ACTIVATION OF NITRIC ACID IN FLUORINATED ALCOHOLS FOR AROMATIC NITRATION AND OXIDATION OF ALCOHOLS

Štefan Možina

Doctoral Dissertation
Jožef Stefan International Postgraduate School
Ljubljana, Slovenia

Supervisor: Prof. Stojan Stavber, Jožef Stefan Institute, Ljubljana, Slovenia
Co-Supervisor: Assoc. Prof. Jernej Iskra, Faculty for Chemistry and Chemical Tehnology, Ljubljana, Slovenia

Evaluation Board:
Prof. Dr. Janez Plavec, Chair, National Institute of Chemistry, Ljubljana, Slovenia
Assist. Prof. Dr. Anton Kokalj, Member, Jožef Stefan Institute, Ljubljana, Slovenia
Prof. Dr. Jurij Svete, Member, Faculty of Chemistry and Chemical Technology, Ljubljana, Slovenia

MEDNARODNA PODIPLOMSKA ŠOLA JOŽEFA STEFANA
JOŽEF STEFAN INTERNATIONAL POSTGRADUATE SCHOOL



Štefan Možina

ACTIVATION OF NITRIC ACID IN FLUORINATED ALCOHOLS FOR AROMATIC NITRATION AND OXIDATION OF ALCOHOLS

Doctoral Dissertation

AKTIVACIJA DUŠIKOVE KISLINE V FLUORIRANIH ALKOHOLIH ZA NITRIRANJE AROMATOV IN OKSIDACIJE ALKOHOLOV

Doktorska disertacija

Supervisor: Prof. Stojan Stavber

Co-Supervisor: Assoc. Prof. Jernej Iskra

Ljubljana, Slovenia, May 2017

Never accept the world as it appears to be, dare to see it for what it could be.

– Dr. Harold Winston

Acknowledgments

I thank the Slovenian Research Agency (ARRS, program Young researchers - MR 36492, ARRS-SP-2990/17) for their funding of my doctoral research. I thank COST (COST action CM1205 CARISMA) for funding my short-term scientific mission at Stockholm University and training school ("A. Corbella" International Summer School).

I thank my supervisor Prof. Dr. Stojan Stavber and my co-supervisor Assoc. Prof. Dr. Jernej Iskra for all their guidance, support and their contribution to my growth as a researcher. I thank them for their proofreading and help in putting this doctoral dissertation into its final shape.

I thank the evaluation board, Dr. Anton Kokalj, Prof. Dr. Janez Plavec, Prof. Dr. Jurij Svete, for their evaluation of my dissertation.

Over the years a lot of people helped in making this dissertation a reality. I would like to express my appreciation to:

National NMR centre, especially to Aleksandar Gačeša and Uroš Javornik, for their help getting excellent NMR spectra and fixing all the problems while I was there.

Dr. Dušan Žigon for the mass spectra (I apologize for that one time when my compound polymerized on the colon of the mass spectra).

Dr. Matic Lozinšek for the X-ray structure analysis.

Blaž Alič for help with the reactions under inert conditions.

Prof. Dr. Janez Štrancar and Dr. Rok Podlipec for measurements as well as analyses of the EPR spectra. Those measurements created a new area for my dissertation. I also thank my other neighbours at the Laboratory of Biophysics for the great atmosphere. I'm sorry I did not get to know you better before.

Anton Kokalj and Matic Poberžnik for help with the DFT studies. It was always great getting to learn completely new mind set to solve problems. Matic thank you for all the help with explaining computational studies to me, helping me with all the errors (small and big), and making my life easier by giving me the necessary tools.

Dr. Belén Martín Matute for our collaboration and accepting me into her group during my stay at Stockholm University. I thank *Antonio Bermejo Gómez* for guiding me during my stay at Stockholm University and teaching me about iridium catalysts. I thank past and present members of the BMM groups, *Elis Erbing*, *Samuel Martínez Erro* and

especially *Greco González Miera* for taking me under your wing and having a great time.

Angela van der Werf, Kilian Colas, Matic Hriberšek, Tony Zhao, Lorn Starmer O'Farrell, Stalin Reddy Pathipati introducing me to Stockholm, making my stay in Stockholm great and full of wonderful memories. I hope I will see you again.

Special thanks go to my present and past co-workers in the K3 Department of Physical and Organic Chemistry, Laboratory of Organic and Bioorganic Chemistry *Katarina Starkl Renar, Jerca Pahor and Klara Čebular.* Katarina thank you for all the help in the office, in the laboratory, and for advises and talks about life outside the institute.

I thank my family for all the love and support in my life. I specially thank my *Mother* & *Father* for creating me. Without them I would not be here. And finally, I thank all my friends around the world, wherever you are, giving my life joy and purpose.

Abstract

The objective of this thesis was to find an alternative way of activating nitric acid and its lower valent analogues to use them as reagents or as catalysts. The research was split into three sections. The first section describes the use of the nitric acid activated by fluorianted solvents (2,2,2-trifluoroethanol-TFE, 1,1,1,3,3,3-hexafluoroisopropanol-HFIP, trifluoroacetic acid-TFA) as a reagent for aromatic nitration. The results obtained with such a method were compared with classic nitration with a mixed acid system. It was found that the activation of HNO_3 with HFIP was of similar strength as in conc. H_2SO_4. For the effective nitration of various aromatic molecules in HFIP 1 equiv. of HNO_3 was used without the addition of external acids. In reactions with 1,3-dimethoxybenzene derivatives new products, i.e., bisphenylnitrosonium nitrates, were identified. Therefore, two mechanistic studies were carried out. In the first mechanism we identified intermediates for the formation of bisphenylnitrosonium nitrates. The reaction path was further explained by DFT calculations. In the second mechanism we explained the nitration of arenes in fluorinated alcohols. In the end we compared our method of nitration of aromatic compounds with HNO_3 in HFIP with other literature methods in terms of the environmental potential by calculating green metrics (atom economy, E factor, etc.). In the second section, the activation of nitric acid for reactions of oxidation was studied. Nitric acid was used as the sole catalyst for the aerobic oxidation of various benzyl alcohols and complete conversion into the corresponding benzaldehydes was obtained. For less reactive aliphatic alcohols an additional iron co-catalyst was used to selectively oxidise the secondary alcohol group. The last section describes the study of aerobic oxidative halogenation in conjunction with an iridium catalyst. This was performed as collaboration with the Martín-Matute group, Stockholm University. We successfully coupled the 1,3-hydride shift in allylic alcohols catalysed by an iridium catalyst with aerobic oxidative iodination. The iodine(I) reagent was generated *in situ* by the aerobic oxidation of iodine using NO_x as a catalyst. The developed method was used for the regioselective synthesis of α-iodoketones from allylic alcohols.

Povzetek

Cilj disertacije je bila raziskava alternativnega načina aktivacije dušikove kisline in njenih nižje valentnih analogov za uporabo kot reagenta ali katalizatorja. Raziskava je razdeljena na tri dele. V prvem delu smo aktivirali dušikovo kislino s fluoriranimi topili (2,2,2-trifluoroetanol, 1,1,1,3,3,3-heksafluoro-propan-2-ol, TFA-trifluoroocetna kislina) in nato smo jo uporabili kot nitrirni reagent za sintezo nitriranih aromatskih spojin. Metodo smo primerjali s klasičnim nitriranjem, kjer se za aktivacijo uporablja H_2SO_4. Nitriranje aromatskih spojin z 1 ekvivalentom HNO_3 v HFIP, je primerljivo s klasičnim nitriranjem v H_2SO_4. Pri reakcijah v HFIP ni bilo potrebe po dodatnih kislinah. Pri reakcijah z 1,3-dimetoksibenzen derivati smo opazili nastanek nov tip produktov, ki so bili okarakterizirali kot bisfenilnitrozonijevi nitrati. Sledila je študija mehanizma nastanka bisfenilnitrozonijevih nitratov in nitriranih aromatskih spojin v fluoriranih alkoholih. Prvi mehanizem razloži mehanizem nastanka bisfenilnitrozonijevih nitratov. Teoretična podlaga k mehanizmu je bila narejena z DFT kalkulacijami. Drugi mehanizem opisuje nastanek nitriranih aromatov v fluoriranih alkoholih. Ugotovljeno je bilo, da v nasprotju s klasičnim nitriranjem, mehanizma potekata po radikalski poti. Raziskavo smo zaključili s primerjavo naše metode (HNO_3 v HFIP) za aromatsko nitriranje z ostalimi literaturnimi metodami z vidika njihovega ekološkega potenciala. Ekološki potencial za metode nitriranja aromatskih spojin je bil ocenjen iz primerjave vrednosti zelenih merilnih enot (atomska ekonomija, E-faktor...). Drugi del disertacije opisuje uporabo aktivirane dušikove kisline kot katalizatorja za aerobno oksidacijo alkoholov. Pri aerobni oksidaciji benzilnih alkoholov dušikova kislina je bila edini katalizator in popolna konverzija v ustrezne benzaldehide je bile dosežena. Za aerobno oksidacijo alifatskih alkoholov smo uporabili železov(III) klorid kot sekundarni katalizator, s katerim je bila dosežena selektivna oksidacija sekundarne alkoholne skupine v ketone brez kakršnekoli reakcije na primarni alkoholni skupini. Zadnji del disertacije vsebuje raziskavo aerobnega oksidativnega halogeniranja v kombinaciji z iridijevim katalizatorjem. To poglavje je bilo izvedeno v sodelovanju z Martín-Matute skupino iz Stockholmske univerze. Z verižno povezavo 1,3-premik hidrida alilnih alkoholih kataliziran z iridijevim katalizatorjem skupaj z aerobnim oksidativnim jodiranjem. Jod(I) spojine so bile pripravljene preko aerobne oksidacije joda, ki je bila katalizirana z NO_x. Razvita metoda je bila uspešno uporabljena za selektivno sintezo α-haloketonov iz alilnih alkoholov.

Contents

List of Figures **xv**

List of Tables **xix**

List of Schemes **xxi**

Abbreviations **xxiii**

Symbols **xxv**

1 Introduction **1**
1.1 Hydrogen bond catalysis . . . 2
1.2 Fluorinated alcohols . . . 5
1.2.1 Mechanistic overview . . . 8
1.2.2 Application of fluorinated alcohols . . . 11
1.2.2.1 Oxidation catalysis . . . 11
1.2.2.2 Reduction catalysis . . . 14
1.2.2.3 Carbon-heteroatom bond formation . . . 16
1.2.2.3.1 Fixation of carbon dioxide . . . 17
1.2.2.4 Carbon–carbon bond formation . . . 18
1.2.2.4.1 C–H functionalizations . . . 19
1.2.2.5 Cycloadditions . . . 21
1.2.2.6 Use in biochemistry . . . 21

2 Aim of the thesis **23**

3 Materials and methods **25**

4 Results and discussion **27**
4.1 Aromatic nitration . . . 27
4.1.1 Introduction . . . 27
4.1.2 Activation of nitric acid under template catalysis . . . 29
4.1.3 Substrate scope . . . 32
4.1.3.1 Oxidation as a side process . . . 35
4.1.3.2 Formation of dinitrated products . . . 38
4.1.4 Bisphenylnitrosonium nitrate . . . 40
4.1.5 Mechanistic study on formation of bisphenylnitrosonium nitrate . . . 45
4.1.6 Mechanism of aromatic nitration in fluorinated alcohols . . . 50
4.1.7 Computational study of formation of bisphenylnitrosonium nitrate . 53
4.1.7.1 Results for calculations with an implicit description of the solvent . . . 56

4.1.7.2 Results for calculations with a hybrid implicit-explicit description of the solvent: SMD_{TFE} + 2×TFE 58
4.1.8 Environmental analysis 62
4.1.9 Experimental data 71
4.1.9.1 Experimental procedure for nitration of 1,3-dimethylbenzene 71
4.1.9.2 Experimental procedure for study of the effect of the ratio solvent/substrate 72
4.1.9.3 Substrate scope 72
4.1.9.4 Study of the formation of dinitrated products 84
4.1.9.5 Study of the formation of bisphenylnitrosonium nitrates . . 85
4.2 Aerobic oxidation of alcohols 88
4.2.1 Introduction 88
4.2.2 Oxidation of benzyl alcohols 89
4.2.3 Mechanism of catalytic oxidation for benzyl alcohols 93
4.2.4 Iron catalysis 97
4.2.5 Mechanism for the iron catalyst 101
4.2.6 Experimental data 105
4.3 Aerobic oxidative iodination 115
4.3.1 Experimental data 121

5 Conclusions **123**

References **125**

Bibliography **141**

Biography **143**

List of Figures

Figure 1.1: Change of the free energy during the transition state due to a catalysts. 1
Figure 1.2: Stabilization of transition state through hydrogen bonds [5]. 4
Figure 1.3: Cooperative effect of hydrogen bond between water molecules. 4
Figure 1.4: Dependence of properties of monomeric HFIP in regard due to conformation of the C-O bond in HFIP. 6
Figure 1.5: Potential energy and dipole moment of HFIP in vacuum (black) or in Polarizable Continuum Model (PCM, red) [18]. 6
Figure 1.6: X-ray structure of single-crystal of HFIP [18]. 7
Figure 1.7: Transition state complex of HFIP-H_2O_2-ethene [21]. 8
Figure 1.8: Energy profile for epoxidation of ethene with H_2O_2 catalysed by HFIP [21]. 8
Figure 1.9: Catalysis of H_2O_2 by HFIP for oxidation of sulfides on the left and the inhibition of further oxidations of sulfoxide through H-bonds with HFIP on the right. 13
Figure 1.10: 2010 Nobel prize winning Pd-catalysed cross coupling. 18
Figure 1.11: SEM images of self-assembled L-Tyr-L-Phe (YF) structures. 21

Figure 4.1: Most common transformations of nitro group. 28
Figure 4.2: Nitration of *m*-xylene (**1**) with different amounts of H_2SO_4. 29
Figure 4.3: Conversion of **1** into **2** in various solvents. 30
Figure 4.4: Comparison of overall conversion between classical system and fluorinated solvents for nitration of *m*-xylene (**1**). 30
Figure 4.5: Yield in dependence to solvent/substrate ratio at nitration of *m*-xylene (**1**). 31
Figure 4.6: Change of selectivity of nitration of *m*-xylene depending on solvent/substrate ratio. 31
Figure 4.7: Products formed in nitration of 1,3-dimethoxybenzene by Gowenlock *et al* [84]. 41
Figure 4.8: The asymetric unit of the bis(2,4,6-trimethoxyphenyl)nitrosonium nitrate (**54**) crystal structure is comprised of one-half of the cation and one-half of the anion ($Z' = 0.5$) - both residing with N-O bonds on the 2-fold rotation axis. 43
Figure 4.9: The course of monitoring of formation of **54** by ^{1}H NMR spectroscopy. 45
Figure 4.10: Change of ^{1}H NMR signals in the aromatic region due to formation of **54**. 46
Figure 4.11: Changes in OH-region in NMR spectra of reaction of **54** and HNO_3 in TFE. 46
Figure 4.12: EPR spectrum of 1st intermediate in formation of the **54**. 47
Figure 4.13: EPR spectrum of 2nd intermediate in formation of **54**. 48
Figure 4.14: EPR spectrum of 3rd intermediate in formation of **54**. 48

Figure 4.15: Time course of nitration of mesitylene (**10a**) into 2-nitromesitylene (**10b**) (peak 1525 cm^{-1}). 50
Figure 4.16: Real-time ATR-IR spectra of nitration of **10a**. 50
Figure 4.17: EPR spectrum at beginning of nitration of mesitylene (**10a**). 51
Figure 4.18: EPR spectrum towards the end of nitration of mesitylene (**10a**). 51
Figure 4.19: $OH^{\bullet}$ extracts a hydrogen atom from TFE solvent molecule and forms H_2O and $CF_3CH_2O^{\bullet}$. 53
Figure 4.20: Energy profile calculated with SMD_{TFE} solvent description and M06-2X functional for alternative mechanism (blue) and classical nitration (red). 56
Figure 4.21: Energy profile for C–N bond stretch for $I1_A$ performed with SMD_{TFE} description of solvent and M06-2X functional. 57
Figure 4.22: Energy profile for C–N bond stretch for $I1_A$ performed with SMD_{TFE} description of solvent and MP2 method. 57
Figure 4.23: Energy profile for C-N bond stretch for $I1_C$ performed with SMD_{TFE} description of solvent and M06-2X functional. 58
Figure 4.24: Optimised structures of NO_2 + 2×TFE in SMD_{TFE} solvent calculated with and M06-2X functional. 58
Figure 4.25: Complexes of TFE molecules with aromate intermediates $I1_A$ and $I1_C$ calculated with SMD_{TFE} solvent description and M06-2X functional. . . 59
Figure 4.26: $I2_A$ and two TFE molecules calculated with SMD_{TFE} solvent description and M06-2X functional. 59
Figure 4.27: Energy profile calculated with SMD_{TFE} + 2×TFE solvent description and M06-2X functional for alternative mechanism (blue) and classical nitration (red). 60
Figure 4.28: Energy profile calculated with SMD_{TFE} + 2×TFE solvent description and M06-2X functional for complete alternative mechanism for formation of **54**. 61
Figure 4.29: AE and RME for different methods of synthesis of nitrotoluene. 68
Figure 4.30: PMI and E factor for different methods of synthesis of nitrotoluene. . . 69
Figure 4.31: Amount of waste depending on its source. 70
Figure 4.32: Cost for synthesis of 1 mol nitrotoluene. 70
Figure 4.33: Influence of solvent HFIP/substrate molar ratio on selectivity and conversion of aerobic oxidation of benzyl alcohol with 5 mol% HNO_3 · . . . 93
Figure 4.34: Real-time FTIR-ATR spectroscopy monitoring of the aerobic oxidation of **67a** with one equivalent of HNO_3. 93
Figure 4.35: Time dependence of stoichiometric oxidation of **67a** (995 cm^{-1}) into **67b** (1696 cm^{-1}), and the temperature of the mixture determined by in situ ATR-IR spectroscopy. 94
Figure 4.36: Time dependence for catalytic oxidation of **67a** (995 cm^{-1}) into **67b** (1696 cm^{-1}), and the temperature of the mixture determined by in situ ATR-IR spectroscopy. 94
Figure 4.37: Enlarged partition of 3D ATR-FTIR spectra for aerobic oxidation of **67a** with 10 mol% HNO_3. 95
Figure 4.38: ATR-IR spectra from decomposition of **67e** in HFIP and in *i*-PrOH. . . 96
Figure 4.39: Lack of signal for usually formed N_2O (2236 cm^{-1}). 96
Figure 4.40: Aerobic oxidation of **77** into **78** catalysed by HNO_3 and metal co-catalyst. 98
Figure 4.41: Influence of amount of $FeCl_3$ on yield of **78**. 98

Figure 4.42: ATR-IR spectra for decomposition of isopentyl nitrite (**94**) catalysed by 1 mol% $FeCl_3$ (peak of aldehyde (**95**) on the left, peak of isopentyl nitrite (**94**) on right. 102
Figure 4.43: Decomposition of isopentyl nitrite (**94**, peak 973 cm^{-1}) into isopentanal (**95**, peak 1710 cm^{-1}). 102
Figure 4.44: UV-VIS spectra of Prussian blue formed in reaction sample and reference. 103

List of Tables

Table 1.1: Physico-ochemical properties of fluorinated alcohols. 5
Table 1.2: Relation between rate constant k and various reactions in fluorinated alcohols. 9
Table 1.3: Effect of solvent in hexafluoroacetone catalysed epoxidation of 3-carene (**I13**). 12
Table 1.4: Solvent effect in palladium-catalysed asymetric hydrogenation. 14

Table 4.1: Aromatic nitration of substrates with activated aromatic ring.[a] 32
Table 4.2: Aromatic nitration of alkylbenzenes.[a] 33
Table 4.3: Aromatic nitration of benzene.[a] 34
Table 4.4: Aromatic nitration of naphthalene.[a] 34
Table 4.5: Aromatic nitration of durene.[a] 35
Table 4.6: Aromatic nitration of 1,3,5-tri-t-butyl-benzene.[a] 36
Table 4.7: Aromatic nitration of anisole.[a] 37
Table 4.8: Aromatic nitration of trifluoromethylbenzene.[a] 39
Table 4.9: Aromatic nitration of nitrobenzene.[a] 39
Table 4.10: Distribution of products in nitration of 1,3-dimethoxybenzene in HFIP.[a] 41
Table 4.11: Distribution of products in nitration of 1,3,5-trimethoxybenzene in fluorinated alcohols.[a] 42
Table 4.12: Reaction with 2,6-dimethoxytoluene (**56**).[a] 44
Table 4.13: Reaction with 3,5-dimethoxytoluene (**60**).[a] 44
Table 4.14: ΔE (in kcal mol^{-1}) for the formation of reaction intermediates in alternative path and in the classical nitration, calculated with three different descriptions of solvents with M06-2X functional. 55
Table 4.15: Methods for aromatic nitration. 65
Table 4.16: Green metrics for methods for aromatic nitration. 66
Table 4.17: Isolation procedure for evaluated methods. 67
Table 4.18: The effect of solvent on oxidation of benzyl alcohol with HNO_3.[a] 89
Table 4.19: Aerobic oxidation of **67a** with catalytic amount of HNO_3.[a] 90
Table 4.20: Catalytic oxidation of various banzyl alcohols.[a] 92
Table 4.21: Selective aerobic oxidation of secondary alcohols.[a] 99
Table 4.22: Reaction with tertiary alcohol.[a] 100
Table 4.23: Solvent effect on selectivity in reaction of iodine(I) with 1-octene-3-ol.[a] 117
Table 4.24: Iridium-catalysed isomerization/aerobic iodination of allyl alcohols.[a] . . 118
Table 4.25: Influence of amount of HCl on catalytic isomerization/iodination of allyl alcohols.[a] 118
Table 4.26: Influence of amount of $NaNO_2$ on catalytic isomerization/iodination of allyl alcohols.[a] 119
Table 4.27: Influence of solvent on catalytic isomerization/iodination of allyl alcohols.[a] 119

List of Schemes

Scheme 1.1: Dynamic kinetic resolution (DKR) of azlactones. . . . 3
Scheme 1.2: Enantioselective Michael addition of acetylacetone to nitrostyrene catalysed by bifunctional thiourea catalyst. . . . 3
Scheme 1.3: Role of catalyst in Michael addition. . . . 3
Scheme 1.4: Alkene epoxidation in perfluorinated alcohols. . . . 11
Scheme 1.5: A novel mechanism with new intermediates for formation Bayer-Villiger product. . . . 12
Scheme 1.6: Selective oxidation of sulfides in HFIP. . . . 12
Scheme 1.7: Oxidation of tiols into disulfide in HFIP. . . . 13
Scheme 1.8: Oxidation of alcohols to carbonyl compounds. . . . 13
Scheme 1.9: Asymmetric hydrogenation of α-fluorinated iminoesters. . . . 15
Scheme 1.10: Asymetric synthesis of fluoroalky amines. . . . 15
Scheme 1.11: Hydrogenation of imines and functionalised ketones. . . . 15
Scheme 1.12: Electrophilic aromatic chlorination catalysed by TFE. . . . 16
Scheme 1.13: Allylic substitution of alcohols with nucleophiles. . . . 16
Scheme 1.14: Asymetric synthesis of α-aminophosphates. . . . 17
Scheme 1.15: Coupling of carbon dioxide and epoxide. . . . 17
Scheme 1.16: Friedel-Crafts intermolekular cyclialkyliation promoted by HFIP. . . . 18
Scheme 1.17: HFIP in aliphatic C(sp^3)–H bond activation. . . . 19
Scheme 1.18: Examples of products formed by different distal directing groups for C–H arene activation. . . . 20
Scheme 1.19: Sulfoxide directed atropodiastereoselective direct functionalizations induced by HFIP. . . . 20
Scheme 1.20: Enantioselective Mukayama-Micheal addition. . . . 20
Scheme 1.21: Rh(I) catalysed [4+2] cycloaddition in TFE. . . . 21

Scheme 4.1: Most common nitrocompounds and their use. . . . 27
Scheme 4.2: Formation of nitronium ion in mixed acids method. . . . 28
Scheme 4.3: Nitration of *m*-xylene. . . . 29
Scheme 4.4: Aromatic nitration of isopropylbenzene. . . . 35
Scheme 4.5: Aromatic nitration of 2-naphthol. . . . 37
Scheme 4.6: Dinitration of *m*-Xylene (**1**). . . . 38
Scheme 4.7: Nitration of 1,2- and 1,4-dimethoxybenzene yields expected nitrated product. . . . 40
Scheme 4.8: Proposed product of nitration of 1,3-dimethoxybenzene by Kochi *et al* [82]. . . . 40
Scheme 4.9: Structure for the 1st intermediate obtained by EPR spectra. . . . 47
Scheme 4.10: Structure for 2nd intermediate obtained from EPR spectra. . . . 48
Scheme 4.11: Structure for 3rd intermediate obtained from EPR spectra. . . . 49
Scheme 4.12: Mechanism for formation of bis(2,4,6-trimethoxyphenyl)nitrosonium nitrate (**54**). . . . 49

Scheme 4.13: Mechanism for classical nitration of aryl compounds. 52
Scheme 4.14: Mechanism for nitration of aryl compounds in HFIP. 52
Scheme 4.15: Proposed alternative path for reactions with HNO_3 in fluorinated alcohols in comparison to classical nitration. 54
Scheme 4.16: Reaction steps in alternative mechanism. 56
Scheme 4.17: Reaction steps in classical nitration mechanism. 56
Scheme 4.18: All reaction steps involved in alternative path for formation of **54**. . . 61
Scheme 4.19: Catalytic transfer of oxygen for oxidation of alcohols. 88
Scheme 4.20: Mechanism for aerobic oxidation of alcohols mediated by HNO_3. . . . 95
Scheme 4.21: Catalytic aerobic oxidation of benzyl alcohols vs. stoichiometric oxidation of aliphatic alcohols. 97
Scheme 4.22: Mechanism for formation of products in reaction with tertiary alcohol. 100
Scheme 4.23: The effect of halogen atom on the oxidation of **78** with $Fe(NO_3)_3$ and HX (X = Cl, Br). 101
Scheme 4.24: Decomposition of nitrite is catalysed by iron salt. 101
Scheme 4.25: Mechanism for aerobic oxidation catalysed by HNO_3 and $FeCl_3$. 103
Scheme 4.26: Selectivity in synthesis of α-haloketones. 115
Scheme 4.27: Tandem 1,3-hydrogen shift/α-functionalisation of allylic alcohols. . . . 116
Scheme 4.28: Synthesis of iodine(I) reagents. 116
Scheme 4.29: Mechanism for catalytic formation of $HICl_2$. 117
Scheme 4.30: Catalytic isomerisation/iodination on other substrates. 120

Abbreviations

AE	...	Atom economy
AN	...	Acceptor number
ATR-IR	...	Attenuated total reflection infrared spectroscopy
EDA	...	Ethydiazoacetate
DCE	...	1,2-dichloroethane
DFT	...	Density functional theory
DKR	...	Dynamic kinetic resolution
E factor	...	Environmental factor
EAN	...	ethylamonium nitrate
ee	...	Enantiomeric excess
EtOH	...	Ethanol
GN	...	guanidine nitrate
HFIP	...	1,1,1,3,3,3-hexafluoropropan-2-ol
HRMS	...	High Resolution Mass Spectrometry
i-Pr	...	Isopropyl
IR	...	Infrared spectroscopy
MeCN	...	Acetonitrile
MTO	...	Methyltrioxorhenium
MW	...	molecular weight
n-Hex	...	*n*-hexane
NMR	...	Nuclear magnetic resonance
PCM	...	Polarizable continuum model
PMI	...	Process mass index
r. t.	...	room temperature
RDX	...	1,3,5-Trinitroperhydro-1,3,5-triazine
RME	...	Reaction mass efficiency
SF	...	Stoichiometric factor
TCE	...	2,2,2-trichloroethanol
TEMPO	...	(2,2,6,6-Tetramethylpiperidin-1-yl)oxyl
TFA	...	Trifluoroacetic acid
TFAA	...	Trifluoroacetic anhydride
TFE	...	2,2,2-trifluoroethanol
TFI	...	Toluene diisocyanate
TLC	...	Thin-layer chromatography
TNT	...	1,3,5-Trinitrobenzene

Symbols

a	...	Hyperfine coupling constant
α	...	Hydrogen bond donor
β	...	Hydrogen bond acceptor
ΔE	...	Reaction energy
η	...	Yield
$E_{\mathrm{T}}^{\mathrm{N}}$	...	Polarity
J	...	Scalar or J-coupling
k	...	Rate constant
m	...	Mass
M	...	Molecular weight
μ	...	Dipole moment
N	...	Nucleophilicity
t_{c}	...	Time correlation
T_{MP}	...	Melting point
Y	...	Ionizing power

Chapter 1

Introduction

The term *catalyst* was conceived by the Swedish chemist Jöns Jacob Berzelius in his report to the Swedish Academy of Science in 1835 [1]. In his description a *catalyst* was a substance which solely by its presence influenced the reaction and remained unaltered throughout the reaction. In the modern definition a catalyst is a compound that influences the reaction rate by reducing the free energy of the transition state without being consumed during the process. The total free energy difference from the reactant to the products, however, does not change (Figure 1.1).

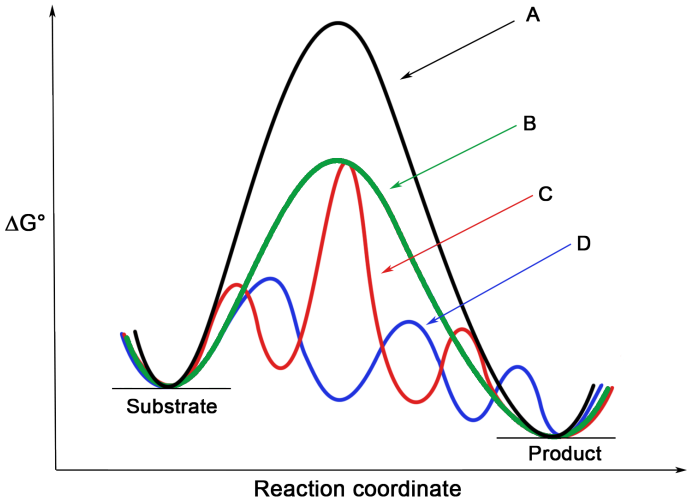


Figure 1.1: Change of the free energy during transition state due to a catalysts. **A** - The uncatalysed path, **B** - A common view of the catalysed path, **C** - More realistic view of how the catalysis is achieved without a the complete change of mechanism (energy to bind reactant to catalyst is required first), **D** - Catalysts can also give a totally new mechanism with a completely new reaction coordinate.

Depending on whether the catalyst is in the same physical phase as the substrate or not we separate catalysts into homogeneous and heterogeneous catalysts. Enzymes or biocatalysts are usually seen as a third separate group. A heterogeneous catalyst is, during the reaction, in a different phase than the substrate. The catalysis typically takes place on the surface of the catalyst. Majority of heterogenous catalysts are in the solid phase. Since active sites are on its surface, it means the bigger the surface is the faster is the reaction. Therefore, a high surface area is desired in regard to the weight of material. This is achieved by reducing the size of particles, commonly to nanoscale particles. The active site represents atoms

(usually transition metals) or crystal faces where the reaction proceeds. Heterogeneous catalysts are in a separate physical state than their surroundings, thus isolation is simple and often just filtration is employed. The effective isolation of a heterogenous catalyst from products and their recycling is important. This is due to their high cost (noble metals) and their biotoxicity (important aspect in, e.g., the pharmaceutical industry).

Homogeneous catalysts are in the same state as the reactants or they are dissolved in solution. Therefore, the probability of encountering a substrate molecule with a catalyst is very high. A higher encounter probability causes a homogeneous catalyst to generally have a greater effectiveness than the heterogeneous counterpart. An additional positive effect of the homogeneous catalyst is an option of using normal chromatographic and spectroscopic techniques in the exploration of mechanism and identifying the intermediates. Acids and bases usually fall under the category of homogeneous catalyst, as well as most of the enzymes and organometallic catalysts [2].

The most commonly used catalysts are noble metals. However, their high cost and future supply risk pose problems [3], [4]. Therefore, a rapidly growing area of research on organocatalysis is important [5]. Based on the mechanism, organocatalytic transformations can be divided in two subgroups - *covalent organocatalysis* and *noncovalent organocatalysis*. In the case of the former, during the catalytic cycle a covalent intermediate is formed between the substrate and catalyst. A typical example is the proline-catalysed aldol reaction, which proceeds through an enamine intermediate [6]. On other hand, noncovalent organocatalysis relies completely on noncovalent interactions, such as the formation of ion pairs and hydrogen bonding. Although organocatalysis began with a "covalent" process, the importance of hydrogen bonding for (stereo)selective organocatalysis has been recognized. An immense amount of development was done in this area in the recent past [5].

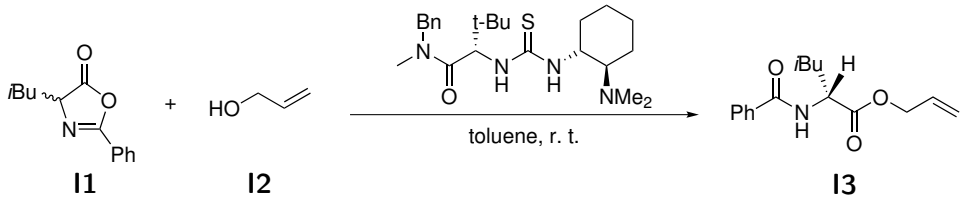
1.1 Hydrogen bond catalysis

Hydrogen bonds are usually formed between polarized X–H and electronegative acceptor atoms (A). The resulting bond X–H$\cdots\cdots$A is weak, but has a significant electrostatic character. Even between neutral molecules hydrogen bonds are a strong directing force keeping the molecules together. Their strength is enough to maintain order and present a powerful directing force in higher structures such as ice. They play a key role in biological systems and are essential for the binding of base pairs in DNA, as well as for binding to receptors, folding of proteins into secondary structures and enzymatic catalysis [5].

Hydrogen bond catalysts are a subgroup of organic catalysts which control organic reactions by the formation of a hydrogen bonds. In reactions catalysed by enzymes the hydrogen bond plays an important role in stabilizing intermediates and lowering the free energy of the transition state [7]. In recent years, new strategies were developed in designing new methods for the synthesis of organic compounds that were inspired by Nature. By harnessing the hydrogen bond power, new small-molecule catalysts emerged. The role of hydrogen bonds in catalysis can be divided into three different ways which are described in the following paragraphs [5].

1. Pre-organization of spatial arrangement of reactants
During the reaction, hydrogen bonds can be used to pre-organize the reactants in an suitable arrangement or to stabilize the transition state or the intermediates [8]. In cases

where the hydrogen bond is attached to a chiral scaffold it can steer the assembly of the well-defined catalyst-substrate complex and therefore determine the stereoselectivity of the reaction. Example of such reaction is dynamic kinetic resolution (DKR) of azlactones (Scheme 1.1). This is a thermodynamic method in which hydrogen bonds are used as an assisting force in the synthesis of organic molecules.

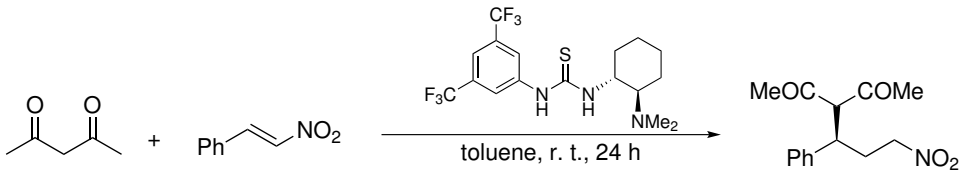


I1 I2 I3

Scheme 1.1: Dynamic kinetic resolution (DKR) of azlactones.

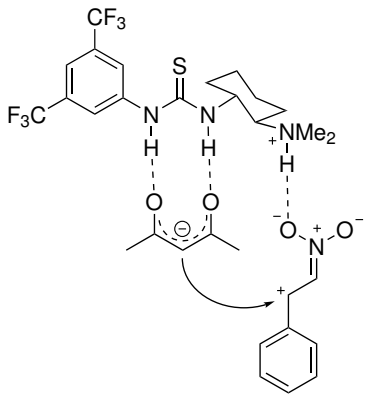
2. Activation of reactants by polarization

The second method uses hydrogen bonds as an assisting force in catalysis. Example of such catalyst is bifunctional thiourea catalyst in reaction of enantioselective addition of acetylacetone to nitrostyrene (Scheme 1.2). Binding through hydrogen bonds changes the electronic densities of reactants. The resulting polarization of the reactants in such catalytic systems leads to their activation (Scheme 1.3). Because of the effect on the reaction rate, this is also known as the kinetic way of using the hydrogen bonds. Polarization of the reactants or substrates can result in their electrophilic activation. It is worth mentioning this represents a third possible known mode for electrophilic activation. Other modes for the electrophilic activation of the reactants are substrate coordination to a metal-based Lewis acid or iminium ion formation.



I4 I5 I6

Scheme 1.2: Enantioselective Michael addition of acetylacetone to nitrostyrene catalysed by bifunctional thiourea catalyst.



Scheme 1.3: Role of catalyst in Michael addition.

3. Stabilization of the charges of the transition state and intermediates
Hydrogen bonds are flexible in terms of angle (90–180°) and length between hydrogen atom and acceptor atom (1.2–3.2 Å). This is very important when charge separation occurs along the reaction path, especially during the transition state. Hydrogen bonds can contract and thus, for example, stabilize the developing (negative) charge. On the other hand, when the product stage comes, the hydrogen bonds can expand and the product-catalyst complex can dissociate. Such an example can be found in olefin epoxidation with H_2O_2 in 1,1,1,3,3,3-hexafluoro-2-propanol (HFIP) [5] (Figure 1.2), where HFIP has a role of hydrogen bond catalyst..

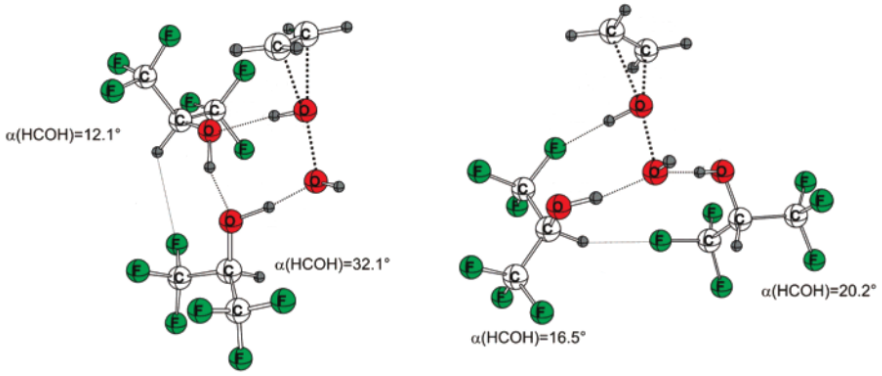


Figure 1.2: Stabilization of transition state through hydrogen bonds [5].

A consequence of hydrogen bonding is the redistribution of the electron density through the covalent bond and this influences further hydrogen bonding. For example, lets look at water molecules. A molecule of water which donates a hydrogen atom to the hydrogen bond has increased electron density on the oxygen atom in the lone pair region. An increased electron density on the oxygen atom favours the acceptance of an additional hydrogen bond. On other hand, the water molecule accepting the hydrogen bond has a reduced electron density on the oxygen atom. Because of that, for such a water molecule it is more energy efficient to further donate the hydrogen bond, but this discourages additional acceptance of the hydrogen bond (Figure 1.3). This electron redistribution therefore results in cooperativity (accepting one hydrogen bond and the donation of another) and anticooperativity (accepting one hydrogen bond disfavours formation of additional one). This is also known as *cooperative hydrogen bonding* [9]. Such catalytic hydrogen bonds can be found in fluorinated alcohols (e.g., HFIP) where higher-order aggregates are formed in an accelerating reaction up to 100,000-fold [5].

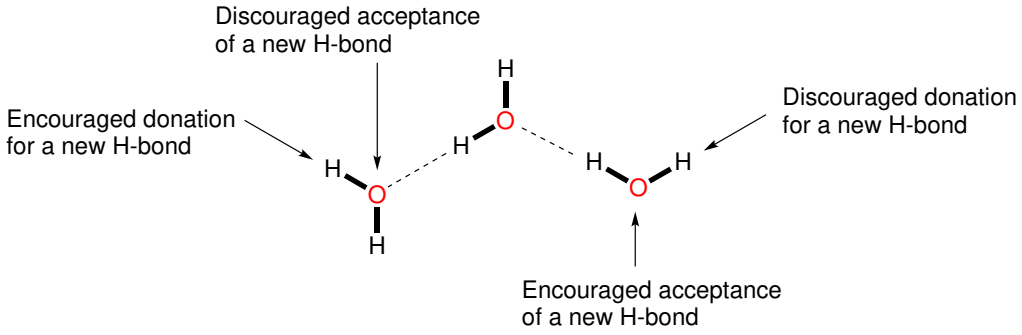


Figure 1.3: Cooperative effect of hydrogen bond between water molecules.

1.2 Fluorinated alcohols

Initially fluorinated alcohols were used in synthetic chemistry as solvents, cosolvents and additives. Next, due to their unique properties they were also used as homogenous catalysts [10]. The first reports were based on biochemical studies where the beneficial effect of fluorinated alcohols was observed in the stabilization of the helix conformation of proteins [11]. In 1996 Eberson *et al.* found that fluorinated alcohols stabilize radical cations due to their unique properties [12]. The most commonly used fluorinated alcohols are 2,2,2-trifluoroethanol (TFE) and 1,1,1,3,3,3-hexafluoro-2-propanol (HFIP), which are commercially available. The special properties of fluorinated alcohols arise from the presence of fluoroalkyl groups. Fluorinated atoms have a strong influence on physico-chemical properties, making fluorinated alcohols unique and distinctly different from their non-fluorinated analogues, as can be seen in Table 1.1 [13].

Table 1.1: Physico-ochemical properties of fluorinated alcohols.

Physico-chemical properties	**EtOH**	**TCE[a]**	**TFE**	**HFIP**
Melting point [°C]	−114	19	−43.5	−5
Boiling point [°C]	78	152	73.8	58.6
Acidity (pKa)	15.9	12.2	12.4	9.3
Polarity (E_T^N)	0.654	0.722	0.898	1.068
Nucleophilicity (N)	0	-	−3.0	−4.23
Ionizing power (Y)	−1.75	-	1.8	3.8
Hydrogen bond donor (α)	0.83	1.36	1.51	1.96
Hydrogen bond acceptor (β)	0.77	0.21	0.18	0 (−0.12)

[a]2,2,2-trichloroethanol

Highly fluorinated alcohols have higher melting points and lower boiling points than their non-fluorinated counterparts [10]. Consequently, they can be easily removed from the reaction mixture by distillation. The strong electron withdrawing effect of fluorine atoms in a CF_3 group leads to increased acidity of the hydrogen of the hydroxyl group. Solvatochromic investigations showed fluorinated alcohols have extremely high polarity. HFIP is even the sole solvent, among 360 investigated compounds, that falls outside of the scale, which is defined by $E_T^N(Me_4Si)=0$ and $E_T^N(water)=1$ while for HFIP E_T^N was determined to be 1.068 [10]. The effect of fluorine atoms extends even further. The influence of fluorinated atoms in TFE and HFIP cause them to be non-nucleophilic, while having high ionizing power [14]. While fluorinated alcohols are strong hydrogen bond donors (α value), on other hand, they are weak hydrogen bond acceptor molecules (β value) [13]. *Hydrogen bond acceptance* (β parameter) is defined from the solvatochromic shift of the longest wavelength in $\pi \longrightarrow \pi^*$ transition for 4-nitrophenol in comparison with 4-nitroanisole. For non-hydrogen bond donor solvent, this experiment measures unambiguously the hydrogen bond acceptance ability of the solvent. Nonetheless, for strong hydrogen bond donors the solvatochromic comparison fails, because the nitro group of 4-nitroanisole is a better hydrogen bond acceptor then the nitro group of 4-nitrophenol. Consequently, the negative values of β are obtained. Therefore, the negative values for most hexafluorinated solvents are assimilated to a value of zero [15].

Non-nucleophilicity of HFIP and its strong interaction with nucleophiles is due to the strong hydrogen bond donor ability. This makes HFIP an excellent solvent for electrochemistry [16]. Fluorinated solvents coordinate a variety of anions (Cl^-, Br^-, NO_3^-,

$SO_4{}^{2-}$, $H_2PO_4{}^-$, OBz^- and OAc^-). They have an even stronger interaction than an analogous isophtalamide-based anion receptor. However, strongly basic anions such as F^- and bicarbonate anions act as Brønsted base and deprotonate the hydroxyl group of fluorinated alcohol. This suggest fluorinated alcohols could be used as pH-switchable receptors that only bind anions when they are "switched on" at low pH [17].

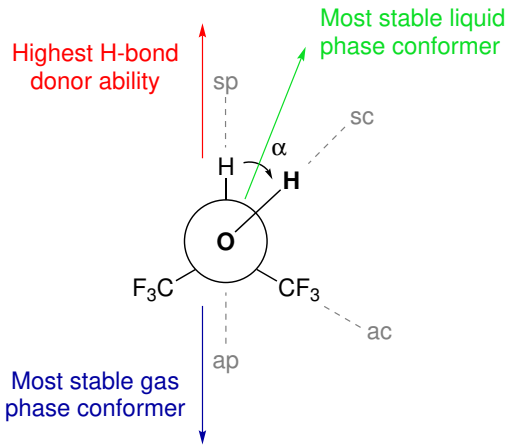


Figure 1.4: Dependence of properties of monomeric HFIP in regard due to conformation of the C-O bond in HFIP.

The hydrogen donor ability of fluorinated alcohols (particularly HFIP) depends on two parameters. The first such parameter is the conformation of the alcohol monomer along the C–O bond (Figure 1.4). The second parameter is the cooperative aggregation to hydrogen bonded clusters [5]. In the gas phase the hydroxy group of HFIP is antiperiplanar (ap, ±150–180°) to the adjacent CH. In a polarizable environment the minimum hydroxy group is in synclinal (sc, 30°to 90°, −30°to -90°) or almost in synperiplanar (sp, 0 ± 30°) conformations (Figure 1.5) [18].

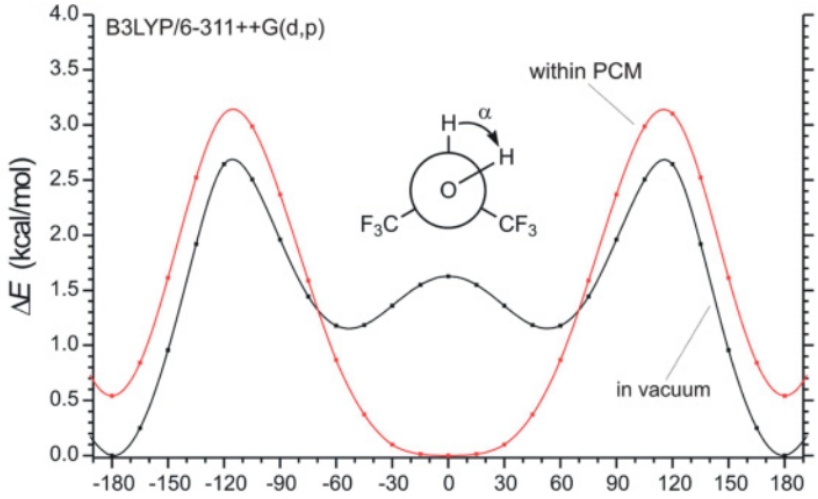
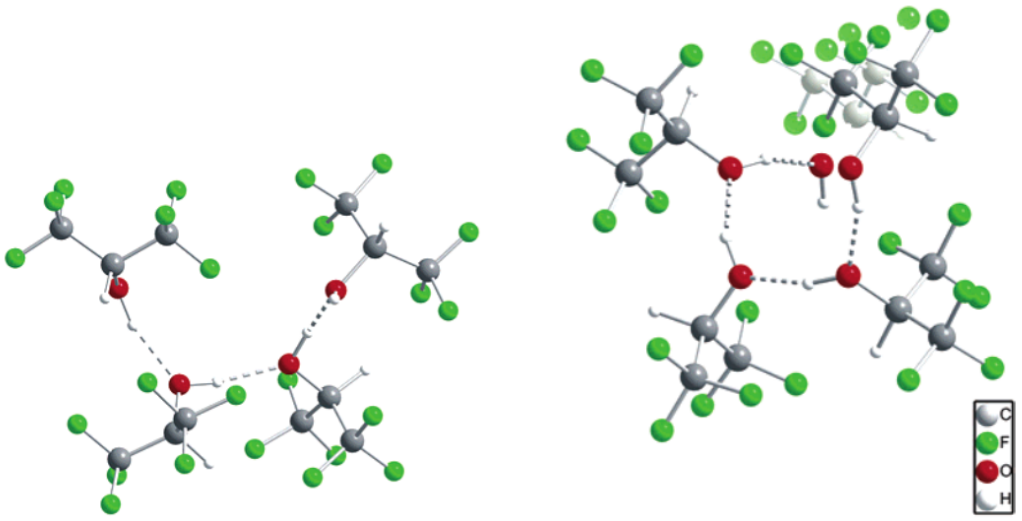


Figure 1.5: Potential energy and dipole moment of HFIP in vacuum (black) or in Polarizable Continuum Model (PCM, red) [18].

In these conformations "the donor orbital energy (σ^*_{OH}) decreased and the dipole moment (μ) increased drastically from ap (antiperiplanar) to sp conformation" [18]. X-ray analyses for HFIP established the synclinal conformation along the C–O bond. HFIP molecules crystallized in infinite helices and zig-zag chains (Figure 1.6) [18].



(a) View perpendicular to the helix axis. (b) View along the helix axis.

Figure 1.6: X-ray structure of single-crystal of HFIP [18].

DFT calculations for the aggregation of HFIP in the liquid state showed the amplified potential to form a H-bond with a highly covalent character. In comparison with *i*-PrOH these effects are twice as pronounced. The coordination of the second and third molecules induces an enhanced polarization of the terminal hydroxyl group. Aggregation beyond trimer, however, does not enhance it further. This means that neglecting aggregation could lead to an underestimation of the potential for fluorinated alcohols as H-bond donors [18].

The proton donor ability increases from EtOH to TFE and finally to HFIP. On the other hand, the basicity of the acceptor molecule decreases as a result, limiting the strength of the hydrogen bond in alcohol clusters. As a consequence, larger clusters of fluorinated alcohols are less strongly bonded compared to non-fluorinated alcohols. An experiment in which a diluted mixture of alcohols are expanded in helium through a pulsed slit jet source showed monomers, dimers and the formation of oligomeric clusters. For EtOH a clear signal for the formation of trimers can be seen, but in the case of HFIP only a weak side band near the signal for dimers is an available candidate for them. It was concluded that the formation of the trimer is disfavoured for HFIP. This comes from destabilization of the trimer ring because of steric and polar interactions [19]. Water-HFIP solutions have microheterogeneity and the formation of clusters. The microheterogeneity between HFIP and water is explained by the tendency of CF_3 groups to cluster, minimizing their contact with water and by formation of network of hydrogen bonds between the HFIP molecules. Strong the tendency for HFIP to cluster was found in 25–35 % volume concentrations [20].

1.2.1 Mechanistic overview

Usually when fluorinated alcohols are used as reaction media their acidity and hydrogen bond donor ability are generally claimed to be major factors responsible for promotion of the transformations. Hydrogen bond donation depends on the temperature and decreases with the rise of the temperature [15]. The most extensive mechanistic studies about the way fluorinated alcohols catalysed reaction were performed on the epoxidation of alkenes with H_2O_2 [21], [22].

DFT calculations showed two possible mechanisms for the epoxidation of ethene and propene with H_2O_2. One follows the homolitic bond cleavage of the peroxide and the π-bond of the alkene. The other mechanism follows concerted polar mechanism. It was found that fluorinated alcohols follow a polar mechanism, however, both mechanisms have similar energy for transition states. Differences between energies for transition states are 0.03–2.26 kcal mol^{-1}. This means both mechanisms could coexist under real conditions. Consequentially, both should be considered until verified or falsified by experimental means. The DFT calculations showed fluorinated alcohols catalyse the reaction of the epoxidation of alkenes with hydrogen peroxide using a combination of three main factors. The first one is the geometrical factor, where the presence of the fluorinated alcohol reduces the bond deformation of the hydrogen peroxide and alkene during the transition state (Figure 1.7) [21].

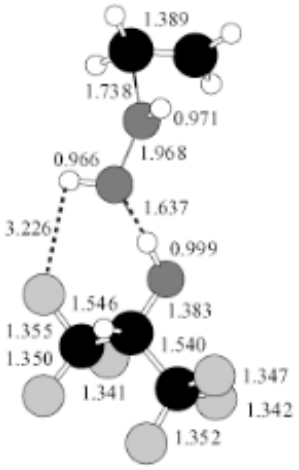


Figure 1.7: Transition state complex of HFIP-H_2O_2-ethene [21]. Numbers represent bond distances in Å.

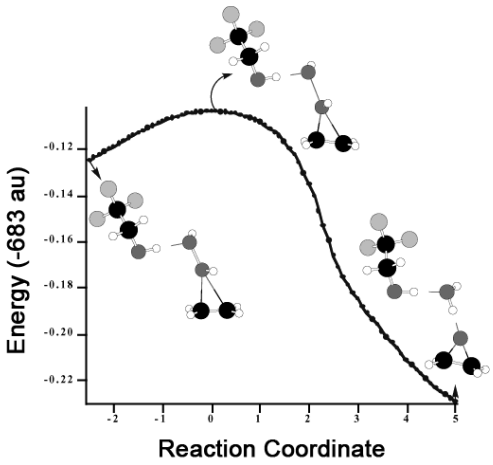


Figure 1.8: Energy profile for epoxidation of ethene with H_2O_2 catalysed by HFIP [21].

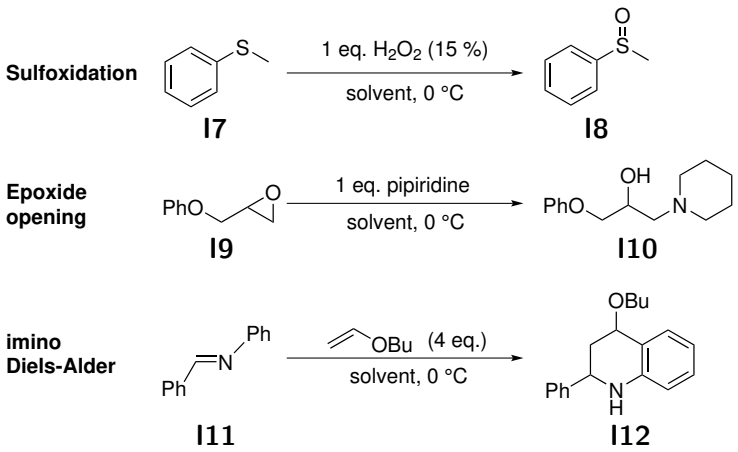
The second two are electronic factors, where fluorinated alcohol increases the polarity of the transition state and acts as a complementary charge template to the hydrogen peroxide and olefin moieties during the transition state (Figure 1.8). Fluorinated alcohol with electrostatic interactions stabilizes the transition state because of the charge complementarity. These interactions are formed especially between the negatively charged fluorine atoms of the fluorinated alcohol and the positively charged hydrogens of H_2O_2 and olefin. This type of catalysis is now known as *template catalysis* and is similar to the "push-pull" activation of hydrogen peroxide in peroxidase heme-enzymes [21].

A kinetic study of the epoxidation of cyclooctene and 1-octene with hydrogen peroxide

was performed in a HFIP/dioxane mixture. The study also included a catalytic reaction with arsonic acid. For both reactions, with and without arsonic acid, two kinetic regimes were found. At low HFIP concentrations ($n_{\mathrm{HFIP}}/n_{\mathrm{total}} \leq 0.15$) both reactions were first order, depending on the HFIP concentration. This is explained as *charge template catalysis* for uncatalysed epoxidation. In the catalysed reaction at a low HFIP concentration an arsonic acid mono-HFIP ester is formed with much higher catalytic properties. At high HFIP concentrations ($n_{\mathrm{HFIP}}/n_{\mathrm{total}} \geq 0.5$) both reaction types showed 12^{th}-order dependence on the HFIP concentration [22]. HFIP at high concentrations forms clusters due to its strong hydrogen bond ability [19], [20], [23]. Therefore, it was concluded in high HFIP concentration that the reaction proceeds inside a coordination sphere comprising *ca.* 12 HFIP molecules. This coordination sphere causes a striking rate acceleration. This resembles a rate acceleration effect by protein matrix in enzymatic catalysis. Usually, co-factors themselves are catalytically active; however, it is the "embedding" into apo enzymes which causes a huge turnover rate typical for enzymes [22].

Promotion of a reactions by fluorinated alcohols can come from their acidity or due to their hydrogen bond donor ability [15]. To understand the role of fluorianetd alcohols three different types of reactions were followed - *sulfoxidation*, *epoxide opening* and *imino Diels-Alder reaction* (Table 1.2). Their rate constants k have been plotted against their pKa value and the AN (acceptor number) values of the alcohols. The corresponding correlation coefficients R^2 were measured [15].

Table 1.2: Relation between rate constant k and various reactions in fluorinated alcohols.



	k [M· mol^{-1}·h^{-1}]		
Solvent	**Sulfide oxidation**	**Epoxide opening**	**Diels-Alder reaction**
EtOH	0	5.9×10^{-2}	0
TFE	2.1	27.6×10^{-2}	0.05
HFIP	676	0	1574
$Ph(CF_3)CHOH$	2.3	56.7×10^{-2}	0
$Ph(CF_3)_2COH$	1.9	8.7×10^{-2}	0
$Allyl(CF_3)_2COH$	1.7	7.5×10^{-2}	0
Correlation coefficient			
R^2 (AN)	0.637	3×10^{-5}	0.635
R^2 (pKa)	0.217	0.017	0.215

Sulfoxidation is an electrophilic process where free H^+ as well as the donation of a hydrogen bond could activate H_2O_2 [15]. For acid activation there was a negative correlation between k and pKa with a low value for $R^2 = 0.217$. This rules out the possibility for acidity to have a major role in the promotion of such a transformation. On the other hand, there was a positive correlation for k and AN with a significant value of $R^2 = 0.637$. As was already assumed in previous investigations, hydrogen bond donation favours reactions [21], although the effect of fluorinated alcohols cannot be attributed solely to hydrogen bond donor ability. Differences between AN values cannot explain the close k values for tertiary hexafluorinated alcohols and TFE. This is even less so for HFIP, where the incredible effect for the promotion of the reaction is seen. The rate constant for HFIP is more than 300 times higher than for other fluorinated alcohols, while the AN value is only 0.4 times higher. Additionally, the absence of a reaction in EtOH was surprising since the AN value for EtOH is only 11 % below that of $Ph(CF_3)_2COH$ ($AN_{EtOH} = 37.1$ vs. $AN_{Ph(CF_3)_2COH} = 41.8$). It is possible that the strong hydrogen bond acceptance of EtOH has a negative effect for H_2O_2 activation [15].

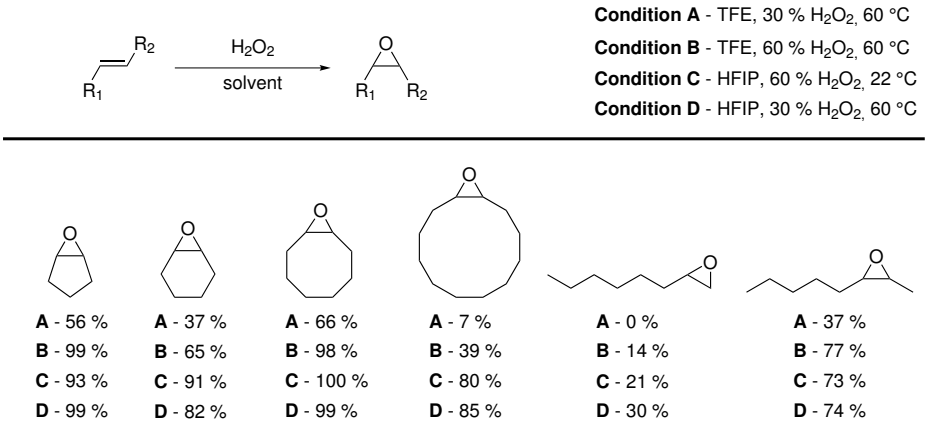
No correlation was found for the reaction of the opening of the epoxide with a piperidine [15]. A correlation with AN gave a slope of almost 0 ($R^2 = 3 \times 10^{-5}$). The correlation with pKa was positive ($R^2 = 0.017$). Therefore, it is clear that neither hydrogen bond donor ability nor acidity can justify the booster effect seen in TFE and $Ph(CF_3)_2COH$. The difference of the reactivity in the imino Diels-Alder reaction is striking since it only occurs in HFIP and TFE. An exceptional reaction rate was obtained for HFIP. On the other hand, the positive correlation for k/AN with ($R^2 = 0.635$) indicates the importance of the hydrogen bond donor ability for the promotion of the reaction. Although, this study is not sufficient to explain why the reaction proceeds only in these two solvents [15].

The authors concluded that the promoter effect of fluorinated alcohols does not stem from Brønsted acidity since for all cases the k/pKa correlation coefficients R^2 are below 0.217 [15]. On other hand, the hydrogen bond donor ability plays an important role in the sulfide oxidation and the imino Diels-Alder reaction. In both reactions an exceptional promoting effect was observed for HFIP, being far more potent than any other fluorinated alcohol. Therefore, this effect cannot be explained exclusively by the hydrogen donor ability [15].

1.2.2 Application of fluorinated alcohols

1.2.2.1 Oxidation catalysis

One of the first studies which determined the ability of fluorinated alcohols to catalyse a reaction was made by Neimann and Neumann [24]. It was discovered that perfluorinated solvents (TFE and HFIP) increased the electrophilic nature of hydrogen peroxide. They exploited this finding for epoxidation of alkenes and for the transformation of ketones into Bayer-Villiger products, where activation by fluorinated alcohols led to reactions with excellent yields and high selectivity. Surprisingly, no additional catalyst was needed for such a reaction to proceed. In the case of TFE 60 % H_2O_2 and an increased temperature were needed to obtain a high conversion. Reactions performed in HFIP could be carried out at r. t. with 60 % H_2O_2 or at 60 °C with 30 % H_2O_2 (Scheme 1.4). The reactivity of the cyclic alkenes was in the order cyclopentene ∼ cyclooctene > cyclohexene > cyclododecene. Low yields (14-30 %) were obtained with terminal alkenes such as 1-octene. In line with expectations the more nucleophilic 2-octene was more reactive and higher yields were obtained (73-77 %). With even more nucleophilic 2,3-dimethyl-2-butene, the epoxide was further transformed into a ring-opened diol and rearranged pinocolone (3,3-dimethyl-2-butanone). The reaction with styrene yielded mostly a C–C bond cleaved product – benzaldehyde [24].

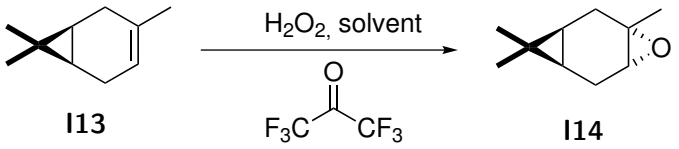


Scheme 1.4: Alkene epoxidation in perfluorinated alcohols.

The oxidation of ketones into the Bayer-Villiger product had limited scope and it could only be done with HFIP. Cyclic ketones were cleanly converted in lactones, while acyclic ketones were unreactive [24]. Epoxidation in fluorinated alcohols was limited to stable epoxides, while acid sensitive epoxides underwent decomposition via hydrolysis or solvolysis. This issue was addressed by Vliet *et al.* [25] by combining fluorinated solvents with a hydrogen peroxide buffer (5 mol% NaH_2PO_4) to obtain sensitive epoxides in high yields. With the less reactive terminal alkenes epoxides were obtained with moderate yields by using HFIP under reflux [25]. By changing the NaH_2PO_4 buffer with a Brønsted acid catalyst (1 mol% *p*-TsOH) they obtained high yields of Bayer-Villiger product from cyclohexanone [26]. The epoxidation of 1-octene was not improved by a simple Brønsted acid, but a clean reaction and a high yield were obtained by using 1 mol% benzenearsonic acid [26] or 0.1 mol% methyltrioxorhenium (MTO) [27]. Hexafluoroacetone as a catalyst in the epoxidation in HFIP represents a path which eliminates the need for a metal or acid catalyst. The best catalytic performance of hexafluoroacetone was observed in the epoxidation of 3-carene (**I13**) in fluorinated solvents (especially in HFIP) (Table 1.3). A mechanistic study of Bayer-Villiger products in HFIP showed a novel mechanism where spiro-bisperoxides (**I16**) were proposed as intermediates [28]. This contributed to the effect of the HFIP to

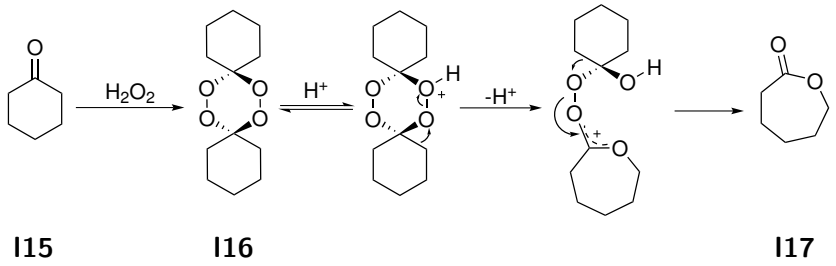
form strong hydrogen bonds with anions and thus stabilize the "naked" cations and cation radicals [12].

Table 1.3: Effect of solvent in hexafluoroacetone catalysed epoxidation of 3-carene (**I13**).



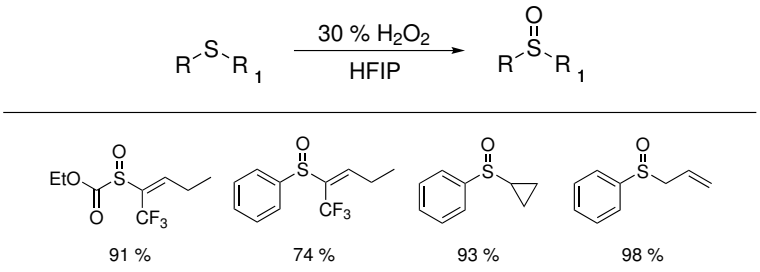
Solvent	Yield (1 h)	Yield (21 h)
DCM	13 %	74 %
$CHCl_3$	9 %	58 %
TFE	15 %	>99 %
HFIP	80 %	>99 %

It was concluded that the properties of HFIP allow the formation of protonated spirobisperoxide and the rearrangement of cations by preventing the competitive intermolecular interception by nucleophiles (Scheme 1.5) [28]. With the H_2O_2/MTO system in a fluorinated alcohols system it was possible to synthesise non-symetric tetroxanes in good yields [29]. The yield and scope of the substrates was furthermore increased by the addition of HBF_4 for the synthesis pharmacologically important 1,2,4,5-tetroxanes [30], [31].



Scheme 1.5: A novel mechanism with new intermediates for formation Bayer-Villiger product.

The activating role of fluorinated alcohols was also used for other types of oxidations. H_2O_2 in the presence of HFIP was used for the selective oxidation of sulfides to sulfoxides (Scheme 1.6) [32], [33].



Scheme 1.6: Selective oxidation of sulfides in HFIP.

In the selective oxidation of sulfides HFIP plays a double role. First, it activates the H_2O_2 with strong hydrogen bonds. The second role of HFIP is to prevent further oxidation to sulfone due to its interaction with sulfoxides. HFIP donates a strong hydrogen bond to an

oxygen atom of the sulfoxide group and consequently decreases the electron density of the sulphur atom, making it less available for further oxidation (Figure 1.9).

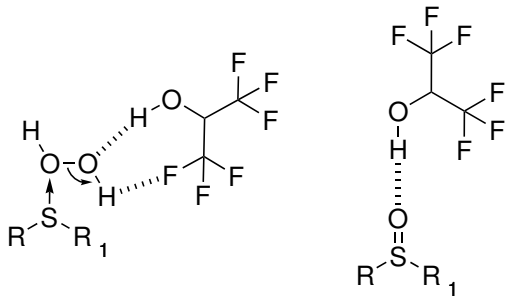
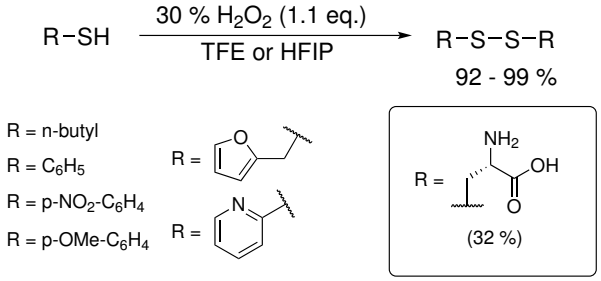


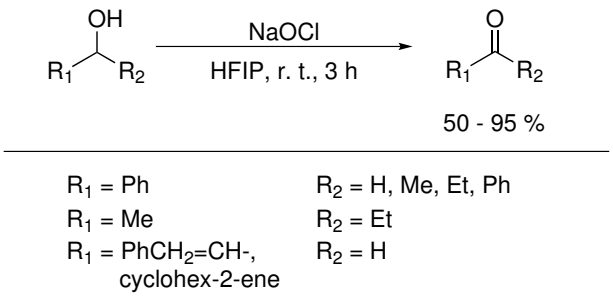
Figure 1.9: Catalysis of H_2O_2 by HFIP for oxidation of sulfides on the left and the inhibition of further oxidations of sulfoxide through H-bonds with HFIP on the right.

Oxidation of tiols with H_2O_2 in fluorinated alcohols yielded disulfides with complete selectivity. No additional metal catalyst was needed. Changing the solvent from HFIP to TFE meant that the reaction time increased from 10 min to 1–6 hours. While high yields were obtained with simple tiols, L-cystine gave only a 32 % yield. This was attributed mostly to the low solubility of L-cystine in a fluorinated medium (Scheme 1.7).



Scheme 1.7: Oxidation of tiols into disulfide in HFIP.

Fluorinated alcohols were used in the catalysis of oxidation for benzyl, allylic and small aliphatic alcohols. Sodium hypochlorite was used as an oxidant and the corresponding carbonyl compounds were obtained (Scheme 1.8). High yields were obtained (90–95 %) for benzylalcohol and cinnamyl alcohol. The lowest yield (50 %) was obtained for the oxidation of 2-butanol which was chosen as a model substrate for aliphatic alcohols. The reaction did not proceed in any other solvents such as DCM, MeCN, toluene, ethanol and TFE [34].



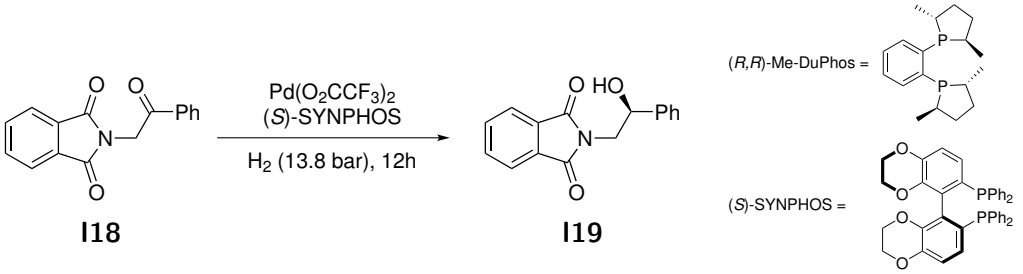
Scheme 1.8: Oxidation of alcohols to carbonyl compounds.

1.2.2.2 Reduction catalysis

In oxidation methods fluorinated alcohols were identified as the key catalyst and great effort was put to identify the mechanism behind the activation of oxidation. On the other hand, in reduction catalysis, where fluorinated alcohols are widespread, little attention was given to elucidate their positive effect on reactions compared to other solvents. In most cases the mechanism behind the catalysis of fluorinated alcohols is unexplored in reduction catalysis.

For the asymmetric hydrogenation of ketones a homogeneous catalyst from palladium(II) trifluoroacetate and (*R*,*R*)-MeDuPHOS was used. A more than 95 % conversion was obtained with 92 % ee for the hydrogination of α-phthalimide ketone (**I18**). Further optimization was performed with the (*S*)-SYNPHOS ligand catalyst. It was discovered that the reaction is very solvent dependent. With TFE good conversion and enantio-selectivity was obtained. DCE was the sole other solvent that gave similar enantio-selectivity; however, the conversion was lower. In all other solvents the low activity of the catalyst was observed (Table 1.4). The mechanism of activation of hydrogenation by TFE was not explained [35].

Table 1.4: Solvent effect in palladium-catalysed asymetric hydrogenation.

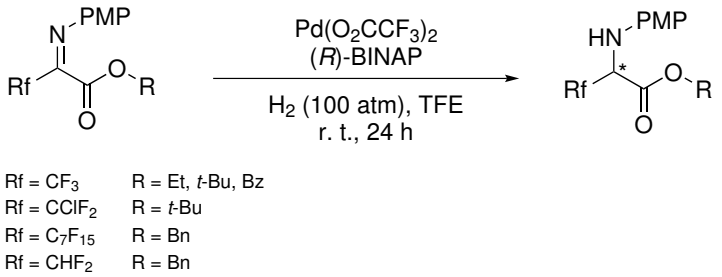


I18 **I19**

Solvent	Conversion (%)	ee (%)
TFE	>95	76.4
EtOH	<5	-
DCE	16	74.4
THF	<5	-

Asymmetric synthesis has grown exponentially over the years. The importance for the synthesis of a single enantiomer comes from need to synthesise chiral drugs in the pharmaceutical industry. Such drugs exhibit different pharmacological effect than their homochiral and racemic forms. The catalytic asymmetric synthesis of fluorinated amino acids is an area of immense interest. One of the most promising routes for the production of chiral centres of α-amino acids is enantio-selective reduction of the imino moiety [36]. An example of the asymmetric hydrogenation of acyclic fluorinated iminoesters catalysed by palladium(II) trifluoroacetate and BINAP complex is shown in Scheme 1.9. The yield and enantio-selectivity were dramatically improved by use of fluorinated alcohol as a solvent, which afforded chiral β-fluorinated α-amino acid derivatives as a products (Scheme 1.9). In other solvents, α-aminoesters were formed in low to moderate yields as well as with low ee. In nucleophilic solvents such as ethanol and methanol the attack of the solvent molecule on imino carbon-atom forming α-alkoxylated aminoesters took place. A decrease of ee in HFIP is explained by racemization. Just by stirring the product in HFIP racemization occurred. It is suggested that hydrogen bond forms between the hydride metal complex and the fluorinated alcohol. Therefore, TFE weakly coordinates to palladium and is easily replaced by fluorinated imines. An additional influence of TFE is to protonate or form

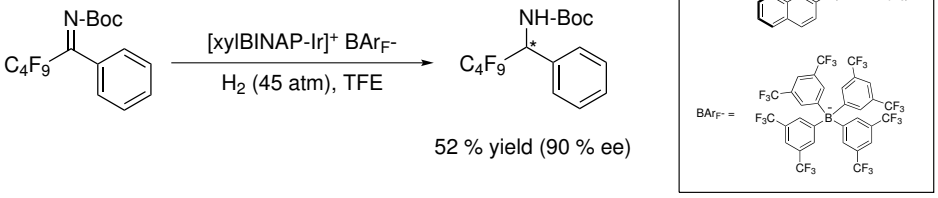
hydrogen bonds with the N-atom of the imine group [37].



Rf = CF_3 R = Et, *t*-Bu, Bz
Rf = $CClF_2$ R = *t*-Bu
Rf = C_7F_{15} R = Bn
Rf = CHF_2 R = Bn

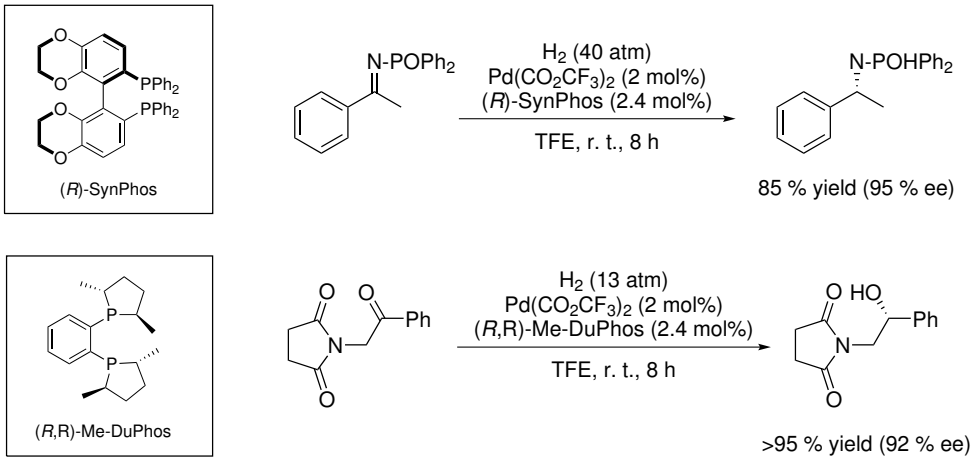
Scheme 1.9: Asymmetric hydrogenation of α-fluorinated iminoesters.

Two examples of asymmetric catalytic reduction of imino group are the synthesis of fluoroalkyl amines by Mikami *et al.* [38] and non-fluorinated amines by Zhou *et al.* [35], [39], [40]. The first reaction was performed in the presence of an iridium complex with BINAP (Scheme 1.10). In the fluorinated solvent (TFE) a massive increase in the enantiomeric selectivity was observed, while the yield was comparable to the reaction performed in DCM. Hydrogen bonds between TFE and the perfluoroalkyl group of imine stabilize the geometry of the imine and prevent its isomerization [38].



Scheme 1.10: Asymetric synthesis of fluoroalky amines.

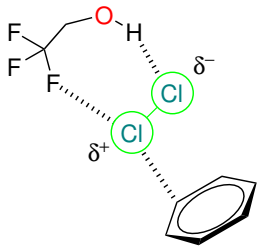
Second reaction, reduction of non-fluorinated imines and fuctionalised ketones, was performed with a palladium catalyst. Only the reaction in TFE was effective in terms of conversion and enantio-selectivety (Scheme 1.11) [36].



Scheme 1.11: Hydrogenation of imines and functionalised ketones.

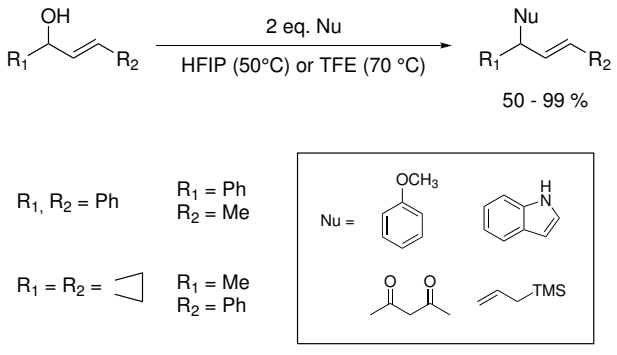
1.2.2.3 Carbon-heteroatom bond formation

Oxidative chlorination is a method of chlorination where the active chlorinating reagent is formed *in situ* by oxidation to obtain HOCl and/or Cl_2. These oxidized species can be used *in situ* for electrophilic halogenation with substrates such as arenes, resulting in the creation of a general and green method for halogenation by using a HCl/H_2O_2 mixture. It was found that TFE catalyses the chlorination of arenes by complementary charge template stabilization [41]. This is similar to epoxidation with H_2O_2 in perfluorinated alcohols. To quantify and determine the effect of TFE on aromatic chlorination Ben-Daniel *et al.* [41] performed reactions in TFE and its non-fluorinated analogue EtOH and four major differences between performing reaction in EtOH or TFE were observed. The first difference is seen in the reaction rates for halogenation. For TFE the reaction rates are essentially the same for anisole as for toluene. The second difference was the chlorination rate of anisole. In TFE it was twice as fast compared to EtOH. The reaction rate for toluene chlorination in TFE increased by three orders of magnitude. The third difference was observed for the reaction with a mixture of substrates (anisole and toluene). Under such conditions in TFE only anisole was chlorinated. The fourth major difference is that the chlorination of anisole in EtOH did not proceed beyond 60 %, while it was completed cleanly in TFE. Based on these results, authors proposed that TFE stabilizes the transition state by acting as a charge template catalyst. Therefore, the OH group stabilizes departing Cl^- by donating hydrogen bond with its hydroxy group. At the same time negative fluorine atoms stabilize the positively charged $Cl^{\delta+}$ (Scheme 1.12). EtOH can stabilize the departing Cl^- group as well; however, its interaction with $Cl^{\delta+}$ is repulsive due to the positive charge on hydrogen atoms [41].



Scheme 1.12: Electrophilic aromatic chlorination catalysed by TFE.

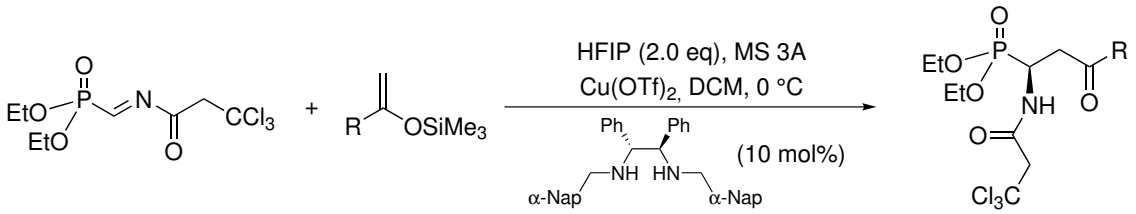
TFE and HFIP were used in metal-free allylic substitution on allylic alcohols (Scheme 1.13). The substitution was made with nitrogen-, silyl- and carbon- nucleophiles. High yields were obtained when (*E*)-1,3-diphenylprop-2-en-1-ol was used as a substrate with a wide range of nucleophiles. Moderate yields were obtained with other substrates [42].



Scheme 1.13: Allylic substitution of alcohols with nucleophiles.

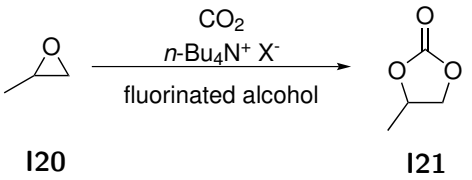
Fluorinated alcohols were used as a catalyst for other types of reactions, such as ring-opening polymerization [43], metal-free *syn*-dihydroxylation of alkenes [44], oxidative hydroxyilation of boronic acid [45], and the formation of N- and O-heterocycles [46], [47]. In the synthesis of α-acyoxy carbonyls fluorinated alcohols stabilized diazoester compounds and made it possible for the reaction to be done under mild conditions, with no additional catalyst [48].

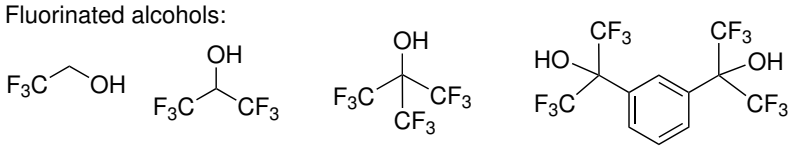
In the synthesis of α-Aminophosphonates from silylenolates and N-acyl-α-iminophosphonates catalysed by chiral copper(II) complex the reaction proceeded smoothly, but with poor enantiomer selectivity. α-aminophosphonate is a strong Lewis base and the release of the Cu catalyst was too slow and the background reaction took place in the absence of a catalyst. HFIP was added to the reaction mixture, which improved the overall yield and enantio-selectivity (>87 ee). The role of HFIP in the reaction was to release the copper catalyst from the product α-aminophosphonate (Scheme 1.14) [49].



Scheme 1.14: Asymetric synthesis of α-aminophosphates.

1.2.2.3.1 Fixation of carbon dioxide Fluorinated alcohols were used as hydrogen bond donors for the fixation of CO_2 onto epoxides forming cyclic carbonates (Scheme 1.15) [8], [50]. Different fluorinated alcohols were used, differentiated by the number of CF_3 groups in their structure. Reactions were performed with stoichiometric amounts in combination with onium organocatalytic salt. Among the different fluorinated alcohols studied, high activity was observed with 1,3-bis(2-hydroxyhexafluoroisopropanol)benzen. The reaction could be performed either under 80 bar with its completion in 30 min or under atmospheric pressure where 10 h were needed for the reaction to be completed [8]. Good conversion was obtained using tetrabutylammonium bromide as co-catalyst. The reaction was carried out under a pressure of 2 MPa, however heating to 60 °C was needed [50].





Scheme 1.15: Coupling of carbon dioxide and epoxide.

A mechanistic insight into the role of fluorinated alcohols in the formation of cyclic car-

bonates was gained using DFT calculations. It was revealed that trifluoromethyl groups significantly improve the stabilization of the transition state and intermediates compared to classical (multi)phenolic activators. Trifluoromethyl groups influence the charge distribution of hydrogen bond donors and strengthen the hydrogen-bond interactions. A correlation between the trifluoromethyl groups and the Gibbs energy was observed. Fluorinated alcohols containing a large number of trifluoromehyl groups strengthen their hydrogen donor ability, leading to better stabilization of intermediates and transition states through hydrogen bonding. Consequently the transition state has a lower Gibbs energy [51].

1.2.2.4 Carbon–carbon bond formation

To create larger organic molecules from smaller structural units new C–C bonds have to be formed. Usually organometallic reagents are used for such a reactions. Most renowned and often used are the Grignard reagent and Suzuki, Heck and Negishi coupling became one of the most important tools in organic chemistry (Figure 1.10) [52]. The last three were awarded a Nobel Prize in Chemistry in 2010 for: "Palladium-catalysed cross coupling in organic chemistry".

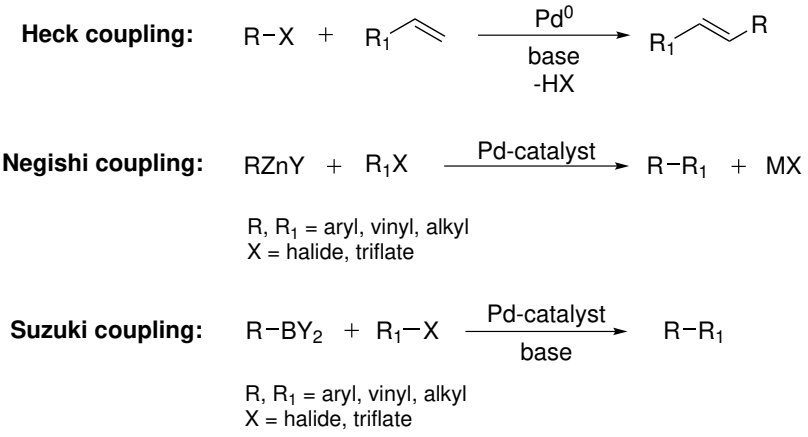
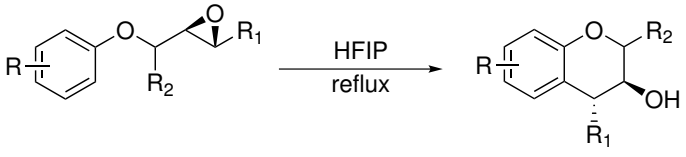


Figure 1.10: 2010 Nobel prize winning Pd-catalysed cross coupling.

Organometallic reagents can be used for the preparation of wide variety of substrates. For specific types of molecules there is a diverse selection of other methods. Few of them use the promoting effect of fluorinated alcohols to proceed. Such a subtype is the Friedel-Craft alkylation of arenes from epoxides (Scheme 1.16). The substrate is refluxed in HFIP and the product is obtained in 5–60 min. No additional catalyst or reagents are needed [53].

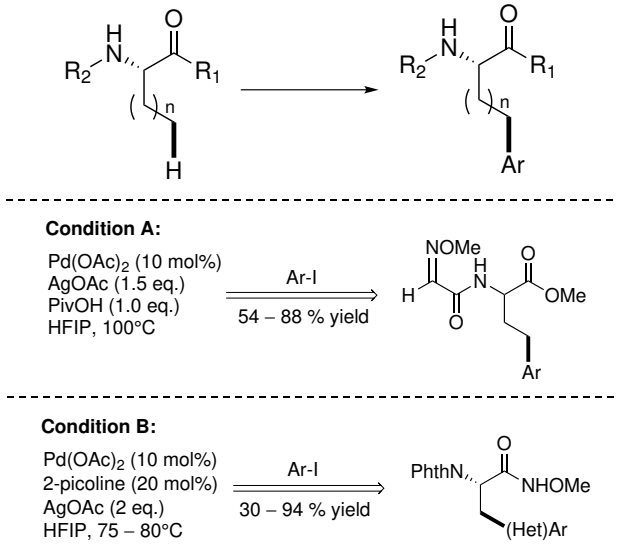


Scheme 1.16: Friedel-Crafts intermolekular cyclialkyliation promoted by HFIP.

The formation of smaller rings such as cyclopropanol from alkenes is done with the $Cu(OTf)_2$/ HFIP system. The method could be used on terminal and cyclic alkenes. The strong hydrogen bond donor ability of HFIP promoted formation of product. With HFIP as solvent dimerization of ethyldiazoacetate (EDA) is limited (<10 %). Also, there was no formation of a solvent inclusion product due to the low nucleophilicity of HFIP [54]. For the synthesis

of heterocycles such as indeno[1,2-*b*]pyridine derivatives [55] TFE was used instead of a metal catalyst. Special properties of fluorinated alcohohols were used for the introduction of a propyl group to the synthesis of 2-propylquinolines [56]. An additional method of alkylation is the formation of tris(indoly)methanes. By using HFIP there was no need to use acids or metal catalysts [34]. In most cases HFIP has a stronger catalytic effect than TFE, although it was opposite in asymmetric α-alkylation between aldehydes and alcohols. For the stereoselective formation of the product an additional secondary chiral amine was added. After $NaBH_4$ reduction enantioriched functionalised primary alcohols were obtained with excellent enantio-selectivity [57].

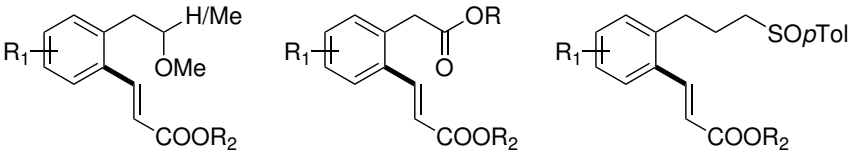
1.2.2.4.1 C–H functionalizations Direct metallation of the C(sp^3)–H is very challenging. A major step forward in the field of C(sp^3)–H activation was achieved by utilizing the potential of a bidentate directing group to enhance such coupling. The bidante directing group induced coupling is tolerant to a wide range of solvents. However, Fernández-Ibáñe and Carretero [58], Ma [59] and Yu [60] have independently observed an additional boost of reactivity by using HFIP. Through strong hydrogen bond donor ability, fluorinated alcohols interact with the directing group of the substrate and accommodate their coordinating properties. The coordinating character of the fluorinated alcohols aids in the controlled assembly of well-defined pre-transition states, therefore it enhancing optimal site- and stereoselectivity. Additionally, fluorinated alcohols act as auxiliary ligand to coordinate Pd-species and stabilize electrophilic catalytic species. In aliphatic substrates, amine ((*N*-2-pyridyl)sulfonyl or 2-methoxyiminoacetyl auxiliaries) or the carboxylate motif was the directing group in the Pd-catalysed direct arylation. The reaction proceeded efficiently in HFIP, while low yields are obtained with traditional solvents (Scheme 1.17) [61].



Scheme 1.17: HFIP in aliphatic C(sp^3)–H bond activation.

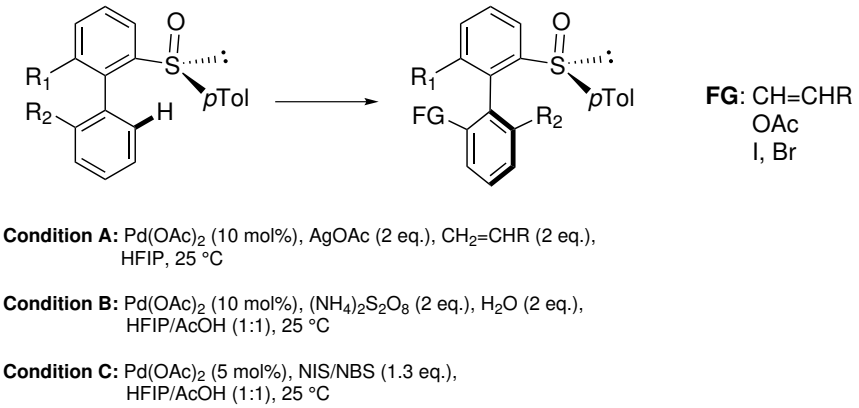
For a long time the *ortho*-functionalisation of the aromatic substrates was possible only by having a coordinating group attached directly to the aromatic ring. The coordinating group accommodated relatively stable, five-membered metallacyclic intermediates during a key step of C–H activation. Using distal directing groups which generate larger metallacyclic intermediates is a considerable synthetic challenge. To develop such transformations, overcoming high entropic barrier was needed due to the presence of freely rotating sp^3 carbon centre between the aromatic ring and the directing group. It was established that such distal C–H functionalisations were possible in HFIP or TFE. Fluorinated alcohols are unique

in their ability to support the *ortho*-olefination of arenes through weakly coordinating distal directing group. Choosing HFIP as solvent has immense value if the reaction occurs *via* a Pd(II)/Pd(IV) (arylation, iodination, acetoxylation), but oxidative Heck reaction following Pd(II)/Pd(0) path works better with *tert*-amyl alcohol (Scheme 1.18) [61].



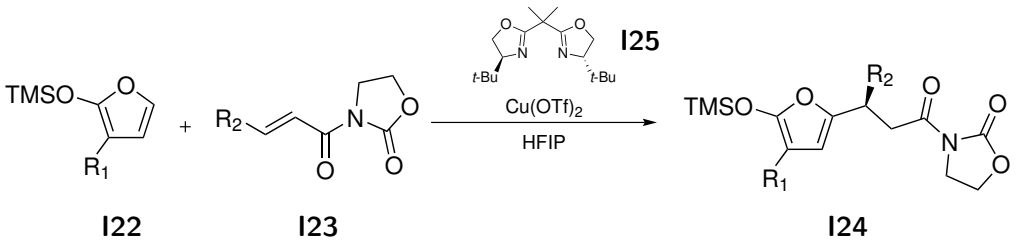
Scheme 1.18: Examples of products formed by different distal directing groups for C–H arene activation.

Fluorinated solvents efficiently control the chiral induction on biaryl substrates with a sulfoxide moiety as a directing group. The chiral auxiliaries were subjected to direct iodination, acetoxylation and olefination. By using fluorinated solvents the desired transformation was performed under mild conditions (Scheme 1.19) [61].



Scheme 1.19: Sulfoxide directed atropodiastereoselective direct functionalizations induced by HFIP.

In Michael the highly enantioselective addition of 2-(trimethylsilyloxy)furans (**I22**) to acrylate (**I23**) with copper(II) trifluoromethanesulfonate/*S,S*-*t*-Bu-box (**I25**) as a catalyst HFIP was essential for achieving a high yield (Scheme 1.20) [10].

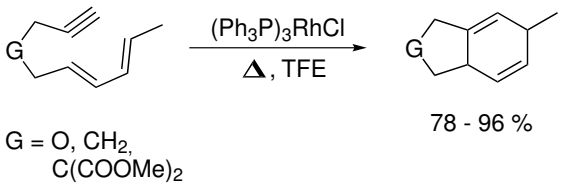


Scheme 1.20: Enantioselective Mukayama-Micheal addition.

HFIP has also a positive effect in a asymmetric Micheal addition catalysed by a lanthanum-linked-BINOL complex. The authors suggested HFIP acts as a proton source and assists in the dissociation of the product from the lanthanum complex. A positive effect was also observed in NH-linked-BINOL ligands [10].

1.2.2.5 Cycloadditions

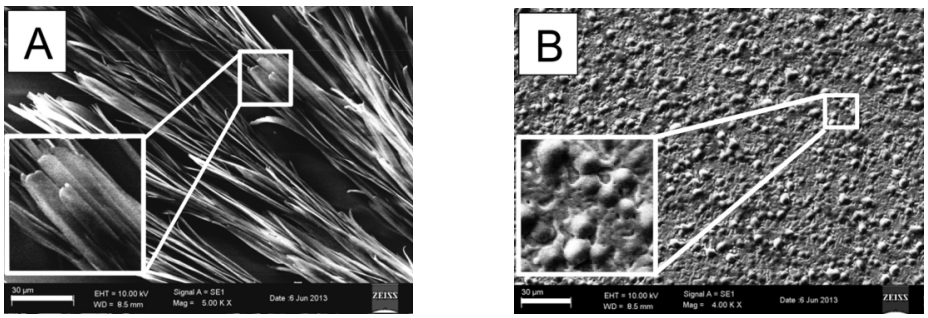
Diels-Alder reactions are a very powerful tool for the stereoselective formation of rings. The [4+2] Diels-Alder reaction is one of the most widely utilized methods for the formation of six-membered rings [62]. Many of Diels-Alder reactions were gathered in review articles from Shuklov *et al.* [10] and Begue *et al.* [13]. An example of this type of reaction is the rhodium-catalysed intramolecular alkyne-diene [4+2] cycloaddition performed with Wilkinson's catalyst-$(PPh_3)_3RhCl$ in mild conditions (Scheme 1.21). The reaction rate was much higher in TFE compared to other solvent, while authors did not provide explanation for such activation [62]. A rhodium catalyst, $[Rh(CO)_2Cl]_2$, was used in the Pausen-Khand reaction ([2+2+1] cycloaddition). The catalyst was most active in TFE as a solvent or in DCE containing 14 equivalents of phenol. TFE is hypothesised to protonate CO in cycloaddition with diene-allenes [63].



Scheme 1.21: Rh(I) catalysed [4+2] cycloaddition in TFE.

1.2.2.6 Use in biochemistry

Alcohol-based cosolvents (such as TFE) were used from the middle of the 20th century to denature proteins and to stabilize the structures of peptides. A special beneficial effect of fluorinated alcohols is to support the formation of the helix conformation of proteins [11], [64]. Fluorinated alcohols (TFE and HFIP) induce the self-assembly of simple aromatic dipeptide L-Tyr-L-Phe (YF). Surface morphology is formed during the evaporation of the solvent and it is solvent dependent. The self-assembled YF structure in the HFIP solvent consists of microribbons (Figure 1.11 (a)). Individual microribbons are assembled in a flower-bouquet-like arrangement. Self-assembled YF structures in TFE form microspeheres (Figure 1.11 (b)). Structures from HFIP showed strong birefringence under polarized light. This means they have a well-defined order structure, crystalline in nature. In contrast no birefringence was observed for the microsphere obtained from TFE solutions. The different structures are a consequence of TFE and HFIP having different modes of interaction with smaller peptides, thereby they induce different conformations [65].



(a) YF microribbons obtained from HFIP (b) YF microspheres obtained from TFE

Figure 1.11: SEM images of self-assembled L-Tyr-L-Phe (YF) structures.

Chapter 2

Aim of the thesis

The objective of this thesis was to find an alternative way to activate nitric acid and its low valent analogues to act as reagents or as catalysts. Classical activators of nitric acid are acids or modern noble metal catalysts. An alternative way of activation for nitric acid is the use of organic catalysis. Organic catalysis is a rapidly growing area of research that was inspired by the action of enzymes. Initially, there was a prevalent idea that an organic catalyst needs to be big in size in order to be effective (similar to enzymes). This notion become obsolete with the forthcoming discoveries of effective catalysts with a low molecular weight. Fluorinated alcohols came to our attention with their unique nature of activation of epoxidation, oxychlorination and Bayer-Villiger oxidation. Having a strong hydrogen bond donor ability, forming strong interactions with nucleophiles while having weak interactions with electrophiles and the trait to form large clusters makes them outstanding media for a wide range of reactions (from oxidation and reduction to C–C bond formation). However, the mechanism behind their boosting properties was mostly not investigated. An exception to this was oxidation reactions with H_2O_2 (epoxidations and Bayer-Villiger reaction) where fluorinated alcohols were identified as template catalysts. We anticipated a similar interaction as was observed between fluorinated alcohol and H_2O_2 can be obtained with HNO_3.

Research in this thesis is divided into three sections. The first part is a study on the activation of nitric acid by fluorinated alcohols on aromatic nitration as a model reaction. The strength of the activation by solvent will be further compared to a classical activation using the mixed acids method (HNO_3/H_2SO_4). To explain the mechanism of nitration in fluorinated alcohols reaction will be performed with 1,3-dimethoxybenzene derivatives where unusual side products are formed. For a study of the mechanism different techniques will be employed, such as ATR-IR, NMR, EPR and DFT calculations. The environmental potential of nitration will be evaluated by calculating the green metrics (atom economy, E-factor, etc.) for our methods and the literature methods.

The second part of the thesis will be a study of the use of activated nitric acid to activate oxidation. Nitric acid will be used as a catalyst for the aerobic oxidation of alcohols. In the case that an additional activation will be needed a metal co-catalyst will be explored. As a co-catalyst a simple iron and copper salt will be explored.

In the final part the research will be expanded on another type of electrophilic reaction, such as halogenation. To prepare the halogenating reagent, catalytic oxidation will be used. In a collaboration with Martín-Matute's group, at Stockholm University, α-haloketones will be prepared from allylic alcohols using a tandem 1,3-hydrogen shift/halogenation.

Chapter 3

Materials and methods

Reagents and solvents
Compounds, reagents and solvents were obtained from commercial sources (Sigma Aldrich, Fluorochem, Merck, Fluka, Alfa Aesar). All reagents were used as obtained with no additional purifying.

TLC chromatography
For TLC analysis 0.2 mm Silica gel on aluminium plate Silica gel/TLC-cards DC-Alufolien-Kieselgel were used from the Fluka distributer. TLC stains were visualised using a UV lamp with 366 nm or a potassium permanganate solution followed by heating the plate. A solution of potassium permanganate was prepared by dissolving 1.5 g $KMnO_4$, 10 g K_2CO_3 and 1.25 mL 10 NaOH in 200 mL of deionized water.

Column chromatography
For stationary phase silica gel Kiselgel 60 was used, obtained from Fluka with a particle size 0.063-0.2 mm.

Infra-red spectroscopy
IR spectra were measured on a Perkin Elmer spectrophotometer Spectrum 400 (FT/IR/FT/FIR Spectrophotometer). Real time measurement of IR spectra of reaction was performed with ATR IR probe ReactIR^{TM} 45 on Easymax 102 Mettler-Toleda reactor.

Nuclear magnetic resonance (NMR)
^{1}H and ^{13}C NMR spectra were measured at the National Institute of Chemistry (Slovenian NMR centre) on Varian Inova 300 spectrometer (300 MHz) at 25 ℃. For ^{1}H spectra measured in $CDCl_3$, TMS was used as internal standard. For ^{13}C NMR spectra $CDCl_3$ was used as standard (77.0 ppm).

X-ray structural analysis
Single-crystal X-ray diffraction data were collected on an Agilent New Gemini, Dual, diffractometer equipped with an Atlas CCD area detector using graphite-monochromatised Cu $K\alpha$ radiation (1.54184 Å). During the data collection a crystal mounted on a glass fibre was kept at 150 K by a cold nitrogen stream. *CrysAlisPro* [66] software was used for the data collection and data reduction. Using *Olex2* [67], the crystal structure was solved with the *ShelXT* [68] structure solution program and refined by least-squares minimisation with a 2016/6 version of *ShelXL* [69]. The figure of the crystal structure was prepared with the program *DIAMOND* [70]

Mass spectroscopy
Mass spectra (ESI) and HR-MS were made on Q-TOF Premier from Water-Micromass producer at Center for mass spectrometry at the Jožef Stefan Institute.

Melting point
Measurement of the melting point was performed in a glass capillary at the Jožef Stefan Institute with Buchi Melting Point M-560 and at Faculty of Chemistry and Chemical Technology, University of Ljubljana with microscope Leica Galen III.

Synthesis of iodine(I) reagents
For the purposes of synthesis of iodine(I) reagents (HIX_2 and $N(CH_3)_3IX_2$; X = Cl, Br) we followed the instructions of the original article [71].

$HICl_2$
127 mg of finely powdered iodine was placed into a flask and dissolved in 1 mL of TFE or HFIP. To this solution 2.0 mmol of 37 % HCl (176.5 μL) and 34 μL H_2O_2 (50 %, 0.6 mmol). After 1 h the reaction was complete. The solvent was removed under reduced pressure.

$HIBr_2$
127 mg of finely powdered iodine was placed into a flask. To this we added 48 % HBr (2.0 mmol, 230 μL) and 34 μL H_2O_2 (50 %, 0.6 mmol). The reaction was complete in 5 min with no more solid iodine present.

$N(CH_3)_4IX_2$
1.0 mmol of HIX_2 (X = Br, Cl) was dissolved in 1 mL of MeCN, followed by the addition of $N(CH_3)_4X$ (X = Br, Cl). The reaction was stopped when the reaction mixture became homogeneous. The solvent was removed under reduced pressure.

Chapter 4

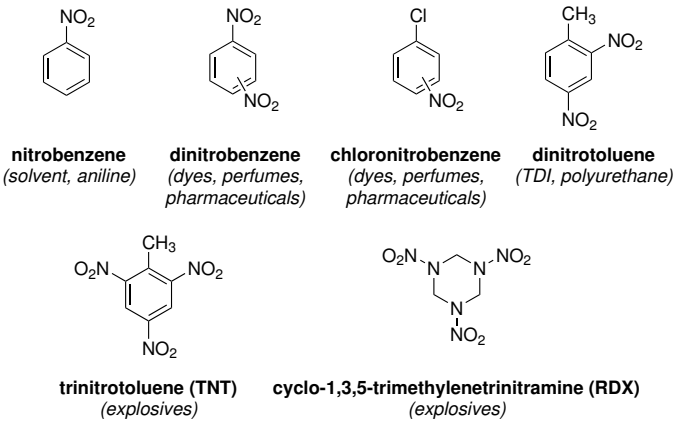
Results and discussion

4.1 Aromatic nitration

4.1.1 Introduction

The first aromatic compounds were obtained by Mitscherlich in 1834 when he treated hydrocarbons obtained from coal tar with fuming nitric acid [72]. The classical or traditional nitration is made by the addition of a strong acid (usually concentrated sulphuric acid) to nitric acid. This mixed acid nitration is the most common method for the nitration of aromatics. On an industrial scale it was first used in 1847 [73] and it is still used today. Aromatic nitration continues to have immense importance in industrial processes. The most known use of nitrated aromatic compounds are explosives, however in much bigger amounts nitrated compounds are used as key intermediates for the preparation of a lot of versatile materials such as polyurethanes, polyamides, pharmaceuticals, dyes, perfumes, plastics and complex target molecules.

Nitrobenzene is the most important nitrated chemical produced on a large scale. It is used as a processing solvent. However, more than 95 % of nitrobenzene is converted to aniline which has hundreds of downstream products [72]. Dinitrobenzene and nitrochlorobenzenes are used as intermediates for the synthesis of dyes, pharmaceuticals and perfumes. Dinitrotoluenes are converted into toluene diisocyanates (TDI) for the manufacture of polyurethanes. Acid catalysed nitrations are also used to manufacture high explosives such as trinitrotoluene (TNT), glyceryl trinitrate (nitrogylcerin), cellulose nitrate, 1,3,5-trinitroperhydro-1,3,5-triazine (RDX) and related nitramines [73] (Scheme 4.1).



Scheme 4.1: Most common nitrocompounds and their use.

The versatile use and importance of nitroarenes comes from their simple synthesis as well as their use as building blocks for further transformation into a wide range of substrates with different functional groups [74] (Figure 4.1).

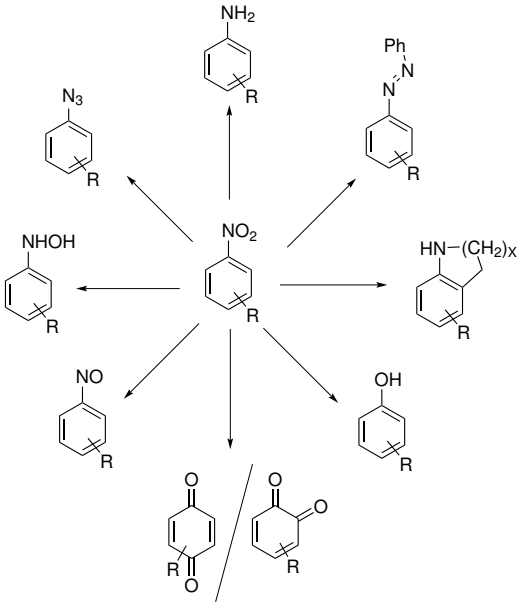


Figure 4.1: Most common transformations of nitro group.

Nitration is divided into three sections *electrophilic*, *nucleophilic* and *free radical* nitration [73]. The broadest and at the same time the most researched nitration is electrophilic nitration. Classical nitration is the most used electrophilic nitration. In classical nitration sulphuric acid is added to rapidly ionize HNO_3 to nitronium ion (NO_2^+) (Scheme 4.2). The nitronium ion is a reactive *species* that acts as a nitrating agent in reactions with hydrocarbons. Usually 2 eq. of H_2SO_4 are added to HNO_3. The first equivalent is needed to ionize nitric acid to a nitronium ion. The second equivalent reacts with a water molecule, formed in first step, which prevents the dilution of acids. In a typical nitration either substrates are added to sulphuric acid followed by the addition of mixture of HNO_3/H_2SO_4 or substrates are added to a mixture of HNO_3/H_2SO_4. The reactions are highly exothermic, which can cause local overheating. Local overheating is a primary cause for side reactions and is a major safety concern [75]. The disadvantages of the classical method are the use of corrosive reagents, the generation of toxic nitrogen oxide fumes (NO_x) and large quantities of waste acids [76]. New, environmentally friendly methods are desired with a high regioselectivity (control of ortho and para substitutions) and the elimination of waste [74] following guidelines from Green chemistry [77].

$$HNO_3 + H_2SO_4 \rightleftharpoons NO_2^+ + HSO_4^- + H_2O$$

$$H_2O + H_2SO_4 \rightleftharpoons H_3O^+ + HSO_4^-$$

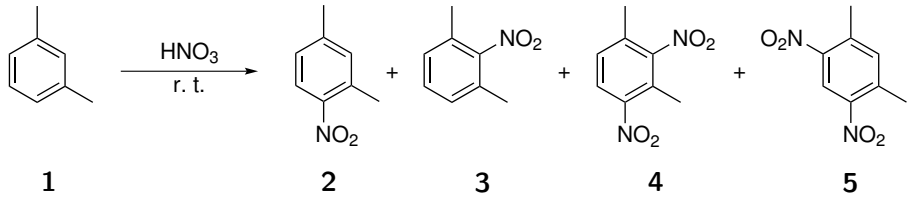
Scheme 4.2: Formation of nitronium ion in mixed acids method.

The successful use of fluorinated alcohols (TFE, HFIP) as a template catalyst in electrophilic reactions such as epoxidation [21], [24], [25], [78], Bayer-Viliger reaction [24], [28] and oxidative electrophilic chlorination [41] led us to believe that they can also be used as the activators of the most renowned electrophilic reaction – aromatic nitration with nitric acid.

4.1.2 Activation of nitric acid under template catalysis

First, we investigated the strength of the activation of nitric acid in fluorinated solvents in comparison with the classical method (sulphuric acid as reaction media). HFIP and TFE were chosen as the most common fluorinated alcohols and commercially available ones. The second most often used reagents for aromatic nitration are acyl nitrites. Amongst them, trifluoroacetyl nitrite is commonly used as a strong nitrating reagent. It is synthesised by a reaction between trifluoroacetanhydride (TFAA) and HNO_3 [76], [79], [80]. As a side product, trifluoroacetic acid (TFA) is formed. This prompted us to investigate and determine whether TFA by itself can activate aromatic nitration.

To compare the reactivity of nitration 1,3-dimethylbenzene (**1**) was chosen as a model substrate (Scheme 4.3). 65 % HNO_3 was used as a nitrating reagent. Its benefits as a reagent are low cost, availability and the formation of water as a side product. At the beginning of our research we investigated the effect of the amount of H_2SO_4 on the conversion as well as the selectivity of the reaction (Figure 4.2). We added 1 mmol of **1**, followed by the addition of the corresponding amount of H_2SO_4 and 1 mmol of HNO_3. The reaction was stirred at room temperature and aliquots were taken at defined time intervals. After micro isolation the aliquotes were analysed with gas chromatography. In line with expectations, increasing the amount of the H_2SO_4 led to higher conversion. However, the yield of **2** started to decrease when more than 2 equiv. of H_2SO_4 were used (Figure 4.3). This was due to further nitration of mono-nitrated products (**2** and **3**), which led to the formation of dinitrated substrates 2,4-dinitro-*m*-xylene (**4**) and 4,6-dinitro-*m*-xylene (**5**).



Scheme 4.3: Nitration of *m*-xylene.

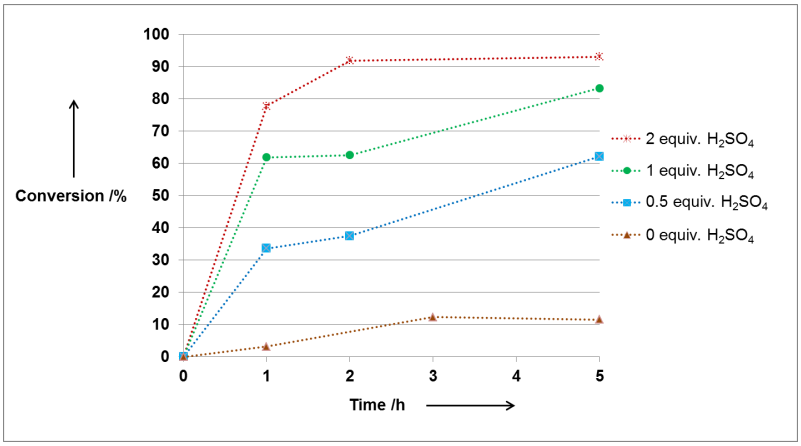


Figure 4.2: Nitration of *m*-xylene (**1**) with different amounts of H_2SO_4.

To improve the selectivity of the classical system, the same nitration in 2 equiv. of H_2SO_4 was also performed in MeCN (Figure 4.4). The conversion was substantially lower, however dinitrated products were not present in the reaction mixture. Fluorinated solvents differentiated among themselves in their activation of HNO_3 for aromatic nitration (Figure 4.4).

TFE was the weakest activator and only trace amounts of product **2** were obtained. Although it seems TFE does not activate HNO_3 for aromatic nitration, its weak activation was observed in substrates with an electron donor group attached to the aromatic ring (*vide infra*). The activation of HNO_3 by HFIP was more pronounced and the nitration with HNO_3 proceeded similarly to a classical system with 1 eq. of H_2SO_4. The biggest difference was observed in the selectivity for **2**, which was the highest in HFIP among all the methods we studied and the ratio **2**:**3** was 10:1 (Figure 4.3). In all other systems the ratio of **2**:**3** was around 5.7:1. The highest conversion was obtained with TFA as a solvent. Under such conditions the reaction was complete in 5 h. In all reactions in fluorinated alcohols no over-nitration was observed.

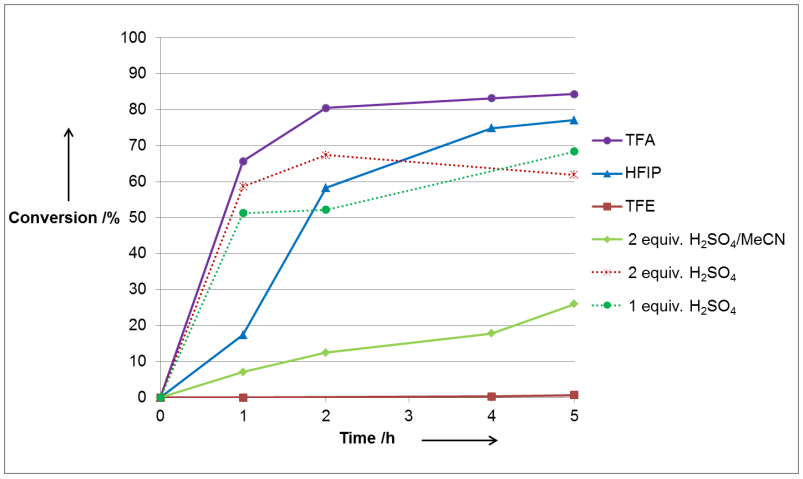


Figure 4.3: Conversion of **1** into **2** in various solvents.

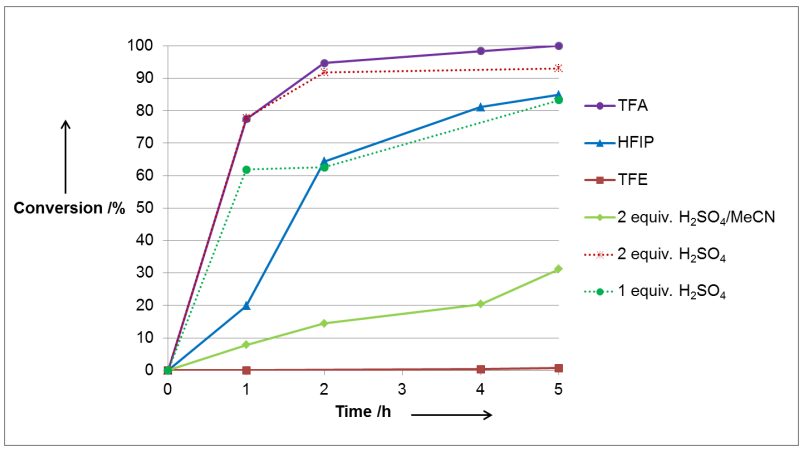


Figure 4.4: Comparison of overall conversion between classical system and fluorinated solvents for nitration of *m*-xylene (**1**).

To gain a deeper insight into the effect of fluorinated solvents, nitration of **1** with 65 % HNO_3 was performed in other solvents. No conversion was obtained in 24 h of nitration of **1** in MeCN and EtOH. In DCM, only a trace amount of product was obtained after 24 h. The highest conversion was obtained in *n*-Hex with 12 % conversion after 24 h. Solvent-free conditions (65 % HNO_3 and no additional catalyst) gave a similar result with 12 % conversion but after 5 h. Low yields of nitration obtained with 65 % HNO_3 in solvents are in agreement with the literature data where it is reported that the rate of reaction strongly depends on the concentration of nitronium ion [81]. In diluted systems it is difficult to form

NO_2^+ and nitration does not proceed. Therefore, the results with HFIP indicate strong activation by the solvent itself. Berkessel *et al.* [22] observed an increase of conversion when there was solvent/substrate ratio of 12. This prompted us to investigate if such a correlation can be observed also for aromatic nitration in fluorinated alcohols. Since reactivity in TFE was low we focused on HFIP. We repeated experiments with **1** and varied the amounts of solvent. After 5 h at room temperature the reaction was stopped. After isolation the reaction mixture was analysed with ^{1}H NMR. The conversion initially increases with a higher ratio of solvent/substrate (Figure 4.5). The highest conversion was obtained when the solvent/substrate ratio was 10, with almost 100 % conversion. An additional increase of solvent/substrate ratio led to a decrease in conversion. The ratio between solvent/substrate did not only influence the conversion, but also influenced the selectivity of the reaction (Figure 4.6). At low amounts of HFIP, 2,6-dimethyl-nitrobenzene (**3**) was dominantly formed. An increase of the solvent/substrate led to a change in selectivity and 2,4-dimethyl-nitrobenzene (**2**) was the major product. In a 10 M reaction mixture, selectivity **2**:**3** was 35:65, while in a reaction with a 0.2 M reaction mixture ($n_{\mathrm{HFIP}}/n_{\mathrm{substrate}}$ = 47) the **2**:**3** ratio was 87:13.

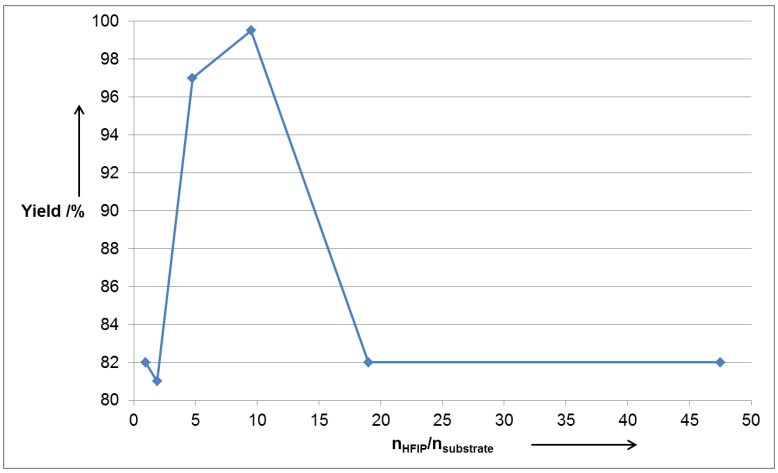


Figure 4.5: Yield in dependence to solvent/substrate ratio at nitration of *m*-xylene (**1**).

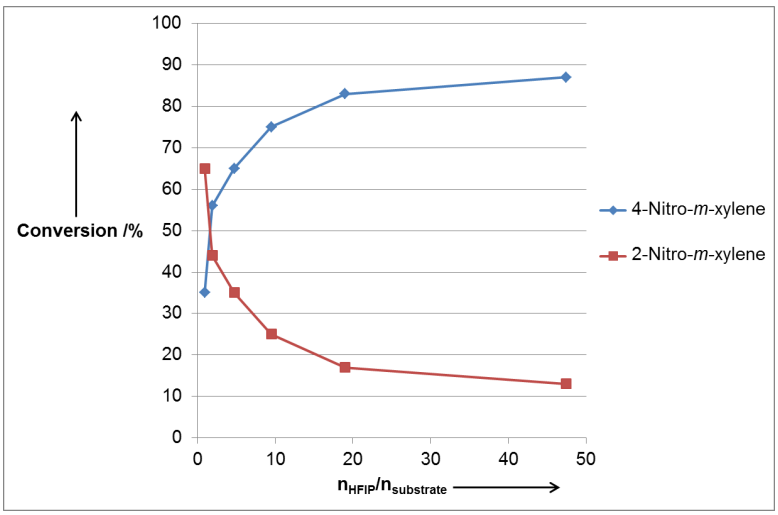
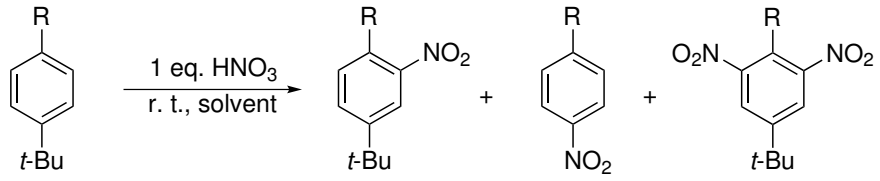


Figure 4.6: Change of selectivity of nitration of *m*-xylene depending on solvent/substrate ratio.

4.1.3 Substrate scope

With an initial study of the effect of reaction parameters on the nitration of *m*-xylene in hand, we expanded our scope to other substrates. For the purposes of a better evaluation, a comparison was made with classical nitration method with 2 eq. H_2SO_4. In a typical reaction all the starting compounds were mixed in an appropriate solvent and stirred at room temperature. The reaction was followed by TLC. After the reaction, the reaction mixture was isolated by classical biphasic extraction and analysed by NMR spectroscopy. For highly reactive substrates with electron donor group attached to an aromatic ring over-nitration represents a major problem. Therefore, classical nitration was performed in a solvent (MeCN) where better results were obtained, as it decreased the over-nitration.

Table 4.1: Aromatic nitration of substrates with activated aromatic ring.[a]



6a - 8a **6b - 8b** **6c - 8c** **6d**

Entry	R	H_2SO_4 [eq.]	Solvent	Time [h]	Yield [%]	Selectivity		
						2-NO_2	4-NO_2	2,6-NO_2
1	OH	2	MeCN	2	93	70	28	2
2	OH	0	TFE	2	95	88	12	-
3	OH	0	HFIP	2	>99	80 (48)	14 (12)	6 (6)
4	OMe	2	MeCN	7	92	74	26	-
5	OMe	0	TFE	7	98	72	28	-
6	OMe	0	HFIP	7	96	73 (67)	27 (27)	-
7	OMe	0	TFA	7	100	75	25	-
8	Me	2	-	6	81	93	7	-
9	Me	0	TFE	6	5	100	-	-
10	Me	0	HFIP	6	74	88	12	-
11	Me	0	TFA	6	90	97 (59)	3 (3)	-

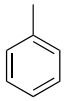
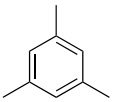
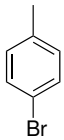
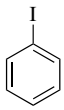
[a] Reaction conditions: 1.0 mmol of substrate, 65 % HNO_3 (1.0 mmol, 69.2 μL), 1 mL of solvent, room temperature. Selectivity and conversion were determined by ^{1}H NMR. Yields in parenthesis represent isolated yield after column chromatography.

High conversions were obtained for all substrates (Table 4.1). Dinitrated products were formed only with 4-*t*-Bu-phenol (**6a**). TFE proved to weakly activate HNO_3 as excellent yields were obtained with both strongly activated substrates, **6a** and 4-*t*-Bu-anisole (**7a**). With 4-*t*-Bu-toluene (**8a**) reaction in TFE had only 5 % conversion. Reactions performed in HFIP gave excellent yields. Even with less activated **8a** a 74 % conversion was obtained. This yield is a very similar to classical nitration with H_2SO_4 where 81 % conversion was obtained. In all cases, the highest conversion was obtained with TFA as a solvent. *Ipso* side products were formed with all three of substrates (**6a**, **7a**, **8a**). This is due to *t*-Bu group being an excellent leaving group in electrophilic substitutions. The formation of *ipso* substituted product was the most prevalent with a substrate **7a** where 26 % of the starting material was converted into the *ipso* product. The reaction with 4-*t*-Bu-aniline

did not proceed in the classical system as well as in fluorinated solvents. No reaction occurred, even if we added HNO_3 in excess amounts (2 eq.). The aniline group is protonated under acid conditions, which deactivates the aromatic system for electrophilic substitution.

We continued our research of aromatic nitration on less-reactive substrates (Table 4.2). As expected from the reaction with **8a**, nitration did not proceed in TFE with these substrates. The only exception was mesitylene (**10a**) where the product **10b** was obtained in a 36 % yield. On other hand, yields obtained in HFIP and TFA were similar or even better than yields obtained in classical nitration. The main difference was in the selectivity of mononitration in fluorinated alcohols, as no dinitrated products were formed. Over nitration was especially problematic in classical nitration with substrates **9a** and **10a**. The best selectivity was obtained for reactions performed in HFIP. It had the lowest formation of 3-nitrotoluene **9** (1 %) and a strong preference for the formation of 4-nitro-1-iodobenzen **12d** (81 %).

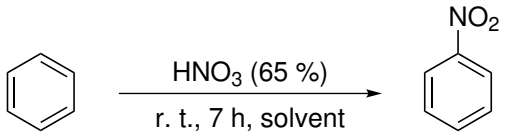
Table 4.2: Aromatic nitration of alkylbenzenes.[a]

Entry	Substrate	H_2SO_4	Solvent	Time [h]	Yield [%]	Selectivity		
						2-NO_2 **(b)**	3-NO_2 **(c)**	4-NO_2 **(d)**
1		2 eq.	-	24	92[b]	53	6	38
2		0	TFE	24	0	-	-	-
3		0	HFIP	23	91	53 (42)	1	46 (38)
4	**9a**	0	TFA	24	94	57	2	42
5		2 eq.	-	7	84[c]	67	-	-
6		0	TFE	7	36	100	-	-
7	**10a**	0	HFIP	7	100	100 (100)	-	-
8		2 eq.	-	7.5	80	65	32	3
9		0	TFE	24	0	-	-	-
10		0	HFIP	24	63	51	38	11
11	**11a**	0	TFA	24	98	57 (50)	35 (32)	8 (7)
12		2 eq.	-	4	94	45	-	55
13		0	TFE	24	1	-	-	100
14		0	HFIP	24	74	19	-	81
15	**12a**	0	TFA	6	100	24 (22)	-	76 (69)

[a] Reaction conditions: 1.0 mmol of substrate, 65 % HNO_3 (1.0 mmol, 69.2 μL), 1 mL of solvent, room temperature. Selectivity and conversion were determined through ^{1}H NMR. Number in parenthesis refers to isolated yield after column chromatography. [b] 3 % 2,4-dinitrotoluene. [c] 33 % 2,6-dinitromesitylene.

Nitration of benzene (**13**, Table 4.3) is of great importance for industry. Complete conversions were obtained for the classical system and the solvent TFA. Although in the classical system traces of dinitrated products were observed. Excellent yield was also obtained in HFIP, however the reaction did not proceed quantitatively.

Table 4.3: Aromatic nitration of benzene.[a]



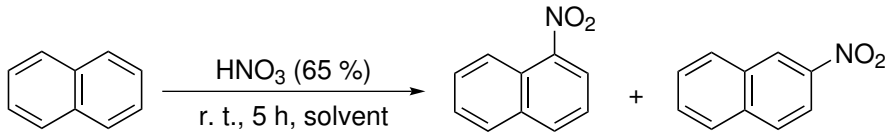
13 **14**

Entry	H_2SO_4 [eq.]	Solvent	Yield [%]
1	2	-	100
2	0	TFE	0
3	0	HFIP	95
4	0	TFA	100 (98)

[a] Reaction conditions: 1.0 mmol of substrate, 65 % HNO_3 (1.0 mmol, 69.2 μL), 1 mL of solvent, room temperature. Selectivity and conversion were determined through ^{1}H NMR. Number in parenthesis refers to isolated yield after column chromatography.

All the methods in the nitration of naphthalene (**15**) had similar results in regard of yield and selectivity (Table 4.4). The lowest yield was obtained with TFE as a solvent where 83 % of **15** was converted into product. Reactions of classical nitration and nitration in TFA and HFIP had 95–96 % conversion. In all of methods **17** was formed as a side product in small amounts (3–5 %).

Table 4.4: Aromatic nitration of naphthalene.[a]



15 **16** **17**

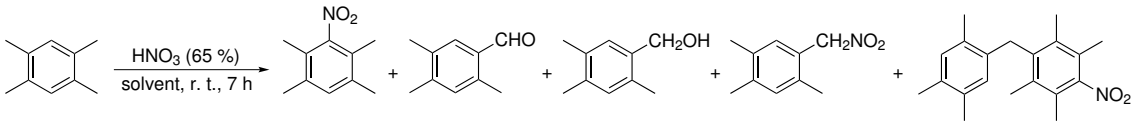
Entry	H_2SO_4	Solvent	Yield [%]	Selectivity	
				16	**17**
1	2	MeCN	96	97	3
2	0	TFE	83	95	5
3	0	HFIP	96	97 (89)	3
4	0	TFA	95	96	4

[a] Reaction conditions: 1.0 mmol of substrate, 65 % HNO_3 (1.0 mmol, 69.2 μL), 1 mL of solvent, room temperature. Selectivity and conversion were determined through ^{1}H NMR. Number in parenthesis refers to isolated yield after column chromatography.

4.1.3.1 Oxidation as a side process

Nitrating reagents, especially HNO_3, are also oxidants. Consequently, oxidation can occur as a side reaction. Reactions were performed as in the previous study. After the isolation, the crude product was analysed by NMR spectroscopy. Products **19**–**23** were separated by column chromatography and the structure determined by comparison with the literature data. The distribution of products in nitration of durene (**18**) was strongly dependent on the method (Table 4.5). For classical nitration, a higher yield was obtained when the reaction was carried out in the solvent MeCN compared to solvent-free conditions (81 % and 31 % respecting). Although the conversion increased by the addition of solvent, the selectivity of reaction was lower and the main product formed was 2,4,5-trimethylbenzaldehyde (**20**). Reaction performed in HFIP had the highest yield and high selectivity for the formation of nitrodurene (**19**). The compound 1,2,4,5-tetramethyl-3-nitro-6-(2,4,5-trimethylbenzyl)benzene (**23**), which was formed in small amount, indicates the possibility of a radical pathway.

Table 4.5: Aromatic nitration of durene.[a]

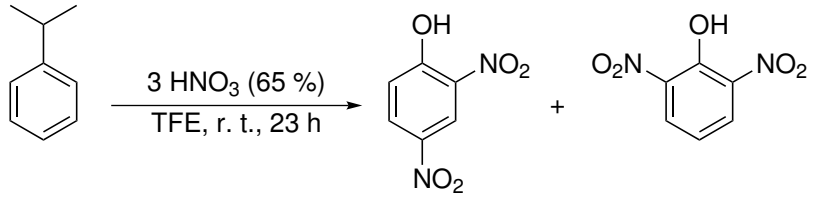


18 **19** **20** **21** **22** **23**

Entry	Solvent	H_2SO_4 [eq.]	Yield [%]	Selectivity				
				19	**20**	**21**	**22**	**23**
1	-	2	31	89	11	0	0	0
2	MeCN	2	81	39	58	0	3	0
3	TFE	0	51	12	36	38	14	0
4	HFIP	0	97	71 (41)	11 (10)	0	9 (7)	8 (1)

[a] Reaction conditions: 1.0 mmol of durene (**18**), 65 % HNO_3 (1.0 mmol, 69.2 μL), 1 mL of solvent, room temperature. Selectivity and conversion were determined through ^{1}H NMR. Number in parenthesis refers to isolated yield after column chromatography.

The formation of phenol was observed as a side product in substrates with a bulky alkyl group, such as *t*-Bu or *i*-Pr, which are good leaving groups. The reaction with isopropylbenzene (**24**) in TFE yielded two products, both after the incorporation of an OH group into the aromatic ring (Scheme 4.4).



24 **25** **26**

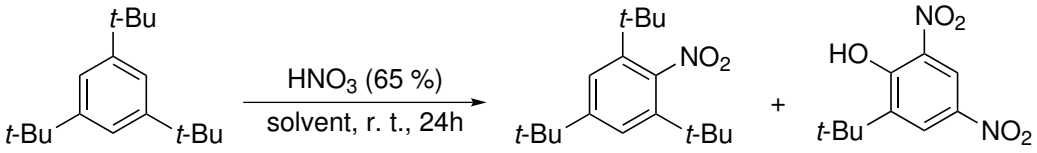
81 % 19 %

Scheme 4.4: Aromatic nitration of isopropylbenzene.

81 % of starting material was converted into 2,4-dinitro-phenol (**25**) and the remaining 19 % was 2,6-dinitro-phenol (**26**). Even for lower amounts of HNO_3 **25** and **26** were the only products formed, albeit at a lower yield. The reaction is similar to the one where phenol is produced from the organic waste.

Nitration of 1,3,5-tri-*t*-butylbenzene (**27**) (Table 4.6) yielded mainly the nitrated product 2-nitro-1,3,5-tri-*t*-butylbenzene (**28**). However, as a side product 5-*t*-butyl-2,3-dinitrophenol (**29**) was formed. In the reaction performed in HFIP a moderate conversion rate was obtained with the substantial formation of **29**. On other hand, for the nitration of **27** in TFA, a high conversion was obtained and an excellent selectivity. 84 % of the starting material was converted into nitrated products, **28** was isolated in 68 % yield and a side product **29** was isolated in a 4 % yield.

Table 4.6: Aromatic nitration of 1,3,5-tri-t-butyl-benzene.[a]



27 **28** **29**

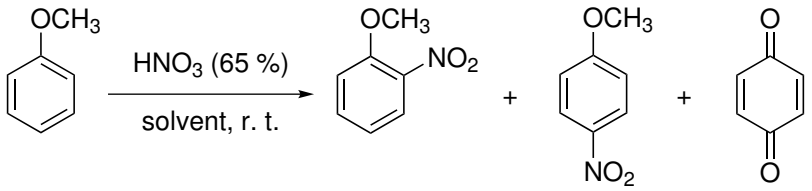
Entry	Solvent	Yield [%]	Selectivity	
			28	**29**
1	HFIP	52	79	21
2	TFA	84	96 (68)	4 (4)

[a] Reaction conditions: 1.0 mmol of 1,3,5-tri-*t*-butylbenzene (**27**), 65 % HNO_3 (1.0 mmol, 69.2 μL), 1 mL of solvent, room temperature. Selectivity and conversion were determined through ^{1}H NMR. Number in parenthesis refers to isolated yield after column chromatography.

Substrates, which already contained oxygen atom in a functional group, are prone to oxidation and quinones could be formed as side products. We have tested two such substrates for nitration – anisole (**30**) and 2-naphtol (**34**).

First, we tried the nitration of anisole (**30** in less activated media, TFE. Nitration proceeded slowly and after 24 h of stirring at room temperature the conversion was 72 %. The main products were both nitrated ones, **31** and **32**, while quinone **33** was formed in a small amount (Table 4.7, entry 1). When the reaction was performed in HFIP a quantitative conversion was achieved in 5 h, although with lower selectivity. In HFIP 15 % of starting material was converted into **33**.

Table 4.7: Aromatic nitration of anisole.[a]

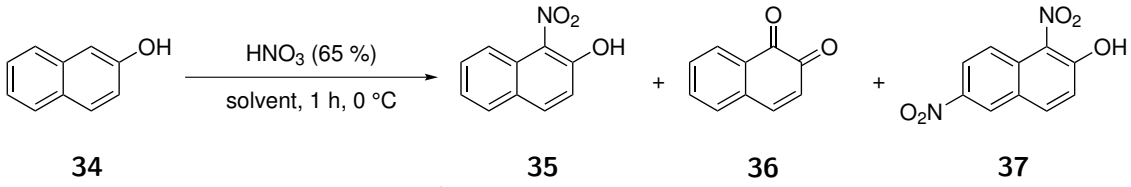


30 **31** **32** **33**

Entry	Solvent	Time	Yield [%]	Selectivity		
				31	**32**	**33**
1	TFE	24	72	40	57	3
2	HFIP	5	100	34 (26)	51 (27)	15

[a] Reaction conditions: 1.0 mmol of anisole (**30**), 65 % HNO_3 (1.0 mmol, 69.2 μL), 1 mL of solvent, room temperature. Selectivity and conversion were determined through ^{1}H NMR. Number in parenthesis refers to isolated yield after column chromatography.

Similar effect of solvent was also observed in nitration of 2-naphthol (**34**). In TFE nitrated product **35** was the main product. On the other hand, in HFIP the main product was quinone (**36**) formed in a 68 % yield.



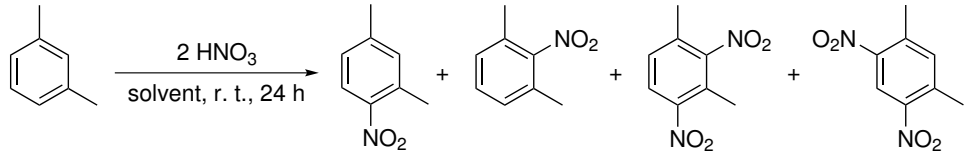
34 **35** **36** **37**

TFE	60 %	37 %	3 %
HFIP	17 %	68 %	15 %

Scheme 4.5: Aromatic nitration of 2-naphthol.

4.1.3.2 Formation of dinitrated products

During a study on the substrate scope we noticed that dinitrated products are not formed in fluorinated alcohols. This was not the case in the classical system, where dinitrated products were formed with substrates mesitylene (**10a**), *m*-xylene (**1**), toluene (**9a**) and 4-*t*-Bu-phenol (**6a**). The only exception where dinitrated side products were also formed in fluorinated alcohols were substrates with high electron donor ability (4-*t*-butylphenol and 2-naphthol). We investigated further the effect of HFIP on the selectivity of nitration for mono- vs. di-nitrated products. Therefore, we repeated a reaction with **1** with 2 equiv. of HNO_3. In HFIP only mono-nitrated products were formed after 24 h at room temperature. Under harsher conditions in TFA 3 % of dinitrated products **4** and **5** were formed after nitration with 2 equiv. of HNO_3 at room temperature in 24 h. On other hand, the reaction performed by the classical method with mixed acids afforded 20 % conversion into dinitrated products with 2 equiv. of HNO_3 and 2 eq. of H_2SO_4 and stirring for 24 h at room temperature. This large difference compared to the fluorinated solvents indicated there is an additional deactivation by fluorinated solvents for further nitration.



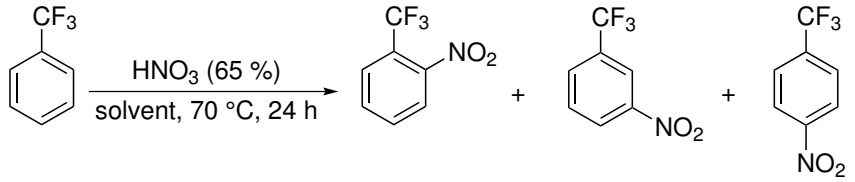
	2	3	4	5
HFIP	90	10	0	0
TFA	84	13	1	2
H_2SO_4 (2 equiv.)	70	11	10	9

Scheme 4.6: Dinitration of *m*-Xylene (**1**).

Fluorinated alcohols are strong hydrogen bond donors and can form hydrogen bonds with nitro group on an aromatic ring. This increases the electrophilic nature of the nitrogen atom in the nitro group and enhances the electron-withdrawing effect of the nitro group, which decreases further the electron density in the aromatic ring. Consequently, the aromatic ring is deactivated for further electrophilic substitution. We wanted to confirm this effect of fluorinated alcohol and we studied the nitration of nitrobenzene (**14**) and trifluoromethylbenzene (**38**). CF_3- and NO_2- groups have strong deactivation effect on the electrophilic aromatic substitution. If our hypothesis is true we would observe a conversion with **38** in HFIP and TFA, as there is no strong interaction between the trifluoromethyl group and the solvent, while on other hand no reaction would occur with **14** due to strong deactivation of the aromatic ring for further nitration.

As could be seen in Table 4.8, trifluoromethylbenzene **38** was nitrated with a similar conversion in H_2SO_4-catalysed reaction in neat and in HFIP. Needless to say, no reaction occurs without H_2SO_4. No additional activation or deactivation was observed in HFIP. The reactivity in TFA was lower, therefore higher amounts of HNO_3 (1.5 eq.) were added. The classical nitration of nitrobenzene (**14**) with mixed acids under solvent-free conditions was of similar reactivity as **38** and 46 % of nitrated products were formed after 24 h reaction at 70 °C. In contrast to the nitration of **38** in HFIP where 54 % conversion was obtained, no conversion was observed for nitration of **14** under similar conditions. Additionally, no reaction occurred in the nitration of **14** in TFA. These results confirm

Table 4.8: Aromatic nitration of trifluoromethylbenzene.[a]



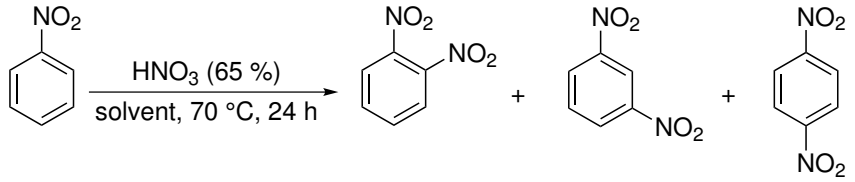
38 **39** **40** **41**

Entry	HNO_3 [eq.]	H_2SO_4 [eq.]	Solvent	Yield [%]	Selectivity		
					39	**40**	**41**
1	1.0	2	-	51	6	88	6
2	1.0	2	HFIP	54	6	89	5
3	1.5	0	TFA	30	7	90	3

[a] Reaction conditions: 1.0 mmol of trifluoromethylbenzene (**38**), 65 % HNO_3 (1.0 mmol, 69.2 μL), 1 mL of solvent, room temperature. Selectivity and conversion were determined through ^{1}H NMR.

our hypothesis that the fluorinated solvent interacts with the nitro group at the aromatic ring, which causes further deactivation for electrophilic aromatic substitutions. Occurrence of dinitrated products with phenols can be explained with solvatocromic investigations. Solvatocromic investigations have already established that strong hydrogen donors such as fluorinated alcohols have a stronger hydrogen bond with 4-nitroanisole compared to 4-nitrophenol [15]. The hydrogen bond strength with nitro-phenols is weaker. Therefore, there is smaller decrease of electron density from the aromatic ring and a lower deactivation for the electrophilic substitutions. Thus, in the nitration of derivatives of phenols in HFIP the formation of dinitrated products can be observed.

Table 4.9: Aromatic nitration of nitrobenzene.[a]



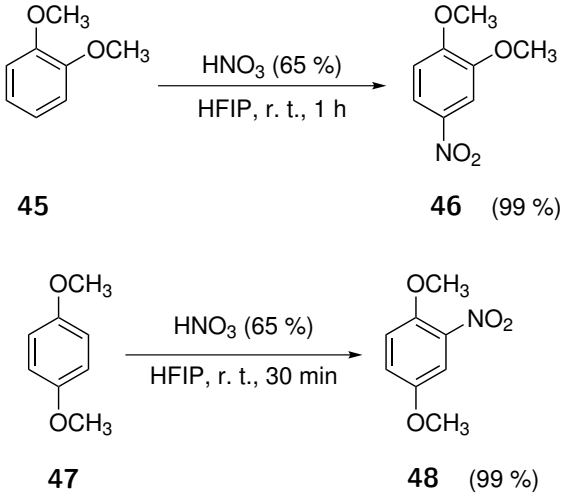
14 **42** **43** **44**

Entry	HNO_3 [eq.]	H_2SO_4 [eq.]	Solvent	Yield [%]	Selectivity		
					22	**23**	**38**
1	1.0	2	-	46	11	87	2
2	1.0	2	HFIP	0	-	trace	-
3	1.5	0	TFA	0	-	-	-

[a] Reaction conditions: 1.0 mmol of nitrobenzene (**14**), 65 % HNO_3 (1.0 mmol, 69.2 μL), 1 mL of solvent, room temperature. Selectivity and conversion were determined through ^{1}H NMR.

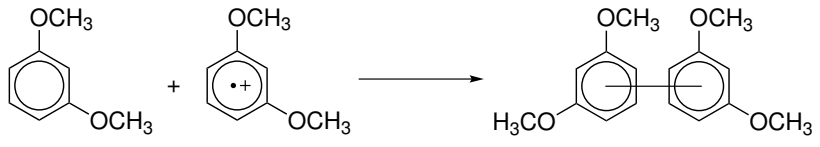
4.1.4 Bisphenylnitrosonium nitrate

Dimethoxybenzenes are highly reactive compounds for electrophilic substitution on an aromatic ring. They were used in a mechanistic study by Kochi *et al.* [82], which confirmed the charge-transfer mechanism. They noted that arene cation radicals are stable enough to be detected. 1,2-Dimethoxybenzene (**45**) and 1,4-dimethoxybenzene (**47**) were nitrated under typical reaction conditions (1 eq. HNO_3, HFIP) and quantitative conversions to nitrated products **46** and **48** were observed in 1 h and 30 min, respectively (Scheme 4.7). However, the reaction with 1,3-dimethoxybenzene (**49**) was different and after the addition of nitric acid to the solution of **49**, an intense dark green colouration formed. A low yield of nitrated product 2,4-dimethoxy-nitrobenzene (**50**) was observed in the NMR spectra of the crude reaction mixture [82].



Scheme 4.7: Nitration of 1,2- and 1,4-dimethoxybenzene yields expected nitrated product.

It was already reported that the direct nitration of **49** produces 2,4-dimethoxy-nitrobenzene (**50**) at surprisingly poor yields (∼30 %) [83]. Kochi *et al.* [82] observed an unusual blue colouration during nitration. Among the dimethoxybenzenes **49** is unique, as it is the only one to produce such an intense colouration upon nitration. Kochie *et al.* attributed such a strong colouration to dimethoxyphenyl dimers, which would form through arene coupling from the cation radical (Scheme 4.8). The formation of such products was an indication of the electron transfer mechanism for electrophilic aromatic substitution. A similar strong colouration was observed for 2,6-dimethoxytoluene and 1,3,5-trimethoxybenzene [82].



Scheme 4.8: Proposed product of nitration of 1,3-dimethoxybenzene by Kochi *et al* [82].

On other hand, Gowenlock *et al.* [84] studied the nitration of **49** with NO_2/N_2O_4 and observed an intense green colouration of the reaction mixture. After stirring the reaction mixture for 48 h the colour changed from green to red and a TLC analysis indicated the presence of two products. They noticed that after the reaction was complete, in a sample standing at room temperature for 20 h, a further six minor side products formed. After

isolation they identified the minor product (15 %) to be **50** and the major product (80 %) was identified as 2,4-dimethoxyanilino-*para*-(2-methoxy)quinone (Figure 4.7).

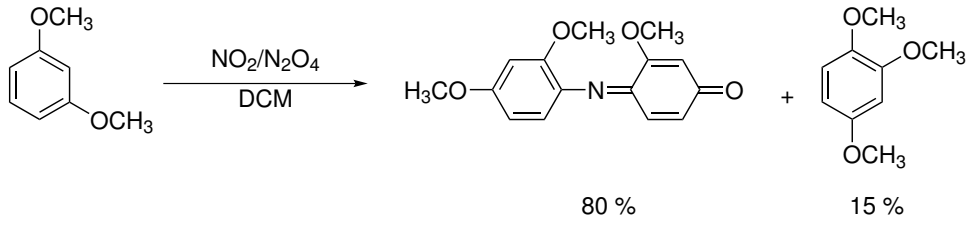
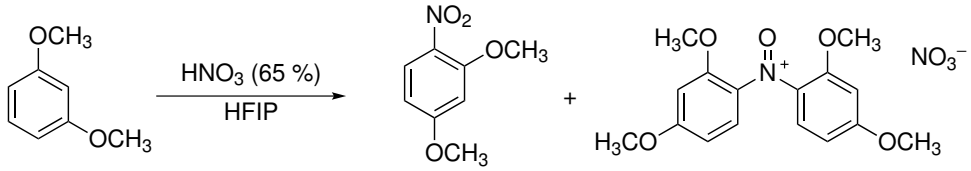


Figure 4.7: Products formed in nitration of 1,3-dimethoxybenzene by Gowenlock *et al* [84].

Due to the different reactivity of **49** in nitration in fluorinated alcohols, we have studied the effect of the solvent and reaction conditions on the reaction of **49** with HNO_3 in fluorinated alcohols. As can be seen from the Table 4.10, the product distribution can be influenced by the amount of solvent and the temperature of the reaction (Table 4.10). For larger amounts of HFIP and higher temperature **50** was predominantly formed. A decrease in the amount of solvent and a decrease of the reaction temperature caused unknown compound to be formed as the major product. By removing **49** and **50** with extraction CCl_4, we were able to isolate the unknown product, which was identified by NMR and HR-MS as bis(2,4-dimethoxyphenyl)nitrosonium nitrate (**51**). **51** is an intense dark green coloured liquid with a high surface tension. It was found that **51** decomposes on silica gel, in polar solvents (H_2O, MeCN, EtOH, DMSO, ...) and at room temperature. After decomposition various red-brown coloured products were formed and the mixture was too complex to be identified. Fluorinated alcohols, especially HFIP, increased the stability of **51** and the product was stable in a solution of fluorinated alcohols.

Table 4.10: Distribution of products in nitration of 1,3-dimethoxybenzene in HFIP.[a]



49 **50** **51**

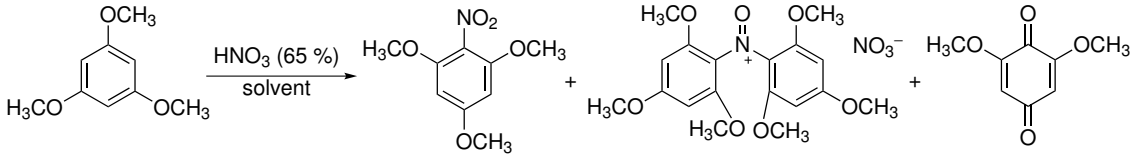
Entry	HFIP [mL]	T [°C]	time [h]	Yield [%]	Selectivity	
					50	**51**
1	0.1	0	6	75	12	88
2	0.2	0	6	81	15	85
3	0.2	0	24	100	9	91 (90)
4	0.5	0	6	100	25	75
5	1.0	0	6	100	36	64
6	1.0	25	6	100	75	25
7	5.0	25	6	100	83 (26)	17

[a] Reaction conditions: 1.0 mmol of 1,3-dimethoxybenzene (**49**), 65 % HNO_3 (1.0 mmol, 69.2 μL), solvent. Selectivity and conversion were determined by ^{1}H NMR. Number in parenthesis refers to isolated yield after column chromatography.

The first bisphenylnitrosoinium salts were proposed in 1919 by Mayer [85], [86] and in 1921 by Kehrmann *et al.* [87]. Although due to analytical methods in that era and the instability of such products, their actual formation is questionable. Products were identified after colour change from green to red, which is caused by decomposition. In 2000, Gowenlock *et al.* [84] reported the formation of bis(2,4,6-trimethoxypheny)nitrosonium nitrate (**54**) in the reaction of 1,3,5-trimethoxybenzene (**52**) and NO_2/N_2O_4. Rubinstein *et al.* confirmed the formation of such a product a few years later based on the crystal structure [88].

Since the successful formation of **54** was already reported in previous studies we continued our research with 1,3,5-trimethoxybenzene **52**. After 1 h of mixing equimolar quantities of **52** and HNO_3 in fluorinated alcohol the reaction mixture coloured into an intense dark blue. Similar to previous experiments with **49** a higher selectivity for the formation of bisphenylnitrosium nitrate was obtained with a lower temperature and smaller amounts of HFIP in the reaction mixture (Table 4.11). However, **52** is more reactive than **49** and a less reactive system can be employed to achieve good conversion. By changing the solvent to TFE the reaction could be performed at 25 °C with excellent conversion and selectivity for **54** (Table 4.11, entry 8). **54** is solid at room temperature and more stable in comparison to **51**.

Table 4.11: Distribution of products in nitration of 1,3,5-trimethoxybenzene in fluorinated alcohols.[a]



52 **53** **54** **55**

Entry	Solvent [mL]	T [°C]	time [h]	Yield [%]	Selectivity		
					53	**54**	**55**
1	0.2 HFIP	0	5	77	4	96	0
2	1.0 HFIP	0	6	99	8	83	7
3	1.0 HFIP	25	6	100	0	61	39
4	5.0 HFIP	25	1	100	24	50	26
5	1.0 TFE	25	1	78	0	100	0
6	1.0 TFE	25	2	87	0	100	0
7	1.0 TFE	25	3	93	0	100	0
8	1.0 TFE	25	4	93	0	97	3
9	1.0 TFE	25	5	100	0	93 (65)	7

[a] Reaction conditions: 1.0 mmol of 1,3,5-trimethoxybenzene (**52**), 65 % HNO_3 (1.0 mmol, 69.2 μL), solvent. Selectivity and conversion were determined by ^{1}H NMR. Number in parenthesis refers to isolated yield after column chromatography.

Monocrystals of **54** product were obtained by diffusion of *n*-hexane into a solution of **54** in $CHCl_3$ at −20 °C. Crystals were metallic lustre brownish red with a trapezoid shape. Single-crystal X-ray diffraction analysis confirmed the structure of **54** (Figure 4.8), which was in line with the literature data [88]. The published crystal structure was refined in $C2/c$ space group with a = 16.015(2) Å, b = 14.1139(18) Å, c = 10.6266(14) Å, β =

127.290(6)°, V = 1911.0(4) Å^3, and Z = 4 at 100 K [88]. However, in this particular case a conventional I-centered cell should be preferred [89]. The crystal structure of **54** was therefore refined in $I2/a$ space group with a = 10.6437(7) Å, b = 14.1647(6) Å, c = 13.0810(11) Å, β = 94.978(7)°, V = 1964.7(2) Å^3, and Z = 4 at 150 K. Transformation of the published $C2/c$ cell into $I2/a$ yields the following cell parameters: a = 10.6267 Å, b = 14.1139 Å, c = 12.7747 Å, β = 94.148 °, V = 1911.0 Å^3. The aforementioned values are in good agreement with the cell parameters reported herein, considering that the crystal structures were measured at different temperatures.

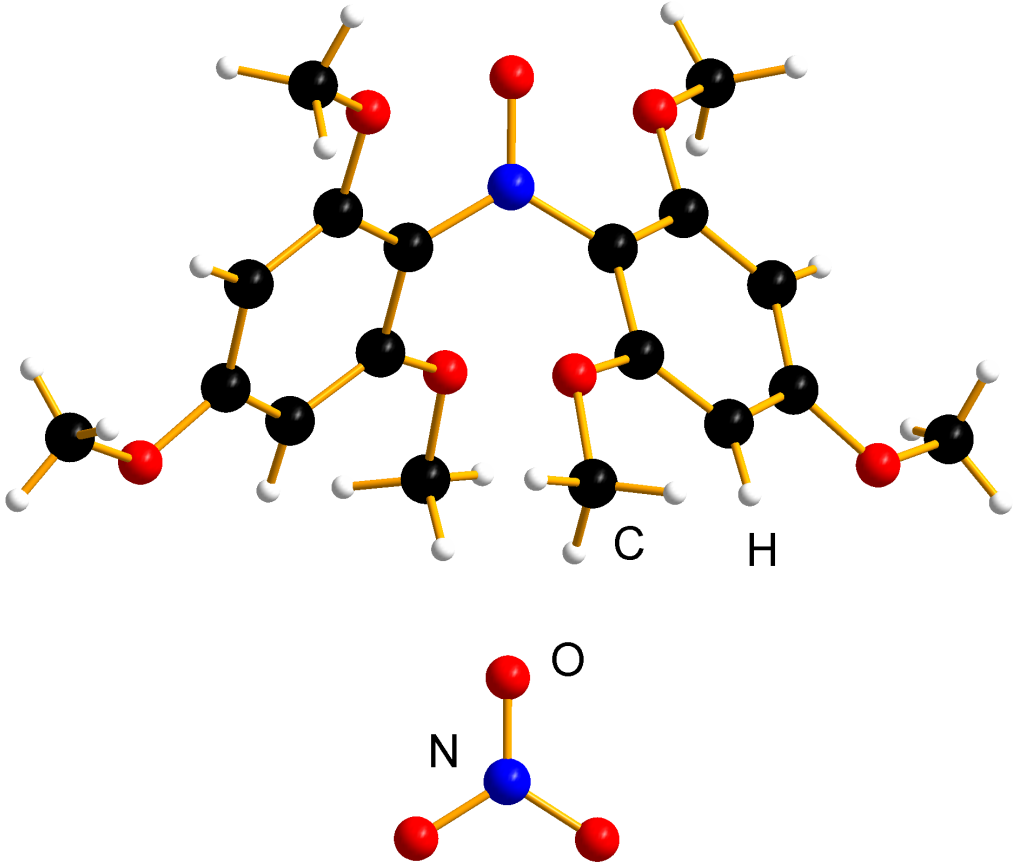
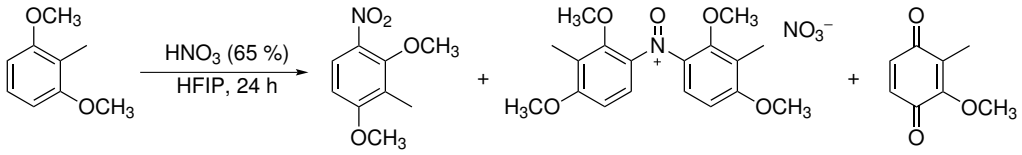


Figure 4.8: The asymetric unit of the bis(2,4,6-trimethoxyphenyl)nitrosonium nitrate (**54**) crystal structure is comprised of one-half of the cation and one-half of the anion (Z' = 0.5) - both residing with N-O bonds on the 2-fold rotation axis. C-carbon, H-hydrogen, O-oxygen, N-nitrogen.

Methoxy groups positioned at 1,3-positions are essential for the formation of bisphenylnitrosonium nitrate. Therefore, we continued our research with 2,6-dimethoxytoluene (**56**) and 3,5-dimethoxytoluene (**60**). We found that bis(2,4-dimethoxy-3-methylephenyl)nitrosonium nitrate (**58**)was also formed, however it decomposed quickly at room temperature. Therefore, lower temperatures were needed for the synthesis. **58** has an intense dark blue colour and similarly to previous substrate lower amounts of HFIP and lower temperature increased selectivity for the formation of **58** (Table 4.12, entry 6).

Table 4.12: Reaction with 2,6-dimethoxytoluene (**56**).[a]



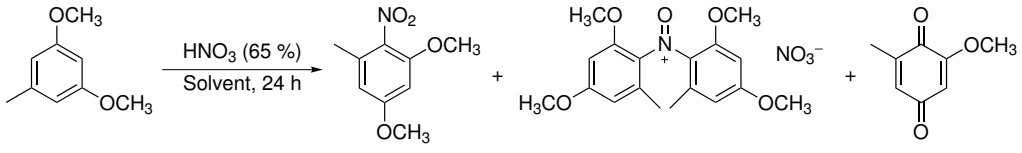
56 **57** **58** **59**

Entry	HNO_3 [eq.]	HFIP [mL]	T [°C]	Yield [%]	Selectivity		
					57	**58**	**59**
1	1.0	0.1	−10	50	45	45	10
2	1.0	0.2	−10	78	55	34	11
3	1.0	0.5	−10	97	57	29	14
4	1.0	1.0	−10	100	69	19	12
5	1.2	0.2	−10	93	54	33	13
6	1.2	0.2	−20	75	33	65 (62)	1

[a] Reaction conditions: 1.0 mmol of 2,6-dimethoxytoluene (**56**), 65 % HNO_3, solvent. Selectivity and conversion were determined by ^{1}H NMR. Number in parenthesis refers to isolated yield after column chromatography.

Similar results were also obtained with 3,5-dimethoxytoluene (60). The highest selectivity for the synthesis of bis(2,4-dimethoxy-6-methylphenyl)nitrosonium nitrate (**62**) was obtained with 0.2 mL HFIP at −10 °C (Table 4.13, entry 3). The colour of **62** was dark green, similar to **51**. At higher temperatures the reaction pathway preferred the formation of 2-nitro-3,5-dimethoxytoluene **61** and 2-methoxy-6-methyl-1,4-benzoquinone (**63**).

Table 4.13: Reaction with 3,5-dimethoxytoluene (**60**).[a]



60 **61** **62** **63**

Entry	Solvent [mL]	T [°C]	Yield [%]	Selectivity		
				61	**62**	**63**
1	1.0 TFE	25	>99	52	16	32
2	0.2 HFIP	0	100	23	63	14
3	0.2 HFIP	−10	79	0	100 (48)	trace

[a] Reaction conditions: 1.0 mmol of 3,5-dimethoxytoluene (**56**), 65 % HNO_3, solvent. Selectivity and conversion were determined by ^{1}H NMR. Number in parenthesis refers to isolated yield after column chromatography.

4.1.5 Mechanistic study on formation of bisphenylnitrosonium nitrate

The question that remains is how non-classical products - bisphenylnitrosonium nitrates - are formed in the reaction of aromatic nitration. Two possibilities can be considered. First, bisphenylnitrosonium nitrates are intermediates from which nitroarenes are formed. To test this we followed the decomposition of bis(2,4-dimethoxyphenyl)nitrosonium nitrate (**51**) at room temperature. A reaction mixture containing mainly **51** was stirred at room temperature for 24 h and a complex mixture of products with no clear indication for the formation of 2,4-dimethoxy-nitrobenzene (**50**) was observed. The second possibility for the formation of bisphenylnitrosonium nitrate **51** is the reaction of nitroarene and the starting material. Pure **50** was synthesized and mixed with **49** in HFIP. However, no reaction occurred and **51** was not formed. The results obtained from these two experiments indicate that bisphenylnitrosonium nitrates are formed through a competitive mechanism to aromatic nitration and could not be transformed into nitroarenes and vice versa. To learn more about the nature of the reaction mechanism we added (2,2,6,6-tetramethylpiperidin-1-yl)oxyl (TEMPO) to the reaction mixture. The reaction was carried out under conditions where both **50** and **51** are formed. The reaction was quenched and neither product was formed, indicating that both products might be formed through a radical mechanism. Further studies were performed with the nitration of 1,3,5-trimethoxybenzene (**52**) in TFE where the selective formation of bis(2,4,6-trimethoxypheny)nitrosonium nitrate (**54**) occurs in high yields. For a mechanistic study it was important that the nitration process was not present. Reaction of formation for **54** in TFE was followed with ^{1}H NMR (Figure 4.9). Due to the needs of the NMR experiment $CDCl_3$ was added as a co-solvent. The addition of equimolar amounts of nitric acid to a solution of **52** in TFE shifted the signal of the OH

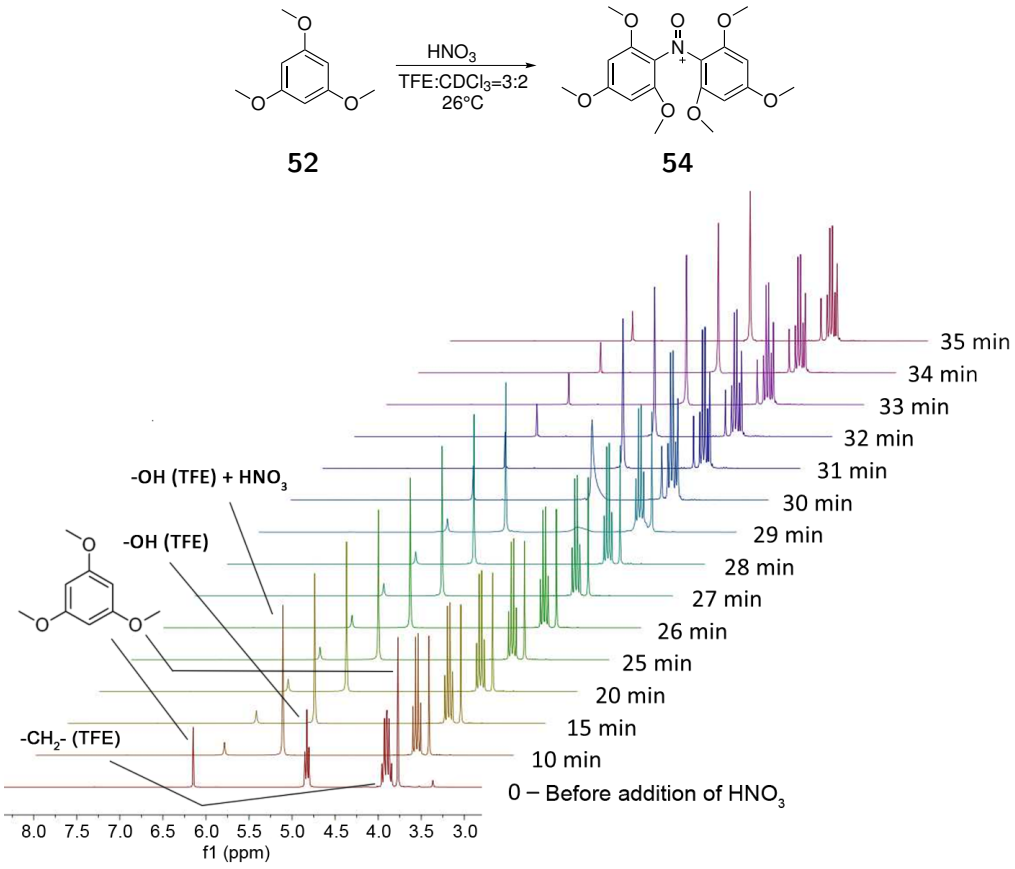


Figure 4.9: The course of monitoring of formation of **54** by ^{1}H NMR spectroscopy.

group from TFE to a higher chemical shift (from 4.83 ppm to 5.48 ppm; Figure 4.11, scan after 10 min). This chemical shift is a consequence of the interaction between HNO_3 and TFE. No other change or new signals were observed for the first 28 min. At 29 min the signal for OH at 4.85 ppm started to increase and the signal at 5.48 ppm to decrease. At the same time we observed a change in the aromatic region of the NMR spectra (Figure 4.10). The signal of **52** at 6.15 ppm was exchanged with the one at 6.25 corresponding to **54** and at 30 min the reaction was already completed. The signal for the TFE OH-group was also completely shifted to 4.86 ppm. The difference in the reaction kinetics compared to the reaction performed in bulk could come from the addition of $CDCl_3$ and a lack of mixing of the reaction mixture.

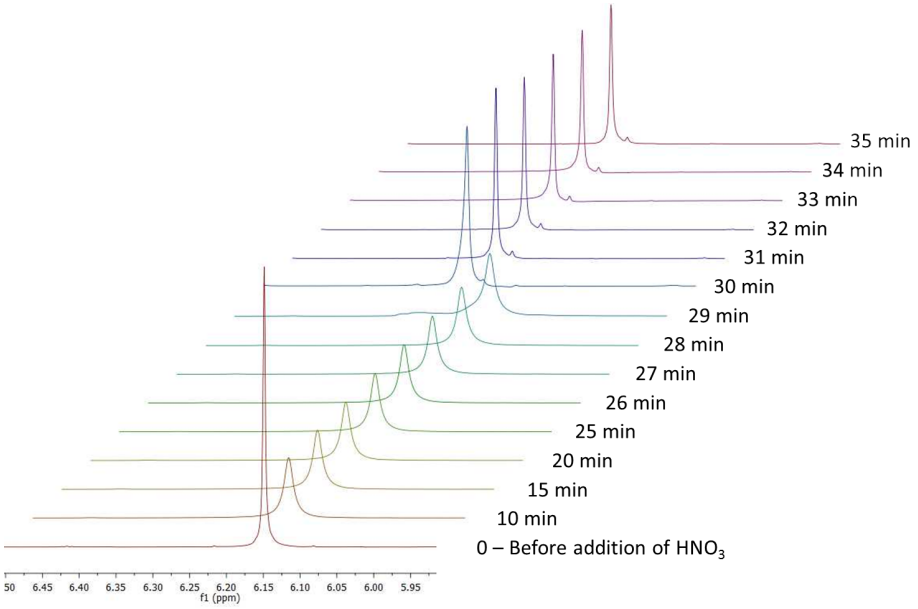


Figure 4.10: Change of ^{1}H NMR signals in the aromatic region due to formation of **54**.

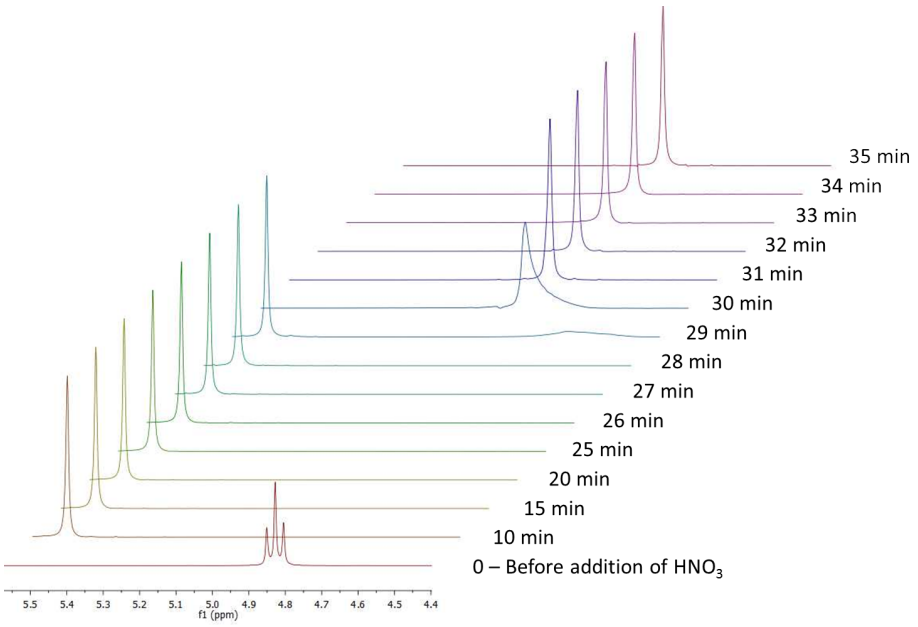


Figure 4.11: Changes in OH-region in NMR spectra of reaction of **54** and HNO_3 in TFE.

The effect of TEMPO and the peculiar kinetics of the reaction led us to try to detect radical intermediates that might be formed during the reaction. Hence, we turned to EPR spectroscopy. The solution of HNO_3 in HFIP was degassed and the substrate **52** was added. EPR was followed at 30 ℃. Immediately, we observed a signal with four peaks (Figure 4.12), which indicates that the radical is localised on carbon atom coupled with 1 nitrogen atom with a_N=5.260 G and 1 hydrogen atom with a_H=6.359 G. Additional coupling was identified to be with 2 equivalent hydrogen atoms (a_{2H}=0.300 G), three equivalent hydrogen atoms (a_{3H}=0.784 G) and six equivalent hydrogen atoms (a_{6H}=0.450 G).

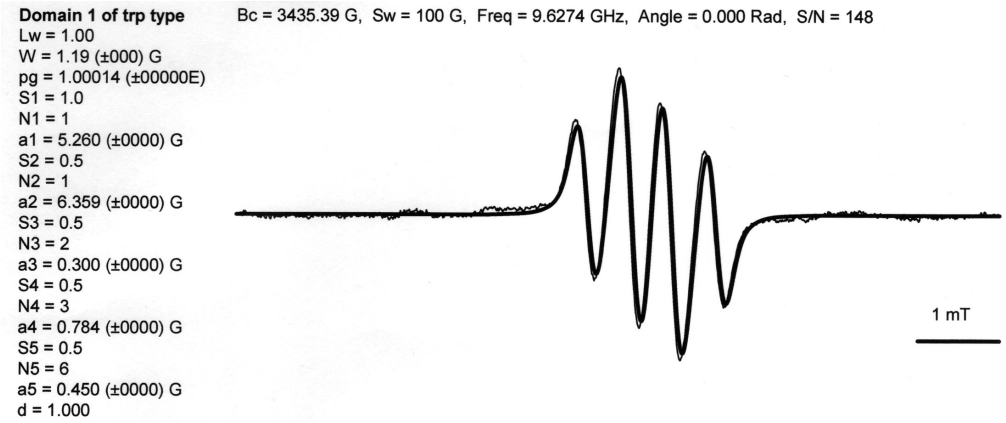
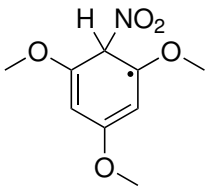


Figure 4.12: EPR spectra of 1st intermediate in formation of the **54** (thin line is observed EPR, thick line is simulated spectrum).

Based on the coupling constants provided by the simulation of the EPR spectra, the structure of 1st intermediate was determined (Scheme 4.9). 1st intermediate is a radical analogue of σ-complex and strongly indicates that the mechanism in fluorinated alcohols is different to the classical mechanism of aromatic nitration.

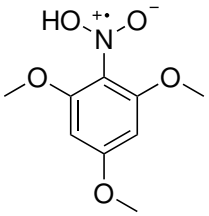


Scheme 4.9: Structure for the 1st intermediate obtained by EPR spectra.

After 1 h of reaction a second signal appeared. Its high intensity then quickly increased. This signal was assigned to a second intermediate with a characteristic doublet-triplet shape (Figure 4.13). Coupling in the EPR spectra for 2nd intermediate indicated that the radical is located at the nitrogen atom (strong coupling of a_N=24.020 G, N=1) and partially on 1 hydrogen atom (a_H=1.662 G, N=0.5). Using these data a second intermediate structure was assigned (Scheme 4.10). Note, that at this time both 1st and 2nd intermediates were present. Their relative weights have been identified to be 30.7 % and 69.3 %, respectively.



Figure 4.13: EPR spectrum of 2nd intermediate in formation of **54** (thin line is observed EPR, thick line is simulated spectrum).



Scheme 4.10: Structure for 2nd intermediate obtained from EPR spectra.

Afterwards, a third intermediate started to appear in the EPR spectrum (Figure 4.14). It was found that it has a slow rotational and rigid structure with a correlation time of 0.44 ns. The radical was located on a nitrogen atom, but the hyperfine coupling constant of a=8.760 G indicated that the electron density at this nitrogen atom is much lower in comparison to the previously identified 2nd intermediate. There are some additional hydrogen atoms which virtually double the signal. A simulation revealed that all three intermediates observed during the reaction are present in the EPR spectra and the 3rd intermediate has 25 % contribution (Figure 4.14).

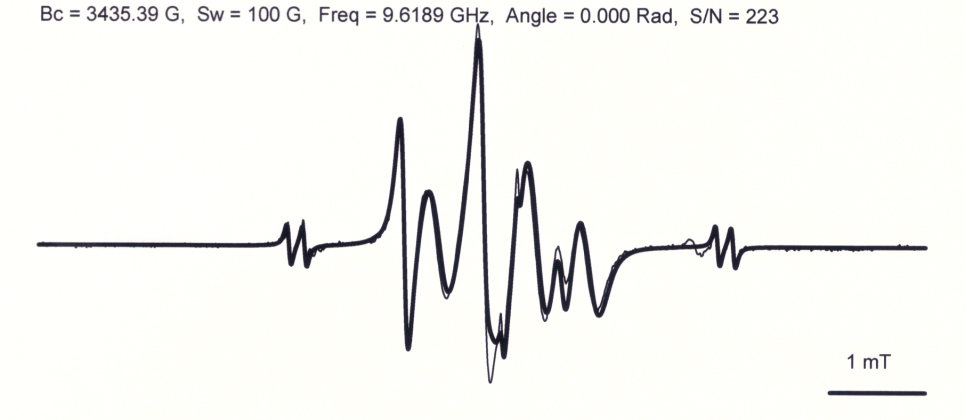
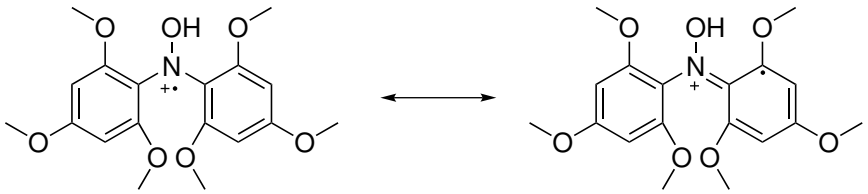


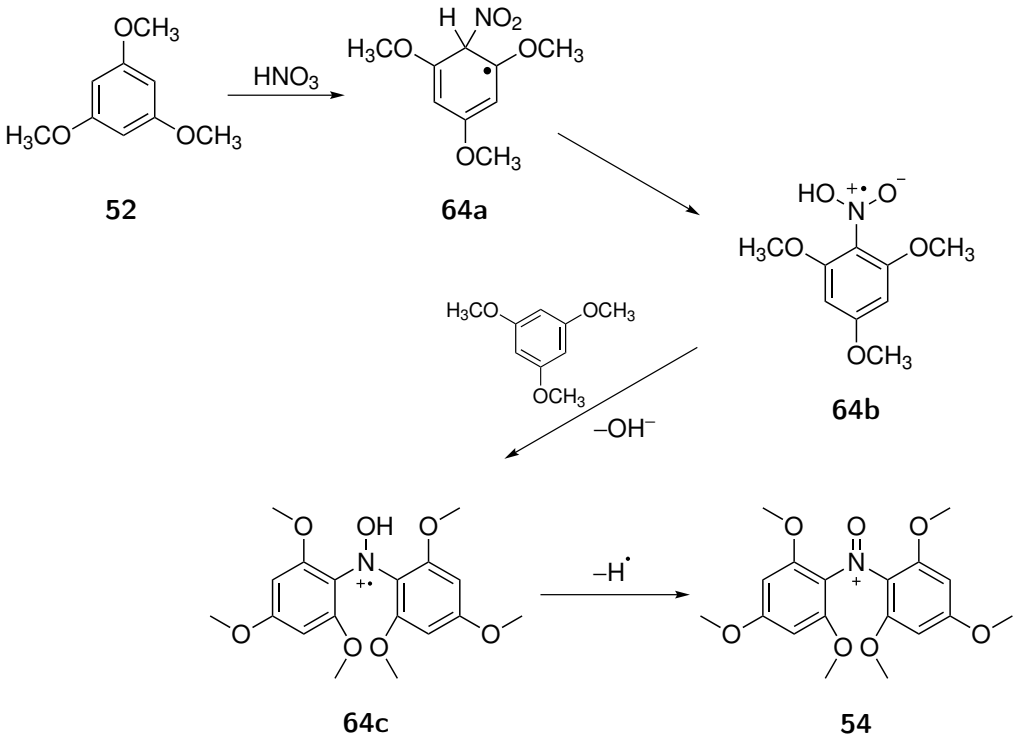
Figure 4.14: EPR spectrum of 3rd intermediate in formation of **54** (thin line is observed EPR, thick line is simulated spectrum).

According to the data, the structure of third intermediate was proposed (Scheme 4.11).



Scheme 4.11: Structure for 3rd intermediate obtained from EPR spectra.

All three intermediates were also observed when the reaction was performed in TFE. However, the reaction performed in TFE had a slower rise of signal for the second intermediate – **64b**. Therefore, the peak height for **64b** was always lower in TFE compared to the measurement obtained in HFIP. The formation of **54** proceeds through three intermediates which we observed with EPR spectroscopy (Scheme 4.12). The key difference compared to classical nitration is the formation of 1st intermediate (**64a**). Therefore, a computational study was made to understand how **64a** could be formed.



Scheme 4.12: Mechanism for formation of bis(2,4,6-trimethoxyphenyl)nitrosonium nitrate (**54**).

4.1.6 Mechanism of aromatic nitration in fluorinated alcohols

Mesitylene (**10a**) was chosen as model substrate to study the nitration of aromatic substrates in HFIP by in-situ ATR-IR spectroscopy as it forms only one nitrated product **10b** with excellent yield. The reaction kinetics was followed with ATR-IR probe. At first we mixed HFIP and 65 % HNO_3 and left stirring for 30 min. In this pre-reaction stage no new signal was formed as well as no change of existing ones occurred (Figure 4.16). Therefore, HFIP and HNO_3 do not react to form a reactive *species* or intermediate. Afterwards, the reaction rate started to increase progressively, as could be seen by an increase in the temperature of the reaction mixture. The maximum temperature was higher by 2.2 K than the defined temperature of the reactor and was reached 30 min after the addition of **10a** (Figure 4.15).

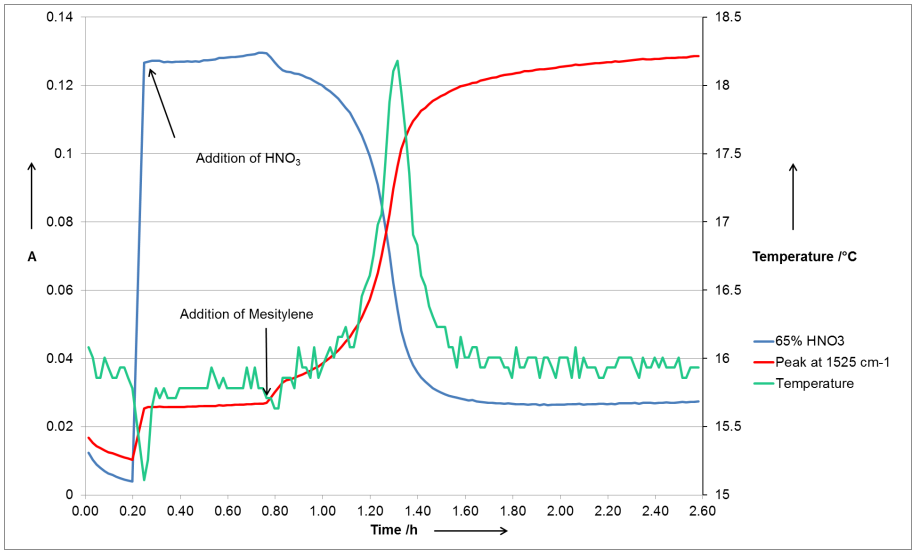


Figure 4.15: Time course of nitration of mesitylene (**10a**) into 2-nitromesitylene (**10b**) (peak 1525 cm^{-1}).

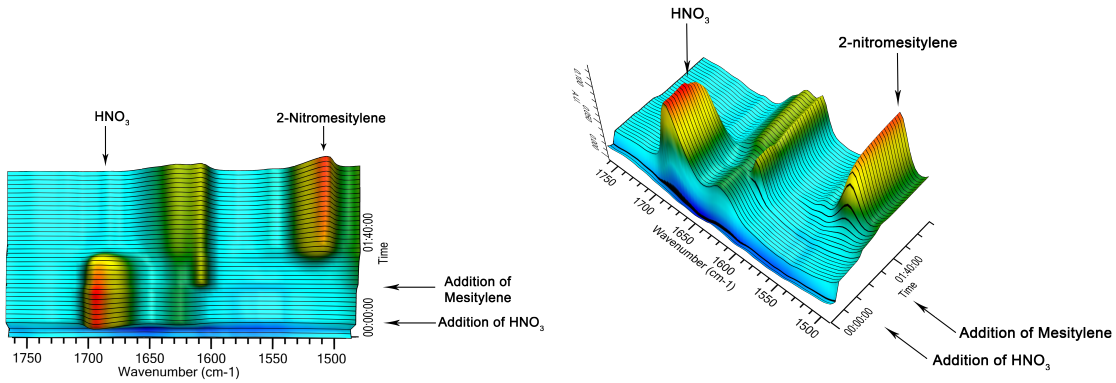


Figure 4.16: Real-time ATR-IR spectra of nitration of **10a**.

Observed kinetics in Figure 4.15 is usual for complex and auto-catalytic reactions. This could not be explained by the classical mechanism for aromatic nitration. To find out more about the mechanism we followed the reaction with EPR spectroscopy. **10a** and 65 % HNO_3 were dissolved in degassed HFIP. Three different radical compounds were observed in the spectrum (Figure 4.17).

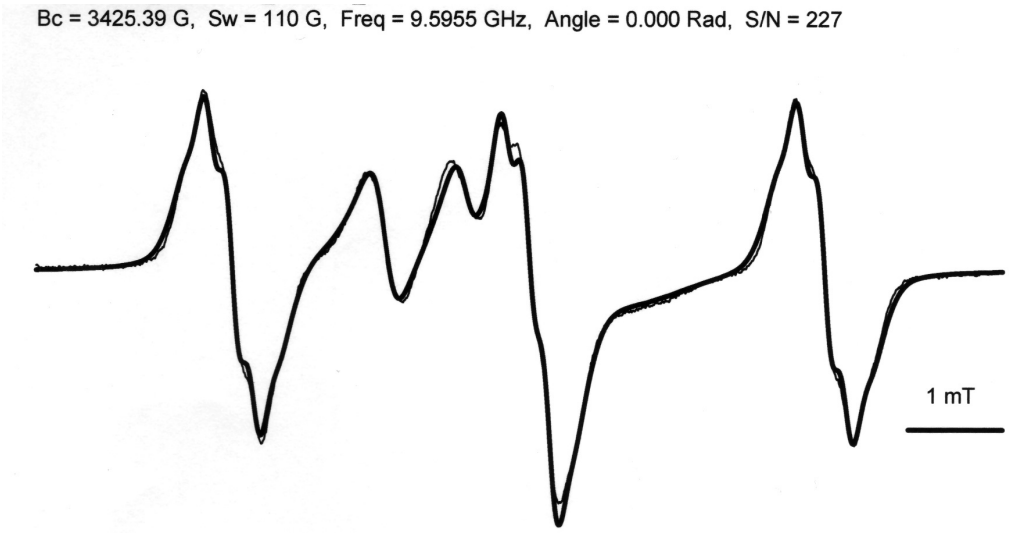


Figure 4.17: EPR spectrum at beginning of nitration of mesitylene (**10a**).

In the first spectrum (Figure 4.17) there are three different radicals. The first radical is "compound 1" which has 49 % contribution to the signal in the EPR spectrum, as shown by simulation of the spectrum. In compound 1 the radical is heavily located on nitrogen atom with a_{N}=33.760 G. It has additional coupling with 4 unequal hydrogen atoms, but with similar hyperfine coupling constants ($a_{1(\mathrm{H})}$=2.732 G, $a_{2(\mathrm{H})}$=2.501 G, $a_{3(\mathrm{H})}$=2.390 G, $a_{4(\mathrm{H})}$=2.299 G). The second compound has a radical electron density that is more distributed, although still localised on the nitrogen atom (a_{N}=9.418 G). The compound was identified as NO_2 with a 17 % contribution to the signal in the EPR spectra. The rest of the signal was explained with the third radical compound that has a radical located on the nitrogen atom. Spin-spin interactions were detected that usually occur when radicals are concentrated. Since radicals with fine coupling (compound 1) were observed at the same time as spin-spin interactions, the reaction mixture is probably heterogeneous.

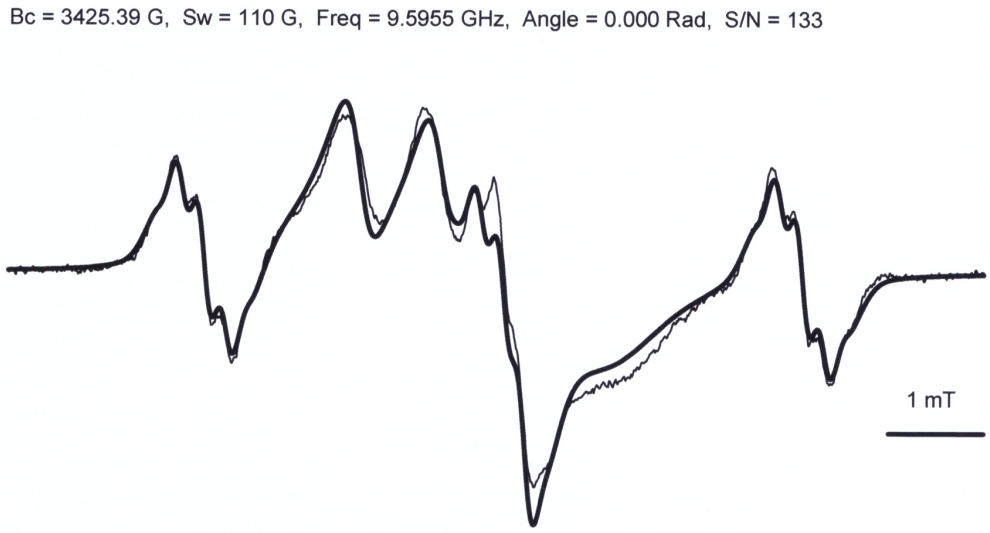


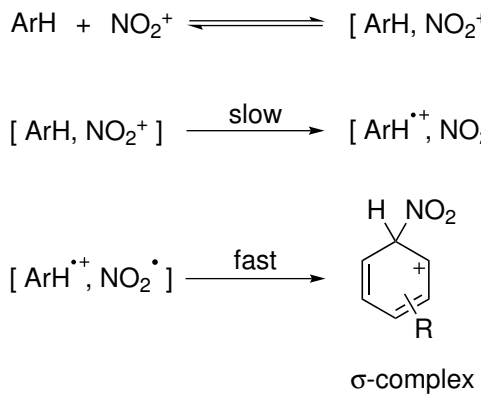
Figure 4.18: EPR spectrum towards the end of nitration of mesitylene (**10a**).

During the reaction the distribution of the radical *species* changed, as can be seen in the second spectrum (Figure 4.18). The compound 1's weight decreased from 49 % to 16 %,

as did the weight of NO_2 radical, from 17 % in the first spectrum (Figure 4.17) to 11 % in the second spectrum. Most of the signal in the second EPR spectrum came from the radical on the nitrogen atom with a spin-spin interaction. It had a 73 % contribution to the signal in the measured EPR spectrum.

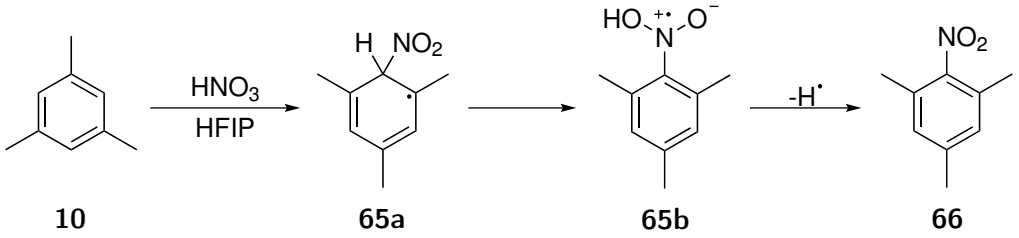
EPR measurements indicated that the system is biphasic, even though the reaction mixture looked homogenous and transparent. The Dynamic Light Scattering (DLS) technique is used to measure the size of micelles and is an excellent method to check whether the reaction mixture is heterogeneous. Unfortunately, the reaction mixture becomes red during the reaction and it absorbs photons from red and green lasers. Due to the light absorption the reaction mixture warmed up and convection starts to occur. This prevented us from measuring any meaningful data.

In the classical electrophilic aromatic nitration mechanism a charge-transfer complex is formed as an intermediate. This complex then proceeds with one-electron transfer between an arene and electrophile NO_2^+ leading to the well-established Wheland or σ-intermediate [90]. In the final step there is a proton elimination, forming the nitrated product (Scheme 4.13).



Scheme 4.13: Mechanism for classical nitration of aryl compounds.

EPR analysis and in-situ ATR-IR spectroscopy showed that aromatic nitration in HFIP proceeds through a different mechanism then classical nitration. EPR results for compound 1 (**65b**) were explained through a comparison of the spectra obtained in reaction of **52** and HNO_3 (chapter 4.1.5). An additional intermediate **65a** is proposed before the formation of **65b**, even though it was not identified in the EPR spectra. The lack of signal for **65a** could be explained by its short lifespan.



Scheme 4.14: Mechanism for nitration of aryl compounds in HFIP.

4.1.7 Computational study of formation of bisphenylnitrosonium nitrate

Calculations were performed within the framework of Density-Functional Theory (DFT) using meta-hybrid M06-2X functional [91] and hybrid B3LYP functional [92] as well as post Hartree-Fock second-order Møller-Plesset pertubation theory (MP2) [93]–[97]. The local Gaussian-type-orbital 6-311++G** basis set was used, which is a triple-zeta basis set modified with polarization and diffuse functions. Molecular calculations were performed using the Gaussian09 program [98]. Molecular graphics were produced with the XCrySDen graphical package [99].

The 2,2,2-trifluoroethanol (TFE) solvent was described implicitly by the SMD continuum solvation model [100] based on Tomasi's polarized continuum model (PCM) using the integral equation formalism [101], [102]. The PCM treats the solvent as a continuum dielectric medium with a molecule trapped within the cavity of the solvent. This level of description of the solvent will be denoted as SMD_{TFE} whereas a hybrid implicit-explicit description of the solvent is denoted as SMD_{TFE} + 1×TFE (one explicit TFE molecule) and SMD_{TFE} + 2×TFE (two explicit TFE molecules).

We chose to perform the computational study for a reaction between 1,3,5-trimethoxybenzene (**52**) and HNO_3 in TFE, where excellent yield and selectivity for bis(2,4,6-trimethoxypheny)-nitrosonium nitrate (**54**) were obtained experimentally. Under such conditions an alternative mechanism is significantly preferred to the classical nitration mechanism, as no nitrated products were formed.

In our computational study we compared the alternative mechanism to classical nitration. In the alternative path the fluorinated alcohol acts as a template catalyst to HNO_3 (Scheme 4.15). In the reaction between HNO_3 and the aromate ring the N–O bond splits homolitically, forming $NO_2^\bullet$ and $OH^\bullet$. In the next step the aromate ring in reaction with $NO_2^\bullet$ donates 1 electron to form the C–N bond, which yields the $I1_A$ intermediate. The $OH^\bullet$ is unstable and reacts immediately with the solvent molecule, forming a water molecule and $CF_3CH_2O^\bullet$ (Figure 4.19).

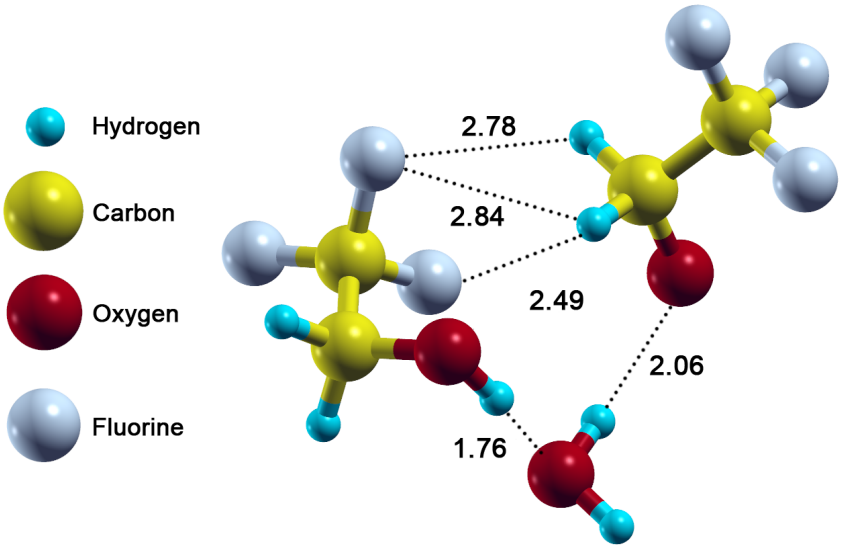
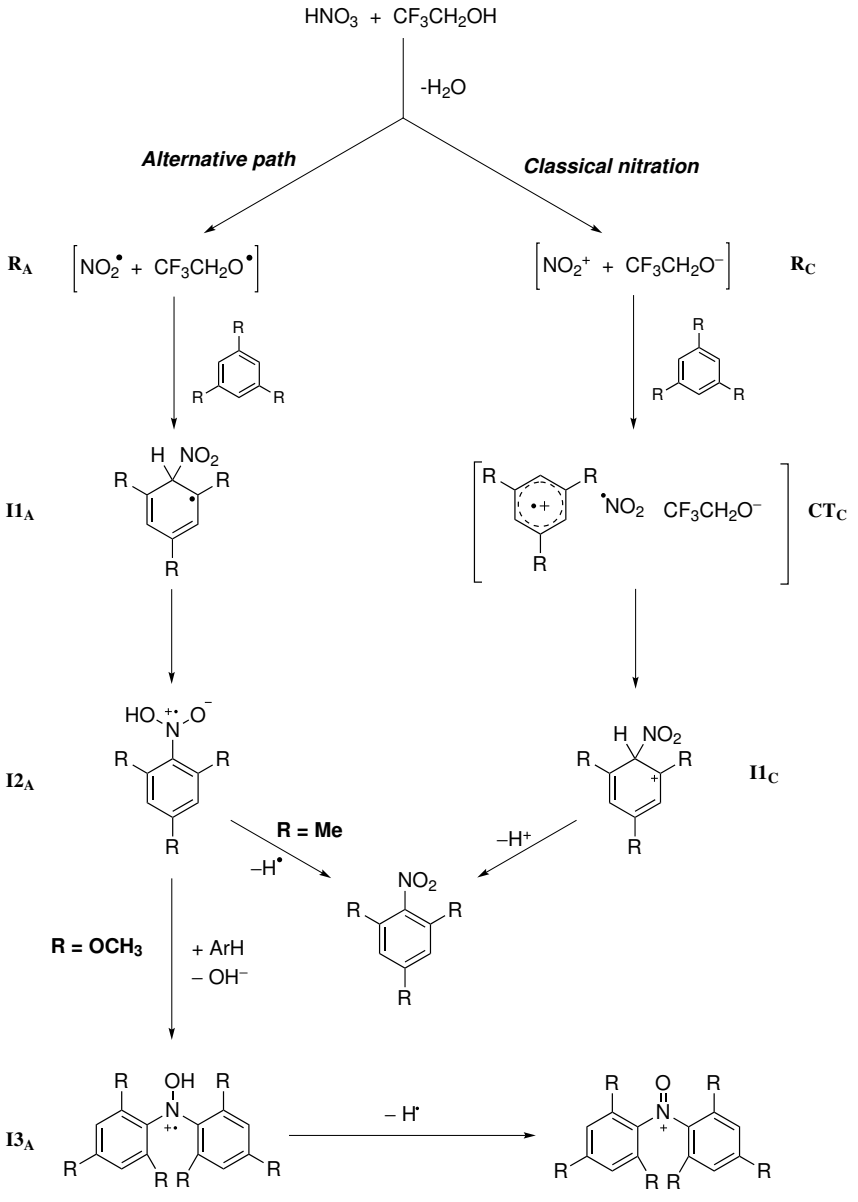


Figure 4.19: $OH^\bullet$ extracts a hydrogen atom from TFE solvent molecule and forms H_2O and $CF_3CH_2O^\bullet$.

In the next step the $I1_A$ rearranges itself into $I2_A$ by a shift of the hydrogen atom from the carbon atom in the aromatic ring onto an oxygen atom in the nitro group. During the rearrangement an aromatic ring is re-established. The experimental results showed a further step depends on the substituents on the aromate ring. With methyl groups attached to the aromatic ring, $I2_A$ converts into a nitrated product by the elimination of the hydrogen atom. However, when methoxy groups were attached to the aromate ring, $I2_A$ reacted again with the initial substrate (**52**) and formed $I3_A$. In the final step of the alternative path there is a hydrogen atom elimination from the $I3_A$, forming the **54** as a product.



Scheme 4.15: Proposed alternative path for reactions with HNO_3 in fluorinated alcohols in comparison to classical nitration.

The first step of the classical nitration consists of a reaction between HNO_3 and TFE, which results in the formation of $NO_2{}^+$. Since TFE has a lower pKa ($pKa_{TFE} = 12.4$) than water ($pKa_{H_2O} = 15.7$), OH^- extracts a proton from the solvent molecule and forms a water molecule and $CF_3CH_2O^-$ as a side product. In next step a single electron transfer

(SET) occurs between the aromate substrate and NO_2^+, which forms a charge-transfer complex [82]. The charge-transfer complex (CT_C) consists of a solvent caged aromatic cation radical together with $NO_2^\bullet$ and $CF_3CH_2O^-$. Kochi *et al.* reported cation radicals formed from electron-rich arenes are persistent enough to be detected [82]. The collapse of the charge transfer complex depends on the solvent's polarity. The ion pair collapse is favoured in nonpolar solvents (benzene, n-haxane, DCM). On the other hand, the radical collapse happens in polar solvents (e.g., MeCN), which results in the formation of a σ-complex ($I1_C$) [82], [103], [104]. In the classical nitration mechanism $I1_C$ transforms into the nitrated product by H^+ elimination.

For each step the reaction energy (ΔE) was calculated by subtracting the energy of the starting compounds (**52** and HNO_3) from the energy of the respective intermediate.

$$\Delta E = E(\text{intermediate}) - E_0 \tag{4.1}$$

ΔE - reaction energy
E(intermediate) - energy of intermediate
E_0 - energy of starting compounds

High ΔE values were obtained when the TFE solvent was described only implicitly (SMD_{TFE}) (Table 4.14). Therefore, to better describe the solvent, we added an explicit TFE molecule (SMD_{TFE} + 1×TFE) to the vicinity of the substrates and reagents. The addition of the explicit TFE molecules resulted in a further stabilisation of the radicals and the charged species as can be seen by the lower ΔE (Table 4.14). The solvent description was further improved by adding the second explicit TFE molecule (SMD_{TFE} + 2×TFE) to surround the substrates and reagents. As expected, the largest stabilization effect by explicit TFE molecules was observed on the charged species, which are formed in the classical nitration method (Table 4.14).

Table 4.14: ΔE (in kcal mol^{-1}) for the formation of reaction intermediates in alternative path and in the classical nitration, calculated with three different descriptions of solvents with M06-2X functional.

Intermediate	SMD_{TFE}	SMD_{TFE} + 1×TFE	SMD_{TFE} + 2×TFE
$\Delta E(R_A)$	50.7	48.7	42.1
$\Delta E(I1_A)$	52.5	49.3	45.7
$\Delta E(I2_A)$	36.6	32.4	24.2
$\Delta E(R_C)$	72.5	62.7	44.7
$\Delta E(CT_C)$	63.8	54.1	44.5
$\Delta E(I1_C)$	29.0	11.6	3.49

4.1.7.1 Results for calculations with an implicit description of the solvent

The calculation performed with the SMD_{TFE} description of the solvent showed the alternative mechanism is less endothermic than the classical nitration. The formation of the radical species R_A ($NO_2^{\bullet}$, $CF_3CH_2O^{\bullet}$) was preferred to the formation of the charged species R_C (NO_2^+, $CF_3CH_2O^-$). Even so, the alternative mechanism consists of high ΔE steps (Figure 4.20). The individual reaction steps for the alternative path are written in Scheme 4.16 and for the classical nitration in Scheme 4.17.

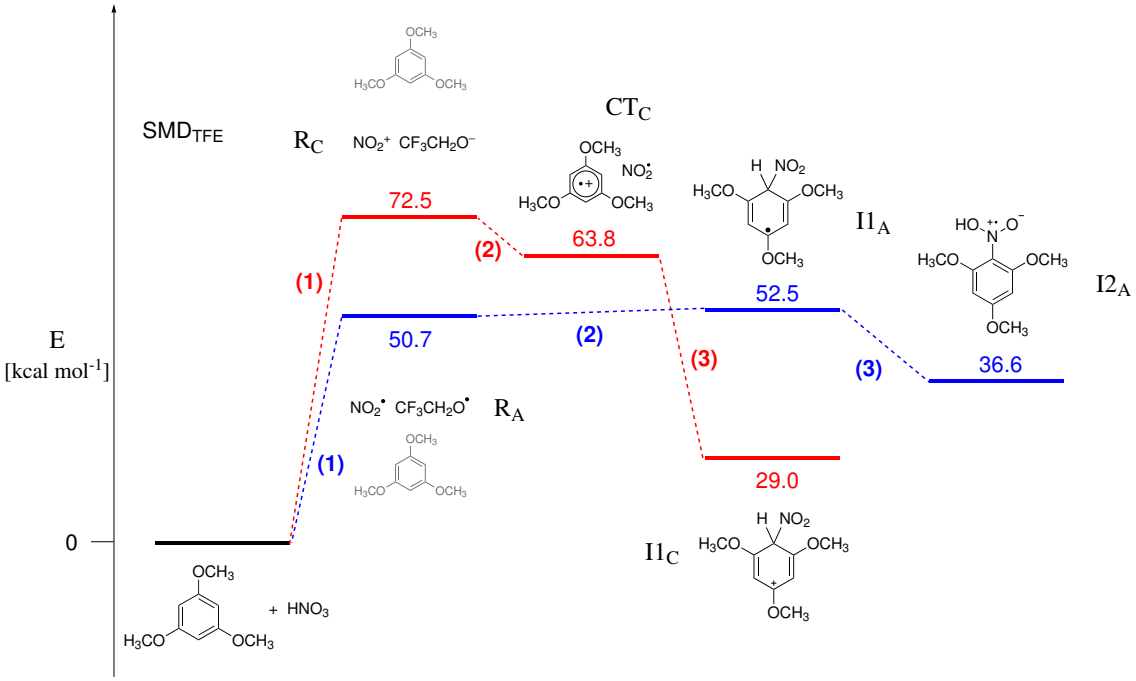
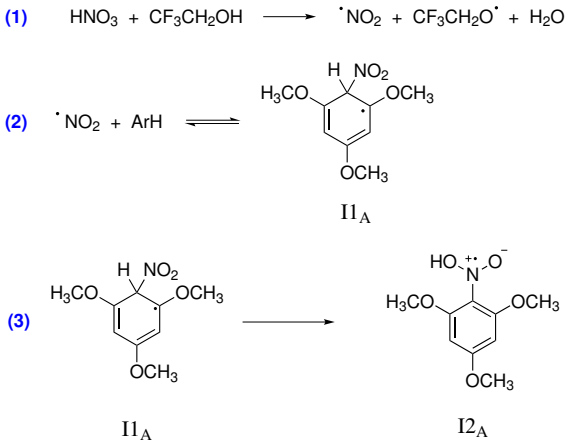
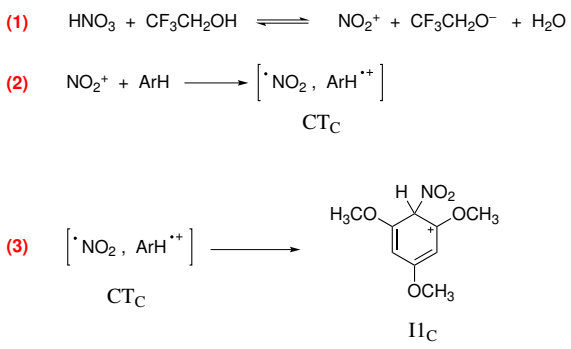


Figure 4.20: Energy profile calculated with SMD_{TFE} solvent description and M06-2X functional for alternative mechanism (blue) and classical nitration (red).

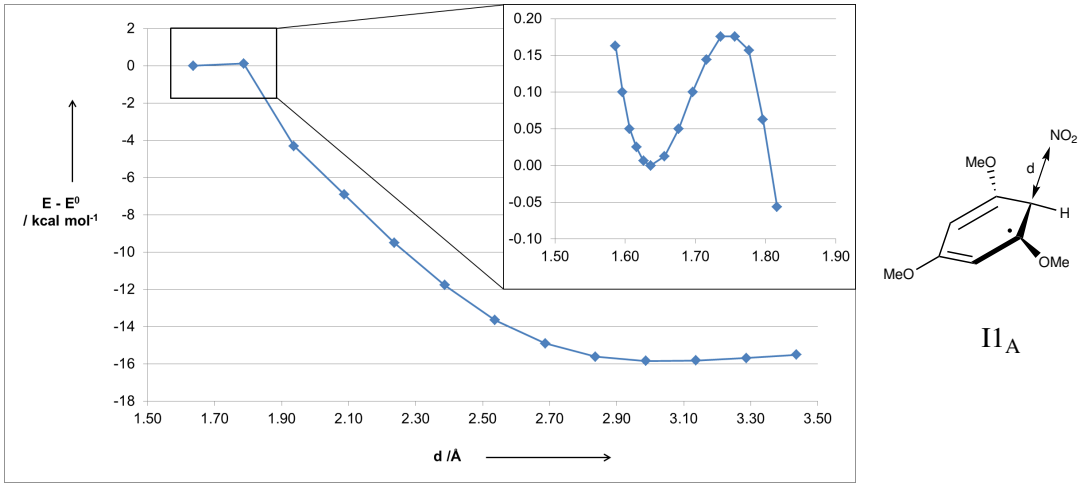


Scheme 4.16: Reaction steps in alternative mechanism.



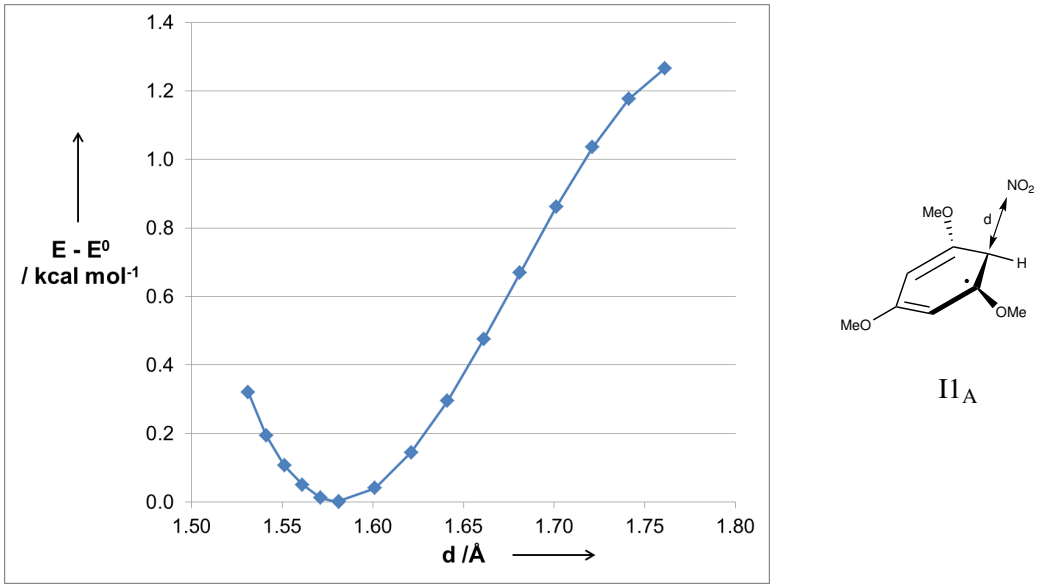
Scheme 4.17: Reaction steps in classical nitration mechanism.

$I1_A$ has a considerably higher ΔE than $I1_C$. To learn more about the nature of $I1_A$ we investigated the stability of $I1_A$ by a stepwise stretch of the C–N bond (Figure 4.21). The calculations showed $I1_A$ is a metastable intermediate with a very shallow minimum. The calculations performed with M06-2X give an energy-barrier value of only 0.18 kcal mol^{-1}. However, the calculations performed with MP2 give a larger, but still very small, energy barrier of 1.3 kcal mol^{-1} (Figure 4.22). It is worth mentioning that with B3LYP functional $I1_A$ is an unstable species.



$I1_A$

Figure 4.21: Energy profile for C–N bond stretch for $I1_A$ performed with SMD_{TFE} description of solvent and M06-2X functional. Curves are drawn to guide the eye.



$I1_A$

Figure 4.22: Energy profile for C–N bond stretch for $I1_A$ performed with SMD_{TFE} description of solvent and MP2 method. Curves is drawn to guide the eye.

Similar as for the C–N bond stretch of $I1_A$, we also evaluated the kinetic stability of σ-complex ($I1_C$). The energy profile was calculated for the formation of $I1_C$ from [$ArH^{\bullet+}$, $NO_2^{\bullet}$] (CT_C) complex with M06-2X (Figure 4.23). We found the energy barrier to form $I1_C$ from CT_C is considerable (9.0 kcal mol^{-1}).

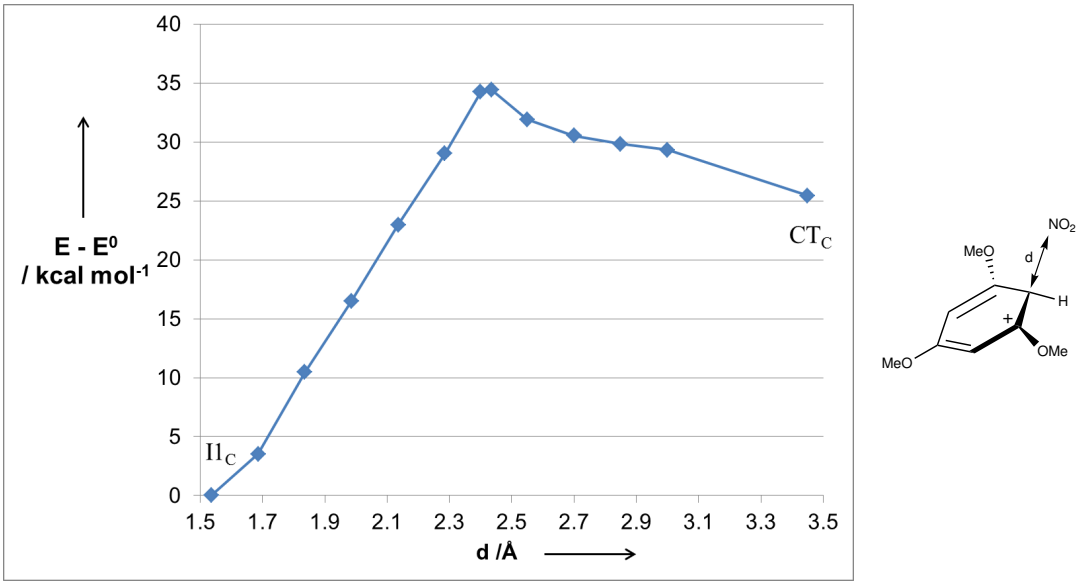
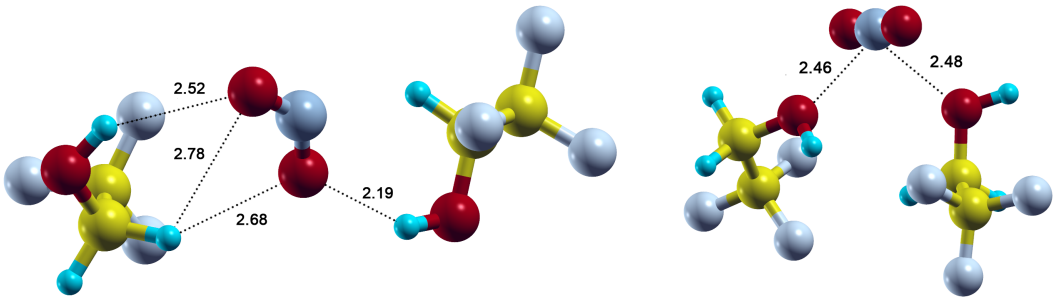


Figure 4.23: Energy profile for C-N bond stretch for $I1_C$ performed with SMD_{TFE} description of solvent and M06-2X functional. Lines are drawn to guide the eye.

4.1.7.2 Results for calculations with a hybrid implicit-explicit description of the solvent: SMD_{TFE} + 2×TFE

Adding explicit TFE molecules to the vicinity of the reagents and substrates has a stabilizing effect. The TFE molecules form hydrogen bonds with $NO_2^{\bullet}$ molecule (Figure 4.24, a). On the other hand, there are only electrostatic interactions between the negatively charged oxygen atoms of TFE and the positively charged nitrogen atom of NO_2^{+} (Figure 4.24, b).

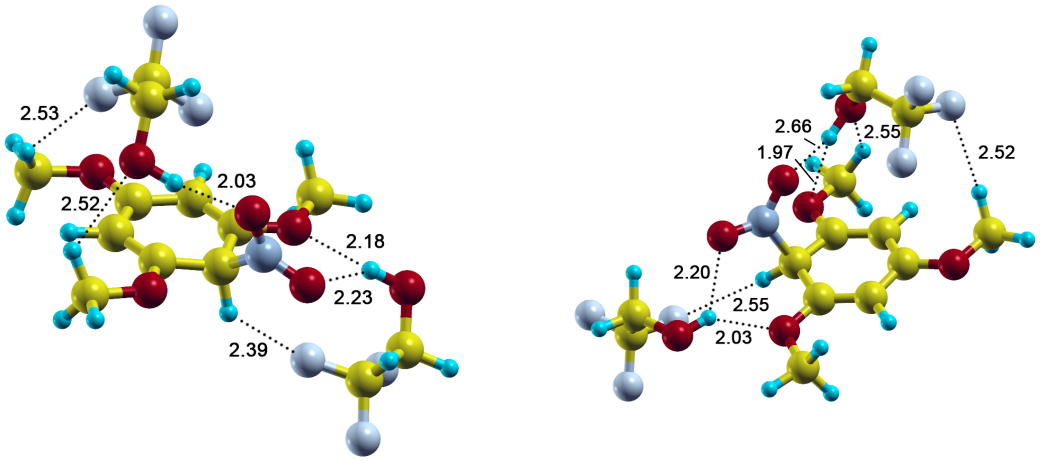


(a) $NO_2^{\bullet}$ + 2×TFE (b) NO_2^{+} + 2×TFE

Figure 4.24: Optimised structures of NO_2 + 2×TFE in SMD_{TFE} solvent calculated with and M06-2X functional.

Stabilisation by explicit TFE molecules was also observed for the aromatic intermediates. The TFE molecules formed hydrogen bonds with the nitro and methoxy groups. Due to their lengths such hydrogen bonds have moderate strength [5]. σ-complex $I1_C$ (Figure 4.25, a) had generally longer hydrogen bonds (by 0.02–0.16 Å) in comparison with $I1_A$ (Figure 4.25, b). We also observed the formation of a hydrogen bond between the hydrogen atom on the aromatic ring and the fluorine atom from the TFE molecule. The C–H$\cdots$F

hydrogen bond was shorter in $I1_C$ (2.39 Å) than in $I1_A$ (2.55 Å). Such bonds are probably weak due to the small C–H$\cdots$F angle. The addition of the second explicit TFE molecule further stabilizes the $I1_A$ and $I1_C$ intermediates.



(a) $I1_C$ + 2×TFE. (b) $I1_A$ + 2×TFE.

Figure 4.25: Complexes of TFE molecules with aromate intermediates $I1_A$ and $I1_C$ calculated with SMD_{TFE} solvent description and M06-2X functional.

$I2_A$ forms stronger complex with TFE molecules than $I1_A$, because $I2_A$ displays slightly shorter hydrogen bonds than $I1_A$ (cf. Figure 4.25, b and Figure 4.26). NO_2H group in $I2_A$ acts as donor as well as acceptor of hydrogen bonds with TFE molecules (Figure 4.26).

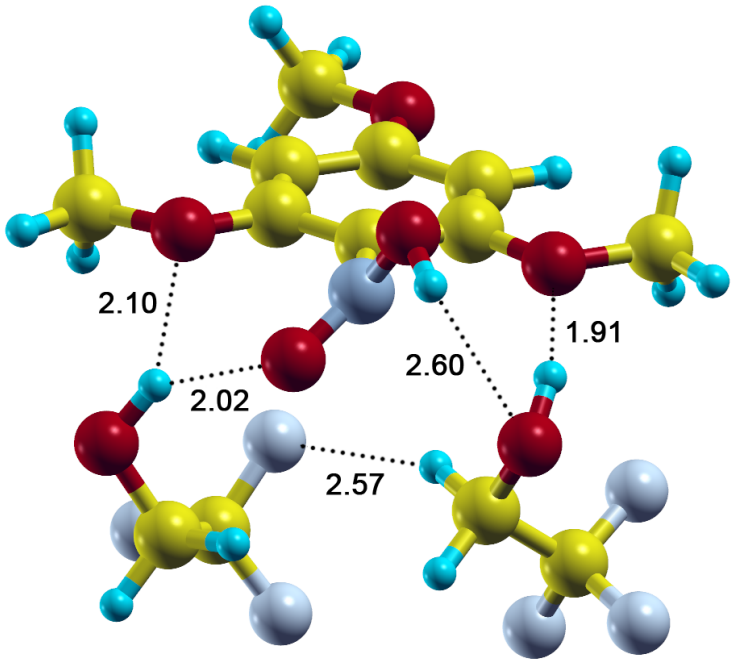


Figure 4.26: $I2_A$ and two TFE molecules calculated with SMD_{TFE} solvent description and M06-2X functional.

With explicit TFE molecules the ΔE was lower for all the species as compared to the results

obtained with only SMD_{TFE} description of the solvent. The corresponding energy profile for the reactions by an alternative path and classical nitration, performed at SMD_{TFE} + 2×TFE description of solvent is presented in Figure 4.27. On this level of the description of the solvent, the homolitic split of the N–O bond is predicted to be 2.6 kcal mol^{-1} more favourable than the heterolytic bond-break. The homolitic break of the N–O bond (R_A) has by 2.6 kcal mol^{-1}, a lower reaction energy than the heterolitic break (R_C). The formation of $I1_A$ from $NO_2^\bullet$ and **52** displays an energy barrier of 3.8 kcal mol^{-1}. The corresponding relative energy ΔE of $I1_A$ is 45.7 kcal mol^{-1}, which is marginally higher than the relative energy of CT_C of the classical path (44.5 kcal mol^{-1}, Figure 4.27). However, the transformation of CT_C to σ-complex displays an energy barrier of 9 kcal mol^{-1}. This implies that the formation of $I1_A$ is kinetically favoured with respect to the formation of $I1_C$.

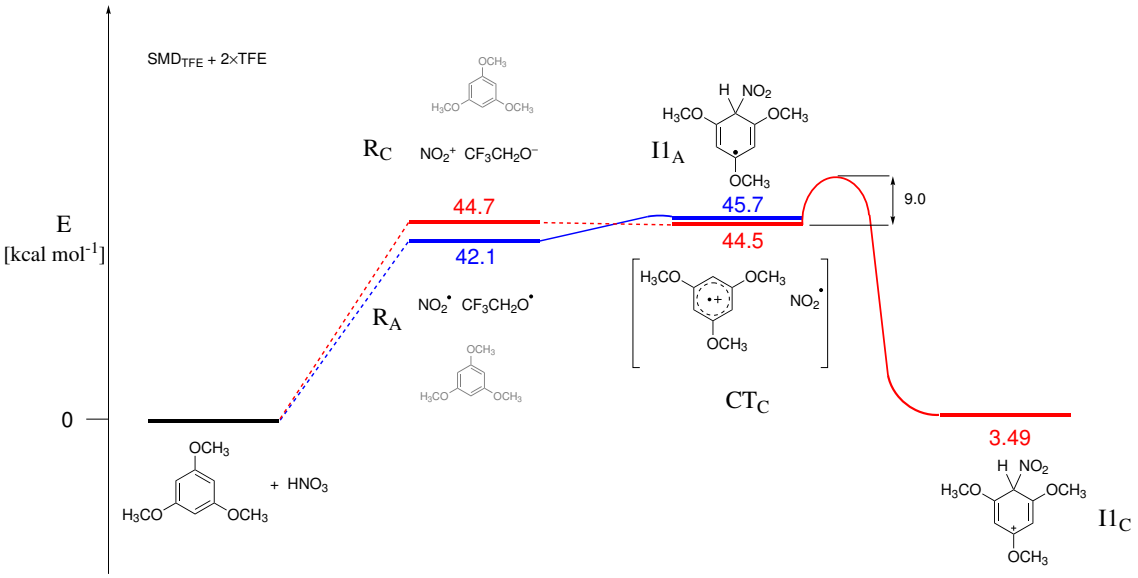


Figure 4.27: Energy profile calculated with SMD_{TFE} + 2×TFE solvent description and M06-2X functional for alternative mechanism (blue) and classical nitration (red).

The energy profile for the complete alternative mechanism, shown in Scheme 4.15 (left) as going from HNO_3 + TFE to $I1_A$, $I2_A$, $I3_A$, and finally **54** is shown in Figure 4.28. This figure reveals that the $I1_A$ is the highest energy intermediate in the whole reaction. The transformations into further intermediates are all exothermic reaction steps. During the rearrangement of $I1_A$ into $I2_A$ 21.5 kcal mol^{-1} of energy is released. In the next step $I2_A$ reacts with one molecule of **52** forming a $I3_A$ intermediate, which releases 37.5 kcal mol^{-1} of energy. In the final step there is the elimination of a hydrogen atom to form **54** (Figure 4.28, Scheme 4.18).

The calculations showed that the energies of corresponding intermediates involved in alternative and classical nitration path are similar, i.e., energy of R_C is similar to R_A and $I1_A$ is similar to CT_C (cf. Figure 4.27). This finding is in agreement with the experimental results. These experimental results show that the reaction selectivity is temperature dependant and at higher temperatures nitrated products are primarily formed. Therefore, an alternative path for the formation of bisphenylnitrosonium nitrates and nitrated products is a competitive reaction with classical nitration. An additional indicator that reactions proceed through an alternative path is the rate of reaction. Classical nitration has a 2^{nd}-order reaction rate. On the other hand, the nitration and the formation of **54** in

fluorinated alcohols show complex reaction rates, which are usually found in autocatalytic reactions. While the experimental and theoretical results indicate reaction proceeds primarily through the alternative path, they do not exclude the possibility that some reaction proceeds through classical nitration.

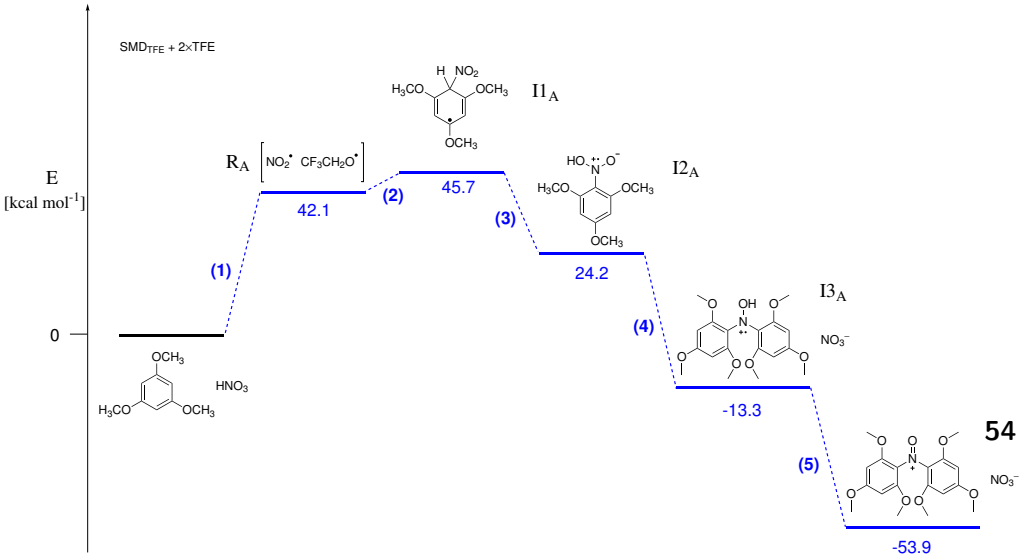
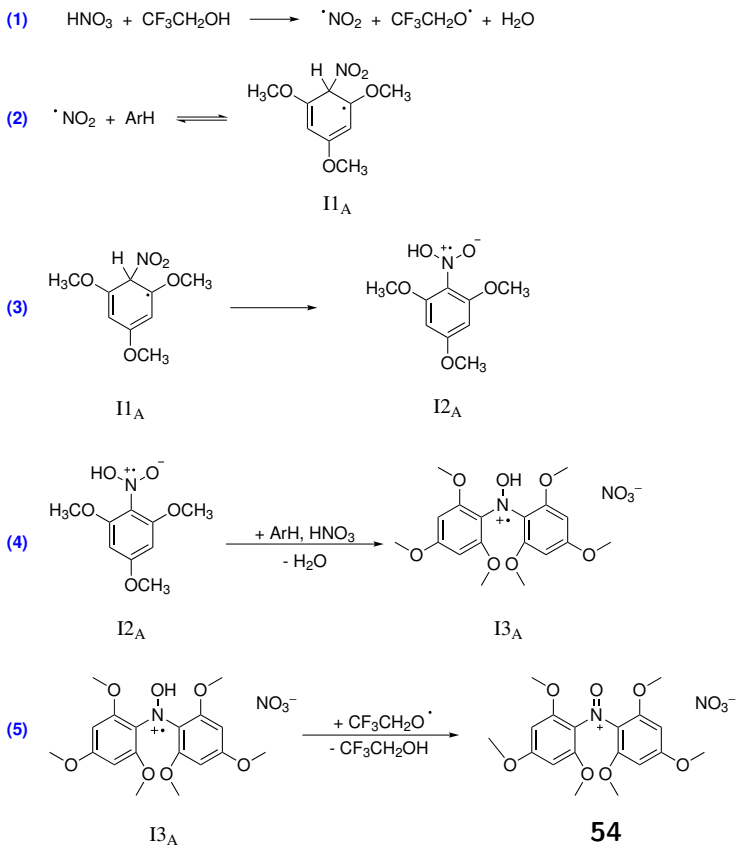


Figure 4.28: Energy profile calculated with SMD_{TFE} + 2×TFE solvent description and M06-2X functional for complete alternative mechanism for formation of **54**.



Scheme 4.18: All reaction steps involved in alternative path for formation of **54**.

4.1.8 Environmental analysis

The goal of green chemistry or sustainable chemistry is to develop new sustainable synthetic methodologies that reduce or eliminate the generation of toxic feedstocks, by-products, solvents and other associated products. At the same time, newly developed methodologies need to be economic in order to have a potential to replace the existing ones [77]. In practise, methods exhibit different "shades of green" [105]. To quantify and distinguish the effectiveness of new methods, green-chemistry metrics were proposed, such as atom economy (AE), reaction mass efficiency (RME), E factor, process mass index (PMI) [105], [106], to name a few.

The concept of atom economy (AE) was introduced by Barry Trost in 1991 [107]. In the past reaction efficiency was measured by selectivity and product yield. Atom economy was created to prompt synthetic chemists to shift their view in term of *how much* of the reactants remain in the final product. The primary goal was to maximize the incorporation of reactant atoms in final products. This method is deliberately simple, by ignoring reaction yield, molar excess of reactants as well as not taking into account solvent and other auxiliary materials. The greatest value of AE comes in the design step of new methodologies as it helps to design synthesis with greatest incorporation of reactants in the final products. AE simplicity is also its flaw, as it does not include auxiliary materials or experimental data. The ideal value for AE would be 100 %, with the whole of the reagent

$$\mathrm{AE}(\%) = \frac{\mathrm{M}_{(\mathrm{products})}}{\Sigma \mathrm{M}_{(\mathrm{reactants})}} \times 100 \tag{4.2}$$

AE - atom economy
M - molecular weight

Reaction mass efficiency (RME) tells us what percentage of the mass of the reactants remains in the product. RME is calculated by the product mass divided by the sum of the masses of the reactants. Therefore, calculations of RME include the atom economy, yield and stoichiometry of the reactants. RME is an improved AE since RME uses experimental data, such as yield and excess of the reactants, for its calculations [105], [106].

$$\mathrm{RME} = \frac{\mathrm{m}_{\mathrm{prod.}}}{\mathrm{m}_{\mathrm{reag.}}} = \eta \cdot \mathrm{AE} \cdot \frac{1}{\mathrm{SF}} \tag{4.3}$$

RME - reaction mass efficiency
η - yield
SF - stoichiometric factor

The environmental factor (E factor) was proposed by Roger Sheldon in the early 1990s. E factor is a metric which quantifies the amount of waste produced during a chemical process. Waste is defined as "anything that is not a desired product" [108]. The E factor is a complimentary green chemistry metric to AE, as E factor offers both fundamental and global evaluations of the synthetic process. The E factor is calculated as the ratio between the total mass of the waste and the mass of the desired product. Since all the waste is undesirable, the ideal value of the E factor is zero. The E factor can be calculated for individual synthetic steps or for the whole process. However, it must be stressed that E factors from individual steps are not additive. In order to determine the E factor from a multi-step synthesis, all the unrecovered waste from individual steps must be put together

and divided by the mass of the final product in the entire synthesis. Adding together the E factors from individual steps results in arbitrarily lower values [105], [106].

$$\text{"E factor"} = \frac{m_{waste}}{m_{prod.}} \tag{4.4}$$

E factor - environmental factor
m - mass (kg)

A corresponding metric to AE for global efficiency did not appear until 1998 when Heinzle *et al.* defined "mass intensity" [109]. In subsequent years "mass intensity" was renamed as "Process mass intensity" (PMI). PMI is calculated by dividing the total mass by the mass of the desired product. Total mass is defined as the "total mass of all the materials used to produce a specified mass of the product". This includes the mass of reactants, reagents, solvents used for the reaction and purification, and the catalyst. The ideal PMI has a value of 1, where all the materials put in a reactor end in the product. Theoretically, the difference between the E factor and the PMI should always be 1 (Equation 4.4). However, one of the main differences between E factor and PMI is that PMI explicitly includes water in its calculations. Also, confusion about what constitutes waste is a reason for reports with vastly different PMI and E factor [105].

$$\text{PMI} = \frac{m_{(\text{all materials})}}{m_{prod.}} = \frac{m_{waste} + m_{prod.}}{m_{prod.}} = \text{"E factor"} + 1 \tag{4.5}$$

PMI - process mass index

It is important to note that one metric does not encompass complete efficiency and greenness. Therefore, it is important to use a combination of multiple metrics to get a better picture of the evaluated methods [105].

In order to compare the new method for aromatic nitration with the old ones, we had to find literature methods and calculate their environmental parameters. Numerous methods for the introduction of a nitro group into arenes exist. Most of them proceed through electrophilic substitution of a hydrogen atom on the aromatic ring. We had to select the best representatives of various methods of aromatic nitration. We have sorted them in separate groups depending on the type of nitrating agent (HNO_3 [110]–[112], $M^+NO_3^-$ [113], akyl nitrite [80], [114]–[116], $NO_2^+X^-$ [117], $NO_{2/}N_2O_4$ [118], [119]). In some methods the nitro group is introduced into the aromatic ring through the ipso-nitration of arylboronic acids [120]–[124] or halogen atoms [125]–[129]. A second alternative path is through the oxidation of primary amines and azides [120]. To obtain a better comparison between the methods we wanted to select a model substrate that has been used in all other methods. Toluene was chosen as substrate because it was the most widely used substrate and it has great industrial importance. Therefore, methods that did not report on the nitration of toluene were not included in the evaluation.

During the evaluation of different methods, we included all the experimental details (amount of solvent, work-up procedure, isolation step...), which were gathered from research articles. Often, we were dealing with the lack of data in the experimental part of the papers. Specifically, isolation steps were not sufficiently detailed and without the data on the quantity of solvent used. Hence, some hypothetical estimations had to be made. We defined the amount of solvents used during isolation step to 10 mL of solvent per 1 mmol of initial substrate. In the case of the neutralisation of acids 5 mL of saturated aquatic solution of

$NaHCO_3$ was used as a predefiend value. The same amount of $NaHCO_3$ was also taken for the isolation procedure where only $NaHCO_3$ was reported but not quantified. Futher steps, such as washing with brine solution, washing with water, drying and separation of different isomers, was predicted to be the same for all methods, since we were using the same substrate. Therefore, it was not included in our calculations of green metrics. Some methods report the recycling of materials; however, no yield for recycling was reported. Eissen and Lenoir [130] in their evaluation of electrophilic bromination of alkenes suggested using a 95 % yield in such cases. They do point out that for practical uses ionic liquids would need to have a 99 % recycling yield to be efficient.

The economy of the process is also a very important parameter and new methods need to match the existing one in order to replace it. Besides green metrics the cost for synthesis of 1 mol of nitrotoluene was also calculated. For some of the evaluated methods the recycling of materials is crucial. Hence, the cost of repeating reactions using recycled materials was also calculated. All materials (auxiliary reagents, solvents) were included in the calculation, except for the cost for toluene, since it is the same for all methods. Costs for the reagents were gathered from the Sigma-Aldrich site (reagent price was gathered on 2. 9. 2016) and we were using the price for the similar quantity of chemical for all methods. The cost of non-commercial reagents was estimated from the cost of their preparation. The Zeolite Hβ was taken from the original article [114].

Table 4.15: Methods for aromatic nitration.

Method	Year	Reagent	Acid/Catalyst	Solvent	T [°C]	t [h]	Yield [%]	Distribution (o/m/p)
1	1834	65 % HNO_3	95 % H_2SO_4	-	r. t.	24	92	49/6/34
2	2017	65 % HNO_3	-	HFIP	r. t.	24	91	45/trace/55
3 [110]	1996	70 % HNO_3	70 % H_2SO_4/Silica-Gel	DCM	25	1.5	99	57/3/40
4 [111]	2009	95 % HNO_3	$La(NTf_2)_3$	$[NH_{444}][NTf_2]$	85	4	96.7	54/2/44
5 [112]	2012	65 % HNO_3	$Bi(OTf)_3$	1,2-DCE	84	6	94	55/4/41
6 [113]	2012	$Bi(NO_3)_3$	-	[bmim]PF_6	85	1.5	100	59/2/39
7 [113]	2012	$Bi(NO_3)_3$	-	1,2-DCE	85	23	100	48/2/50
8 [118]	1996	NO_2/O_2	$Fe(acac)_3$	1,2-DCE	0	12	>99	55/2/43
9 [119]	2011	N_2O_5	PEG_{200}-DAIL	CCl_4	50	2	97.1	54/2/44
10 [114]	1998	90 % HNO_3	Hβ	Ac_2O	r. t.	0.5	>99	18/3/79
11 [115]	2002	96 % $N(Me)_4NO_3$	Tf_2O	DCM	−78 - r. t.	24	100	62/1/37
12 [80]	2011	EAN	-	Tf_2O	−5 – r. t.	0.5	100	54/trace/28
13 [80]	2011	EAN	-	TFAA	−5 – r. t.	0.75	86	59/trace/41
14 [116]	2004	GN	85 % H_2SO_4	-	0 – 5	3	82	64/-/18

EAN - ethylamonium nitrate
GN - guanidine nitrate

Table 4.16: Green metrics for methods for aromatic nitration.

Method	Reagent	Yield	AE [%]	RME [%]	PMI	E factor	E factor (isolation)	Price [€]	Price (recycling) [€]
1	HNO_3/H_2SO_4	91	88.4	76.0	26	1.8	25	15.3	15.3
2	HNO_3/HFIP	92	88.4	80.4	35	1.4	23	1846	189
3 [110]	HNO_3/Silica−Gel	99	88.4	85.2	56	49	49	293	174
4 [111]	$HNO_3/La(NTf_2)_3$	96.7	88.4	73.7	60	0.24	53	2507	134
5 [112]	$HNO_3/Bi(OTf)_3$	94	88.4	78.1	66	26	65	163	118
6 [113]	$Bi(NO_3)_3$/[bmim]PF_6	100	28.2	20.0	106	41	102	13365	1217
7 [113]	$Bi(NO_3)_3$/1.2-DCE	100	28.2	20.0	94	41	93	321	321
8 [118]	$NO_2/O_2/Fe(acac)_3$	>99	74.5	8.7	132	38	131	1837	1837
9 [119]	N_2O_5/$PEG_2$00-DAIL	97.1	68.5	64.6	468	373	451	6772	6676
10 [114]	$AcONO_2$/Zeolite Hβ	>99	53.3	42.7	2.6	1.3	1.3	101	95
11 [115]	$C(NH_2)_3NO_3/H_2SO_4$	100	26.9	24.5	89	55	88	1824	1824
12 [80]	EAN/Tf_2O	100	28.4	12.3	79	3.55	75	1427	1328
13 [80]	EAN/TFAA	86	33.4	14.0	75	2.5	70	356	262
14 [116]	GN/H_2SO_4	82	64.0	52.5	294	23	292	186	186

Table 4.17: Isolation procedure for evaluated methods.

Method	Isolation steps
1	Addition of 2x 1 mL of DCM and 1 mL of saturated solution of $NaHCO_3$. The layer was separated and the organic layer was dried with Na_2SO_4. After the filtration of Na_2SO_4 the solvent was removed with distillation under reduced pressure.
2	HFIP was removed with distillation under reduced pressure. Addition of 2x 1 mL of DCM and 2 mL water. The organic phase was dried with Na_2SO_4. Na_2SO_4 was filtered and the solvent was removed with distillation under reduced pressure.
3	Filtration, solvent was removed with distillation under reduced pressure. Catalyst washed with solvent.
4	Extraction with solvent mixture hexane-diethy ether (estimations: 1:1 solvent volume ratio, 10 mL/mmol of toluene), washing with saturated $NaHCO_3$ solution, drying with $MgSO_4$. Solvent was removed with distillation under reduced pressure.
5	Decantation, washing flask with 1,2-DCE (estimation: 2 mL/mmol of toluene), addition of $NaHCO_3$ to get pH = 7 (estimation: 1 equivalent).
6	Extraction from ion liquid with EtOAc/Et_2O = 2:3 vol/vol (estimation: 10 mL/mmol of toluene). Organic fraction was then washed with 10 % $NaHCO_3$ (estimation 5 mL/mmol), dryed with $MgSO_4$. Solvent was removed with distillation under reduced pressure.
7	Addition of 5 mL of DCM, washing organic layer with 10 % $NaHCO_3$ (estimation 5 mL/mmol of toluene), drying with $MgSO_4$. Solvent was removed with distillation under reduced pressure.
8	Extraction with 1,2-DCE (estimation 10 mL/mmol of toluene). Organic extraction was washed with water, brine solution and dryed with Na_2SO_4. Solvent was removed with distillation under reduced pressure.
9	Filtration, washing with 10 % $NaHCO_3$ (50 mL), washing twice with water (50 mL), drying with $MgSO_4$. Solvent was removed with distillation under reduced pressure.
10	Distillation of acetic acid under reduced pressure (30 mm Hg). Distillation of substrate under reduced pressure (0.2 mm Hg, 70 ℃)
11	Reaction was stopped with 15 mL 5 % $NaHCO_{3(aq)}$. Organic phase was washed with 5x 25 mL of water. Combined water fraction were washed with 25 mL DCM. Both DCM fractions were combined and dried with $MgSO_4$. Solvent was removed with distillation under reduced pressure.
12	Reaction mixture was extracted with 3-4x with dried Et_2O or chloroform-hexane mixture (1:2) or with EtOAc/hexane=1:3 (estimation: 10 mL/mmol of toluene). Combined extractions were washed with 8 % water solution of $NaHCO_3$ (estimation: 5 mL/mmol of toluene). Followed with washing with brine solution and drying with $MgSO_4$. Solvent was removed with distillation under reduced pressure.

13	Reaction mixture was extracted with 3-4x with dried Et_2O or chloroform-hexane mixture (1:2) or with EtOAc/hexane=1:3 (estimation: 10 mL/mmol of toluene). Combined extractions were washed with 8 % water solution of $NaHCO_3$ (estimation: 5 mL/mmol of toluene). Followed with washing with brine solution and drying with $MgSO_4$. Solvent was removed with distillation under reduced pressure.
14	When reaction was complete reaction mixture was poured onto ice (100 mL). Extraction was carried out with $CHCl_3$ (4x 50 mL). Organic extractions were combined and washed with 10 % water solution of $NaHCO_3$ (2x 25 mL), water (2x 25 mL) and dried with Na_2SO_4. Solvent was removed with distillation under reduced pressure.

Methods that we used for comparison were performed on a laboratory scale. Therefore, this calculation of the green metrics represents a rough estimation. This needs to be taken into account before extrapolating the results to an industrial scale. The Sigma-Aldrich site was taken as the source for an estimation of the costs of reagents as most of the reagents were available there. However, for special chemicals, such as ionic liquids or fluorinated solvents, a lower price can be obtained with specialised distributors. AE tells us how much of the reagents are incorporated into the product, but does not take into account the auxiliary materials (solvents, catalyst) or any experimental data (yield, excess of reagents). This is why in our evaluation of the methods for aromatic nitration the best results with the AE metric were obtained for methods that used HNO_3 as a nitrating reagent. Namely, only water is formed as a side product after nitration with HNO_3 (Figure 4.29). RME is an improved AE metric as it already incorporates experimental data into the calculation. A quantitative reaction with no excess of reagents would have the same value for AE and RME. For most methods in our evaluation RME is slightly lower than AE. The best results were still obtained with methods which use HNO_3 as a nitrating agent with AE over 85 % and RME over 75 %. The lowest RME was obtained for the $NO_2/Fe(acac)_3$ method (RME = 8.7 %). Although the AE for this method is 74.5 %, which puts it just under those that use nitric acid, the use of excess of nitrating reagent results in the largest difference among the AE and RME values of the selected methods (Figure 4.29).

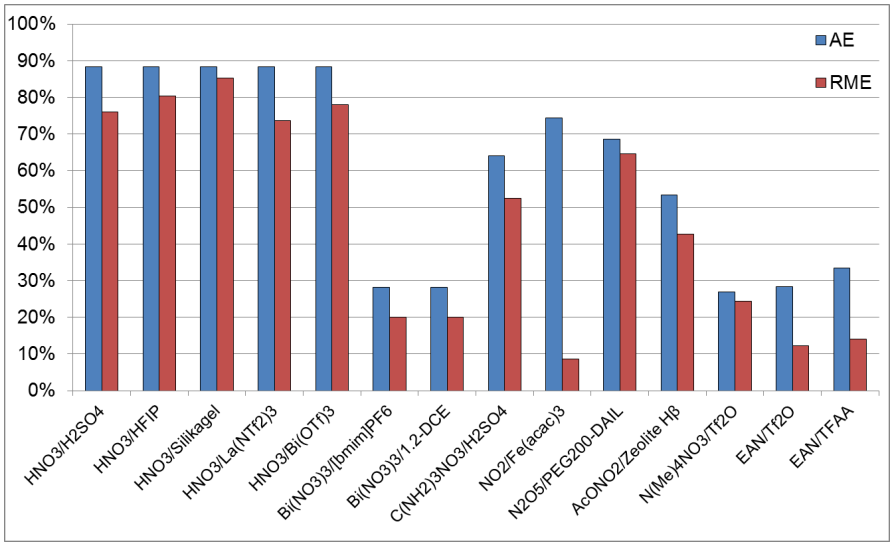


Figure 4.29: AE and RME for different methods of synthesis of nitrotoluene.

Initially, E factor included in the calculations only materials used in the reaction step. Afterwards, E factor also included an isolation step. The E factor therefore includes in the equation all the materials used in the reaction step, isolation step and purification step, except for water and recycled materials. The calculation of the PMI metric includes the reaction and the isolation. In Figure 4.30 a comparison of values for the E factor of the reaction step, and the one with an incorporated isolation step and the PMI value of various methods for the nitration of toluene is presented. To our surprise the calculation showed that classical nitration is one of the least polluting methods (E factor = 1.8, E factor(isolation) = 25, PMI = 26). Nitration with HNO_3 in HFIP had a slightly better E factor (E factor = 1.4, E factor(isolation) = 23) and a slightly worse PMI (PMI = 35) in comparison with classical nitration. The best result (E factor and PMI) was obtained for the method of Smith *et al.* [114] with only 1.3 kg of waste produced per kg of product. They did not use aqueous work-up and isolated the product by distillation. This is an energy-consuming process, but energy is not included in the calculation. This method of isolation is only suitable for volatile products. For the majority of methods, most of the waste is produced during the isolation steps.

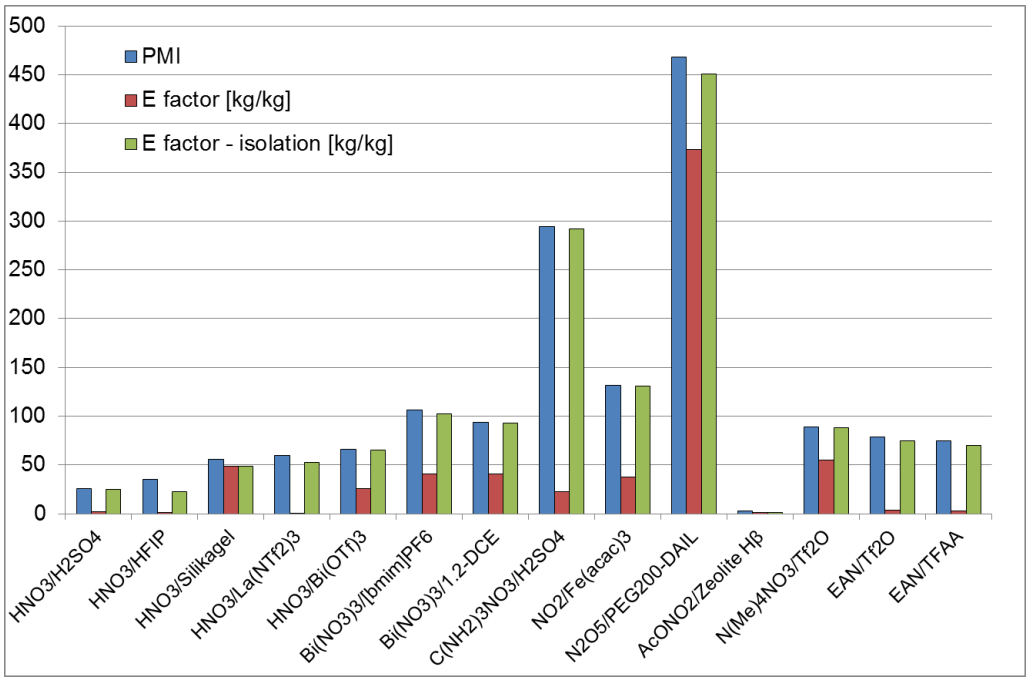


Figure 4.30: PMI and E factor for different methods of synthesis of nitrotoluene.

While most of the methods are optimised in respect to reagents and catalysts, the highest amount of waste is produced by solvents used during the reaction and in the isolation step (Figure 4.31) [105].

Next, we estimated the cost of each method as the economic aspect of developing new methods is very important and serves as an indication of the potential of the method for its application. An estimation of the cost showed that the reason for the dominant use of classical nitration in industry is its low cost compared to other known methods. For the laboratory scale synthesis of 1 mol of nitrotoluene the cost is 15.3 € (Figure 4.32). This is almost ten times more cost effective than other modern nitration methods. The method using ionic liquids was one of the most expensive methods (method 6-13 365 €). In method 9 the authors used CCl_4, which is nowadays avoided due to its high ozone depleting strength and consequently it now has a high price. Therefore, this was the second-most expensive

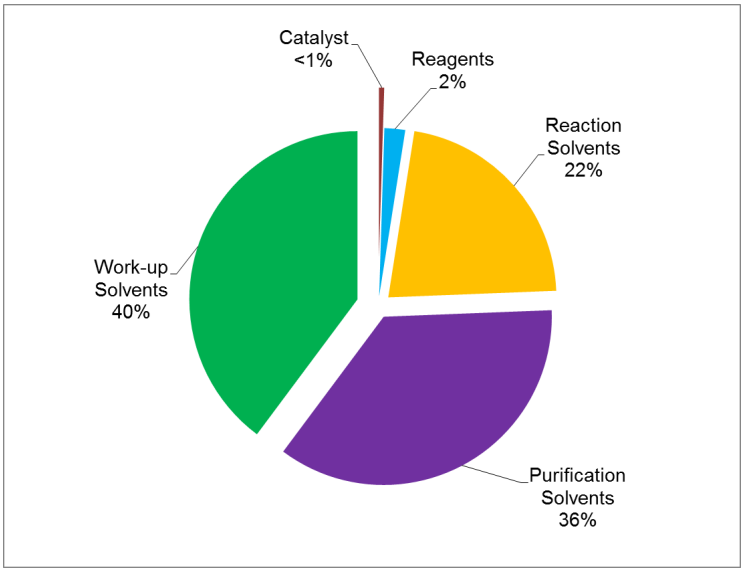


Figure 4.31: Amount of waste depending on its source.

method in our evaluation with a cost of 6772 € for 1 mol of nitrotoluene. Method 10 by Smith *et al.*, which had the lowest E factor, had the second lowest cost, with 101 € for 1 mol of nitrotoluene.

Recycling of reaction component or solvent is an important aspect in industry. We have estimated the component that could be regenerated and excluded that component from the calculation. Thus we obtained the cost of the second reaction. Calculating a cost for the reaction with recycled materials proved important, as for many methods the cost drastically decreased when recycled materials were reused. The biggest decrease of the cost due to the use of recycled materials was determined for methods 2, 4 and 6 with up to ten times of the initial reaction cost (Figure 4.32).

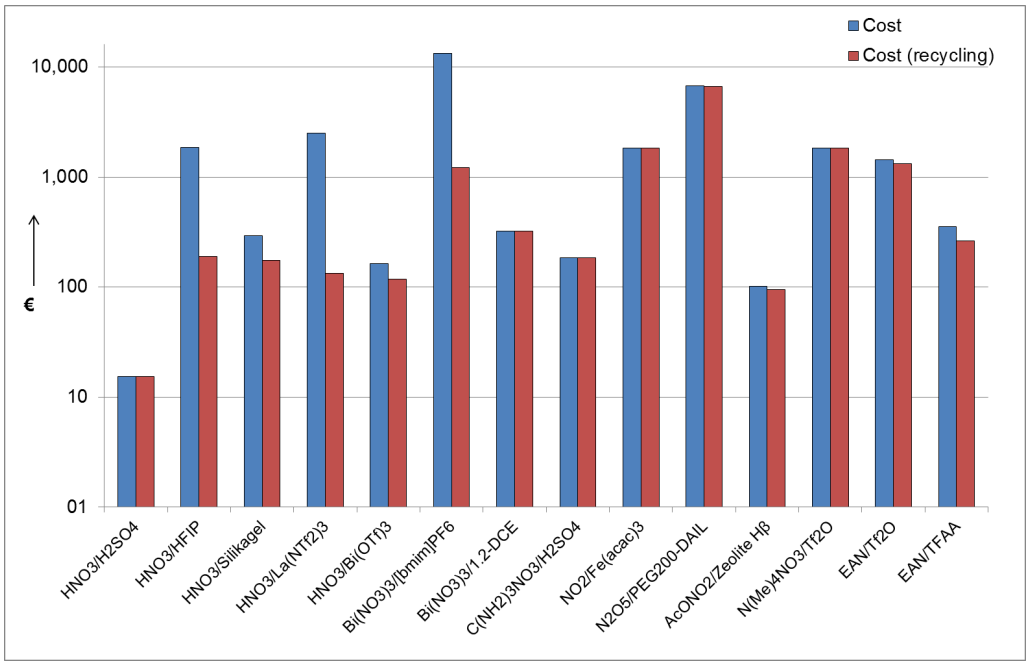


Figure 4.32: Cost for synthesis of 1 mol nitrotoluene.

4.1.9 Experimental data

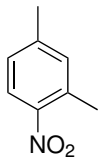
4.1.9.1 Experimental procedure for nitration of 1,3-dimethylbenzene

Aromatic nitration with mixed acids
To 1.0 mmol of 1,3-dimethylbenzene (**1**) (123.0 μL) was added (0, 0.1, 0.5, 1, 2 mmol) of H_2SO_4 followed by the addition of 1.0 mmol of HNO_3 (65 %, 69.7 μL). The reaction mixture was stirred at room temperature. The reaction conversion was followed by GC. An aliquot of reaction mixture was taken at a determined time. On a sample a mini extraction was performed by adding 0.5 mL of water and 0.5 mL of EtOAc. The mixture was mixed and then left for the phases to separate. 1 μL of organic phase was taken for GC analysis. After 6 h, 4 mL of DCM and 4 mL of water were added. The water phase was neutralised by the addition of $NaHCO_{3(s)}$. The phases were separated and the organic phase was dried with Na_2SO_4. After filtration the solvent was removed under reduced pressure. Conversion and product distribution were determined by NMR spectroscopy and the structure confirmed by a comparison with the literature data.

Aromatic nitration with mixed acids with solvent
1.0 mmol of 1,3-dimethylbenzene (**1**) (123.0 μL) was dissolved in 1 mL of MeCN. Afterwards 2 mmol of H_2SO_4 (96 %, 111.4 μL) was added and followed by the addition of 1.0 mmol of HNO_3 (65 %, 69.7 μL). The reaction mixture was stirred at room temperature. The reaction conversion was followed by GC. A sample of reaction mixture was taken at a determined time. On a sample a mini extraction was performed by adding 0.5 mL of water and 0.5 mL of EtOAc. The mixture was mixed and then left for the phases to separate. 1 μL of organic phase was taken for GC analysis. After 6 h, 4 mL of DCM and 4 mL of water were added. The water phase was neutralised by the addition of $NaHCO_{3(s)}$. The phases were separated and the organic phase was dried with Na_2SO_4. After filtration the solvent was removed under reduced pressure. Conversion and product distribution were determined by NMR spectroscopy and structure confirmed by comparison with the literature data.

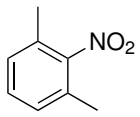
Aromatic nitration in fluorinated solvents
1.0 mmol of 1,3-dimethylbenzene (**1**) (123.0 μL) was dissolved in 1 mL of solvent (TFE, HFIP or TFA) followed by the addition of 1.0 mmol of HNO_3 (65 %, 69.7 μL). The reaction mixture was stirred at room temperature. The reaction conversion was followed by GC. A sample of reaction mixture was taken at a determined time. On a sample a mini extraction was performed by adding 0.5 mL of water and 0.5 mL of EtOAc. The mixture was mixed and then left for the phases to separate. 1 μL of organic phase was taken for the GC analysis. After 6 h, 4 mL of DCM and 4 mL of water were added. The water phase was neutralised by the addition of $NaHCO_{3(s)}$. The phases were separated and the organic phase was dried with Na_2SO_4. After filtration the solvent was removed under reduced pressure. The conversion and product distribution were determined by NMR spectroscopy and the structure was confirmed by comparison with the literature data.

2,4-Dimethyl-nitrobenzene - (**2**) [131]



$C_8H_9NO_2$, MW = 151.16
Reaction solvent: TFA
Mobile phase for column chromatography: DCM/*n*-Hex = 1/2
Yield: 42 %, 197.3 mg , yellow oil
^{1}H NMR (300 MHz, $CDCl_3$): δ 2.40 (s, 3H), 2.59 (s, 3H), 7.13 (m, 2H), 7.92 (m, 1H)
^{13}C NMR (76 MHz, $CDCl_3$): δ 20.58, 21.18, 124.77, 127.36, 133.25, 133.67, 144.10, 146.80
IR ν_{max} (cm^{-1}): 2930, 1613, 1589, 1511, 1338, 835, 749
HR-MS (ESI^+): calculated ($C_8H_{10}NO_2$) 152.0712, measured ($C_8H_{10}NO_2$) 152.0715

2,6-Dimethyl-nitrobenzene - (**3**) [124]



$C_8H_9NO_2$, MW = 151.16
Reaction solvent: TFA
Mobile phase for column chromatography: DCM/*n*-Hex = 1/2
Yield: 4 %, 11 mg, yellow oil
^{1}H NMR (300 MHz, $CDCl_3$): δ 2.31 (s, 6H), 7.12 (m, 2H), 7.26 (m, 1H)

4.1.9.2 Experimental procedure for study of the effect of the ratio solvent/substrate

1.0 mmol of 1,3-dimethylbenzene (**1**) (123.0 μL) was dissolved in (0.1, 0.2, 0.5, 1, 2. 5 mL) of HFIP followed by the addition of 1.0 mmol of HNO_3 (65 %, 69.7 μL). The reaction mixture was stirred at room temperature. After 5 h, 4 mL of DCM and 4 mL of water were added. The water phase was neutralised by the addition of $NaHCO_{3(s)}$. The phases were separated and the organic phase was dried with Na_2SO_4. After filtration the solvent was removed under reduced pressure. Conversion and product distribution were determined by NMR spectroscopy and the structure was confirmed by a comparison with the literature data.

4.1.9.3 Substrate scope

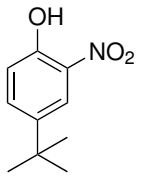
Aromatic nitration with mixed acids (Procedure A)
To 1.0 mmol of substrate was added (0 or 1 mL) of MeCN. Afterwards, 2 mmol of H_2SO_4 (96 %, 111.4 μL) was added followed by the addition of 1.0 mmol of HNO_3 (65 %, 69.7 μL). The reaction mixture was stirred at room temperature. The reaction conversion was followed by TLC. When the reaction was complete, 4 mL of DCM and 4 mL of water were added. The water phase was neutralised by the addition of $NaHCO_{3(s)}$. The phases

were separated and the organic phase was dried with Na_2SO_4. After filtration the solvent was removed under reduced pressure. The conversion and product distribution were determined by NMR spectroscopy and the structure confirmed by a comparison with the literature data.

Aromatic nitration in fluorinated alcohols (Procedure B)
1.0 mmol of substrate was dissolved in 1 mL of solvent (TFE or HFIP) followed by the addition of 1.0 mmol of HNO_3 (65 %, 69.7 μL). Reaction conversion was followed by TLC. When the reaction was complete, 4 mL of DCM was added and dried with Na_2SO_4. After filtration the solvent was removed under reduced pressure. The conversion and product distribution were determined by NMR spectroscopy and GC analysis and structure was confirmed by comparison with the literature data.

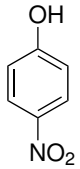
Aromatic nitration in trifluoroacetic acid (Procedure C)
1.0 mmol of substrate was dissolved in 1 mL of solvent TFA which was followed by the addition of 1.0 mmol of HNO_3 (65 %, 69.7 μL). The reaction conversion was followed by TLC. After the end of reaction 6 mL of H_2O and 6 mL of DCM were added. The water phase was neutralised by the addition of $NaHCO_{3(s)}$. After neutralisation the organic phase was separated and dried with Na_2SO_4. After filtration the solvent was removed under reduced pressure. The conversion and product distribution were determined by NMR spectroscopy and the structure confirmed by comparison with the literature data.

4-*t*-Bu-2-nitrophenol - (**6b**) [132]



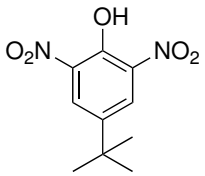
$C_{10}H_{13}NO_3$, MW = 195.22
Yield: 48 %, 92.8 mg, yellow oil
Reaction conditions: Procedure B
Mobile phase for column chromatography: DCM/*n*-Hex/CH_3COOH = 1/1/0.01
^{1}H NMR (300 MHz, $CDCl_3$): δ 1.33 (s, 9H), 7.10 (d, J = 8.9 Hz, 1H), 7.64 (dd, J = 8.9 Hz, J = 2.8 Hz, 1H), 8.07 (d, J = 2.4 Hz, 1H), 10.47 (br, 1H)
^{13}C NMR (76 MHz, $CDCl_3$): δ 31.02, 34.32, 119.49, 120.87, 133.00, 135.42, 143.67, 153.03
IR ν_{max} (cm^{-1}): 3251, 2964, 1629, 1533, 1318, 832, 588
HR-MS (ESI^+): calculated ($C_{10}H_{12}NO_3$) 194.0817, measured ($C_{10}H_{12}NO_3$) 194.0813

4-Nitrophenol - (**6c**) [133]



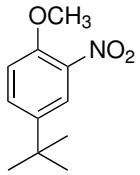
$C_6H_5NO_3$, MW = 139.03
Reaction conditions: Procedure B
Mobile phase for column chromatography: DCM/*n*-Hex/CH_3COOH = 1/1/0.01
Yield: 12 %, 16.3 mg, yellow powder
^{1}H NMR (300 MHz, $CDCl_3$): δ 7.69 (m, 2H), 8.17 (m, 2H), 10.86 (br, 1H)

4-*t*-Bu-2,6-dinitrophenol - (**6d**) [134]



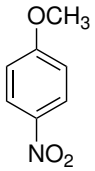
$C_{10}H_{12}N_2O_5$, MW = 240.07
Reaction conditions: Procedure B
Mobile phase for column chromatography: DCM/*n*-Hex/CH_3COOH = 1/1/0.01
Yield: 6 %, 15.3 mg, yellow oil
^{1}H NMR (300 MHz, $CDCl_3$): δ 1.38 (s, 9H), 8.33 (s, 2H), 11.30 (br, 1H)

4-*t*-Bu-2-nitroanisole - (**7b**) [135]



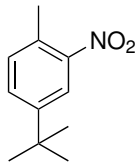
$C_{11}H_{15}NO_3$, MW = 209.11
Reaction conditions: Procedure B
Mobile phase for column chromatography: DCM/*n*-Hex = 1/1
Yield: 67 %, 106.4 mg, yellow oil
^{1}H NMR (300 MHz, $CDCl_3$): δ 1.32 (s, 9H), 3.94 (s, 3H), 7.03 (d, J = 8.9 Hz, 1H), 7.56 (dd, J = 8.7 Hz, J = 2,4 Hz, 1H), 7.84 (d, J = 2.6 Hz, 1H)
^{13}C NMR (76 MHz, $CDCl_3$): δ 31.13, 34.27, 56.51, 113.21, 122.49, 131.24, 139.16, 143.74, 150.75
IR ν_{max} (cm^{-1}): 2963, 1621, 1526, 1350, 1268, 1018, 829, 819, 630
HR-MS (ESI^+): calculated ($C_{11}H_{16}NO_3$) 210.1130, measured ($C_{11}H_{16}NO_3$) 210.1124

4-Nitroanisole - (**7**) [124]



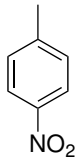
$C_6H_5NO_3$, MW = 139.11
Reaction conditions: Procedure B
Mobile phase for column chromatography: DCM/*n*-Hex = 1/1
Yield: 27 %, 41.5 mg, white powder
^{1}H NMR (300 MHz, $CDCl_3$): δ 3.91 (s, 3H), 6.97 (m, 2H), 8.20 (m, 2H)
^{13}C NMR (76 MHz, $CDCl_3$): δ 56.92, 113.95, 125.84, 141.43, 164.54
IR ν_{max} (cm^{-1}): 1590, 1495, 1329, 845, 750, 616
$\boldsymbol{T}_{MP}$**:** 51,3 – 52,1 ℃ (Lit.: 54 ℃)

4-*t*-Bu-2-nitrotoluene - (**8b**) [136]



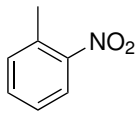
$C_{11}H_{15}NO_2$, MW = 193.24
Reaction conditions: Procedure C
Mobile phase for column chromatography: gradient change from DCM/*n*-Hex = 1/4 to DCM/*n*-Hex = 3/1
Yield: 59 %, 114.7 mg, yellow oil
^{1}H NMR (300 MHz, $CDCl_3$): δ 1.34 (s, 9H), 2.56 (s, 3H), 7.26 (d, J = 7.9 Hz, 1H), 7.52 (dd, J = 7.9 Hz, J = 2,0 Hz, 1H), 7.97 (d, J = 2.0 Hz, 1H)
^{13}C NMR (76 MHz, $CDCl_3$): δ 19.92, 31.05, 34.65, 121.43, 130.19, 130.48 132.41, 149.03, 150.61
IR ν_{max} (cm^{-1}): 2965, 2871, 1524, 1343, 830
HR-MS (ESI^+): calculated ($C_{11}H_{16}NO_2$) 194.1181, measured ($C_{11}H_{16}NO_2$) 194.1186

4-Nitrotoluene - (**8c**) [124]



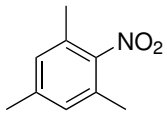
$C_7H_7NO_2$, MW = 137.14
Reaction conditions: Procedure C
Mobile phase for column chromatography: gradient change from DCM/*n*-Hex = 1/4 to DCM/*n*-Hex = 3/1
Yield: 3 %, 4.2 mg, yellow oil
^{1}H NMR (300 MHz, $CDCl_3$): δ 2.47 (s, 3H), 7.32 (m, 2H), 8.12 (m, 2H)

2-Nitrotoluene - (**9b**) [124]



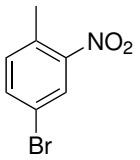
$C_7H_7NO_2$, MW = 137.14
Reaction conditions: Procedure B
Isolated 107.8 mg mixture of 2-nitrotoluene and 4-nitrotoluene (2-NO_2/4-NO_2) = 53/47)
^{1}H NMR (300 MHz, $CDCl_3$): δ 2.60 (s, 3H), 7.30 (m, 2H), 7.50 (td, J = 7.5 Hz, J = 1.5 Hz, 1H), 7.95 (dd, J = 8.7 Hz, J = 1.5 Hz, 1H)

2-Nitromesitylene - (**10b**) [137]



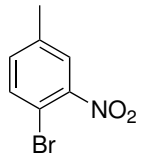
$C_9H_{11}NO_2$, MW = 165.19
Reaction conditions: Procedure B
Yield: 100 %, 151 mg, yellow oil
^{1}H NMR (300 MHz, $CDCl_3$): δ 2.28 (s, 6H), 2.31 (s, 3H), 6.92 (s, 2H)
^{13}C NMR (76 MHz, $CDCl_3$): δ 17.37, 20.88, 129.32, 130.29, 140.20, 149.67
IR ν_{max} (cm^{-1}): 2928, 1518, 1363, 853, 834, 603

4-Bromo-2-nitrotoluene - (**11b**) [138]



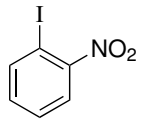
$C_7H_6BrNO_2$, MW = 216.03
Reaction conditions: Procedure C
Mobile phase for column chromatography: DCM/*n*-Hex = 10/1
Yield: 166.5 mg mixture of all products (**11b**/**11c**/**8c** = 50/32/7)
^{1}H NMR (300 MHz, $CDCl_3$): δ 2.55 (s, 3H), 7.28 (d, J = 8.2 Hz, 1H), 7.64 (dd, J = 7.9 Hz, J = 1.8 Hz, 1H), 8.11 (d, J = 2.1 Hz, 1H)

4-Bromo-3-nitrotoluene - (**11c**) [139]



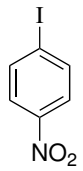
$C_7H_6BrNO_2$, MW = 216.03
Reaction conditions: Procedure C
Mobile phase for column chromatography: DCM/*n*-Hex = 10/1
Yield: 166.5 mg mixture of all products (**11b**/**11c**/**8c** = 50/32/7)
^{1}**H NMR (300 MHz, CDCl$_3$):** δ 2.55 (s, 3H), 7.28 (d, J = 8.2 Hz, 1H), 7.64 (dd, J = 7.9 Hz, J = 1.8 Hz, 1H), 8.11 (d, J = 2.1 Hz, 1H)

2-Nitroiodobenzene - **12b** [140]



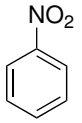
$C_6H_4INO_2$, MW = 249.01
Reaction conditions: Procedure C
Mobile phase for column chromatography: DCM
Yield: 91 %, 226.5 mg mixture of **12b** and **12d** (24:76)
^{1}**H NMR (300 MHz, CDCl$_3$):** δ 7.27 (m, 1H), 7.50 (m, 1H), 7.86 (dd, J = 8.1 Hz, J = 1.7 Hz, 1H), 8.05 (dd, J = 7.9 Hz, J=1.4 Hz, 1H)

4-Nitroiodobenzene - **12d** [141]



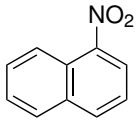
$C_6H_4INO_2$, MW = 249.01
Reaction conditions: Procedure C
Mobile phase for column chromatography: DCM
Yield: 91 %, 226.5 mg mixture of **12b** and **12d** (24:76)
^{1}**H NMR (300 MHz, CDCl$_3$):** δ 7.90-7.97 (m, 4H))

Nitrobenzene - (**14**) [124]



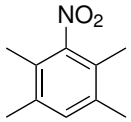
$C_6H_5NO_2$, MW = 123.11
Reaction conditions: Procedure C
Yield: 98 %, 106.1 mg, yellow oil
^{1}H NMR (300 MHz, $CDCl_3$): δ 7,55 (m, 2H) ,7,71 (m, 1H), 8.24 (m, 2H)
^{13}C NMR (76 MHz, $CDCl_3$): δ 123.32, 129.20, 134.51, 148.06
IR ν_{max} (cm^{-1}): 2923, 1519, 1344, 851, 729, 701, 680

1-Nitronaphthalene - (**16**) [124]



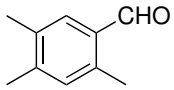
$C_{10}H_7NO_2$, MW = 173.17
Reaction conditions: Procedure B
Mobile phase for column chromatography: gradient change from DCM/EtOH = 10/1 **Yield**: 89 %, 154 mg, orange powder
^{1}H NMR (300 MHz, $CDCl_3$): δ 7.54 (t, J = 7.8 Hz, 1H), 7.72 (ddd, J = 8.2 Hz, J = 7.0 Hz, J = 1.2 Hz 1H), 7.62 (ddd, J = 8.4, J = 6.9, J = 1.4 Hz Hz, 1H), 7.95 (d, J = 8.1 Hz, 1H), 8.12 (d, J = 8.2 Hz, 1H), 8.23 (dd, J = 7.6 Hz, J = 1.2 Hz, 1H), 8.57 (d, J = 8.7 Hz, 1 H)
^{13}C NMR (76 MHz, $CDCl_3$): δ 123.00, 123.91, 124.04, 125.02, 127.26, 128.52, 129.35, 134.24, 134.59, 146.47
IR ν_{max} (cm^{-1}): 1600, 1515, 1335, 803, 759
***T*$_{MP}$:** 54,3 – 55,5 °C (Lit.: 56 – 59 °C)
HR-MS (ESI^+): calculated ($C_{10}H_8NO_2$) 174.0555, measured ($C_{10}H_8NO_2$) 174.0559

Nitrodurene - (**19**) [142]



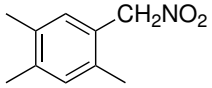
$C_{10}H_{13}NO_2$, MW = 179.22
Reaction conditions: Procedure B
Mobile phase for column chromatography: DCM/*n*-Hex = 1/1
Yield: 41 %, 81 mg, white crystals
^{1}H NMR (300 MHz, $CDCl_3$): δ 2.12 (s, 6H), 2.25 (s, 6H), 7.04 (s, 1H)
^{13}C NMR (76 MHz, $CDCl_3$): δ 13.90, 19.61, 124.25, 132.34, 135.22, 153.07
IR ν_{max} (cm^{-1}): 2924, 1494, 1380, 1013, 898, 769
***T*$_{MP}$:** 97,7 °C – 99,7 °C (Lit.: 113 °C)

2,4,5-Trimethylbenzaldehide - (**20**) [142]



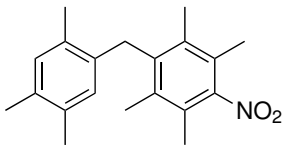
$C_{10}H_{12}O$, MW = 148.20
Reaction conditions: Procedure B
Mobile phase for column chromatography: DCM/*n*-Hex = 1/1
Yield: 10 %, 16 mg, orange oil
^{1}H NMR (300 MHz, $CDCl_3$): δ 2.29 (s, 6H), 2.59 (s, 3H), 7.03 (s, 1H), 7.55 (s, 1H), 10.19 (s, 1H)
^{13}C NMR (76 MHz, $CDCl_3$): δ 18.84, 19.05, 19.96, 132.09, 133.01, 133.13, 134.57, 138.05, 143.38, 192.52
IR ν_{max} (cm^{-1}): 3676, 2972, 1684, 1264, 1066, 735, 704
HR-MS (ESI^+): calculated ($C_{10}H_{13}O$) 149.0966, measured ($C_{10}H_{13}O$) 149.0963

1,2,4-Trimethyl-5-(nitromethyl)benzene - (**22**) [142]



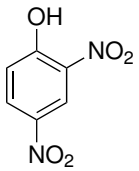
$C_{10}H_{13}NO_2$, MW = 179.22
Reaction conditions: Procedure B
Mobile phase for column chromatography: DCM/*n*-Hex = 1/1
Yield: 7 %, 14 mg, yellow oil
^{1}H NMR (300 MHz, $CDCl_3$): δ 2.24 (s, 6H), 2.32 (s, 3H), 5.42 (s, 2H), 7.03 (s, 1H), 7.11 (s, 1H)

1,2,4,5-Tetramethyl-3-nitro-6-(2,4,5-trimethylbenzyl)benzene - (**23**) [143]



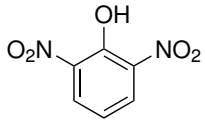
$C_{20}H_{25}NO_2$, MW = 311.42
Reaction conditions: Procedure B
Mobile phase for column chromatography: DCM/*n*-Hex = 1/1
Yield: 1 %, 3.5 mg, white solid
^{1}H NMR (300 MHz, $CDCl_3$): δ 2.07 (s, 3H), 2.11 (s, 6H), 2.19 (s, 9H), 2.36 (s, 3H), 3.88 (s, 2H), 6.20 (s, 1H), 6.99 (s, 1H)
^{13}C NMR (76 MHz, $CDCl_3$): δ 15.04, 16.24, 19.14, 19.31, 29.70, 33.15, 124.12, 127.50, 131.41, 133.19, 133.89, 134.11, 135.10, 138.88, 152.19, 163.94

2,4-Dinitrophenol - (**25**) [144]



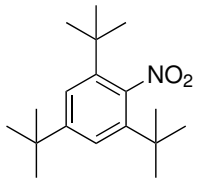
$C_6H_4N_2O_5$, MW = 184.11
Reaction conditions: Procedure B
Mobile phase for column chromatography: DCM/CH_3COOH = 10/0.1
Yield: 16 % 30.0 mg (mixture of **25**/**26** = 82/18)
^{1}H NMR (300 MHz, $CDCl_3$): δ 7.35 (d, J = 9.2 Hz, 1H), 8.47 (dd, J = 9.3, 2.8 Hz, 1H), 9.09 (d, J = 2.8 Hz, 1H), 11.02 (brs, 1H)

2,6-Dinitrophenol - (**26**) [145]



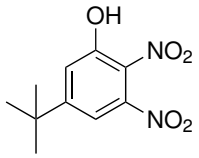
$C_6H_4N_2O_5$, MW = 184.11
Reaction conditions: Procedure B
Mobile phase for column chromatography: DCM/CH_3COOH = 10/0.1
Yield: 16 % 30.0 mg (mixture of **25**/**26** = 82/18)
^{1}H NMR (300 MHz, $CDCl_3$): δ 7.17 (t, J = 8.3 Hz, 1H), 8.35 (d, J = 8.3 Hz, 2H), 11.48 (br s, 1H)

2,4,6-Tri(*terc*-butyl)-nitrobenzene - (**28**) [146]



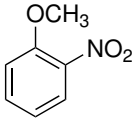
$C_{18}H_{29}NO_2$, MW = 291.43
Reaction conditions: Procedure C
Mobile phase for column chromatography: n-Hex
Yield: 68 %, 198.4 mg, white crystals
^{1}H NMR (300 MHz, $CDCl_3$): δ 1.32 (s, 9H), 1.38 (s, 18H), 7.44 (s, 2H)
^{13}C NMR (76 MHz, $CDCl_3$): δ 32.23, 35.16, 36.28, 123.50, 140.09, 147.04, 151.31
IR ν_{max} (cm^{-1}): 2962, 1528, 1376, 1364, 878, 841, 768
$\boldsymbol{T}_{MP}$**:** 202 - 203 ℃ (Lit. 205 - 206 ℃)

5-*t*-Butyl-2,3-dinitrophenol - (**29**) [147]



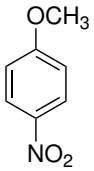
$C_{10}H_{12}N_2O_5$, MW = 240.21
Reaction conditions: Procedure C
Mobile phase for column chromatography: *n*-Hex
Yield: 4 %, 8.5 mg, yellow powder
^{1}H NMR (300 MHz, $CDCl_3$): δ 1.50 (s, 9H), 8.46 (d, J = 2.8 Hz, 1H), 8.97 (d, J = 2.8 Hz, 1H), 12.01 (br, 1H)
^{13}C NMR (76 MHz, $CDCl_3$): δ 28.97, 36.22, 119.64, 128.58, 133.11, 139.24, 142.89, 158.89
IR ν_{max} (cm^{-1}): 3107, 2971, 1606, 1560, 1339, 1268, 1148, 704
$\boldsymbol{T}_{MP}$**:** 103 - 115 ℃ (Lit. 124 - 125 ℃)
HR-MS (ESI^-): calculated ($C_{10}H_{11}N_2O_5$) 239.0668, measured ($C_{10}H_{11}N_2O_5$) 239.0671

2-Nitroanisole - (**31**) [148]



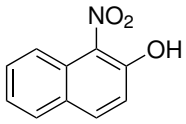
$C_7H_7NO_3$, MW = 153.14
Reaction conditions: Procedure B
Mobile phase for column chromatography: DCM/*n*-Hex = 1/1
Yield: 26 %, 40.2 mg, white powder
^{1}H NMR (300 MHz, $CDCl_3$): δ 3.96 (s, 3H), 7.03 (ddd, J = 8.1 Hz, J = 7.5 Hz, J = 1.2 Hz, 1H), 7.09 (dd, J = 8.6 Hz, J = 1.2 Hz, 1H), 7.55 (ddd, J = 8.4 Hz, J = 7.3 Hz, J = 1.7 Hz, 1H), 7.84 (dd, J = 8.1 Hz, J = 1.7 Hz, 1H)
^{13}C NMR (76 MHz, $CDCl_3$): δ 56.41, 113.42, 120.20, 125.62, 134.19, 139.63, 152.90
IR ν_{max} (cm^{-1}): 2497, 2845, 1608, 1519, 1489, 1348, 1276, 1256, 1165, 1016, 855, 741, 662

4-Nitroanisole - (**32**) [124]



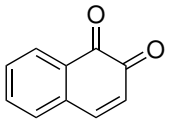
$C_7H_7NO_3$, MW = 153.14
Reaction conditions: Procedure B
Mobile phase for column chromatography: DCM/*n*-Hex = 1/1
Yield: 27 %, 41.9 mg, white powder
^{1}H NMR (300 MHz, $CDCl_3$): δ 3.91 (s, 3H), 6.97 (m, 2H), 8.20 (m, 2H)
^{13}C NMR (76 MHz, $CDCl_3$): δ 55.92, 113.95, 125.84, 141.43, 164.54
IR ν_{max} (cm^{-1}): 1607, 1589, 1496, 1329, 1261, 1173, 1105, 845, 750, 691
$\boldsymbol{T}_{MP}$**:** 51.3 – 52.1 ℃ (Lit. 54 ℃)

1-Nitronaphthalen-2-ol - (**35**) [149]



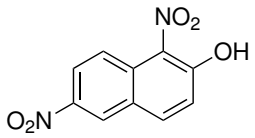
$C_{10}H_7NO_3$, MW = 189.17
Reaction conditions: Procedure B
Mobile phase for silica plate chromatography: DCM/*n*-Hex = 9/1
Yield: 33 %, 62 mg, yellow crystals
^{1}H NMR (300 MHz, $CDCl_3$): δ 7.24 (d, J = 9.2 Hz, 1H), 7.50 (m, 1H), 7.72 (m, 1H), 7.80 (m, 1H), 7.99 (d, J = 9.2 Hz, 1H), 8.90 (m, 1H), 12.18 (s, 1H)
^{13}C NMR (76 MHz, $CDCl_3$): δ 119.28, 123.15, 125.57, 126.81, 128.05, 128.59, 129.24, 130.90, 139.15, 158.77
IR ν_{max} (cm^{-1}): 2922, 1621, 1432, 1376, 1133, 838, 758, 731
$\boldsymbol{T}_{MP}$**:** 98.0 – 102.9 ℃ (Lit. 100 - 102 ℃
HR-MS (ESI^-): calculated ($C_{10}H_6NO_3$) 188.0344, measured ($C_{10}H_6NO_3$) 188.0348

Naphthalene-1,2-dione - (**36**) [150]



$C_{10}H_6O_2$, MW = 158.15
Reaction conditions: Procedure B
Mobile phase for silica plate chromatography: DCM/*n*-Hex = 9/1
Yield: 14 %, 23 mg, black powder
^{1}H NMR (300 MHz, $CDCl_3$): δ 6.44 (d, J = 10.1 Hz, 1H), 7.38 (m, 1H), 7.46 (d, J = 10.1 Hz, 1H), 7.51 (m, 1H), 7.66 (m, 1H), 8.10 (m, 1H)
^{13}C NMR (76 MHz, $CDCl_3$): δ 127.94, 129.82, 130.24, 130.86, 131.63, 134.78, 135.81, 145.33, 178.89, 180.86
IR ν_{max} (cm^{-1}): 3343, 1653, 1286, 849, 762
$\boldsymbol{T}_{MP}$**:** 116.3 – 117.9 ℃ (Lit. 119 - 121 ℃)
HR-MS (ESI^+): calculated ($C_{10}H_7O_2$) 159.0446, measured ($C_{10}H_7O_2$) 159.0442

1,6-Dinitronaphthalen-2-ol - (**37**) [149]



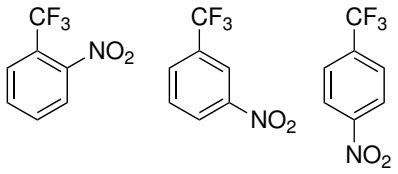
$C_{10}H_6N_2O_5$, MW = 243.17
Reaction conditions: Procedure B
Mobile phase for silica plate chromatography: DCM/*n*-Hex = 9/1
Yield: 3 %, 6 mg, yellow powder
^{1}H NMR (300 MHz, $CDCl_3$): δ 7.45 (d, J = 9.2 Hz, 1H), 8.17 (d, J = 9.2 Hz, 1H), 8.48 (dd, J = 9.6 Hz, J = 2.4 Hz, 1H), 8.75 (d, J = 2.4 Hz, 1H), 9.06 (d, J = 9.6 Hz, 1H), 12.20 (s, 1H)
^{13}C NMR (76 MHz, $CDCl_3$): δ 122.14, 124.02, 124.90, 124.97, 127.69, 128.36, 130.28, 139.63, 144.66, 160.51
IR ν_{max} (cm^{-1}): 3075, 1612, 1531, 1490, 1460, 1338, 1214, 1146, 906, 829, 732
HR-MS (ESI^-): calculated ($C_{10}H_5N_2O_5$) 233.0198, measured ($C_{10}H_5N_2O_5$) 233.0195

4.1.9.4 Study of the formation of dinitrated products

Aromatic nitration with mixed acids
To 1.0 mmol of substrate was added (0 or 1 mL) of HFIP. Afterwards 2 mmol of H_2SO_4 (96 %, 111.4 μL) was added and followed by the addition of 1.0 mmol of HNO_3 (65 %, 69.7 μL). The reaction mixture was put in a pilot reactor, type Mettlet Toledo Easy Max 102, which was heated to 70 ℃. The reaction mixture was stirred for 24 h. After 24 h the reaction mixture was left to cool to room temperature. Next, 4 mL of DCM and 4 mL of water were added. The water phase was neutralised by the addition of $NaHCO_{3(s)}$. The phases were separated and the organic phase was dried with Na_2SO_4. After filtration the solvent was removed under reduced pressure. The conversion and product distribution were determined by NMR spectroscopy and the structure was confirmed by a comparison with the literature data.

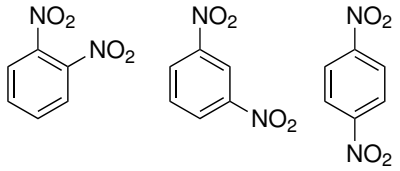
Aromatic nitration in trifluoroacetic acid
To 1.0 mmol of substrate 1 mL of TFA was added, followed by the addition of 1.0 mmol of HNO_3 (65 %, 69.7 μL). The reaction mixture was put in the pilot reactor type Mettlet Toledo Easy Max 102, which was heated to 70 ℃. The reaction mixture was stirred for 24 h. After 24 h the reaction mixture was left to cool to room temperature. Next, 4 mL of DCM and 4 mL of water were added. The water phase was neutralised by the addition of $NaHCO_{3(s)}$. The phases were separated and the organic phase was dried with Na_2SO_4. After filtration the solvent was removed under reduced pressure. The conversion and product distribution were determined by NMR spectroscopy and the structure confirmed by a comparison with the literature data.

Trifluoromethyl-nitrobenzene - 39, **40**, **41** [151], [152]



$C_7H_4F_3NO_2$, MW = 191.11
Reaction conditions: TFA
Reaction mixture: 30 %, 120.3 mg (**39**/**40**/**41** = 7/90/3). NMR chemical shift values for the respective isomers were determined directly from the reaction mixture.
39: **^{1}H NMR (300 MHz, $CDCl_3$):** δ 7.70-7.78 (m, 2H), 7.81-7.88(m, 1H), 7.85-7.93 (m, 1H)
39: **^{1}H NMR (300 MHz, $CDCl_3$):** 7.75 (m, 1H), 7.99 (m, 1H), 8.46 (m, 1H), 8.51 (m, 1H)
41: **^{1}H NMR (300 MHz, $CDCl_3$):** δ 7.80-7.96 (m, 2H), 8.31-8.37 (m, 2H)

Dinitrobenzene - 42, 43, 44 [80]



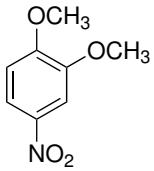
$C_6H_4N_2O_4$, MW = 168.11
Reaction conditions: H_2SO_4
Reaction mixture: 46 %, 132.1 mg (**42**/**43**/**44** = 11/87/2). NMR chemical shift values for the respective isomers were determined directly from the reaction mixture.
42: **^{1}H NMR (300 MHz, $CDCl_3$):** δ 7.79 (m, 2H), 7.93 (m, 2H)
43: **^{1}H NMR (300 MHz, $CDCl_3$):** δ 7.85 (dt, J = 0.46 Hz, J = 8.24 Hz, 1H), 8.60 (dd, J = 2.14 Hz, J = 8.24 Hz, 2H), 9.07 (dt, J = 0.46 Hz, J = 2.14 Hz, 1H)
44: **^{1}H NMR (300 MHz, $CDCl_3$):** δ 8.44 (s, 4H)

4.1.9.5 Study of the formation of bisphenylnitrosonium nitrates

1.0 mmol of substrate was dissolved in 0.2, 1.0, 5.0 mL of solvent (TFE, HFIP) followed by the addition of 1.0 mmol of HNO_3 (65 %, 69.7 μL). The reaction mixture was mixed at an appropriate temperature (-20, -10, 0, 25 ℃). After the reaction was complete, 2 mL of DCM and Na_2SO_4 were added. After filtration the solvent was removed under reduced pressure. The sample was kept in a freezer before measurement of the NMR. The conversion and product distribution were determined by NMR spectroscopy. Known structures were confirmed by a comparison with the literature data.

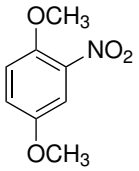
0.5 mmol of 3,5-dimethoxytoluene (74.7 μL) was dissolved in 0.1 mL of HFIP followed by the addition of 0.5 mmol of HNO_3 (65 %, 34.6 μL). The reaction mixture was mixed at -10 ℃. After the reaction was complete 2 mL of DCM and Na_2SO_4 were added. After filtration the solvent was removed under reduced pressure. The sample was kept in a freezer before the measurement of the NMR. Isolation was performed by washing a sample with CCl_4.

1,2-Dimethoxy-4-nitrobenzene - (**46**) [124]



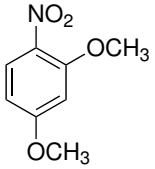
$C_8H_9NO_4$, MW = 183.16
Mobile phase for column chromatography: DCM
Yield: 98 %, 180 mg, yellow powder
^{1}H NMR (300 MHz, $CDCl_3$): δ 3.97 (s, 3H), 3.99 (s, 3H), 6.93 (d, J = 9.0 Hz, 1H), 7.76 (d, J = 2.6 Hz, 1H), 7.93 (dd, J = 9.0 Hz, J = 2.6 Hz, 1H)
^{13}C NMR (76 MHz, $CDCl_3$): δ 56.18, 56.33, 106.30, 109.74, 117.67, 141.35, 148.74, 154.39
IR ν_{max} (cm^{-1}): 2841, 1586, 1497, 1343, 1234, 1013, 849, 740
$\boldsymbol{T}_{MP}$**:** 96.6 – 98.8 ℃ (Lit. 96 ℃)

1,4-Dimethoxy-2-nitrobenzene - (**48**) [153]



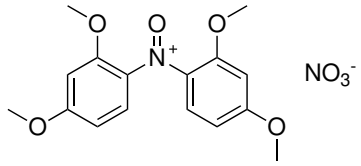
$C_8H_9NO_4$, MW = 183.16
Yield: 98 %, 179.7 mg, yellow powder
^{1}H NMR (300 MHz, $CDCl_3$): δ 3.82 (s, 3H), 3.92 (s, 3H), 7.03 (d, J = 9.2 Hz, 1H), 7.12 (dd, J = 9.2, 3.1 Hz, 1H), 7.40 (d, J = 3.0 Hz, 1H)
^{13}C NMR (76 MHz, $CDCl_3$): δ 55.84, 56.87, 109.85, 114.96, 120.60, 139.27, 147.13, 152.65

2,4-Dimethoxy-nitrobenzene - (**50**) [154]



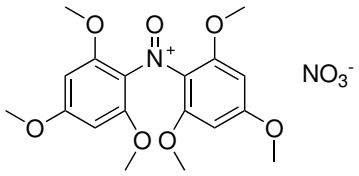
$C_8H_9NO_4$, MW = 183.16
Mobile phase for column chromatography: DCM
Yield: 26 %, 47 mg
^{1}H NMR (300 MHz, $CDCl_3$): δ 3.89 (s, 3H), 3.95 (s, 3H), 6.63 – 6.35 (m, 2H), 7.99 (d, J = 8.9 Hz, 1H)
^{13}C NMR (76 MHz, $CDCl_3$): δ 55.85, 56.36, 99.46, 104.71, 128.37, 132.68, 155.60, 164.76
IR ν_{max} (cm^{-1}): 2954, 1606, 1589, 1494, 1343, 1266, 1216, 1092, 1017, 830, 747

bis(2,4-Dimethoxyphenyl)nitrosonium nitrate - (**51**)



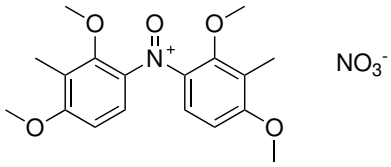
$C_{16}H_{18}N_2O_8$, MW = 366.32
Isolation: washing reaction mixture with CCl_4
Yield: 90 %, 165.1 mg, intense dark green liquid
^{1}H NMR (300 MHz, $CDCl_3$): δ 3.97 (s, 6H), 4.13 (s, 6H), 6.66 (d, J = 2.4 Hz, 2H), 6.76 (dd, J = 9.4, 2.3 Hz, 2H), 7.61 (d, J = 9.4 Hz, 2H)
^{13}C NMR (76 MHz, $CDCl_3$): δ 57.80, 57.84, 97.69, 112.86, 131.98, 138.93, 160.37, 173.18
HR-MS (ESI^-): calculated ($C_{16}H_{18}NO_5$) 304.1185, measured ($C_{16}H_{18}NO_5$) 304.1181

bis(2,4,6-Trimethoxyphenyl)nitrosonium nitrate - (**54**) [88]



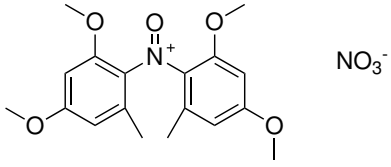
$C_{18}H_{22}N_2O_{10}$, MW = 426.37
Isolation: washing reaction mixture with CCl_4
Yield: 65 %, 138.8 mg , intense dark blue solid
Crystalisation: $CHCl_3$/*n*-Hex
^{1}H NMR (300 MHz, $CDCl_3$): δ 3.89 (s, 12H), 4.10 (s, 6H), 6.28 (s, 4H)
^{13}C NMR (76 MHz, $CDCl_3$): δ 56.45, 57.78, 92.89, 132.26, 160.06, 171.37
HR-MS (ESI$^-$): calculated ($C_{18}H_{22}NO_7$) 364.1396, measured ($C_{18}H_{22}NO_7$) 364.1393
X-Ray: Structure was in line with literature data [88].

bis(2,4-Dimethoxy-3-methylephenyl)nitrosonium nitrate - (**58**)



$C_{18}H_{22}N_2O_8$, MW = 394.38
Isolation: washing reaction mixture with *n*-Hex
Yield: 62 %, 121.4 mg, intense dark blue liquid
^{1}H NMR (300 MHz, $CDCl_3$): δ 2.21 (s, 6H), 3.71 (s, 6H), 4.12 (s, 6H), 6.93 (d, J = 9.39 Hz, 2H), 7.62 (d, J = 9.39 Hz, 2H)
^{13}C NMR (76 MHz, $CDCl_3$): δ 8.58, 9.35, 57.08, 57.67, 62.36, 62.88, 108.87, 109.10, 115.68, 123.74, 126.80, 131.71, 131.91, 142.03, 157.13, 157.23, 171.59, 171.72
HR-MS (ESI$^-$): calculated ($C_{18}H_{22}NO_5$) 332.1498, measured ($C_{18}H_{22}NO_5$) 332.1503

bis(2,4-Dimethoxy-6-methylephenyl)nitrosonium nitrate - (**62**)



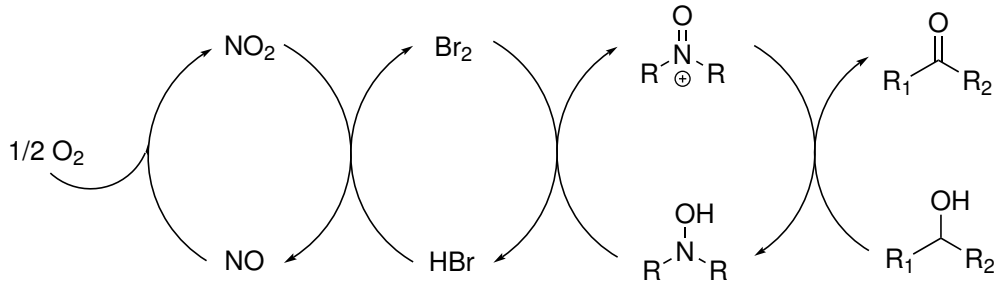
$C_{18}H_{22}N_2O_8$, MW = 394.38
Isolation: washing reaction mixture with CCl_4
Yield: 48 %, 47.7 mg, intense dark green liquid
^{1}H NMR (300 MHz, $CDCl_3$): δ 2.33 (s, 6H), 3.81 (s, 6H), 4.08 (s, 6H), 6.48 (d, J = 2.4 Hz, 2H), 6.59 (d, J = 2.4 Hz, 2H)
^{13}C NMR (76 MHz, $CDCl_3$): δ 20.34, 57.35, 57.78, 96.32, 114.91, 140.57, 143.58, 160.54, 170.53
HR-MS (ESI$^-$): calculated ($C_{18}H_{22}NO_5$) 332.1498, measured ($C_{18}H_{22}NO_5$) 332.1492

4.2 Aerobic oxidation of alcohols

4.2.1 Introduction

Green chemistry emerged at the beginning of the 1990s. Its goal was to design methods that would reduce (or even eliminate) the generation of toxic reagents, by-products, solvents and other auxiliary substances and would be economically efficient [77]. This prompted the search for new methodologies, with Nature becoming a model system. The focus on developing new oxidation methods shifted from stoichiometric oxidants (high amount of waste with hazardous properties) to catalytic processes using inexpensive and clean oxidants such as H_2O_2 and O_2.

Two billion years ago oxygen started accumulating in the Earth's atmosphere, known as *The great oxygenation event* [155]. This happened after O_2 released from cyanobacteria oxidized most of the iron(II) resources in the oceans into ferric minerals. Although O_2 is a powerful oxidant, the high energy barrier of the transition state kinetically disfavours a reaction with organic molecules. The problem was solved by mimicking Nature, which bypasses the unfavorable kinetics of direct oxidation by an aerobic respiratory chain [156]. Oxygen transfer cycles were developed (Scheme 4.19) often using (2,2,6,6-tetramethylpiperidin-1-yl)oxyl (TEMPO) and its derivatives as well as transition metals as catalysts [3], [157]–[162].



Scheme 4.19: Catalytic transfer of oxygen for oxidation of alcohols.

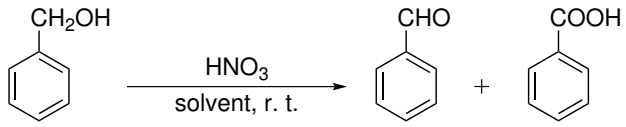
There has been considerable progress made in recent years in aerobic oxidation catalysis by persistent dialkyl nitroxide radicals such as TEMPO and its derivatives, however they are rather expensive and efficient recycling is an important issue [163]. Metal catalysts are often based on noble metals such as Pd, Au and Pt. The development of a cheap catalyst for selective oxidations is desired. Iron is the second most abundant metal in the Earth's crust after aluminium. In living organisms it is responsible for the transportation of oxygen and it helps in the oxidation of substrates by electron transport from oxygen. Iron is also much lower on the supply-risk index for chemical elements compared to noble metals [3], [4]. Furthermore, the platinum group of metals is also considerably more toxic compared to iron, which is why their presence in products for the pharmaceutical industry must be very low. The difference is such that platinum group metals are *Class 1 metals: metals with significant safety concern*, on the other hand, iron is under *Class 3 metals: metals of minimal safety concerns* [3].

Nitric acid is an inexpensive reagent with remarkable selectivity. Together with $NaNO_2$ it is a source of nitrogen oxides that have been successfully used in the aerobic oxidation of alcohols [164]. Usually, the presence of a different co-catalyst is needed, such as bromine [165], a carbon-based catalyst [166] and TEMPO [167]–[169]. When just nitric acid is used as the catalyst for aerobic oxidation, harsh conditions are needed, which can be obtained by performing the reaction in concentrated sulfuric acid [170] or at 100 °C and 5 bar O_2 in dioxane. However, the terminal production of N_2O is a problem [171], [172].

4.2.2 Oxidation of benzyl alcohols

Continuing our research on the activation of nitric acid we investigated whether the activation of nitric acid using fluorinated alcohols is strong enough to be used for the oxidation of alcohols. To confirm our hypothesis we compared the reactions for the oxidation of benzyl alcohol (**67a**) with HNO_3 as an oxidant in different solvents (Table 4.18).

Table 4.18: The effect of solvent on oxidation of benzyl alcohol with HNO_3.[a]



67a **67b** **67c**

Entry	Solvent	Time	Conversion [%]	Selectivity **67b**/**67c**
1	HFIP	10 min	100	100/0
2	TFE	3 h	96	100/0
3	EtOH	6 h	0[b]	-
4	*i*-PrOH	6 h	0[b]	-
5	MeCN	6 h	0	-
6	DCM	6 h	17	100/0
7	*n*-Hex	6 h	92	100/0
8	-	4 h	95	83/17

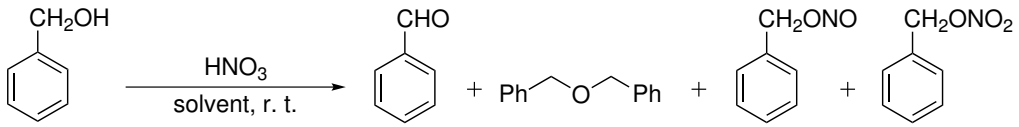
[a] Reaction conditions: benzyl alcohol **67a** (1 mmol), 65 % aq. HNO_3 (1 mmol, 69.2 µL), 1 mL of solvent, room temperature. Selectivity and conversion were determined by NMR spectroscopy based on the starting compound. [b] No reaction was observed between the solvent and HNO_3.

Equimolar amounts of benzyl alcohol and 65 % aqueous HNO_3 were dissolved in HFIP and complete conversion into benzaldehyde (**67b**) was obtained in just 10 min with the formation of red-brown gas NO_2/N_2O_4. Reactivity in TFE was lower and it took 3 h for the reaction to obtain 96 % conversion. Surprisingly, no conversion was obtained when polar solvents (EtOH, *i*-PrOH, MeCN) were used (Table 4.18, entry 3-5). Oxidations in *n*-Hex and DCM proceeded with 92 % and 17 % conversion after 6 h, respectively. The reaction mixture was heterogeneous with HNO_3 in a separate layer that might be the reason for a better conversion in those solvents. The reaction proceeded also in solvent-free conditions, however over oxidation was observed and benzoic acid (**67c**) was formed (Table 4.18, entry 8). In HFIP a quantitative conversion to **67b** was obtained already after 10 min and no over oxidation into **67c** was detected, even after 2 h.

Since the strong activation of HNO_3 for the oxidation of **67a** was observed by HFIP, we studied whether the system can be used in sub-stoichiometric amounts with molecular oxygen working as a terminal oxidant. To do this a balloon filled with air or O_2 was attached to the reaction mixture containing **67a** in HFIP with various amounts of HNO_3. As can be seen in Table 4.19 complete and selective conversion into **67b** was obtained with 10 mol% HNO_3 in an O_2 atmosphere. When we used air as the source of oxygen, a lower conversion was obtained and twice the amount of HNO_3 was needed to obtain the same results as in an O_2 atmosphere. In reactions with lower amounts of catalyst dibenzyl ether (**67d**) was formed. A similar effect was observed when the reaction was performed at higher temperature of 40 ℃.

The active role of HFIP was confirmed by performing catalytic oxidation in *n*-hexane and under solvent-free conditions. Although these latter reactions worked with a stoichiometric amount of HNO_3, oxidation with 10 mol% of HNO_3 under an O_2 atmosphere did not proceed in *n*-hexane, while under solvent-free conditions 5 % of **67b** was formed. The reactions performed under an inert atmosphere (argon) failed to give a larger amount of the product than could be achieved by oxidation with HNO_3, proving that O_2 is a true terminal oxidant. Only 7 % of **67a** was converted into **67b** with 10 mol% HNO_3. Not having molecular oxygen present, NO could not be oxidised back into NO_2/HNO_2 and the catalytic cycle stopped. With 20 mol% of HNO_3 36 % conversion into **67b** was observed, while with 50 mol% of HNO_3 conversion was 92 % with the formation of benzyl nitrite (**67e**) in a 22 % yield (Table 4.19). Having the latter reaction performed under molecular oxygen only **67b** was obtained.

Table 4.19: Aerobic oxidation of **67a** with catalytic amount of HNO_3.[a]



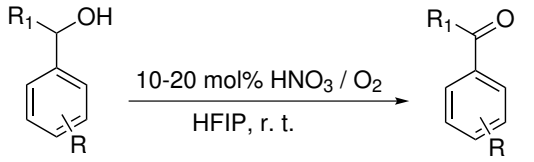
67a **67b** **67d** **67e** **67f**

Entry	HNO_3 [mol%]	Atmosphere	Conversion [%]	Selectivity **67b**/**67d**
1	2	O_2	21	100/0
2	5	O_2	53	100/0
3	10	O_2	>99	100/0
4	2	Air	8	50/50
5	5	Air	4	100/0
6	10	Air	55	100/0
7	20	Air	97	94/6[b]
8	10	Argon	7	100/0
9	20	Argon	36	100/0
10	50	Argon	92	78/22[c]

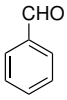
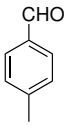
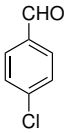
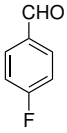
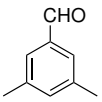
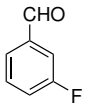
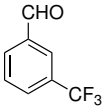
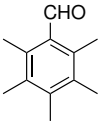
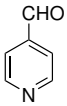
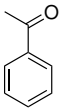
[a] Reaction conditions: 1 mmol benzyl alcohol **67a** (103.5 µL), 1 mL HFIP, 65 % aq. HNO_3, balloon of O_2 (air or Ar), room temperature, 24 h. Selectivity and conversion were determined by NMR spectroscopy based on starting compound. [b] Benzyl nitrate (**67f**). [c] Benzyl nitrite (**67e**).

Obtaining a reaction system for the catalytic aerobic oxidation of benzyl alcohol we investigated the oxidising abilities of other various benzylic alcohols (Table 4.20). For the reaction to be quantitative, 10–20 mol% of 65 % HNO_3 had to be used. In none of the substrates over oxidation into benzoic acid occurred. Heterocycle (**75a**) (Table 4.20, row 9) and pentamethylbenzyl alcohol (**74a**) (Table 4.20, row 8) were unreactive. For the former the most likely cause of inactivity was the steric hindrance of methyl groups preventing access of the reagent to the alcohol group to react with it and form a product. Since no conversion was observed with **75a**, we repeated the reaction under similar conditions using **75a**·HCl to prevent the formation of its salt with HNO_3. Even so, no product was formed. The reaction was also performed with 4-OMe-, 4-NH_2-, 4-OH-substituted benzylic alcohols. In all three cases polymerization occurred and no formation of the desired alcohol was observed. According to Giacco *et al.* [173] polymerization is a result of the formation of benzyl cation. The benzyl cation is stabilized by a strong electron-donating group and reacts with another aromatic molecule. Polymerization could not be avoided even if we reduced the amount of HNO_3 or the amount of HFIP. Secondary benzyl alcohol (**76a**) was less reactive and an increase of the catalyst loading to 20 mol% was needed. Oxidation of the aliphatic alcohols did not occur under catalytic conditions and a stoichiometric amount of HNO_3 was needed.

Table 4.20: Catalytic oxidation of various banzyl alcohols.[a]



67a - 76a R_1 = –H, –CH_3 **67b - 76b**

Entry	Product		HNO_3 [mol%]	Time	Conversion (yield) [%]
1		**67b**	10	22	100 (97)
2		**68b**	10	6	100 (93)
3		**69b**	10	24	26
			15	23	100 (97)
4		**70b**	10	23	100 (99)
5		**71b**	10	5	100 (>99)
6		**72b**	10	23	45
			15	22	100 (86)
7		**73b**	10	23	19
			20	23	100 (>99)
8		**74b**	20	24	n. r.
9		**75b**	20	24	n. r.
10		**76b**	20	23	97 (70)

[a] Reaction conditions: 1 mmol of substrate, 1 mL HFIP, 65 % aq. HNO_3, O_2, room temperature, 6–24 hours. n. r. – no reaction

4.2.3 Mechanism of catalytic oxidation for benzyl alcohols

Berkessel *et al.* [22] showed the importance of the concentration of HFIP in the reaction mixture. In the epoxidation of 1-octene an increase of the reaction rate with an increasing amount of HFIP was observed. The reaction rate immensely increased at the solvent/substrate ratio of 12 [22]. Therefore, we studied the effect of the amount of solvent on the reaction rate and the selectivity of the aerobic benzyl oxidation that was catalysed by nitric acid (Figure 4.33). For a better understanding of the influence of the molar ratio between the solvent and the substrate, a reaction was performed with 5 mol% HNO_3 as the catalyst to avoid a complete conversion. The initial increase of the amount of solvent from the equimolar amount increases the conversion and selectivity for the oxidation of benzyl alcohol (**67a**) to benzaldehyde (**67b**). Complete selectivity for **67b** and high conversion was obtained when ratio was approximately 10 molecules of HFIP to 1 molecule of **67a**. A further increase in the amount of solvent resulted in a lower conversion and an increase in the formation of benzyl ether (**67d**).

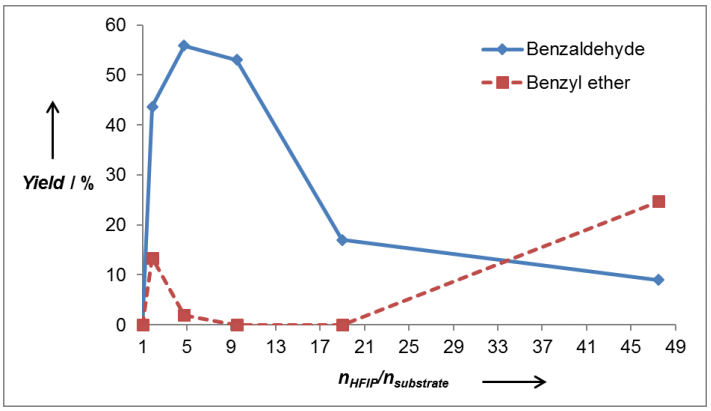


Figure 4.33: Influence of solvent HFIP/substrate molar ratio on selectivity and conversion of aerobic oxidation of benzyl alcohol with 5 mol% HNO_3 ·

The reaction was followed in situ using an ATR-IR probe. It was found that the kinetics strongly depends on the ratio of HNO_3 and the substrate. In a reaction with 1 equivalent amount of HNO_3 the reaction was complete within minutes after the addition of HNO_3 (Figure 4.35). No induction period was observed, indicating the absence of the autocatalytic process (Figure 4.34) [167], [174].

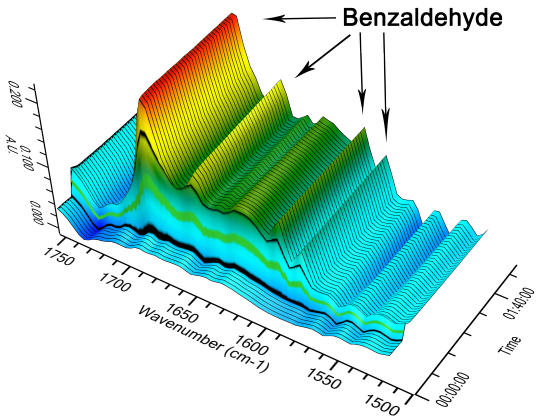


Figure 4.34: Real-time FTIR-ATR spectroscopy monitoring of the aerobic oxidation of **67a** with one equivalent of HNO_3.

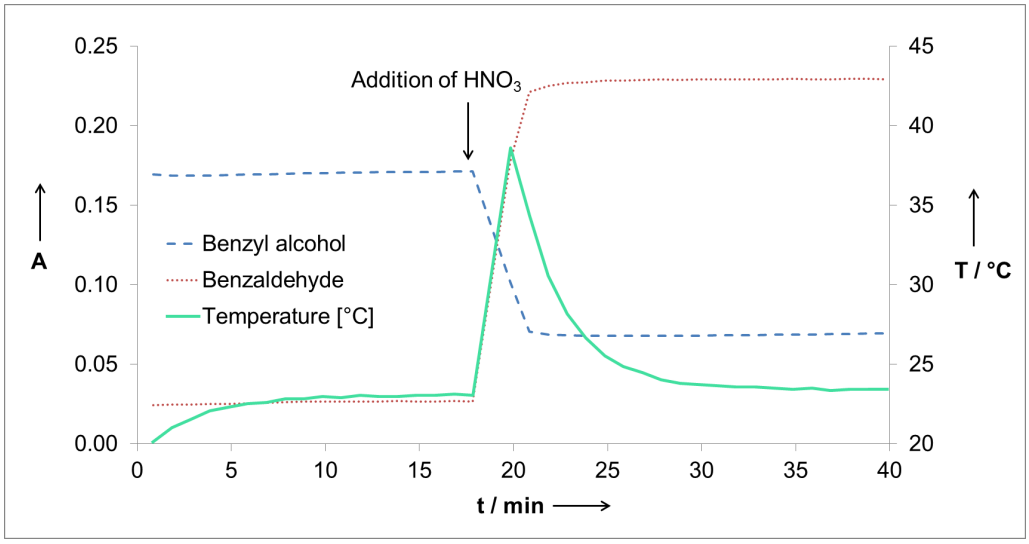


Figure 4.35: Time dependence of stoichiometric oxidation of **67a** (995 cm^{-1}) into **67b** (1696 cm^{-1}), and the temperature of the mixture determined by in situ ATR-IR spectroscopy.

In the case of using a substoichiomteric amount of HNO_3, initially the reaction was fast with an increase of the temperature of the reaction mixture for app. 2 °C (Figure 4.36). This is contributed to the reaction with HNO_3. After an initial amount of HNO_3 was consumed the concentration of **67b** started to increased linearly, which indicates a zero-order reaction rate (Figure 4.37). This is due to the slow diffusion of oxygen from the gas phase into the reaction mixture and is consequently a rate-limiting step.

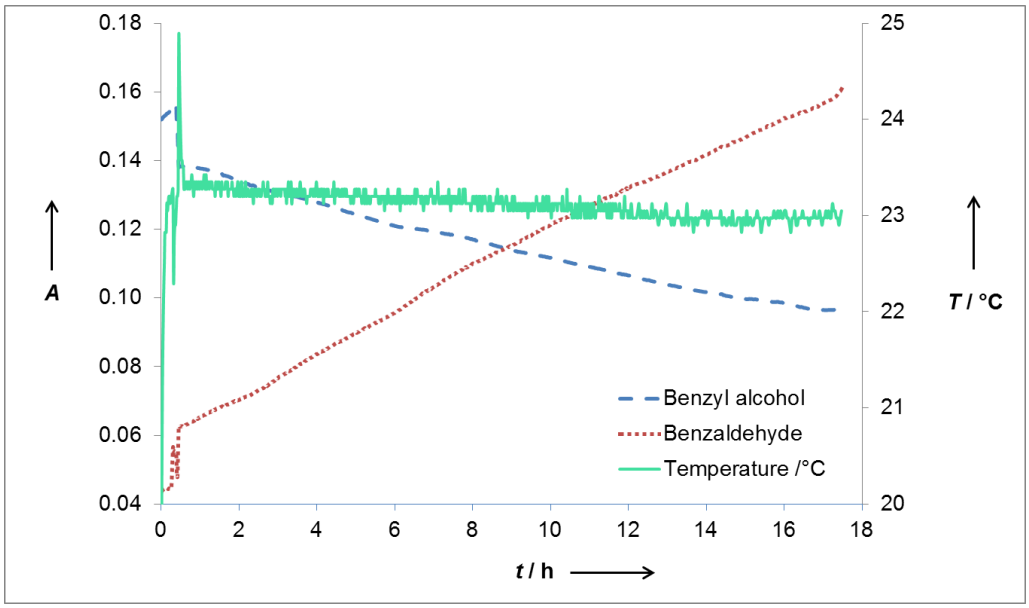
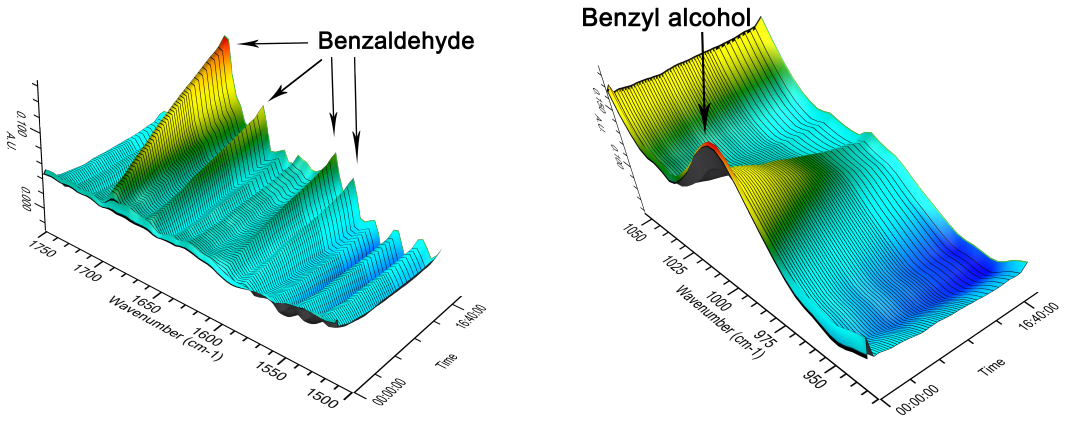


Figure 4.36: Time dependence for catalytic oxidation of **67a** (995 cm^{-1}) into **67b** (1696 cm^{-1}), and the temperature of the mixture determined by in situ ATR-IR spectroscopy.

The mechanism for the aerobic oxidation of benzyl alcohols mediated by HNO_3 was studied by Aellig *et al.* (Scheme 4.20) [167], [171], [175]. They proposed a reaction path where HNO_2 reacts with **67a** and forms nitrite **67e** that is further transformed into benzadeldehyde **67b** by acid-catalysed decomposition. HNO is formed as a side product and is regenerated into HNO_2 by aerobic oxidation through the NO/NO_2 cycle. The true termi-



(a) (b)

Figure 4.37: Enlarged partition of 3D ATR-FTIR spectra for aerobic oxidation of **67a** with 10 mol% HNO_3. (a) Linear increase of signal of benzaldehyde (**67b**, 1696 cm^{-1}) with time. (b) Decrease of signal for benzyl alcohol (**67a**) at 995 cm^{-1}.

nal oxidant in such a reaction is O_2. However, a competitive terminal reaction is present, where two molecules of HNO react with each other and form N_2O (Scheme 4.20).

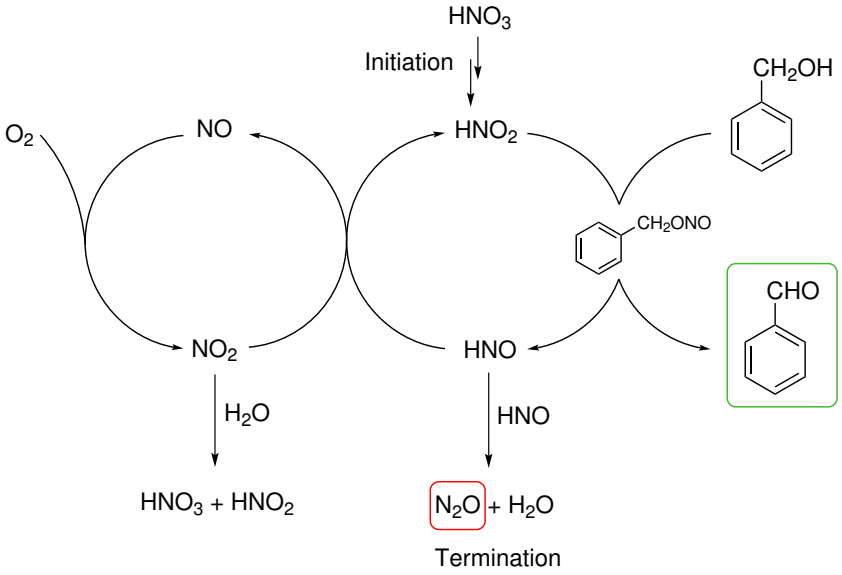
Aellig *et al.* initiation:

$$4\ HNO_3 \rightleftharpoons 4\ NO_2 + 2\ H_2O + O_2$$

$$2\ NO_2 + H_2O \rightleftharpoons N_2O_4 + H_2O \longrightarrow HNO_3 + HNO_2$$

HNO_3 in HFIP initiation:

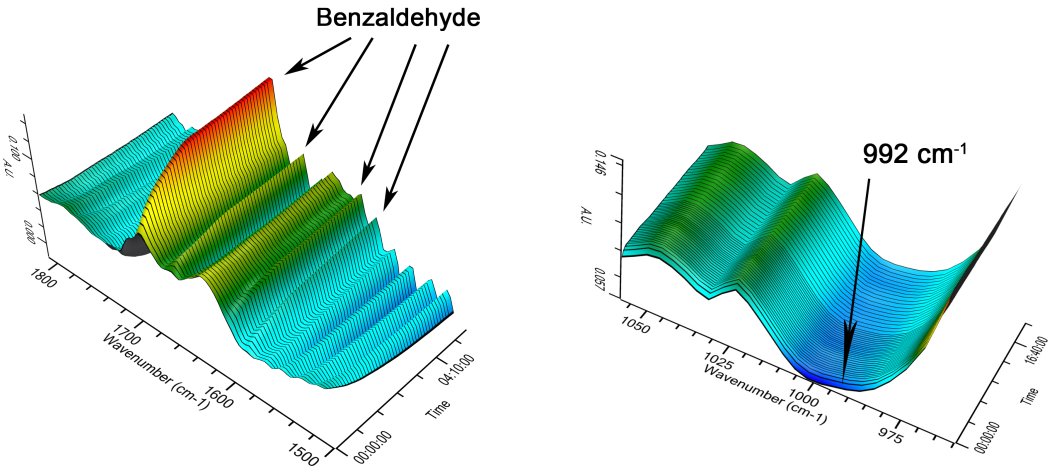
$$HNO_3 + PhCH_2OH \longrightarrow HNO_2 + PhCHO$$



Scheme 4.20: Mechanism for aerobic oxidation of alcohols mediated by HNO_3.

In reactions involving O_2 and HNO_3, HFIP can act as a template catalyst similar to reactions involving H_2O_2. To understand the role of HFIP in the reaction, **67e** was prepared

independently [176]. Upon stirring a solution of **67e** in HFIP at room temperature in situ ATR-IR spectroscopy clearly showed the formation of **67b** and after removing the solvent under reduced pressure **67b** was obtained in quantitative amounts. On the other hand, when **67e** was stirred in *i*-PrOH ATR-IR spectroscopy showed no change during stirring. After removing the solvent **67e** decomposed back to **67a**, therefore hydrolysis in the former case had to occur while removing the solvent (Figure 4.38).



(a) (b)

Figure 4.38: ATR-IR spectra from decomposition of **67e** in HFIP and in *i*-PrOH. (a) Stirring in HFIP. Rise of the signal of benzaldehyde (**67b**) with time can be clearly seen. (b) Stirring in *i*-PrOH (peak of benzyl alcohol **67a** at 992 cm^{-1} remains unchanged).

As opposed to the acid co-catalysed HNO_3 mediated oxidation of benzyl alcohols in dioxane [175], the signal for N_2O (at 2236 cm^{-1} in the IR spectrum) was not observed (Figure 4.39). This is attributed to the lower reaction temperature and the highly polar and strong ionizing nature of HFIP.

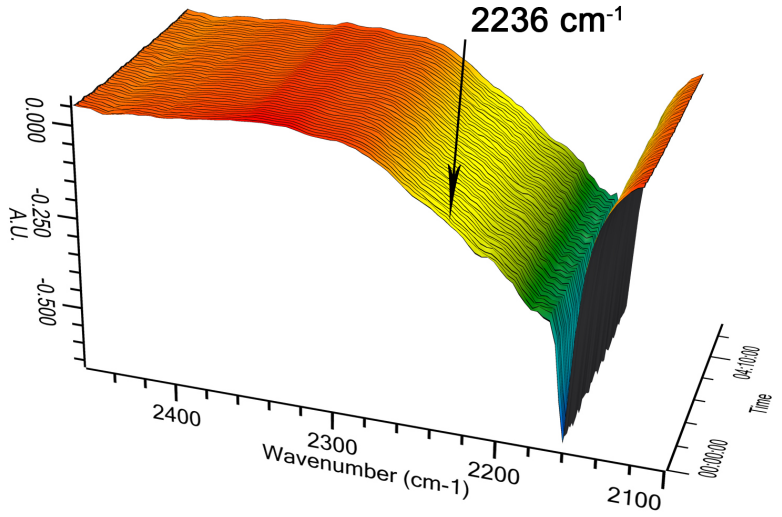
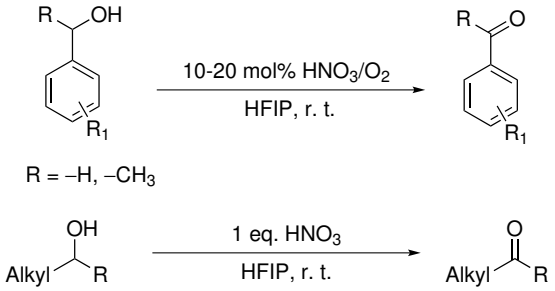


Figure 4.39: Lack of signal for usually formed N_2O (2236 cm^{-1}).

4.2.4 Iron catalysis

The synthesis of natural and complex molecules usually involves multiple-oxygen containing functional groups. Often, there is a need to selectively oxidize only a primary or secondary alcohol group in the same molecule [177]. The transformation from biomass-derived carbohydrates into value-added chemicals is reasonable because of their abundant functionality. The challenge is in controlling the selective transformation of the functionality of polyols into the final product [178]. Therefore, there is a clear need for the reagents to be able to distinguish and selectively react only with one type of alcohol group (primary, secondary or the allylic alcohol group). Primary alcohols have a less crowded environment compared to secondary alcohols [179]. Some methods use this characteristic for the selective oxidation of primary alcohols into aldehydes and acids with no reaction occurring on the secondary alcohol group [161]. On the other hand, thermodynamics usually favour the oxidation of secondary alcohols over primary ones, since the oxidation potential from primary alcohols into aldehydes is usually higher than the oxidation of secondary alcohols into ketones [179]. A lot of commonly used reagents react faster with secondary alcohols than primary ones, but the difference in the reaction rates is too small for practical use. Another strategy for selective oxidation of one alcohol group is by the introduction of a protecting group, however this increases the number of steps needed, increases the formation of waste and decreases the overall yield [177].

The previously mentioned aerobic oxidation of alcohols with HNO_3 as a catalyst has limited substrate scope as it could only oxidise benzyl alcohols. The oxidation of primary benzyl alcohols was successful, while for secondary benzyl alcohols a higher loading of HNO_3 was needed. The oxidation of other alcohols could only be achieved by using stoichiometric amounts of HNO_3 (Scheme 4.21).



Scheme 4.21: Catalytic aerobic oxidation of benzyl alcohols vs. stoichiometric oxidation of aliphatic alcohols.

On this basis we decided to search for a co-catalyst that would improve the conversion rate of the aerobic HNO_3-catalysed oxidation of aliphatic alcohols. We focused on simple iron and copper salts since they have better sustainability potential and a lower price compared to noble metals. We chose 2-octanol (**77**) as the model substrate and the screening of the metal co-catalyst for the oxidation of **77** was performed with 1 mol% of metal salt and 5 mol% HNO_3 in HFIP. All the reaction components were mixed in HFIP and a balloon filled with molecular oxygen was attached to the flask. Among the tested co-catalysts, the best result was obtained with $FeCl_3$, where a quantitative conversion into 2-octanone (**78**) was observed in 24 h (Figure 4.40). A chloride anion as a counter ion is essential for a high conversion. The oxidation of **77** with $K_3[Fe(CN)_6]$ and $Fe(NO_3)_3$ was very low. The chloride anion itself is not enough for the reaction to proceed since with $AlCl_3$ and NaCl as a catalyst **78** was formed only in trace amounts. With HCl as a co-catalyst quantitative

conversion was also obtained. However, it was found to be less active than $FeCl_3$ when it was used as co-catalyst on less reactive substrates such as cyclopentanol (**81**) that failed to react. In contrast to the research of Wang et al. [180] where $FeCl_3$ was used as a co-catalyst in the presence of TEMPO, we observed a large difference between Fe^{3+} and Fe^{2+} salts. Although the difference could come from the lower solubility of Fe^{2+} in HFIP compared to Fe^{3+}.

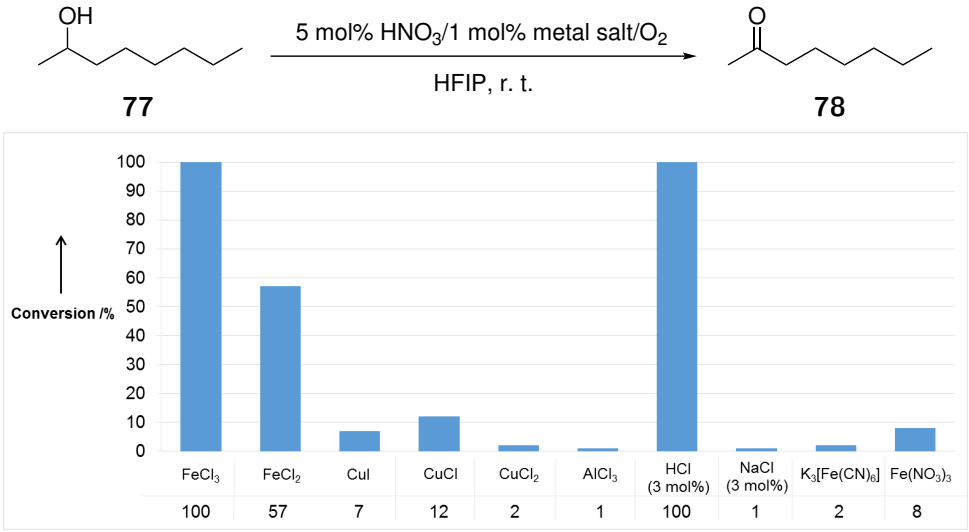


Figure 4.40: Aerobic oxidation of **77** into **78** catalysed by HNO_3 and metal co-catalyst (number under each column is conversion of **77**).

Next, we investigated how the amount of $FeCl_3$ catalyst influenced the conversion of **77** into **78**. The best result was obtained with our already used initial amount of 1 mol% of $FeCl_3$. In the case where we decreased the amount of $FeCl_3$ catalyst below 0.5 mol% the reaction did not proceed as the product was obtained only in trace amounts. An increase of the $FeCl_3$ catalyst loading had a negative effect on the conversion.

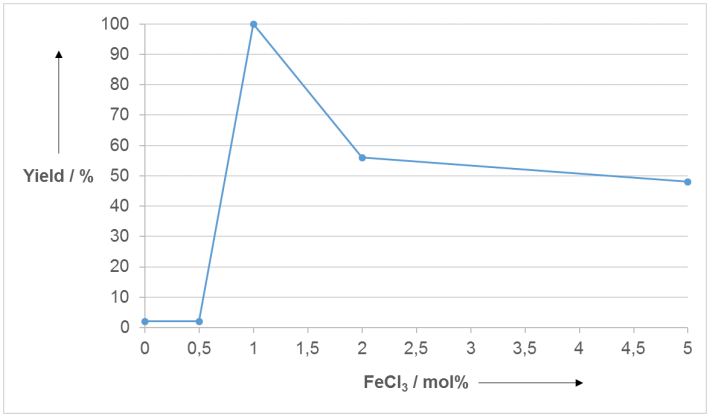
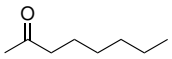
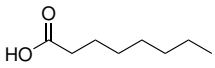
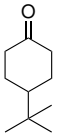
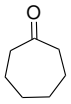
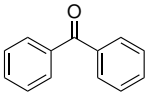
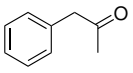
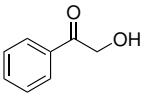
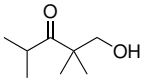
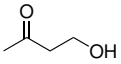


Figure 4.41: Influence of amount of $FeCl_3$ on yield of **78**.

The influence of the solvent was re-examined in this metal-co-catalyzed aerobic oxidation in order to elucidate the possible role of HFIP as a templated catalyst. The reaction under optimised conditions (5 mol% HNO_3 and 1 mol% $FeCl_3$) was repeated in various solvents (TFE, EtOH, MeCN, DCM and 2-Me-THF), but in all cases the product was obtained only in trace amounts. This indicates that HFIP has an essential role in this aerobic HNO_3 and $FeCl_3$ catalysed oxidation reaction. Having a working system in hand, we expanded our

research to other aliphatic alcohols (Table 4.21).

Table 4.21: Selective aerobic oxidation of secondary alcohols.[a]

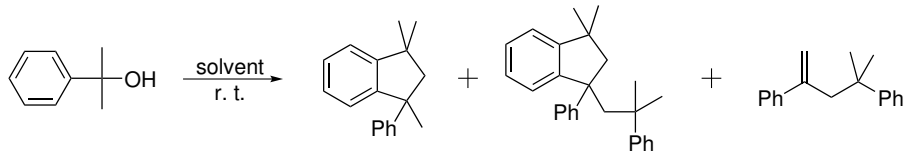
Entry	Product		HNO_3 [mol%]	time [h]	Conversion (Yield) [%]
1		**78**	5	24	100 (100)[b]
2		**79**	10	24	n. r.
			1 eq.	23	100
3		**80**	12	7	100 (77)[b]
4		**81**	10	23	43
			20	23	100 (88)
5		**82**	15	6.5	100 (74)
6		**83**	15	23	90 (59)
7		**84**	12	5	100 (83)
8		**85**	10	5	97 (83)
9		**86**	15	22	96 (95)
10		**87**	12	5	100 (96)
11		**88**	10	22	98 (98)[c]

[a] Reaction conditions: 1 mmol of substrate, 1 mL HFIP, 65 % aq. HNO_3, 1 mol% $FeCl_3$ (1.7 mg), O_2, room temperature, 5–24 hours. n. r. – no reaction
[b] Yield obtained from ^{1}H NMR with naphthalene as internal standard.
[c] Yield obtained from ^{1}H NMR with naphthalene as internal standard with no isolation.

Other substrates showed a lower reactivity and an increase in the catalytic amount of HNO_3 to 10–15 mol% was needed. The exception to this was **81**, which was the least reactive substrate, hence the increase of HNO_3 to 20 mol% was needed. Selective oxidation of secondary alcohols was obtained with an excellent yield. No reaction occurred on the primary aliphatic alcohols. This selectivity was present even when the primary and secondary alcohol groups were present in the same molecule (Table 4.21, entry 9–11). The oxidation of 1-octanol into octanoic acid (**79**) was possible only by using 1 equivalent of HNO_3 to achieve a complete conversion (Table 4.21, entry 2). Since no reaction was ob-

served with the primary alcohols, we further investigated whether the reaction proceeds with aldehyde. 10 mol% of HNO_3 and 1 mol% of $FeCl_3$ were added to a hexanal solution in HFIP under a molecular oxygen atmosphere. After 22 h only a 13 % conversion was obtained. This would indicate the oxidation was mostly by nitric acid itself and no catalytic cycle was obtained. In the final part of the study on the aerobic oxidation of alcohols, allyl alcohols and tertiary alcohols were examined. All the reactions with allyl alcohols ended in polymerisation. Contrary to expectation, the reaction with tertiary alcohol proceeded smoothly and 2-phenyl-propan-2-ol (**89**) was converted to three products and the distribution of the products was markedly influenced by the solvent. While in HFIP the main product was **90**, in TFE **92** was the main product (Table 4.22). The reaction did not proceed in the absence of a catalyst (Table 4.22, entry 5).

Table 4.22: Reaction with tertiary alcohol.[a]

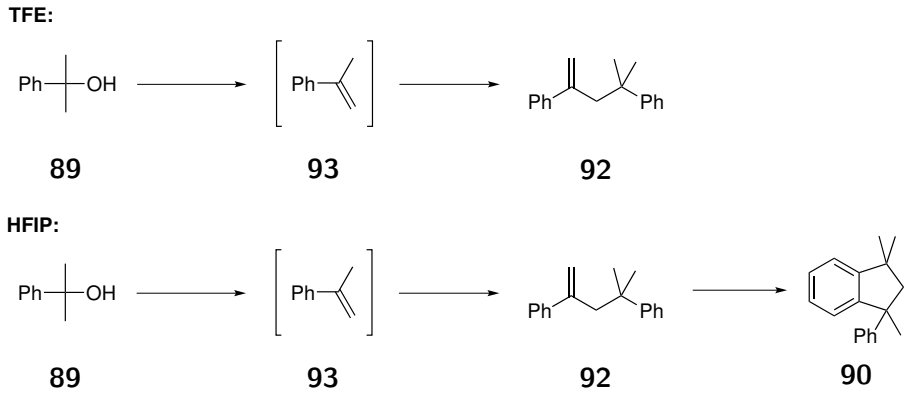


89 **90** **91** **92**

Entry	HNO_3 [mol%]	$FeCl_3$ [mol%]	Solvent	Time [h]	Conversion [%]	Selectivity **90**/**91**/**92**
1	10	1	HFIP	2	100	93/0/0
2	10	0	HFIP	2	100	65/35/0
3	0	1	HFIP	3	100	76(57)/24(18)/0
4	0	1	TFE	3	100	7/9/84(62)
5	0	0	HFIP	22	0	-/-/-

[a] Reaction conditions: 2-phenyl-propan-2-ol (**89**) (1.0 mmol, 140.4 mg), 1 mL solvent, 65 % aq. HNO_3 (0–10 mol%), $FeCl_3$ (0–1 mol%), room temperature, 3–22 hours.

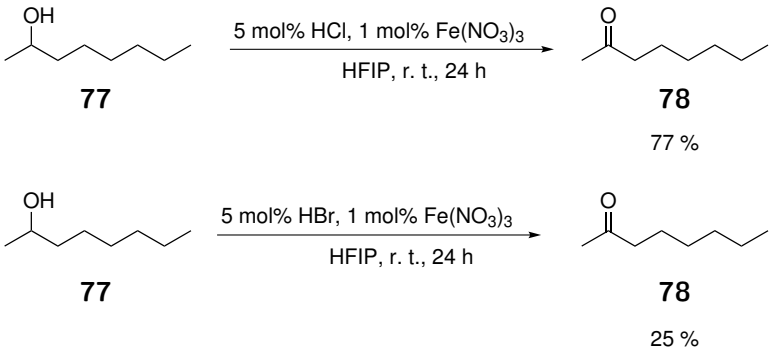
Initially, the tertiary alcohol (**89**) is dehydrated to the corresponding alkene **93** (Scheme 4.22). This could react with other **93** or **89** to form **92** which is the main product that we obtained in the TFE solvent. In HFIP the reaction proceeds further and the compound **90** is formed through the intramolecular cyclisation of **92** (Scheme 4.22). A similar reaction was observed by Stavber *et al.* [181] in their work.



Scheme 4.22: Mechanism for formation of products in reaction with tertiary alcohol.

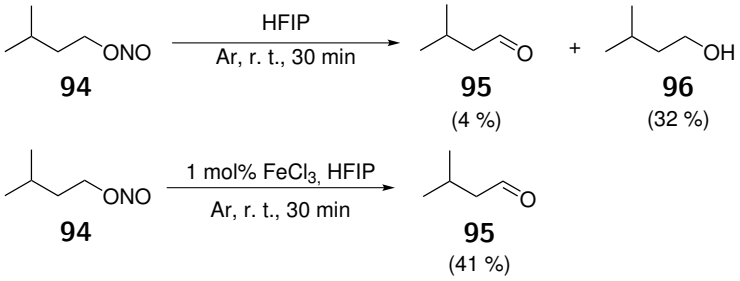
4.2.5 Mechanism for the iron catalyst

In the oxidation of **77** into **78** a similar reactivity was obtained with $FeCl_3$ and HCl as a co-catalyst. We noticed that chloride anions from the iron salt were essential for the system to work. In the next step we investigated whether the sources of chloride and nitrate ions were important or whether could they be interchanged. We performed a reaction in which the source of nitrate was an iron salt (1 mol% $Fe(NO_3)_3$) and the source of the chloride anions was HCl (5 mol%). In such a case we obtained a 77 % conversion of **77** into **78**. In the system where we replaced HCl (5 mol%) with HBr (5 mol%) and using $Fe(NO_3)_3$ as a co-catalyst we observed a 25 % conversion of **77** into **78** (Scheme 4.23). This indicates the formation of NOX (X=Cl or Br) *in situ* and works as a reactive species. NOCl is more polarized compared to NOBr. This step defines the reactivity of the nitrogen atom of NOCl as being more electrophilic and reacts at a higher rate [182]. This would explain the lower conversion obtained with HBr compared to HCl.



Scheme 4.23: The effect of halogen atom on the oxidation of **78** with $Fe(NO_3)_3$ and HX (X = Cl, Br).

It is possible to oxidise **77** without $Fe(NO_3)_3$ with only a HNO_3/HCl system, However, this system is limited and the less reactive alcohol **81** did not react without the presence of $Fe(NO_3)_3$. NOCl in the presence of alcohol forms alkyl nitrites. As we showed before, benzyl nitrites are unstable in HFIP and decompose into ketones or to aldehydes. Alkyl nitrites are more stable and some of them are commercially available. We used iso-pentyl nitrite (**94**) as a model compound to study the transformation of the nitrite **94** into a carbonyl compound. We have stirred the solution of **94** in HFIP and found that after 30 minutes **94** was mostly hydrolysed, forming 32 % of alcohol **96** and only 4 % of aldehyde **95**. However, the decomposition of alkyl nitrites substantially increased in the presence of 1 mol% of iron(III) salt in the reaction mixture (Scheme 4.24).



Scheme 4.24: Decomposition of nitrite is catalysed by iron salt.

Next, we followed the conversion of isopentyl nitrite **94** in HFIP with an in-situ ATR-IR probe. The IR spectra of the reaction clearly showed that **94** with 1 mol% $FeCl_3$ in HFIP

under argon converted into aldehyde **95** (Figure 4.42). Most of the decomposition occurred in the first 6 h (Figure 4.43). After 20 h only **95** was isolated.

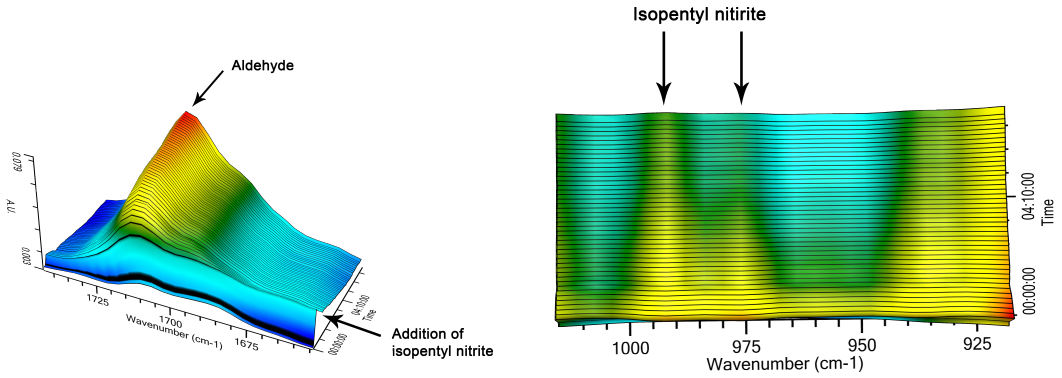


Figure 4.42: ATR-IR spectra for decomposition of isopentyl nitrite (**94**) catalysed by 1 mol% $FeCl_3$ (peak of aldehyde (**95**) on the left, peak of isopentyl nitrite (**94**) on right.

We could not detect end product of the nitrogen part of the starting nitrite in the ATR IR spectra due to the overlap of the bands for C=O and N=O of HNO, while no formation of N_2O (peak at 2236 cm^{-1}) could be detected.

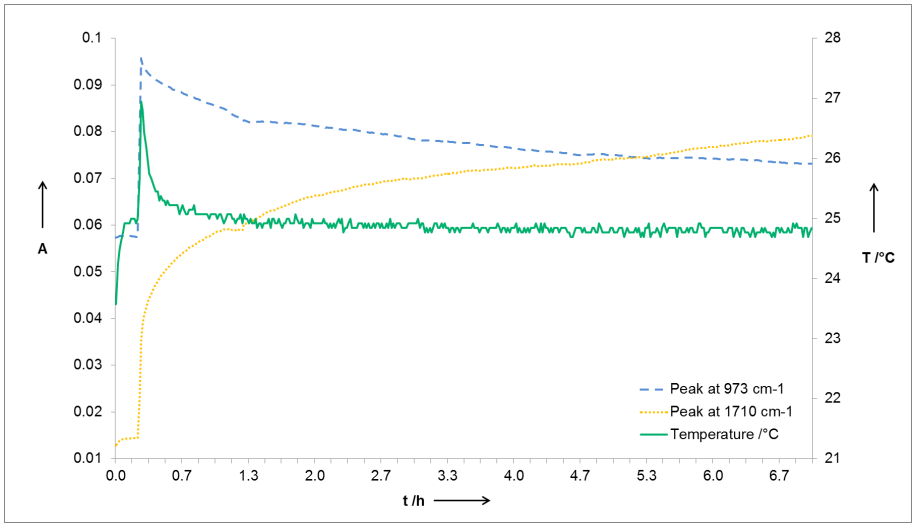


Figure 4.43: Decomposition of isopentyl nitrite (**94**, peak 973 cm^{-1}) into isopentanal (**95**, peak 1710 cm^{-1}).

The iron catalyst usually works as a single electron transfer catalyst [183]. We showed that iron(III) plays a crucial role in the decomposition of the nitrite. The action could be due to its Lewis acid properties or it could act as one-electron oxidant. To determine whether the redox mechanism is operative, we tried to determine the formation of Fe^{2+} during the reaction. The reaction mixture was mixed for 1 h without the presence of molecular oxygen so that all the molecular oxygen in the system would react and $FeCl_3$ convert to its reduced form in the reaction cycle. After 1 h we added $K_3[Fe(CN)_6]$ to the reaction mixture, followed by the addition of 3 mL of water. The reaction turned blue and the UV-VIS spectrum of the reaction mixture was identical to an independently prepared sample of Prussian blue ($Fe_4[Fe(CN)_6]_3 \cdot xH_2O$) (Figure 4.44).
The results point to the conclusion that iron can have two roles in the HNO_3-catalyzed

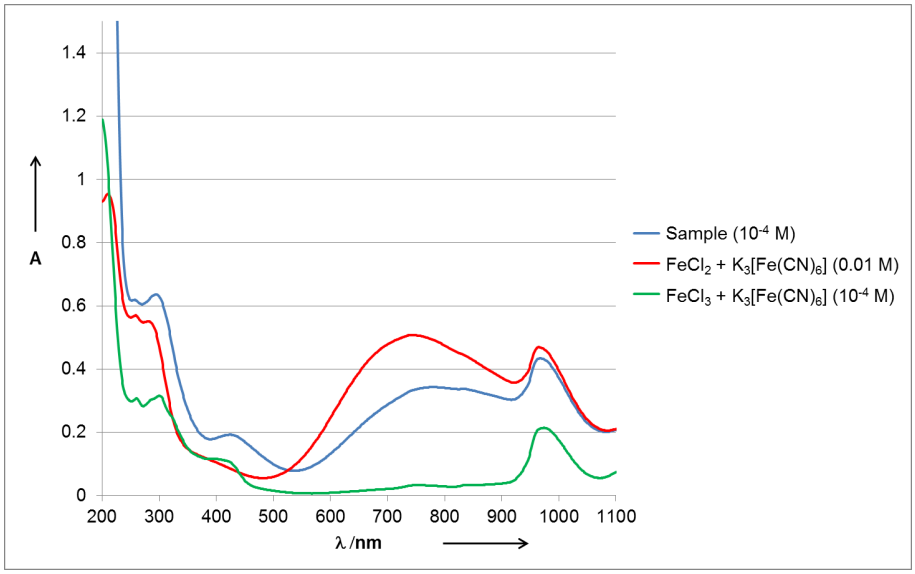
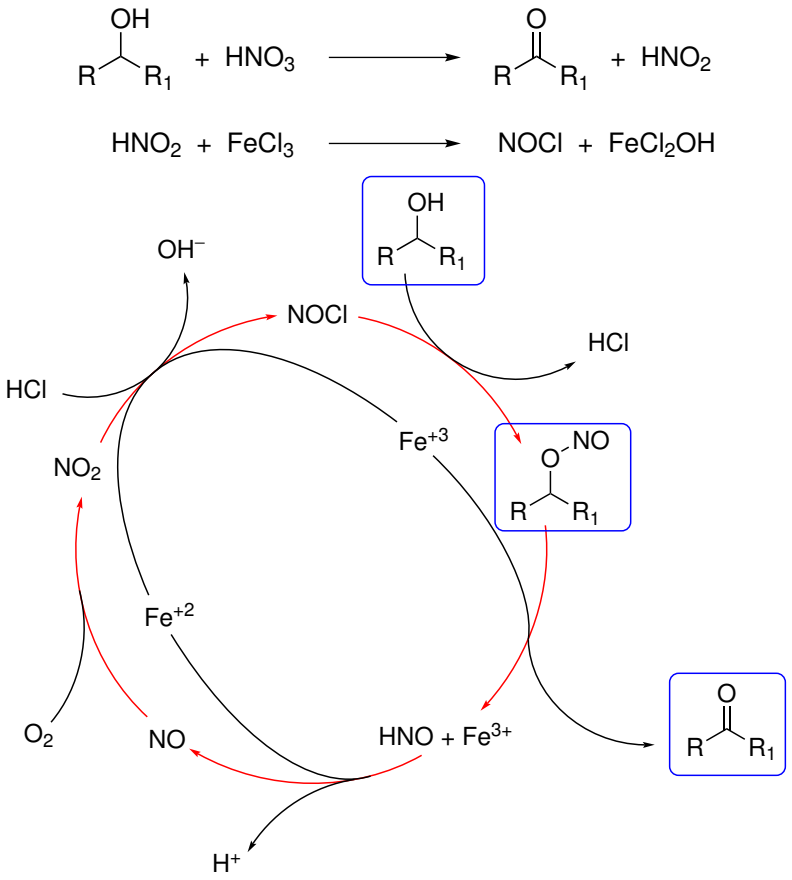


Figure 4.44: UV-VIS spectra of Prussian blue formed in reaction sample and reference.

aerobic oxidation of alcohols. First, it accelerates the decomposition of alkyl nitrite into a carbonyl compound and HNO, as was confirmed by the in-situ ATR-IR experiments. The HNO formed after the decomposition of alkyl nitrite can rapidly dimerize and yield N_2O [167].



Scheme 4.25: Mechanism for aerobic oxidation catalysed by HNO_3 and $FeCl_3$.

The second role of Fe^{3+} is to prevent dimerization of HNO into N_2O by working as a single electron catalyst by oxidising HNO into NO. NO can be further oxidised by molecular oxygen into NO_2. The iron catalyst is renewed into the Fe(III) form by oxidation with NO_2 and the reactive species NOCl is formed (Scheme 4.25). The ability of NO_2 to oxidise Fe^{2+} was confirmed by the following experiment. H_2SO_4 was added to the flask containing $NaNO_2$ to form NO_2, which was transferred by diffusion to a second flask connected to the first one by a tube. The second flask contained the solution of $FeCl_2$ in HFIP. After 1 h the reaction was stopped and solution of $K_4[Fe(CN)_6]$ was added. Prussian blue was immediately formed (proved by UV-VIS spectra) confirming the formation of Fe^{3+} species with NO_2. A blank reaction with $FeCl_2$ did not form any colouration, which was clearly confirmed with the UV-VIS spectroscopy.

4.2.6 Experimental data

General procedure for studying of the effect of the solvent in the oxidation with HNO_3
1.0 mmol (103.5 μL) of benzyl alcohol (**67a**) was dissolved in 1.0 mL of solvent (HFIP, TFE, EtOH, *i*-PrOH, MeCN, DCM, *n*-Hex) and then 1.0 mmol (69.7 μL) of 65 % HNO_3 was added. The reaction mixture was stirred for 10 min to 6 h at room temperature. The reaction conversion was followed with TLC chromatography. After the reaction was completed 2 mL of DCM and 2 mL of water were added. The water phase was neutralised with $NaHCO_{3(s)}$. The organic phase was separated from the water phase and dried with Na_2SO_4. The solvent was evaporated under reduced pressure. The conversion and selectivity of reaction were determined by ^{1}H NMR analysis.

General procedure for study of the effect of atmosphere in oxidation with HNO_3
1.0 mmol (103.5 μL) of benzyl alcohol (**67a**) was dissolved in 1.0 mL of 1,1,1,3,3,3-hexafluoro-2-propanol (HFIP) and then (2, 5, 10, 20 or 50 mol%) of 65 % HNO_3 (1.39, 3.49, 6.97, 13.94, 34.85 μL)was added. A balloon filled with (O_2 or air) was attached to a round bottom flask with the reaction mixture. The reaction performed under an inert atmosphere had gases removed from the bottle with a vacuum pump. The bottle was then refilled with argon. This was repeated twice before the addition of the substrates, solvent and reagents. The reaction mixture was stirred for 24 h at room temperature. After 24 h 2 mL of DCM and 2 mL of water were added to the reaction mixture. The water phase was neutralised with $NaHCO_{3(s)}$. The organic phase was separated from the water phase and dried with Na_2SO_4. The solvent was evaporated under reduced pressure. The conversion and selectivity of the reaction were determined by ^{1}H NMR analysis.

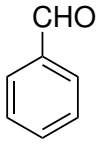
General procedure for *in situ* ATR-IR experiments
First 3.0 mL of 1,1,1,3,3,3-hexafluoro-2-propanol (HFIP) and 65 % HNO_3 (3.0 mmol – 209.1 μL or 0.3 mmol – 20.91 μL) were put in a reactor. In the case of catalytic oxidation (0.3 mmol HNO_3) a balloon filled with molecular oxygen was attached to reactor. With an ATR-IR probe the spectra was measured for 10 min. After 10 min 3.0 mmol (310.5 μL) of benzyl alcohol (**67a**) was added to the reactor. IR spectrum was measured for 24 h. After the reaction was complete 4 mL of DCM and 4 mL of water were added. The water phase was neutralised with $NaHCO_{3(s)}$. The organic phase was separated from the water phase and dried with Na_2SO_4. The solvent was evaporated under reduced pressure. The conversion and selectivity of the reaction were determined by ^{1}H NMR analysis.

General procedure for the synthesis of benzyl nitrite [176]
1.0 mmol (103.5 μL) of benzyl alcohol (**67a**) was dissolved in 3.0 mL of $CHCl_3$ followed by the addition of 1.1 mL of *t*-butyl nitrite. The reaction mixture was stirred for 4 h at room temperature. After 4 h, the reaction was stopped and the solvent was evaporated under reduced pressure. The conversion and selectivity of the reaction were determined by ^{1}H NMR analysis.

General procedure for the decomposition of benzyl nitrite
Benzyl nitrite synthesized using the previous method was put in a reactor and 1.0 mL of HFIP was added. The reaction was stirred for 20 h at 25 °C. The reaction was followed with an *in-situ* ATR-IR probe. After 20 h the reaction was stopped and the solvent was evaporated under reduced pressure. The conversion and selectivity of the reaction were determined by ^{1}H NMR analysis.

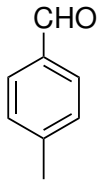
General procedure for oxidation of benzyl alcohols
1.0 mmol of substrate was dissolved in 1.0 mL of 1,1,1,3,3,3-hexafluoro-2-propanol (HFIP) and then 10, 15 or 20 mol% of 65 % HNO_3 (6.97, 10.46 or 13.94 μL) was added. A balloon filled with molecular oxygen was attached to a round bottle flask containing the reaction mixture. The reaction mixture was stirred for 5-24 h at room temperature. After the reaction was completed 2 mL of DCM was added, followed by washing with brine solution. The organic phase was separated from the water phase and dried with Na_2SO_4. The solvent was evaporated under reduced pressure. In some cases additional purification was needed with column chromatography on silica gel. The conversion and selectivity of the reaction were determined by ^{1}H NMR analysis. In some cases additional purification was needed with column chromatography on silica gel with the eluent n-Hex:EtOAc = 10:1 or DCM.

Benzaldehyde - 67b [184]



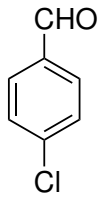
C_7H_6O, MW = 106.12
Conditions: 10 mol% of HNO_3
Yield: 97 %, 103.0 mg, bright yellow oil
^{1}H NMR (300 MHz, $CDCl_3$): δ 7.51-7.56 (m, 2H), 7.61-7.66 (m, 1H), 7.87-7.90 (m, 2H), 10.02 (s, 1H)
^{13}C NMR (76 MHz, $CDCl_3$): δ 128.93, 129.68, 134.40, 136.34, 192.34

4-Methylbenzaldehyde – 68b [185]



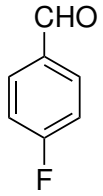
C_8H_8O, MW = 120.15
Conditions: 10 mol% of HNO_3
Yield: 93 %, 113.8 mg, yellow oil
^{1}H NMR (300 MHz, $CDCl_3$): δ 2.44 (s, 3H), 7.33 (AA'BB', J = 8 Hz, 2H), 7.78 (AA'BB', J = 8.0 Hz, 2H), 9.96 (s, 1H)
^{13}C NMR (76 MHz, $CDCl_3$): δ 21.86, 129.69, 129.84, 134.14, 145.57, 192.05

4-Chlorobenzaldehyde – 69b [152]



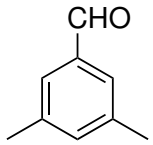
C_7H_5ClO, 140.57
Conditions: 15 mol% of HNO_3
Yield: 97 %, 135.9 mg, white powder
^{1}H NMR (300 MHz, $CDCl_3$): δ 7.52 (AA'BB', J = 8.5 Hz, 2H), 7.83 (AA'BB', J = 8.5 Hz, 1H), 9.99 (s, 1H)
^{13}C NMR (76 MHz, $CDCl_3$): δ 129.43, 130.87, 134.69, 140.93, 190.81

4-Fluorobenzaldehyde – 70b [185]



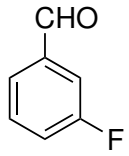
C_7H_5FO, MW = 124.11
Conditions: 10 mol% of HNO_3
Yield: 99 %, 122.3 mg, yellow oil
^{1}H NMR (300 MHz, $CDCl_3$): δ 7.21 (m, 2H), 7.91 (m, 2H), 9.96 (s, 1H)
^{13}C NMR (76 MHz, $CDCl_3$): δ 116.24 (d, J = 22.5 Hz), 132.17 (d, J = 9.8 Hz), 132.83 (d, J = 2.6 Hz), 166 (d, J = 257.0 Hz, CF), 190.59

3,5-Dimethylbenzaldehyde – 71b [185]



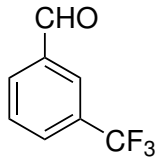
$C_9H_{10}O$, MW = 134.18
Conditions: 10 mol% of HNO_3
Yield: 99 %, 133.6 mg, yellow oil
^{1}H NMR (300 MHz, $CDCl_3$): δ 2.39 (d, J = 0.7 Hz, 6 H), 7.27 (m, 1H), 7.48 (m, 2H), 9.93 (s, 1H)
^{13}C NMR (76 MHz, $CDCl_3$): δ 21.03, 127.58, 136.27, 136.50, 138.75, 192.97

3-Fluorobenzaldehyde – **72b** [184]



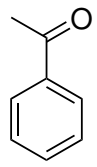
C_7H_5FO, MW = 124.11
Conditions: 15 mol% of HNO_3
Yield: 82 %, 107.3 mg, yellow oil
^{1}H NMR (300 MHz, $CDCl_3$): δ 7.34 (tdd, J = 8.3, 2.7, 1.2 Hz, 1H) 7.48-7.57 (m, 2H), 7.68 (dt, J = 7.6, 1.2 Hz, 1H), 10.00 (s, 1H)
^{13}C NMR (76 MHz, $CDCl_3$): δ 115.32 (d, J = 21.7 Hz), 121.56 (d, J = 21.8 Hz), 126.02 (d, J = 2.8 Hz), 130.76 (d, J = 7.6 Hz), 138.37 (d, J = 6.7 Hz), 163.07 (d, J = 249.4 Hz, CF), 190.88

3-(Trifluoromethyl)benzaldehyde - 73b [152]



$C_8H_5F_3O$, MW = 174.12
Conditions: 20 mol% of HNO_3
Yield: 99 %, 174.0 mg, yellow oil
^{1}H NMR (300 MHz, $CDCl_3$): δ 7.64-7.74 (m, 1H), 7.89 (d, J = 7.7 Hz, 1H), 8.09 (d, J = 8.1 Hz, 1H), 8.15 (s, 1H), 10.09 (s, 1H)
^{13}C NMR (76 MHz, $CDCl_3$): δ 123.46 (q, J = 272.46 Hz, CF3), 126.20 (q, J = 3.9 Hz), 129.68, 130.66 (q, J = 3.6 Hz), 131.63 (q, J = 33.3 Hz), 132.63, 136.68, 190.68

Acetophenone – **76b** [184]



C_8H_8O, MW = 120.15
Conditions: 20 mol% of HNO_3
Yield: 70 %, 83.6 mg, bright yellow oil
^{1}H NMR (300 MHz, $CDCl_3$): δ 2.58 (s, 3H), 7.41-7.46 (m, 2H), 7.52-7.57 (m, 1H), 7.93-7.96 (m, 2H)
^{13}C NMR (76 MHz, $CDCl_3$): δ 26.40, 128.12, 128.39, 132.93, 136.92, 197.95

General procedure for the scope of the metal co-catalyst
1.0 mol% of metal salt ($FeCl_3$, $FeCl_2$, CuI, CuCl, $CuCl_2 \cdot 2\,H_2O$, $AlCl_3$, $K_3[Fe(CN)_6]$, $Fe(NO_3)_3$) or 3.0 mol% of catalyst (NaCl, HCl) was added to 1.0 ml of HFIP followed by the addition of 65 % HNO_3 (5 mol%, 3.49 μL). At the end 1.0 mmol (158.8 μL) of 2-octanol (**77**) was added to the reaction mixture. A balloon filled with molecular oxygen was attached to a round bottom flask with the reaction mixture. The reaction mixture was stirred for 24 h at room temperature. After 24 h, 2 mL of DCM was added and the solution was washed with brine solution. An organic phase was separated from the water phase and dried with Na_2SO_4. The solvent was evaporated under reduced pressure. The conversion and selectivity of the reaction were determined by ^{1}H NMR analysis.

General procedure for the influence of the amount $FeCl_3$
0 – 5.0 mol% $FeCl_3$ were added to 1.0 ml of HFIP followed by the addition of 65 % HNO_3 (5 mol%, 3.49 μL). At the end 1.0 mmol (158.8 μL) of 2-octanol (**77**) was added to the reaction mixture. A balloon filled with molecular oxygen was attached to a round bottom flask with the reaction mixture. The reaction mixture was stirred for 24 h at room temperature. After 24 h, 2 mL of DCM was added and the solution was washed with brine solution. The organic phase was separated from the water phase and dried with Na_2SO_4. The solvent was evaporated under reduced pressure. The conversion and selectivity of the reaction were determined by ^{1}H NMR analysis.

General procedure for the $Fe(NO_3)_3$ + HX reactions
1.0 mol% of $Fe(NO_3)_3$ (4.0 mg) was added to 1.0 ml of HFIP followed by addition of 5 mol% of HX (HCl - 37 %, 4.2 μL; HBr - 48 %, 5.65 μL). At the end 1.0 mmol (158.8 μL) of 2-octanol (**77**) was added to the reaction mixture. A balloon filled with molecular oxygen was attached to a round bottom flask with the reaction mixture. The reaction mixture was stirred for 23 h at room temperature. After 23 h, 2 mL of DCM was added and the solution was washed with brine solution. The organic phase was separated from the water phase and dried with Na_2SO_4. The solvent was evaporated under reduced pressure. The conversion and selectivity of the reaction were determined by ^{1}H NMR analysis.

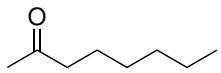
Procedure for experiments with isopentyl nitrite (94)
Initially, the oxygen was removed from the reactor under a nitrogen flow. 0 or 1.0 mol% (5.1 mg) $FeCl_3$ was added to 3.0 ml of HFIP followed by the addition of 3.0 mmol (418 μL) of isopentyl nitrite (**94**). A balloon filled with argon was attached to the reaction mixture. The reaction mixture was stirred for 20 h at room temperature. The conversion and selectivity of the reaction were determined by ^{1}H NMR analysis without additional isolation.

Confirmation of the formation of Fe^{2+} ions in the reaction mixture
1.0 mol% (1.7 mg) $FeCl_3$ was added to 1.0 ml of HFIP followed by the addition of 5 mol% (3.49 μL) of 65 % HNO_3. At the end 1.0 mmol of 2-octanol (**77**) was added to the reaction mixture. The reaction mixture was stirred for 2 h at room temperature. After 2 h 2 mL of water was added. The sample was taken for UV-VIS measurements. This was followed by the addition of 2.2 mg of $K_3[Fe(CN)_6]$ and an additional 1 mL of water. The sample sizes taken for the UV-VIS spectroscopy were 150 μL.

Confirmation of formation of Fe^{3+} ions in reaction with $FeCl_2$ and NO_2
69.0 mg (1.0 mmol) of $NaNO_2$ and 55.7 of 96 % H_2SO_4 were mixed in the first flask, where the balloon with molecular oxygen was attached. The first flask was connected by a glass tube to a second flask. The second flask contained a solution of $FeCl_2$ (0.1 mmol, 19.9 mg) in 1.0 mL of HFIP. After 23 h 4 mL of water and 31.6 mg (0.075 mmol) of $K_4[Fe(CN)_6]$ were added to the second flask. Solution turned to a blue-green colour. The sample taken (150 μL) for UV-VIS spectroscopy was diluted with water to $9.4 \cdot 10^{-5}$ M in regard to $K_4[Fe(CN)_6]$.

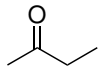
General procedure for the oxidation of alcohols with an iron catalyst
1.0 mol% (1.7 mg) $FeCl_3$ was added to 1.0 ml of HFIP followed by the addition of (5–20 mol%) 65 % HNO_3. At the end 1.0 mmol of substrate was added to the reaction mixture. A balloon filled with molecular oxygen was attached to a round bottom flask with the reaction mixture. The reaction mixture was stirred for 5–24 h at room temperature. After the reaction was complete, 2 mL of DCM was added and the reaction solution was washed with a brine solution. An organic phase was separated from the water phase and dried with Na_2SO_4. The solvent was evaporated under reduced pressure. In some cases additional purification was needed with column chromatography on silica gel.

2-Octanone - 78 [186]



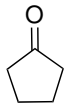
$C_8H_{16}O$, MW = 128.21
Yield: 100 % - determined through NMR with internal standard, colourless oil
^{1}H NMR (300 MHz, $CDCl_3$): δ 0.78-0,98 (m, 3H), 1.28 (m, 6H), 1.57 (m, 2H), 2.14 (s, 3H), 2.43 (t, J = 7.5 Hz, 2H)
^{13}C NMR (76 MHz, $CDCl_3$): δ 13.98, 22.45, 23.81, 28.81, 29.79, 31.54, 43.82, 210.01

2-Butanone - 80 [187]



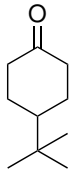
C_4H_8O, MW = 72.11
Yield: 77 %, colourless liquid
^{1}H NMR (300 MHz, $CDCl_3$): δ 1.06 (t, J = 7.3 Hz, 3H), 2.14 (s, 3H), 2.46 (q, J = 7.3 Hz, 2H)
^{13}C NMR (76 MHz, $CDCl_3$): δ 7.83, 29.44, 36.87, 209.68

Cyclopentanone - 81 [186]



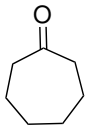
C_5H_8O, MW = 84.12
Yield: 88 %, 73.7 mg, colourless oil
^{1}H NMR (300 MHz, $CDCl_3$): δ 1.97 (m, 4H), 2.18 (m, 4H)
^{13}C NMR (76 MHz, $CDCl_3$): δ 23.19, 38.39, 224.63

4-*t*-Butylcyclohexan-1-one - 82 [188]



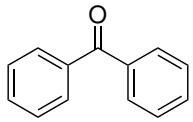
$C_{10}H_{18}O$, MW = 154.25
Mobile phase for column chromatography: DCM/MeOH = 20/1
Yield: 74 %, 111.7 mg
^{1}H NMR (300 MHz, $CDCl_3$): δ 0.92 (s, 9H), 1.47 (m, 3H), 2.10 (m, 2H), 2.38 (m, 4H)
^{13}C NMR (76 MHz, $CDCl_3$): δ 27.58, 32.45, 41.29, 46.69, 212.55

Cycloheptanone - 83 [186]



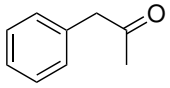
$C_7H_{12}O$, MW = 112.17
Mobile phase for column chromatography: *n*-Hex/EtOAc = 4/1
Yield: 59 %, 65.9 mg
^{1}H NMR (300 MHz, $CDCl_3$): δ 1.69 (m, 8H), 2.50 (m, 4H)
^{13}C NMR (76 MHz, $CDCl_3$): δ 24.26, 30.34, 43.80, 215.56

Benzophenone - 84 [187]



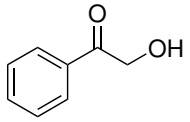
$C_{13}H_{10}O$, MW = 182.22
Mobile phase for column chromatography: DCM
Yield: 83 %, 151.2 mg
^{1}**H NMR (300 MHz, $CDCl_3$):** δ 7.45-7.50 (m, 4H), 7.56-7.61 (m, 2H), 7.79-7.82 (m, 4H)
^{13}**C NMR (76 MHz, $CDCl_3$):** δ 128.24, 130.02, 132.38, 137.56, 196.72

1-Phenylpropan-2-one - 85 [189]



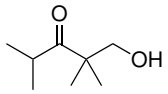
$C_9H_{10}O$, MW = 134.18
Yield: 83 %, 154.3 mg
^{1}**H NMR (300 MHz, $CDCl_3$):** δ 2.15 (s, 3H), 3.69 (s, 2H), 7.21 (m, 2H), 7.27-7.36 (m, 3H)
^{13}**C NMR (76 MHz, $CDCl_3$):** δ 29.26, 51.04, 127.05, 128.74, 129.37, 134.22, 206.40

2-Hydroxy-1-phenylethan-1-one - 86 [190]



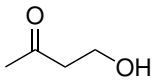
$C_8H_8O_2$, MW = 136.15
Mobile phase for column chromatography: *n*-Hex/EtOAc = 2/1
Yield: 95 %, 133.5 mg, white crystals
^{1}**H NMR (300 MHz, $CDCl_3$):** δ 3.50 (t, J = 4.7 Hz, OH), 4.88 (d, J = 4.7 Hz, 2H), 7.51 (m, 2H), 7.63 (m, 1H), 7.92 (m, 2H)
^{13}**C NMR (76 MHz, $CDCl_3$):** δ 65.43, 127.66, 128.94, 133.35, 134.26, 198.35

1-Hydroxy-2,2,4-trimethylpentan-3-one - 87 [191]



$C_8H_{16}O_2$ MW = 144.21
Mobile phase for column chromatography:DCM/MeOH = 10/1
Yield: 96 %, 138.3 mg, white powder
^{1}**H NMR (300 MHz, $CDCl_3$):** δ 1.06 (d, J = 6.7 Hz, 6H), 1.18 (s, 6H), 2.38 (br s, 1H), 3.09 (hept, J = 6.7 Hz, 1H), 3.55 (s, 2H)
^{13}**C NMR (76 MHz, $CDCl_3$):** δ 19.88, 21.11, 34.59, 49.61, 69.43, 221.81

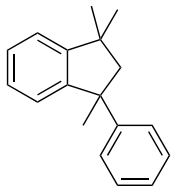
4-Hydroxybutan-2-one - 88 [192]



$C_4H_8O_2$, MW = 88.11
Yield: 98 % - determined through NMR with internal standard
^{1}**H NMR (300 MHz, $CDCl_3$):** δ 2.20 (s, 3H), 2.70 (t, J = 5.5 Hz, 2H), 2.78 (br s, 1H), 3.85 (t, J = 5.5 Hz, 2H)
^{13}**C NMR (76 MHz, $CDCl_3$):** δ 30.35, 45.30, 57.60, 209.37

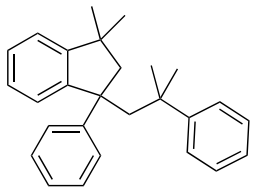
General procedure for oxidation of terciary alcohols
1 mol% of $FeCl_3$ (1.7 mg) was dissolved in 1.0 mL of solvent (HFIP, TFE) followed by addition of 1.0 mmol of 2-phenyl-propan-2-ol (**89**). The reaction mixture was stirred for 3 h. After the reaction was complete, 2 mL of DCM was added and the reaction solution was washed with brine solution. An organic phase was separated from the water phase and dried with Na_2SO_4. The solvent was evaporated under reduced pressure. The substrates were separated with column chromatography on silica gel with n-Hex:DCM = 20:1 mobile phase.

1,1,3-Trimethyl-3-phenyl-2,3-dihydro-1*H*-indene - 90 [181]



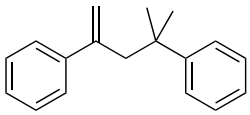
$C_{18}H_{20}$, MW = 236.35
Yield: 57 %, 67.5 mg, colourless oil
^{1}**H NMR (300 MHz, $CDCl_3$):** δ 1.03 (s, 3H), 1.34 (s, 3H), 1.69 (s, 3H), 2.19 (d, J = 13.0 Hz, 1H), 2.42 (d, J = 13.0 Hz, 1H), 7.32 – 7.07 (m, 9H)
^{13}**C NMR (76 MHz, $CDCl_3$):** δ 30.36, 30.67, 30.88, 42.84, 50.78, 59.22, 76.58, 77.00, 77.42, 122.52, 124.97, 125.45, 126.60, 126.65, 127.17, 127.95, 148.68, 150.97, 152.16

1,1-Dimethyl-3-(2-methyl-2-phenylpropyl)-3-phenyl-2,3-dihydro-1*H*-indene - 91



$C_{27}H_{30}$, MW = 354.53
Yield: 18 %, 19.6 mg
^{1}H NMR (300 MHz, $CDCl_3$): δ 0.66 (s, 3H), 1.06 (s, 3H), 1.12 (2s, 6H), 1.95 (d, J = 13.5 Hz, 1H), 2.02 (d, J = 13.5 Hz, 1H), 2.39 (d, J = 15.0 Hz, 1H), 2.84 (d, J = 15.0 Hz, 1H), 7.04 – 7.35 (m, 13H), 7.45 (m, 1H)
^{13}C NMR (76 MHz, $CDCl_3$): δ 28.63, 29.57, 29.64, 33.88, 38.84, 42.39, 51.23, 54.89, 55.62, 76.58, 77.00, 77.42, 122.53, 125.29, 125.35, 125.70, 125.77, 127.17, 127.42, 127.70, 128.02, 147.56, 149.65, 150.40, 151.69, 153.92.

(4-Methylpent-1-ene-2,4-diyl)dibenzene - 92 [181]

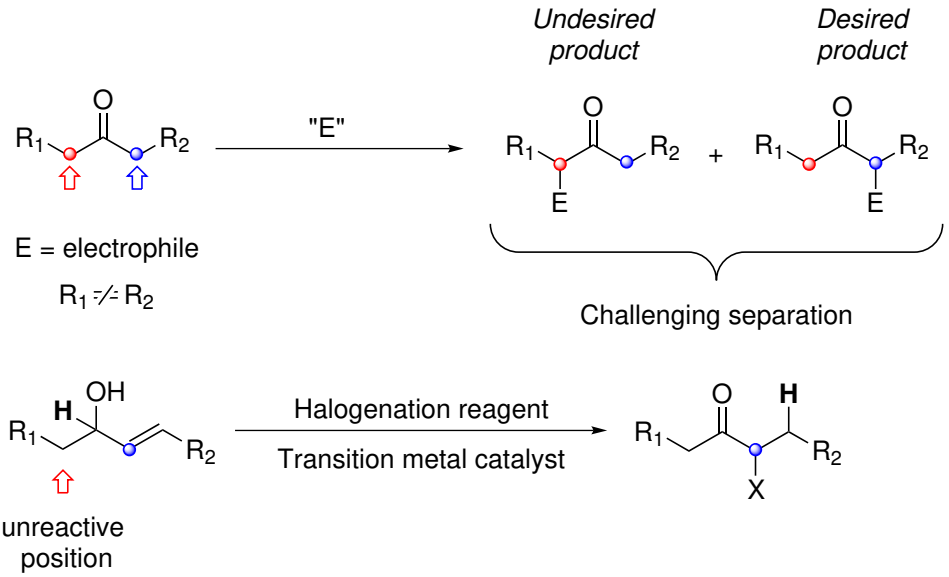


$C_{18}H_{20}$, MW = 236.35
Yield: 62 %, 73.3 mg
^{1}H NMR (300 MHz, $CDCl_3$): δ 1.22 (s, 6H), 2.83 (s, 2H), 4.78 (m, 1H), 5.14 (d, J = 1.9 Hz, 1H), 6.95 – 7.52 (m, 10H)
^{13}C NMR (76 MHz, $CDCl_3$): δ 28.73, 38.65, 49.56, 76.58, 77.00, 77.42, 116.85, 125.41, 125.90, 126.48, 126.79, 127.79, 127.98, 143.44, 146.67, 149.37.

4.3 Aerobic oxidative iodination

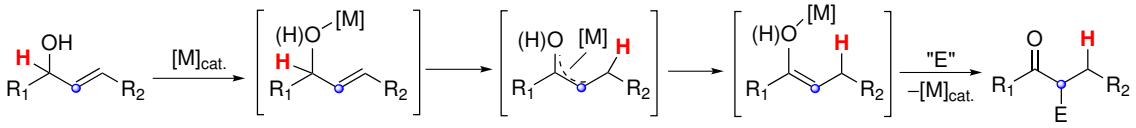
α-Halocarbonyl compounds have high synthetic values as they are used as building blocks. This is due to a variety of functional groups that can be selectively introduced, both at the halogenated α-carbon atom and the carbonyl group [193]. They readily undergo various reactions such as substitutions [193]–[196], cross-coupling reaction [197]–[200] and for formation of heterocycles [201].

Methods for the synthesis of α-halocarbonyl compounds suffer from two distinct problems. The first problem comes from use of environmentally hazardous molecules, long reaction times, harsh conditions and/or inconvenient work-up procedures [202]. The selectivity of the reaction represents the second problem because of the formation of α,α-dihalogenated products and limits the selective halogenation to a substrates with only one enolizable position [203]. The reaction with unsymmetrical aliphatic ketones is challenging (Scheme 4.26). To achieve regioselective functionalization of carbonyl compounds, most methods rely on steric and electronic differentiations [203]. However, with some substrates enolization cannot be obtained at the desired position and complete regioselectivity cannot be achieved. The formation of a mixture of α-halocarbonyl compounds limits the yield and utility of the methods because of the challenging separation of constitutional isomers [203]. Complete regiocontrol was achieved by Belén *et al.* through a 1,3-hydrogen shift on allylic alcohols and tandem halogenation catalysed by transition metals (Scheme 4.26) [203]–[205].



Scheme 4.26: Selectivity in synthesis of α-haloketones.

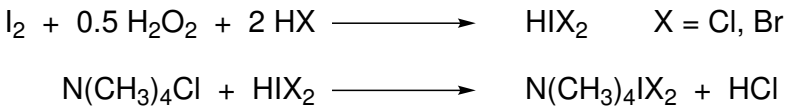
The allylic alcohols can be isomerised into carbonyl compounds by addition of the transition metal catalyst. The isomerisation occurs through formation of the transition metal enolates. However, if the electriphiles are present in the reaction media, α-functionalised carbonyl compounds are formed regiospecifically (Scheme 4.27) [204], [206].



Scheme 4.27: Tandem 1,3-hydrogen shift/α-functionalisation of allylic alcohols.

Even though various methods have been developed for the synthesis of α-haloketones there is significant lack of methods for the synthesis of α-iodoketones. This limitation is due to the low electrophilic character of molecular iodine and the strong leaving group ability of iodide [207]. The electrophilic iodination of the α-carbonyl site was thus far synthesised by the activation of iodine with cerium(IV) ammonium nitrate [208], SeO_2 [209] or with an excess of iodine, which worked as a Lewis acid [210]. The second type of methods uses iodine salt in combination with an oxidising agent such as NH_4I/Oxone [211] or $NaI/H_2O_2/H_2SO_4$ [212]. α-iodoketones were also prepared through nucleophilic substitutions [213], iodination of enol acetales with *N*-iodosuccinimide [214] and IBX/I_2 mediated oxidation of alkenes [215].

Hypervalent iodine, e.g., iodine(I) compounds are much more reactive than iodine itself. Iodine(I) reagents can be simply synthesized through the reaction of I_2, H_2O_2 and HX (X=Cl, Br), which produces HIX_2 (Scheme 4.28) [216]. By using H_2O_2 or O_2 to produce iodine(I) reagents such methods have "green" potential. The electrophilic properties of iodine(I) were successfully used for the preparation of iodoarenes and the addition to alkenes [71], [153], [216]. The reactivity of the reagents was increased when performed in TFE.

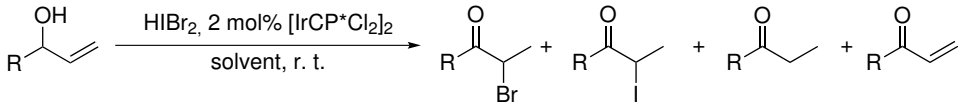


Scheme 4.28: Synthesis of iodine(I) reagents.

Our plan was to combine $[IrCp^*Cl_2]_2$ catalyst for 1,3-hydrogen shift with HIX_2 reagent for the electrophilic addition of an iodine atom to an α-carbon atom. It was envisioned that the reactivity of the iodine(I) species can be further increased by the use of fluorinated alcohols. For a model substrate we chose 1-octene-3-ol. We found that $HICl_2$ and $N(CH_3)_4ICl_2$ have a high reactivity and the addition to a double bond proceeds too fast for the iridium catalyst to work.

Therefore, we continued our research with $HIBr_2$ as an iodine(I) reagent. Its lower reactivity was a step in the right direction as we obtained α-bromoketone (**98**) and α-iodoketones (**99**). The selectivity of the reaction was highly dependent on the the choice of solvent (Table 4.23). High selectivity for **98** was obtained with the solvent mixture THF:H_2O=1:1 (Table 4.23, entry 4). In MeCN and HFIP only addition of the $HIBr_2$ on double bond occurred, forming 1,2-dibromo-octane-3-ol and 1-bromo-2-iodo-octane-3-ol. Separation of products proved to be problematic and we were unsuccessful in their characterisation with HR-MS.

Table 4.23: Solvent effect on selectivity in reaction of iodine(I) with 1-octene-3-ol.[a]

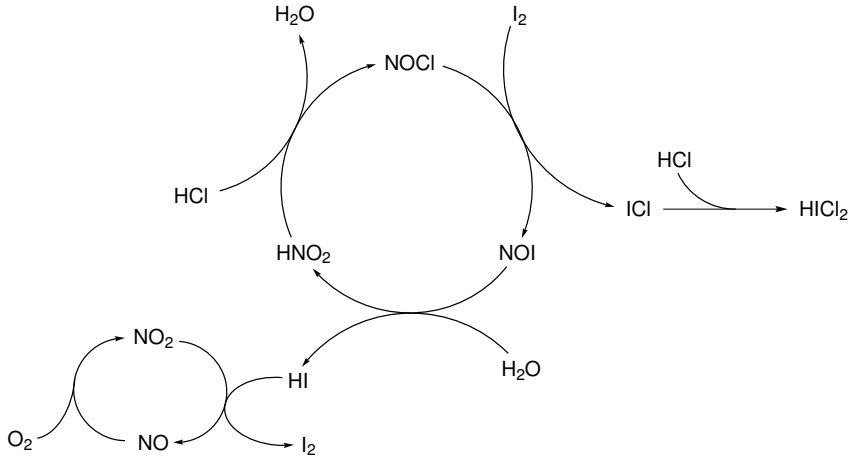


97 R = $-(CH_2)_4CH_3$ **98** **99** **100** **101**

Entry	Solvent	time [h]	Conversion [%]	**98**	**99**	**100**	**101**	Addition products
1	MeCN	23	95	0	0	0	0	100
2	THF	23	92	33	0	7	0	60
3	HFIP	1	96	0	0	0	0	100
4	THF:H_2O=1:1	16	73	81	0	16	3	0
5	THF:H_2O=1:1[b]	20	81	80	0	20	0	0
6	THF:EtOH=1:1	22	70	32	35	15	8	10
7	EtOH:H_2O=2:3	25	77	21	56	8	<1	15

[a] Reaction conditions: 1-octene-3-ol (**97**; 1.0 mmol, 157.5 μL), 1.0 mmol $HIBr_2$, 2 mol% $[IrCp^*Cl_2]_2$ (12.3 mg), 5.0 mL of solvent mixture, room temperature, 1 – 25 h. Selectivity and conversion were determined through ^{1}H NMR.
[b] $N(CH_3)_4ICl_2$ used as iodine(I) reagent.

However, a saturated ketone was formed as a side product in a substantial amount. Changing the reagent from $HIBr_2$ to $N(CH_3)_4ICl_2$ did not improve the reaction selectivity. In solvent mixtures containing EtOH α-iodoketone **99** was formed in a larger amount. The best result for the formation of **99** was obtained in EtOH:H_2O=2:3 (Table 4.23, entry 7), where the iodo product **99** was formed in a 56 % yield. Since control of the reaction selectivity was challenging we decided to produce $HICl_2$ in a catalytic amount to reduce the side reactions. Recently, the catalytic formation of $HICl_2$ *in situ* was reported by Iskra *et al.* [153], who used nitrogen oxide gases as an oxidant and oxygen as a terminal oxidant (Scheme 4.29). Following their example we modified the procedure by using $NaNO_2$ as a source of NO_x gases and HCl was added in sub-stoichiometric amounts.

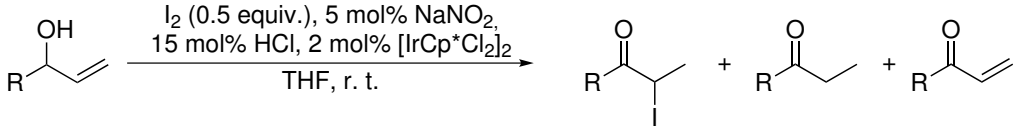


Scheme 4.29: Mechanism for catalytic formation of $HICl_2$.

First, we tested tandem aerobic iodination/catalytic 1,3-hydride shift reaction under an O_2 atmosphere. As an initial solvent we chose THF, with which we observed the formation

of α-haloketone in previous reactions with $HIBr_2$. The reaction was performed by adding THF to 2 mol% of iridium catalyst, 5 mol% of $NaNO_2$ and 1 equiv. of I_2. During stirring of the reaction mixture 15 mol% of HCl was added, followed by the addition of **97**. In the last step balloon with the desired atmosphere (O_2 or air) was attached to the flask. The difference was small between the reactions performed under oxygen or an air atmosphere. While complete conversion was obtained under molecular oxygen atmosphere, it also had a lower selectivity for iodinated product (Table 4.24). Therefore, the future reactions were performed under air.

Table 4.24: Iridium-catalysed isomerization/aerobic iodination of allyl alcohols.[a]



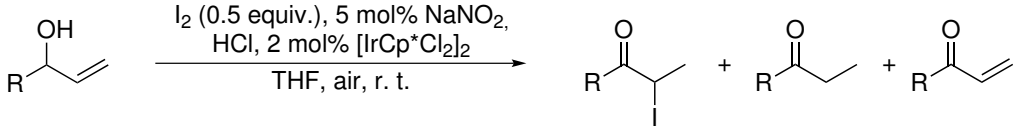
97 R = $-(CH_2)_4CH_3$ **99** **100** **101**

Entry	Atmosphere	Time [h]	Conversion [%]	**99**	**100**	**101**
1	O_2	23	100	59	36	5
2	Air	22	92	61	25	14

[a] Reaction conditions: 1-octene-3-ol (**97**; 0.2 mmol, 30.9 μL), 5 mol% $NaNO_2$ (0.7 mg), HCl (15 mol%, 2.46 μL), 2 mol% $[IrCp^*Cl_2]_2$ (0.004 mmol, 3.2 mg), 1 mL of THF, room temperature, 22 h. Selectivity and conversion were determined through ^{1}H NMR.

In next step we looked at the influence of the amount of HCl on the selectivity of the reaction. Interestingly, a decrease in the amount of HCl increased the selectivity for iodo ketone **99**, while the conversion was still high. A high conversion was obtained even in the absence of HCl (Table 4.25, entry 3). Chlorine atoms, needed for the formation of reactive species $ICl/HICl_2$, could come from the Ir-catalyst. Therefore, no additional source of chlorine atoms is needed. Decreasing the amount of HCl increased the yield of iodo-ketone **99** and decreased the formation of saturated ketone **100**.

Table 4.25: Influence of amount of HCl on catalytic isomerization/iodination of allyl alcohols.[a]



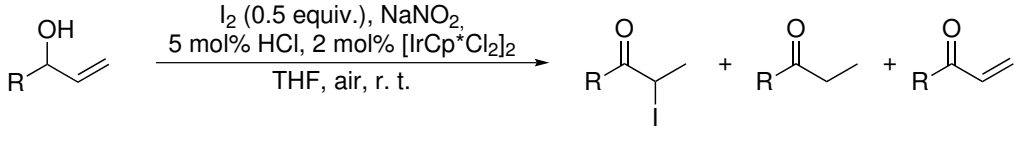
97 R = $-(CH_2)_4CH_3$ **99** **100** **101**

Entry	HCl [mol%]	Time [h]	Conversion [%]	**99**	**100**	**101**
1	15	22	100	56	36	5
2	5	22	91	57	26	16
3	0	22	91	64	25	11

[a] Reaction conditions: 1-octene-3-ol (**97**; 0.2 mmol, 30.9 μL), I_2 (0.1 mmol, 25.4 mg), 5 mol% $NaNO_2$ (0.7 mg), HCl, 2 mol% $[IrCp^*Cl_2]_2$ (0.004 mmol, 3.2 mg), 1 mL of THF, room temperature, 22 h. Selectivity and conversion were determined through ^{1}H NMR.

An increase of $NaNO_2$ had the opposite effect and the yield of iodinated product **99** increased, while the saturated ketone **100** decreased (Table 4.25). At a higher loading of $NaNO_2$ complete conversion was observed and saturated ketone **100** was not formed at all. However, unsaturated ketone **101** was still formed in a 12 % yield.

Table 4.26: Influence of amount of $NaNO_2$ on catalytic isomerization/iodination of allyl alcohols.[a]



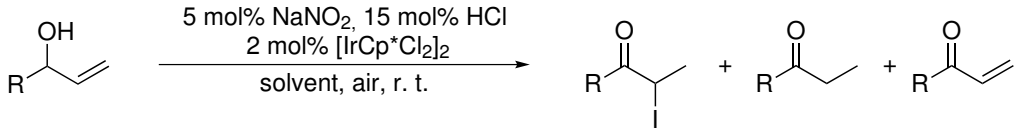
97 R = $-(CH_2)_4CH_3$ **99** **100** **101**

Entry	$NaNO_2$ [mol%]	Time [h]	Conversion [%]	**99**	**100**	**101**
1	10	22	100	88	0	12
2	5	22	91	57	26	17
3	2	22	72	43	47	10

[a] Reaction conditions: 1-octene-3-ol (**97**; 0.2 mmol, 30.9 μL), I_2 (0.1 mmol, 25.4 mg), $NaNO_2$, HCl (5 mol%, 0.82 μL), 2 mol% $[IrCp^*Cl_2]_2$ (0.004 mmol, 3.2 mg), 1 mL of THF, room temperature, 22 h. Selectivity and conversion were determined through ^{1}H NMR.

In our final step we checked the influence of the solvent (Table 4.27). The non-polar solvent *n*-hexane in comparison with THF had a higher selectivity for **99** but a low conversion.

Table 4.27: Influence of solvent on catalytic isomerization/iodination of allyl alcohols.[a]



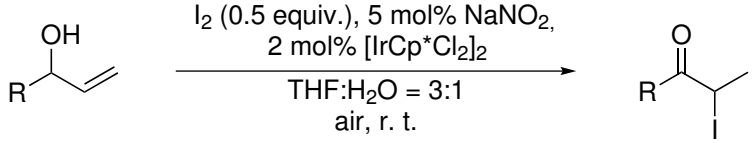
97 R = $-(CH_2)_4CH_3$ **99** **100** **101**

Entry	Solvent	Time [h]	Conversion [%]	**99**	**100**	**101**
1	THF	22	100	59	36	5
2	*n*-Hex	22	36	71	17	9
3	HFIP	22	Complex mixture			
4	EtOH:H_2O=2:3	22	32	66	34	0
5	THF:H_2O=1:1	22	64	66	23	5
6	THF:H_2O=2:1	22	66	82	11	8
7[b]	THF:H_2O=3:1	6	>99	93	0	7

[a] Reaction conditions: 1-octene-3-ol (**97**; 0.2 mmol, 30.9 μL), I_2 (0.1 mmol, 25.4 mg), 5 mol% $NaNO_2$ (0.7 mg), HCl (15 mol%, 2.46 μL), 2 mol% $[IrCp^*Cl_2]_2$ (0.004 mmol, 3.2 mg), 1 mL of solvent, room temperature, 22 h. Selectivity and conversion were determined through ^{1}H NMR.
[b] Reaction performed with absence of HCl and with 1.3 mL of solvent.

HFIP, which was thus far successfully used as a template catalyst, had poor selectivity. Its interaction with an iridium catalyst and its activating nature to activate electrophiles caused the formation of multiple products. Using a THF-water mixture there was an improved selectivity for the formation of **99**. At higher THF/water ratios a higher selectivity and conversion were obtained. The best result was obtained with THF:H_2O=3:1 with no HCl in the reaction mixture. Under such conditions the reaction was complete in 6 h and a 93 % conversion into **99** was obtained.

With optimised conditions we iodinated other substrates. With 1-pentene-3-ol (**102**) we obtained a high conversion into α-iodoketone (**103**). As a side product α-chloroketone (**104**, 7 %) was formed. Chlorine atoms could come only from the iridium catalyst. On the other hand, a in reaction with 3-phenyl-prop-1-en-3-ol (**105**) a poor yield was obtained for 2-iodo-1-phenylpropanone (**106**, 35 %) with unsaturated ketone formed as side product (5 %). According to the NMR spectra the rest was the starting compound **105** and therefore a substrate-specific optimisation is needed.



R = -CH_2CH_3	93	**103**
R = -$(CH_2)_4CH_3$	93	**99**
R = -Ph	35	**106**

Scheme 4.30: Catalytic isomerisation/iodination on other substrates.

4.3.1 Experimental data

Procedure for reactions under different atmosphere conditions In a flask 5 mol% $NaNO_2$ (0.01 mmol, 0.7 mg) was added, followed by 2 mol% $[IrCp^*Cl_2]_2$ (0.004 mmol, 3.2 mg) and 0.5 eq. I_2 (0.1 mmol, 25.4 mg). Next, 1 mL of THE was added, followed by the addition of 15 mol% of HCl (37 %, 2.46 μL). In the last step 1-octene-3-ol (**97**) was added (0.2 mmol) and a balloon with air or O_2 was attached to the flask. The reaction mixture was mixed at room temperature for 22–23 h. The reaction mixture was then transferred in a separatory funnel. The flask and magnet were washed with 2 ml DCM and 2 mL of water. In the case of poor phase separation some NaCl was added. The organic phase was separated from the water phase and dried with Na_2SO_4. Na_2SO_4 was filtered away and the solvents were removed under reduced pressure. The conversion and selectivity of the reaction were determined by ^{1}H NMR analysis without additional isolation.

Procedure for investigation of the influence of the amount of HCl on the reaction selectivity In a flask 5 mol% $NaNO_2$ (0.01 mmol, 0.7 mg) was added, followed by 2 mol% $[IrCp^*Cl_2]_2$ (0.004 mmol, 3.2 mg) and 0.5 eq. I_2 (0.1 mmol, 25.4 mg). Next, 1 mL of THE was added, followed by the addition of 0, 5 or 15 mol% of 37 % HCl (0, 0.82 μL or 2.46 μL). In the last step 1-octene-3-ol (**97**) was added (0.2 mmol) and a balloon with air was attached to the flask. The reaction mixture was mixed at room temperature for 22–23 h. The reaction mixture was then transferred in a separatory funnel. The flask and magnet were washed with 2 ml DCM and 2 mL of water. In the case of poor phase separation some NaCl was added. The organic phase was separated from the water phase and dried with Na_2SO_4. The Na_2SO_4 was filtered away and the solvents were removed under reduced pressure. The conversion and selectivity of the reaction were determined by ^{1}H NMR analysis, without any additional isolation.

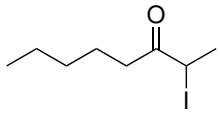
Procedure for investigation of the influence of the amount of $NaNO_2$ on the reaction selectivity In a flask 2, 5 or 10 mol% $NaNO_2$ (0.3, 0.7 or 1.4 mg) was added, followed by 2 mol% $[IrCp^*Cl_2]_2$ (0.004 mmol, 3.2 mg) and 0.5 eq. I_2 (0.1 mmol, 25.4 mg). Next, 1 mL of THE was added, followed by the addition of 15 mol% of HCl (37 %, 2.46 μL). In the last step 1-octene-3-ol (**97**) was added (0.2 mmol) and a balloon with air was attached to the flask. The reaction mixture was mixed at room temperature for 22–23 h. The reaction mixture was then transferred in a separatory funnel. The flask and magnet were washed with 2 ml DCM and 2 mL of water. In the case of poor phase separation some NaCl was added. The organic phase was separated from the water phase and dried with Na_2SO_4. The Na_2SO_4 was filtered away and the solvents were removed under reduced pressure. The conversion and selectivity of the reaction were determined by ^{1}H NMR analysis, without any additional isolation.

General procedure for investigation of the solvent's effect on the reaction selectivity In a flask 5 mol% $NaNO_2$ (0.01 mmol, 0.7 mg) was added, followed by 2 mol% $[IrCp^*Cl_2]_2$ (0.004 mmol, 3.2 mg) and 0.5 eq. I_2 (0.1 mmol, 25.4 mg). Next, 1 mL of solvent was added (exception was THF:H_2O=3:1 solvent mixture where 1.3 mL was used). In last step 1-octene-3-ol (**97**) was added (0.2 mmol) and a balloon with air was attached to the flask. The reaction mixture was mixed at room temperature for 22–23 h. The reaction mixture was then transferred in a separatory funnel. The flask and magnet were washed with 2 ml DCM and 2 mL of water. In the case of poor phase separation some NaCl was added. The organic phase was separated from the water phase and dried with Na_2SO_4. The Na_2SO_4 was filtered away and solvents were removed under reduced pressure. The conversion and selectivity of the reaction were determined by ^{1}H NMR analysis, without

any additional isolation.

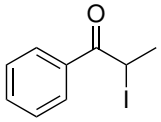
General procedure for the synthesis of α-iodoketones In a flask 5 mol% $NaNO_2$ (0.01 mmol, 0.7 mg) was added, followed by 2 mol% $[IrCp^*Cl_2]_2$ (0.004 mmol, 3.2 mg) and 0.5 eq. I_2 (0.1 mmol, 25.4 mg). After that the solvents were added – 1 mL THF and 0.3 mL H_2O - followed by turning on the stirring. Next, the substrate was added (0.2 mmol) and a balloon with air was attached to the flask. The reaction mixture was mixed at room temperature until the reaction was complete. The reaction mixture was transferred in a separatory funnel. The flask and magnet were washed with 2 ml DCM and 2 mL of water. In the case of poor phase separation some NaCl was added. The organic phase was separated from the water phase and dried with Na_2SO_4. The Na_2SO_4 was filtered away and solvents were removed under reduced pressure. The conversion and selectivity of the reaction were determined by ^{1}H NMR analysis, without any additional isolation.

2-iodooctan-3-one - 99 [211]



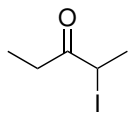
$C_8H_{15}IO$, MW = 254.11
^{1}H NMR (300 MHz, $CDCl_3$): δ 0.90 (t, J = 6.8 Hz, 3H), 1.32 (m, 6H), 1.64 (m, 3H), 1.89 (d, J = 6.8 Hz, 3H), 2.60 (m, 1H), 2.84 (m, 1H), 4.62 (q, J = 6.8 Hz, 1H).

2-iodo-1-phenylpropan-1-one - 103 [211]



C_9H_9IO, MW = 260.07
^{1}H NMR (300 MHz, $CDCl_3$): δ 2.08 (d, J = 6.7 Hz, 3H), 5.50 (q, J = 6.7 Hz, 1H), 7.47 (m, 2H), 7.58 (m, 1H), 8.01 (m, 2H).

2-iodopentan-3-one - 106 [217]



C_5H_9IO, MW = 212.03
^{1}H NMR (300 MHz, $CDCl_3$): δ 1.14 (t, J = 7.3 Hz, 3H), 1.89 (d, J = 6.8 Hz, 3H), 2.59 (m, 1H), 2.96 (m, 1H), 4.64 (q, J = 6.9 Hz, 1H).

Chapter 5

Conclusions

In conclusion, we developed a new method for the activation of nitric acid. This was achieved by using fluorinated alcohols as template catalysts.

In the first section of the thesis we described use of nitric acid (activated by fluorinated alcohols) as a reagent for aromatic nitration. We observed that 2,2,2-trifluoroethanol (TFE) is a weak activator of nitric acid. Therefore, TFE was successfully used as a template catalyst only on substrates with a strong electron-donor group present in the aromatic ring. With highly reactive substrates we obtained high yields for the nitrated products. Due to the TFE low activation power of the nitric acid smaller amounts of oxidation side products were formed, compared to classical nitration and nitration in 1,1,1,3,3,3-hexafluoroisopropanol (HFIP). The nitric acid was strongly activated by the HFIP template catalyst. Even with less reactive substrates we obtained high conversions into nitrated products. The conversion was similar to the classical system but with better selectivity. Trifluoroacetic acid (TFA), while it has the highest acidity of the tested solvents, also strongly activated the process of aromatic nitration. Excellent yields were obtained, even with substrates having a deactivated aromatic ring. We observed that dinitrated products were not formed in fluorinated solvents, as compared to a classical system. The only exceptions were highly reactive phenols derivatives, where dinitrated products were formed in small amounts. The lack of formation of dinitrated products was explained by the interaction of the fluorinated solvent and the nitro group. This interaction takes place in the form of a hydrogen bond. The electron density on the nitrogen atom is decreased due to the hydrogen bond being formed between the fluorinated solvent and the nitro group. The increase in the electrophilic nature of the nitrogen atom attracts electrons from the aromatic ring. This causes additional deactivation of the aromatic ring for electrophilic substitution. Reactions with 1,3-dimethoxybenzene derivatives resulted in the formation of unknown compounds, which were identified as bisphenylnitrosonium nitrates. Such compounds were unstable at room temperature and decomposed rapidly in polar solvents or on silica gel. Fluorinated alcohols (especially HFIP) had a stabilizing effect.

A mechanistic study was performed for aromatic nitration and the formation of bisphenylnitrosonium nitrates in fluorinated alcohols. We used different methods (ATR-IR, NMR, EPR and DFT calculations) to explain the reaction mechanisms. For both mechanisms (aromatic nitration and the formation of bisphenylnitrosonium nitrates in fluorinated alcohols) the radical pathway was identified. Aromatic nitration proceeds through two radical intermediates. Bisphenylnitrosonium nitrates, on the other hand, are formed through three radical intermediates. The first two are analogous to intermediates in aromatic nitration. The nitro product is formed by the elimination of the hydrogen atom from the second intermediate. On the other hand, to form a bisphenylnitrosonium nitrate a second inter-

mediate reacts with the initial substrate to form a third radical intermediate. In the final step the third radical intermediate transforms into a final product, yielding bisphenylnitrosonium nitrate. We made a comparison of our nitration method in fluorinated solvents with other novel nitration methods and classical nitration. We found that the classical nitration method is one of the least polluting methods. Our method had a slightly better E factor than the classical method and a slightly worse PMI. Among various considered methods for which we estimated green metrics, the classical nitration method was the most cost-effective method.

The second section describes our work where we used nitric acid as a catalyst for the aerobic oxidation of alcohols. The oxidation of benzyl alcohols proceeded with an excellent yield under an oxygen atmosphere with 10–20 mol% HNO_3 in HFIP. On the other hand, aliphatic alcohols were less reactive and the conversion was obtained with only stoichiometric amounts of HNO_3. By using 1 mol% of $FeCl_3$ as co-catalyst aerobic oxidation of aliphatic alcohols catalysed by HNO_3 proceeded with excellent yields. The reaction proved to be selective for oxidation of the secondary alcohol group, while no reaction occurred on the primary alcohol group, even when present in the same molecule. $FeCl_3$ has two functions in the catalytic cycle. The first role is to act as a source of chlorine atoms needed for the *in situ* formation of NOCl as a reactive species. The second role is that iron ions act as a single electron transfer (SET) catalysts for the transformation of HNO into NO and NO_2 into HNO_2/NOCl.

The last section describes the formation of α-haloketones from allylic alcohols. Aerobic oxidative iodination was catalysed by NO_x and $[IrCP^*Cl_2]_2$. The nitrogen oxide gases work as a catalyst in the oxidation of iodine into the iodine(I) reagent. The iridium catalyst was used for the 1,3-hydrogen shift on allylic alcohol, which forms electron-rich α-carbon atom besides the carbonyl group. The iodine(I) reagent reacts with the α-carbon atom, forming the final product. We obtained a high conversion into α-iodketones (2-iodooctan-3-one and 2-iodopentan-3-one). Further work in this area of research will continue in the future.

References

[1] J. J. Berzelius, "Årsberättelsen om framsteg i fysik och kemi, afgiven den 31 mars," Royal Swedish Academy of Sciences, 1835.

[2] E. Anslyn and D. Dougherty, *Modern physical organic chemistry*. University Science, 2006, ISBN: 9781891389313.

[3] Q. Cao, L. M. Dornan, L. Rogan, N. L. Hughes, and M. J. Muldoon, "Aerobic oxidation catalysis with stable radicals," *Chemical Communications*, vol. 50, no. 35, pp. 4524–4543, 2014.

[4] British Geological Survey. (2016). Risk list 2015, [Online]. Available: `http://www.bgs.ac.uk/mineralsuk/statistics/riskList.htmlr` (visited on 12/05/2016).

[5] P. Pihko, *Hydrogen bonding in organic synthesis*. John Wiley & Sons, 2009, ISBN: 9783527318957.

[6] S. Mukherjee, J. W. Yang, S. Hoffmann, and B. List, "Asymmetric enamine catalysis," *Chemical Reviews*, vol. 107, no. 12, pp. 5471–5569, 2007.

[7] W. Cleland and M. Kreevoy, "Low-barrier hydrogen bonds and enzymic catalysis," *Science*, vol. 264, no. 5167, pp. 1887–1890, 1994.

[8] S. Gennen, M. Alves, R. Méreau, T. Tassaing, B. Gilbert, C. Detrembleur, C. Jerome, and B. Grignard, "Fluorinated alcohols as activators for the solvent-free chemical fixation of carbon dioxide into epoxides," *ChemSusChem*, vol. 8, no. 11, pp. 1845–1849, 2015.

[9] M. Chaplin. (2016). Water structure and science, [Online]. Available: `http://www1.lsbu.ac.uk/water` (visited on 12/01/2016).

[10] I. A. Shuklov, N. V. Dubrovina, and A. Boerner, "Fluorinated alcohols as solvents, cosolvents and additives in homogeneous catalysis," *Synthesis*, vol. 39, no. 19, pp. 2925–2943, 2007.

[11] M. Buck, "Trifluoroethanol and colleagues: Cosolvents come of age. Recent studies with peptides and proteins," *Quarterly Reviews of Biophysics*, vol. 31, no. 3, pp. 297–355, 1998.

[12] L. Eberson, M. P. Hartshorn, O. Persson, and F. Radner, "Making radical cations live longer," *Chemical Communications*, no. 18, pp. 2105–2112, 1996.

[13] J.-P. Begue, D. Bonnet-Delpon, and B. Crousse, "Fluorinated alcohols: A new medium for selective and clean reaction," *Synlett*, vol. 15, no. 01, pp. 18–29, 2004.

[14] F. L. Schadt, P. v. R. Schleyer, and T. Bentley, "Hexaflouroisopropanol - a solvent of high ionizing power and low nucleophilicity," *Tetrahedron Letters*, vol. 15, no. 27, pp. 2335–2338, 1974.

[15] D. Vuluga, J. Legros, B. Crousse, A. M. Slawin, C. Laurence, P. Nicolet, and D. Bonnet-Delpon, "Influence of the structure of polyfluorinated alcohols on Brønsted acidity/hydrogen-bond donor ability and consequences on the promoter effect," *The Journal of Organic Chemistry*, vol. 76, no. 4, pp. 1126–1133, 2011.

[16] L. Eberson, M. P. Hartshorn, J. J. McCullough, O. Persson, and F. Radner, "1,1,1,3,3,3-hexafluoropropan-2-ol (HFP) as a solvent for electrochemistry," *Acta Chemica Scandinavica*, vol. 52, no. 52, pp. 1024–1028, 1998.

[17] N. Busschaert, J. Jaramillo-Garcia, M. E. Light, J. Herniman, G. J. Langley, and P. A. Gale, "An anion-binding fluorinated alcohol isophthalamide isostere," *RSC Advances*, vol. 4, no. 11, pp. 5389–5393, 2014.

[18] A. Berkessel, J. A. Adrio, D. Hüttenhain, and J. M. Neudörfl, "Unveiling the "booster effect" of fluorinated alcohol solvents: Aggregation-induced conformational changes and cooperatively enhanced h-bonding," *Journal of the American Chemical Society*, vol. 128, no. 26, pp. 8421–8426, 2006.

[19] H. Schaal, T. Häber, and M. A. Suhm, "Hydrogen bonding in 2-propanol. The effect of fluorination," *The Journal of Physical Chemistry A*, vol. 104, no. 2, pp. 265–274, 2000.

[20] M. Fioroni, K. Burger, A. E. Mark, and D. Roccatano, "Model of 1,1,1,3,3,3-hexafluoro-propan-2-ol for molecular dynamics simulations," *The Journal of Physical Chemistry B*, vol. 105, no. 44, pp. 10 967–10 975, 2001.

[21] S. P. De Visser, J. Kaneti, R. Neumann, and S. Shaik, "Fluorinated alcohols enable olefin epoxidation by H_2O_2: Template catalysis," *The Journal of Organic Chemistry*, vol. 68, no. 7, pp. 2903–2912, 2003.

[22] A. Berkessel and J. A. Adrio, "Kinetic studies of olefin epoxidation with hydrogen peroxide in 1,1,1,3,3,3-hexafluoro-2-propanol reveal a crucial catalytic role for solvent clusters," *Advanced Synthesis & Catalysis*, vol. 346, no. 2-3, pp. 275–280, 2004.

[23] D. P. Hong, M. Hoshino, R. Kuboi, and Y. Goto, "Clustering of fluorine-substituted alcohols as a factor responsible for their marked effects on proteins and peptides," *Journal of the American Chemical Society*, vol. 121, no. 37, pp. 8427–8433, 1999.

[24] K. Neimann and R. Neumann, "Electrophilic activation of hydrogen peroxide: Selective oxidation reactions in perfluorinated alcohol solvents," *Organic Letters*, vol. 2, no. 18, pp. 2861–2863, 2000.

[25] M. C. van Vliet, I. W. Arends, and R. A. Sheldon, "Fluorinated alcohols: Effective solvents for uncatalysed epoxidations with aqueous hydrogen peroxide," *Synlett*, vol. 12, no. 02, pp. 0248–0250, 2001.

[26] A. Berkessel and M. R. Andreae, "Efficient catalytic methods for the Baeyer–Villiger oxidation and epoxidation with hydrogen peroxide," *Tetrahedron Letters*, vol. 42, no. 12, pp. 2293–2295, 2001.

[27] J. Iskra, D. Bonnet-Delpon, and J.-P. Bégué, "Methyltrioxorhenium-catalysed epoxidation of alkenes: Enhancement of reactivity in hexafluoro-2-propanol," *Tetrahedron Letters*, vol. 43, no. 6, pp. 1001–1003, 2002.

[28] A. Berkessel, M. R. Andreae, H. Schmickler, and J. Lex, "Baeyer–Villiger oxidations with hydrogen peroxide in fluorinated alcohols: Lactone formation by a nonclassical mechanism," *Angewandte Chemie International Edition*, vol. 41, no. 23, pp. 4481–4484, 2002.

[29] J. Iskra, D. Bonnet-Delpon, and J.-P. Bégué, "One-pot synthesis of non-symmetric tetraoxanes with the H_2O_2/MTO/fluorous alcohol system," *Tetrahedron Letters*, vol. 44, no. 33, pp. 6309–6312, 2003.

[30] K. Žmitek, S. Stavber, M. Zupan, D. Bonnet-Delpon, S. Charneau, P. Grellier, and J. Iskra, "Synthesis and antimalarial activities of novel 3,3,6,6-tetraalkyl-1,2,4,5-tetraoxanes," *Bioorganic & Medicinal Chemistry*, vol. 14, no. 23, pp. 7790–7795, 2006.

[31] K. Žmitek, S. Stavber, M. Zupan, D. Bonnet-Delpon, and J. Iskra, "Fluorinated alcohol directed formation of dispiro-1,2,4,5-tetraoxanes by hydrogen peroxide under acid conditions," *Tetrahedron*, vol. 62, no. 7, pp. 1479–1484, 2006.

[32] K. S. Ravikumar, Y. M. Zhang, J.-P. Bégué, and D. Bonnet-Delpon, "Role of hexafluoro-2-propanol in selective oxidation of sulfide to sulfoxide: Efficient preparation of glycosyl sulfoxides," *European Journal of Organic Chemistry*, vol. 1998, no. 12, pp. 2937–2940, 1998.

[33] K. Ravikumar, F. Barbier, J.-P. Bégué, and D. Bonnet-Delpon, "Selective oxidation of sulfides: Selective preparation of 1-trifluoromethyl vinyl sulfoxides," *Journal of Fluorine Chemistry*, vol. 95, no. 1–2, pp. 123–125, 1999.

[34] S. Khaksar and S. M. Talesh, "Transition metal-free oxidation of activated alcohols to aldehydes and ketones in 1,1,1,3,3,3-hexafluoro-2-propanol," *Journal of Fluorine Chemistry*, vol. 140, pp. 95–98, 2012.

[35] Y.-Q. Wang, S.-M. Lu, and Y.-G. Zhou, "Palladium-catalyzed asymmetric hydrogenation of functionalized ketones," *Organic Letters*, vol. 7, no. 15, pp. 3235–3238, 2005.

[36] T. Sugiishi, M. Matsugi, H. Hamamoto, and H. Amii, "Enhancement of stereoselectivities in asymmetric synthesis using fluorinated solvents, auxiliaries, and catalysts," *RSC Advances*, vol. 5, no. 22, pp. 17 269–17 282, 2015.

[37] H. Abe, H. Amii, and K. Uneyama, "Pd-catalyzed asymmetric hydrogenation of α-fluorinated iminoesters in fluorinated alcohol: A new and catalytic enantioselective synthesis of fluoro α-amino acid derivatives," *Organic Letters*, vol. 3, no. 3, pp. 313–315, 2001.

[38] K. Mikami, T. Murase, L. Zhai, S. Kawauchi, Y. Itoh, and S. Ito, "Sequential perfluoroalkylation and asymmetric reduction of nitriles triggered with perfluoroalkyl titanates: Catalytic asymmetric synthesis of perfluoroalkyl amines," *Tetrahedron Letters*, vol. 51, no. 10, pp. 1371–1373, 2010.

[39] Y.-Q. Wang and Y.-G. Zhou, "Highly enantioselective Pd-catalyzed asymmetric hydrogenation of N-diphenylphosphinyl ketimines," *Synlett*, vol. 17, no. 08, pp. 1189–1192, 2006.

[40] Y.-Q. Wang, S.-M. Lu, and Y.-G. Zhou, "Highly enantioselective Pd-catalyzed asymmetric hydrogenation of activated imines," *The Journal of Organic Chemistry*, vol. 72, no. 10, pp. 3729–3734, 2007.

[41] R. Ben-Daniel, S. P. De Visser, S. Shaik, and R. Neumann, "Electrophilic aromatic chlorination and haloperoxidation of chloride catalyzed by polyfluorinated alcohols: A new manifestation of template catalysis," *Journal of the American Chemical Society*, vol. 125, no. 40, pp. 12 116–12 117, 2003.

[42] P. Trillo, A. Baeza, and C. Nájera, "Fluorinated alcohols as promoters for the metal-free direct substitution reaction of allylic alcohols with nitrogenated, silylated, and carbon nucleophiles," *The Journal of Organic Chemistry*, vol. 77, no. 17, pp. 7344–7354, 2012.

[43] O. Coulembier, D. P. Sanders, A. Nelson, A. N. Hollenbeck, H. W. Horn, J. E. Rice, M. Fujiwara, P. Dubois, and J. L. Hedrick, "Hydrogen-bonding catalysts based on fluorinated alcohol derivatives for living polymerization," *Angewandte Chemie International Edition*, vol. 48, no. 28, pp. 5170–5173, 2009.

[44] S. Picon, M. Rawling, M. Campbell, and N. C. Tomkinson, "Alkene dihydroxylation with malonoyl peroxides: Catalysis using fluorinated alcohols," *Organic Letters*, vol. 14, no. 24, pp. 6250–6253, 2012.

[45] L. Wang, D.-Y. Dai, Q. Chen, and M.-Y. He, "Rapid and green synthesis of phenols catalyzed by a deep eutectic mixture based on fluorinated alcohol in water," *Journal of Fluorine Chemistry*, vol. 158, pp. 44–47, 2014.

[46] S. Khaksar, "Fluorinated alcohols: A magic medium for the synthesis of heterocyclic compounds," *Journal of Fluorine Chemistry*, vol. 172, pp. 51–61, 2015.

[47] S. Fustero, R. Román, J. F. Sanz-Cervera, A. Simón-Fuentes, A. C. Cunat, S. Villanova, and M. Murguia, "Improved regioselectivity in pyrazole formation through the use of fluorinated alcohols as solvents: Synthesis and biological activity of fluorinated tebufenpyrad analogs," *The Journal of Organic Chemistry*, vol. 73, no. 9, pp. 3523–3529, 2008.

[48] L. Dumitrescu, K. Azzouzi-Zriba, D. Bonnet-Delpon, and B. Crousse, "Nonmetal catalyzed insertion reactions of diazocarbonyls to acid derivatives in fluorinated alcohols," *Organic Letters*, vol. 13, no. 4, pp. 692–695, 2011.

[49] S. Kobayashi, H. Kiyohara, Y. Nakamura, and R. Matsubara, "Catalytic asymmetric synthesis of α-amino phosphonates using enantioselective carbon-carbon bond-forming reactions," *Journal of the American Chemical Society*, vol. 126, no. 21, pp. 6558–6559, 2004.

[50] M. Alves, B. Grignard, S. Gennen, R. Méreau, C. Detrembleur, C. Jérôme, and T. Tassaing, "Organocatalytic promoted coupling of carbon dioxide with epoxides: A rational investigation of the cocatalytic activity of various hydrogen bond donors," *Catalysis Science & Technology*, vol. 5, no. 9, pp. 4636–4643, 2015.

[51] M. Alves, R. Méreau, B. Grignard, C. Detrembleur, C. Jerome, and T. Tassaing, "A comprehensive density functional theory study of the key role of fluorination and dual hydrogen bonding in the activation of the epoxide/CO_2 coupling by fluorinated alcohols," *RSC Advances*, vol. 6, no. 43, pp. 36 327–36 335, 2016.

[52] J. Clayden, N. Greeves, and S. Warren, *Organic chemistry*. OUP Oxford, 2012, ISBN: 9780199270293.

[53] G.-X. Li and J. Qu, "Friedel–Crafts alkylation of arenes with epoxides promoted by fluorinated alcohols or water," *Chemical Communications*, vol. 46, no. 15, pp. 2653–2655, 2010.

[54] K. Azzouzi-Zriba, D. Bonnet-Delpon, and B. Crousse, "Transition metal-catalyzed cyclopropanation of alkenes in fluorinated alcohols," *Journal of Fluorine Chemistry*, vol. 132, no. 10, pp. 811–814, 2011.

[55] M. Daryabari and S. Khaksar, "Green synthesis of highly substituted pyridines via the one-pot multi-component reaction in 2,2,2-trifluoroethanol," *Journal of Molecular Liquids*, vol. 198, pp. 263–266, 2014.

[56] C. Venkateswarlu, P. Balaji, K. De, B. Crousse, B. Figadère, and J. Legros, "Straightforward synthesis of 2-propylquinolines under multicomponent conditions in fluorinated alcohols," *Journal of Fluorine Chemistry*, vol. 152, pp. 94–98, 2013.

[57] J. Xiao, K. Zhao, and T.-P. Loh, "The acid free asymmetric intermolecular α-alkylation of aldehydes in fluorinated alcohols," *Chemical Communications*, vol. 48, no. 29, pp. 3548–3550, 2012.

[58] N. Rodríguez, J. A. Romero-Revilla, M. Á. Fernández-Ibáñez, and J. C. Carretero, "Palladium-catalyzed N-(2-pyridyl) sulfonyl-directed C(sp^3)–H γ-arylation of amino acid derivatives," *Chemical Science*, vol. 4, no. 1, pp. 175–179, 2013.

[59] M. Fan and D. Ma, "Palladium-catalyzed direct functionalization of 2-aminobutanoic acid derivatives: Application of a convenient and versatile auxiliary," *Angewandte Chemie International Edition*, vol. 52, no. 46, pp. 12 152–12 155, 2013.

[60] W. Gong, G. Zhang, T. Liu, R. Giri, and J.-Q. Yu, "Site-selective C(sp^3)–H functionalization of di-, tri-, and tetrapeptides at the N-terminus," *Journal of the American Chemical Society*, vol. 136, no. 48, pp. 16 940–16 946, 2014.

[61] J. Wencel-Delord and F. Colobert, "A remarkable solvent effect of fluorinated alcohols on transition metal catalysed C–H functionalizations," *Organic Chemistry Frontiers*, vol. 3, no. 3, pp. 394–400, 2016.

[62] R. S. Jolly, G. Luedtke, D. Sheehan, and T. Livinghouse, "Novel cyclization reactions on transition metal templates. The catalysis of intramolecular [4+2] cycloadditions by low-valent rhodium complexes," *Journal of the American Chemical Society*, vol. 112, no. 12, pp. 4965–4966, 1990.

[63] P. A. Wender, M. P. Croatt, and N. M. Deschamps, "Metal-catalyzed [2+2+1] cycloadditions of 1,3-dienes, allenes, and CO," *Angewandte Chemie International Edition*, vol. 45, no. 15, pp. 2459–2462, 2006.

[64] J. F. Povey, C. M. Smales, S. J. Hassard, and M. J. Howard, "Comparison of the effects of 2,2,2-trifluoroethanol on peptide and protein structure and function," *Journal of Structural Biology*, vol. 157, no. 2, pp. 329–338, 2007.

[65] S. M. M. Reddy, G. Shanmugam, and A. B. Mandal, "1,1,1,3,3,3-hexafluoro-2-propanol and 2,2,2-trifluoroethanol solvents induce self-assembly with different surface morphology in an aromatic dipeptide," *Organic & Biomolecular Chemistry*, vol. 12, no. 32, pp. 6181–6189, 2014.

[66] Rigaku Oxford Diffraction, *CrysAlisPro software system, version 1.171.38.43, Rigaku Coorporation*, 2015.

[67] O. V. Dolomanov, L. J. Bourhis, R. J. Gildea, J. A. Howard, and H. Puschmann, "*OLEX2*: A complete structure solution, refinement and analysis program," *Journal of Applied Crystallography*, vol. 42, no. 2, pp. 339–341, 2009.

[68] G. M. Sheldrick, "Crystal structure refinement with *SHELXL*," *Acta Crystallographica Section C: Structural Chemistry*, vol. 71, no. 1, pp. 3–8, 2015.

[69] ——, "*SHELXT*–Integrated space-group and crystal-structure determination," *Acta Crystallographica Section A: Foundations and Advances*, vol. 71, no. 1, pp. 3–8, 2015.

[70] K. Brandenburg and M. Berndt, "*DIAMOND*: Visual crystal structure information system," *3.1, Crystal Impact GbR, Bonn, Germany*, 2005.

[71] L. Bedrač and J. Iskra, "Iodine (I) reagents in hydrochloric acid-catalyzed oxidative iodination of aromatic compounds by hydrogen peroxide and iodine," *Advanced Synthesis & Catalysis*, vol. 355, no. 7, pp. 1243–1248, 2013.

[72] G. Booth, "Nitro compounds, aromatic," in *Ullmann's Encyclopedia of Industrial Chemistry*. Wiley Online Library, 2000, ISBN: 9783527306732.

[73] G. A. Olah, R. Malhotra, and S. C. Narang, *Nitration: Methods and mechanisms*, ser. Organic Nitro Chemistry. Wiley-VCH, 1989, ISBN: 9780471186953.

[74] N. Ono, *The nitro group in organic synthesis*, ser. Organic Nitro Chemistry. John Wiley & Sons, 2003, vol. 9, ISBN: 9780471458463.

[75] P. Zhang, M. Cedilote, T. P. Cleary, and M. E. Pierce, "Mono-nitration of aromatic compounds via their nitric acid salts," *Tetrahedron Letters*, vol. 48, no. 49, pp. 8659–8664, 2007.

[76] K. Smith and G. A. El-Hiti, "Use of zeolites for greener and more para-selective electrophilic aromatic substitution reactions," *Green Chemistry*, vol. 13, no. 7, pp. 1579–1608, 2011.

[77] P. Anastas and J. Warner, *Green chemistry: Theory and practice*. Oxford University Press, 1998, ISBN: 9780198502340.

[78] M. C. van Vliet, I. W. Arends, and R. A. Sheldon, "Hexafluoroacetone in hexafluoro-2-propanol: A highly active medium for epoxidation with aqueous hydrogen peroxide," *Synlett*, vol. 12, no. 08, pp. 1305–1307, 2001.

[79] N. L. Lancaster and V. Llopis-Mestre, "Aromatic nitrations in ionic liquids: The importance of cation choice," *Chemical Communications*, no. 22, pp. 2812–2813, 2003.

[80] G. Aridoss and K. K. Laali, "Ethylammonium nitrate (EAN)/Tf_2O and EAN/TFAA: Ionic liquid based systems for aromatic nitration," *The Journal of Organic Chemistry*, vol. 76, no. 19, pp. 8088–8094, 2011.

[81] G. A. Olah, S. J. Kuhn, S. H. Flood, and J. C. Evans, "Aromatic substitution. XIII. 1a Comparison of nitric acid and mixed acid nitration of alkylbenzenes and benzene with nitronium salt nitrations," *Journal of the American Chemical Society*, vol. 84, no. 19, pp. 3687–3693, 1962.

[82] S. Sankararaman, W. A. Haney, and J. K. Kochi, "Annihilation of aromatic cation radicals by ion-pair and radical pair collapse. Unusual solvent and salt effects in the competition for aromatic substitution," *Journal of the American Chemical Society*, vol. 109, no. 25, pp. 7824–7838, 1987.

[83] J. D. Loudon and J. Ogg, "2: 3-dihydro-3-oxobenz-1: 4-oxazines," *Journal of the Chemical Society.*, no. 0, pp. 739–744, 1955.

[84] B. G. Gowenlock, B. King, and J. Pfab, "Reactions of 1,2-and 1,3-dimethoxy-and 1,3,5-trimethoxybenzene with nitrogen dioxide/dinitrogen tetraoxide in dichloromethane," *Journal of Chemical Research*, vol. 2000, no. 6, pp. 276–277, 2000.

[85] K. H. Meyer and H. Gottlieb-Billroth, "Übe die einwirkung der salpetersäure auf phenol-äther," *Berichte der deutschen chemischen Gesellschaft (A and B Series)*, vol. 52, no. 8, pp. 1476–1489, 1919.

[86] K. H. Meyer and W. Reppe, "Über die reduktionsstufen von arylderivaten der salpetersäure," *Berichte der deutschen chemischen Gesellschaft (A and B Series)*, vol. 54, no. 2, pp. 327–337, 1921.

[87] F. Kehrmann and H. Decker, "Über die oxoniumsalze aus phenol-äthern und phenolen, II. mitteilung: F. kehrmann und ch. schmajewski: Über die zersetzung der oxoniumsalze aus thymol-äthyläther und aus anisol durch wasser oder alkalisch reagierende stoffe," *Berichte der deutschen chemischen Gesellschaft (A and B Series)*, vol. 54, no. 9, pp. 2435–2440, 1921.

[88] A. Rubinstein, P. Jiménez-Lozanao, J. J. Carbó, J. M. Poblet, and R. Neumann, "Aerobic carbon–carbon bond cleavage of alkenes to aldehydes catalyzed by first-row transition-metal-substituted polyoxometalates in the presence of nitrogen dioxide," *Journal of the American Chemical Society*, vol. 136, no. 31, pp. 10 941–10 948, 2014.

[89] A. D. Mighell, "Conventional cells: Monoclinic I- and C-centered cells," *Acta Crystallographica Section B: Structural Science*, vol. 59, no. 2, pp. 300–302, 2003.

[90] J. F. d. Queiroz, J. W. d. M. Carneiro, A. A. Sabino, R. Sparrapan, M. N. Eberlin, and P. M. Esteves, "Electrophilic aromatic nitration: Understanding its mechanism and substituent effects," *The Journal of Organic Chemistry*, vol. 71, no. 16, pp. 6192–6203, 2006.

[91] Y. Zhao and D. G. Truhlar, "The M06 suite of density functionals for main group thermochemistry, thermochemical kinetics, noncovalent interactions, excited states, and transition elements: Two new functionals and systematic testing of four M06-class functionals and 12 other functionals," *Theoretical Chemistry Accounts: Theory, Computation, and Modeling (Theoretica Chimica Acta)*, vol. 120, no. 1, pp. 215–241, 2008.

[92] A. D. Becke, "Density-functional thermochemistry. III. The role of exact exchange," *The Journal of Chemical Physics*, vol. 98, no. 7, pp. 5648–5652, 1993.

[93] M. J. Frisch, M. Head-Gordon, and J. A. Pople, "A direct MP2 gradient method," *Chemical Physics Letters*, vol. 166, no. 3, pp. 275–280, 1990.

[94] ——, "Semi-direct algorithms for the MP2 energy and gradient," *Chemical Physics Letters*, vol. 166, no. 3, pp. 281–289, 1990.

[95] M. Head-Gordon, J. A. Pople, and M. J. Frisch, "MP2 energy evaluation by direct methods," *Chemical Physics Letters*, vol. 153, no. 6, pp. 503–506, 1988.

[96] S. Sæbø and J. Almlöf, "Avoiding the integral storage bottleneck in LCAO calculations of electron correlation," *Chemical Physics Letters*, vol. 154, no. 1, pp. 83–89, 1989.

[97] M. Head-Gordon and T. Head-Gordon, "Analytic MP2 frequencies without fifth-order storage. theory and application to bifurcated hydrogen bonds in the water hexamer," *Chemical Physics Letters*, vol. 220, no. 1-2, pp. 122–128, 1994.

[98] M. J. Frisch, G. W. Trucks, H. B. Schlegel, G. E. Scuseria, M. A. Robb, J. R. Cheeseman, G. Scalmani, V. Barone, B. Mennucci, G. A. Petersson, H. Nakatsuji, M. Caricato, X. Li, H. P. Hratchian, A. F. Izmaylov, J. Bloino, G. Zheng, J. L. Sonnenberg, M. Hada, M. Ehara, K. Toyota, R. Fukuda, J. Hasegawa, M. Ishida, T. Nakajima, Y. Honda, O. Kitao, H. Nakai, T. Vreven, J. A. Montgomery Jr., J. E. Peralta, F. Ogliaro, M. Bearpark, J. J. Heyd, E. Brothers, K. N. Kudin, V. N. Staroverov, R. Kobayashi, J. Normand, K. Raghavachari, A. Rendell, J. C. Burant, S. S. Iyengar, J. Tomasi, M. Cossi, N. Rega, J. M. Millam, M. Klene, J. E. Knox, J. B. Cross, V. Bakken, C. Adamo, J. Jaramillo, R. Gomperts, R. E. Stratmann, O. Yazyev, A. J. Austin, R. Cammi, C. Pomelli, J. W. Ochterski, R. L. Martin, K. Morokuma, V. G. Zakrzewski, G. A. Voth, P. Salvador, J. J. Dannenberg, S.

Dapprich, A. D. Daniels, Ö. Farkas, J. B. Foresman, J. V. Ortiz, J. Cioslowski, and D. J. Fox, *Gaussian 09 Revision A.1*, Gaussian Inc. Wallingford CT, 2009.

[99] A. Kokalj, "XCrySDen—a new program for displaying crystalline structures and electron densities," *Journal of Molecular Graphics and Modelling*, vol. 17, no. 3, pp. 176–179, 1999, Code available from http://www.xcrysden.org/.

[100] A. V. Marenich, C. J. Cramer, and D. G. Truhlar, "Universal solvation model based on solute electron density and on a continuum model of the solvent defined by the bulk dielectric constant and atomic surface tensions," *The Journal of Physical Chemistry B*, vol. 113, no. 18, pp. 6378–6396, 2009.

[101] E. Cances, B. Mennucci, and J. Tomasi, "A new integral equation formalism for the polarizable continuum model: Theoretical background and applications to isotropic and anisotropic dielectrics," *The Journal of chemical physics*, vol. 107, no. 8, pp. 3032–3041, 1997.

[102] B. Mennucci, E. Cances, and J. Tomasi, "Evaluation of solvent effects in isotropic and anisotropic dielectrics and in ionic solutions with a unified integral equation method: Theoretical bases, computational implementation, and numerical applications," *The Journal of Physical Chemistry B*, vol. 101, no. 49, pp. 10 506–10 517, 1997.

[103] S. Sankararaman, W. Haney, and J. K. Kochi, "Aromatic nitration with ion radical pairs [ArH·+, NO_2·] as reactive intermediates. Time-resolved studies of charge-transfer activation of dialkoxybenzenes," *Journal of the American Chemical Society*, vol. 109, no. 17, pp. 5235–5249, 1987.

[104] E. Kim, T. Bockman, and J. Kochi, "Electron-transfer mechanism for aromatic nitration via the photoactivation of EDA (electron donor-acceptor) complexes. Direct relationship to electrophilic aromatic substitution," *Journal of the American Chemical Society*, vol. 115, no. 8, pp. 3091–3104, 1993.

[105] A. Dicks and A. Hent, *Green chemistry metrics: A guide to determining and evaluating process greenness*. Springer, 2014, ISBN: 9783319105017.

[106] D. J. Constable, A. D. Curzons, and V. L. Cunningham, "Metrics to 'green' chemistry—which are the best?" *Green Chemistry*, vol. 4, no. 6, pp. 521–527, 2002.

[107] B. Trost, "The atom economy–a search for synthetic efficiency," *Science*, vol. 254, no. 5037, pp. 1471–1477, 1991.

[108] R. A. Sheldon, "Organic synthesis-past, present and future," *Chemistry and Industry*, no. 23, pp. 903–6, 1992.

[109] E. Heinzle, D. Weirich, F. Brogli, V. H. Hoffmann, G. Koller, M. A. Verduyn, and K. Hungerbühler, "Ecological and economic objective functions for screening in integrated development of fine chemical processes. 1. Flexible and expandable framework using indices," *Industrial & Engineering Chemistry Research*, vol. 37, no. 8, pp. 3395–3407, 1998.

[110] J. M. Riego, Z. Sedin, J. Zaldívar, N. C. Marziano, and C. Tortato, "Sulfuric acid on silica-gel: An inexpensive catalyst for aromatic nitration," *Tetrahedron Letters*, vol. 37, no. 4, pp. 513–516, 1996.

[111] S. Wang, S. Jiang, and J. Nie, "Lanthanide bis [(trifluoromethyl) sulfonyl] imides as reusable catalysts for mononitration of substituted benzenes in ionic liquids," *Advanced Synthesis & Catalysis*, vol. 351, no. 11-12, pp. 1939–1945, 2009.

[112] W. Zhu, Y. Liu, G. Niu, Q. Wang, J. Li, X. Zhu, Y. Li, H. Xue, and G. Yang, "First application of bismuth triflate as an efficient, non-transition metallic and reusable catalyst for aromatic nitration," *Catalysis Communications*, vol. 29, pp. 145–148, 2012.

[113] J. Jacoway, G. N. Kumar, and K. K. Laali, "Aromatic nitration with bismuth nitrate in ionic liquids and in molecular solvents: A comparative study of $Bi(NO_3)_3 \cdot 5H_2O$/[bmim][PF_6] and $Bi(NO_3)_3 \cdot 5H_2O$/1,2-DCE systems," *Tetrahedron Letters*, vol. 53, no. 50, pp. 6782–6785, 2012.

[114] K. Smith, A. Musson, and G. A. DeBoos, "A novel method for the nitration of simple aromatic compounds," *The Journal of Organic Chemistry*, vol. 63, no. 23, pp. 8448–8454, 1998.

[115] S. A. Shackelford, M. B. Anderson, L. C. Christie, T. Goetzen, M. C. Guzman, M. A. Hananel, W. D. Kornreich, H. Li, V. P. Pathak, A. K. Rabinovich, *et al.*, "Electrophilic tetraalkylammonium nitrate nitration. II. Improved anhydrous aromatic and heteroaromatic mononitration with tetramethylammonium nitrate and triflic anhydride, including selected microwave examples," *The Journal of Organic Chemistry*, vol. 68, no. 2, pp. 267–275, 2003.

[116] M. Ramana, S. Malik, and J. Parihar, "Guanidinium nitrate: A novel reagent for aryl nitrations," *Tetrahedron Letters*, vol. 45, no. 47, pp. 8681–8683, 2004.

[117] G. A. Olah, H. C. Lin, J. A. Olah, and S. C. Narang, "Electrophilic and free radical nitration of benzene and toluene with various nitrating agents," *Proceedings of the National Academy of Sciences*, vol. 75, no. 3, pp. 1045–1049, 1978.

[118] H. Suzuki, S. Yonezawa, N. Nonoyama, and T. Mori, "Iron (III)-catalysed nitration of non-activated and moderately activated arenes with nitrogen dioxide–molecular oxygen under neutral conditions," *Journal of the Chemical Society, Perkin Transactions 1*, no. 19, pp. 2385–2389, 1996.

[119] P.-C. Wang and M. Lu, "Regioselectivity nitration of aromatics with N_2O_5 in PEG-based dicationic ionic liquid," *Tetrahedron Letters*, vol. 52, no. 13, pp. 1452–1455, 2011.

[120] G. Yan and M. Yang, "Recent advances in the synthesis of aromatic nitro compounds," *Organic & Biomolecular Chemistry*, vol. 11, no. 16, pp. 2554–2566, 2013.

[121] S. Salzbrunn, J. Simon, G. S. Prakash, N. A. Petasis, and G. A. Olah, "Regioselective nitration of arylboronic acids," *Synlett*, vol. 11, no. 10, pp. 1485–1487, 2000.

[122] G. S. Prakash, C. Panja, T. Mathew, V. Surampudi, N. A. Petasis, and G. A. Olah, "ipso-Nitration of arylboronic acids with chlorotrimethylsilane-nitrate salts," *Organic Letters*, vol. 6, no. 13, pp. 2205–2207, 2004.

[123] H. Yang, Y. Li, M. Jiang, J. Wang, and H. Fu, "General copper-catalyzed transformations of functional groups from arylboronic acids in water," *Chemistry–A European Journal*, vol. 17, no. 20, pp. 5652–5660, 2011.

[124] S. Manna, S. Maity, S. Rana, S. Agasti, and D. Maiti, "ipso-Nitration of arylboronic acids with bismuth nitrate and perdisulfate," *Organic Letters*, vol. 14, no. 7, pp. 1736–1739, 2012.

[125] G. Prakash and T. Mathew, "ipso-Nitration of arenes," *Angewandte Chemie International Edition*, vol. 49, no. 10, pp. 1726–1728, 2010.

[126] S. Saito and Y. Koizumi, "Copper-catalyzed coupling of aryl halides and nitrite salts: A mild ullmann-type synthesis of aromatic nitro compounds," *Tetrahedron Letters*, vol. 46, no. 28, pp. 4715–4717, 2005.

[127] P. LaBeaume, M. Placzek, M. Daniels, I. Kendrick, P. Ng, M. McNeel, R. Afroze, A. Alexander, R. Thomas, A. E. Kallmerten, *et al.*, "Microwave-accelerated fluorodenitrations and nitrodehalogenations: Expeditious routes to labeled PET ligands and fluoropharmaceuticals," *Tetrahedron Letters*, vol. 51, no. 14, pp. 1906–1909, 2010.

[128] B. P. Fors and S. L. Buchwald, "Pd-catalyzed conversion of aryl chlorides, triflates, and nonaflates to nitroaromatics," *Journal of the American Chemical Society*, vol. 131, no. 36, pp. 12 898–12 899, 2009.

[129] P. A. Joseph, S. Priyadarshini, M. L. Kantam, and H. Maheswaran, "Copper catalyzed ipso-nitration of iodoarenes, bromoarenes and heterocyclic haloarenes under ligand-free conditions," *Tetrahedron Letters*, vol. 53, no. 12, pp. 1511–1513, 2012.

[130] M. Eissen and D. Lenoir, "Electrophilic bromination of alkenes: Environmental, health and safety aspects of new alternative methods," *Chemistry-A European Journal*, vol. 14, no. 32, pp. 9830–9841, 2008.

[131] M. Shi and S.-C. Cui, "Electrophilic aromatic nitration using a mixed catalyst of lithium, molybdenum, ytterbium on silica gel," *Advanced Synthesis & Catalysis*, vol. 345, no. 12, pp. 1329–1333, 2003.

[132] W. Zhang, J. Zhang, S. Ren, and Y. Liu, "Palladium-catalyzed aromatic C–H bond nitration using removable directing groups: Regiospecific synthesis of substituted o-nitrophenols from related phenols," *The Journal of Organic Chemistry*, vol. 79, no. 23, pp. 11 508–11 516, 2014.

[133] C. Zhu, R. Wang, and J. R. Falck, "Mild and rapid hydroxylation of aryl/heteroaryl boronic acids and boronate esters with N-Oxides," *Organic Letters*, vol. 14, no. 13, pp. 3494–3497, 2012.

[134] J. Rojo, J.-M. Lehn, G. Baum, D. Fenske, O. Waldmann, and P. Müller, "Self-assembly, crystal structure, and magnetic properties of a phenoxo-bridged tetranuclear cuii complex of the [2 × 2] grid type," *European Journal of Inorganic Chemistry*, vol. 1999, no. 3, pp. 517–522, 1999.

[135] P. Maslak and W. H. Chapman, "Photochemically generated ion and radical pairs. self-destructive charge-transfer complexes," *The Journal of Organic Chemistry*, vol. 55, no. 26, pp. 6334–6347, 1990.

[136] R. Reuter and H. A. Wegner, "Meta-oligoazobiphenyls–synthesis via site-selective mills reaction and photochemical properties," *Beilstein journal of Organic Chemistry*, vol. 8, no. 1, pp. 877–883, 2012.

[137] M. Reitti, P. Villo, and B. Olofsson, "One-pot C-H functionalization of arenes by diaryliodonium salts," *Angewandte Chemie*, vol. 128, no. 31, pp. 9074–9078, 2016.

[138] M.-L. Yao, G. W. Kabalka, D. W. Blevins, M. S. Reddy, and L. Yong, "Halodeboronation of organotrifluoroborates using tetrabutylammonium tribromide or cesium triiodide," *Tetrahedron*, vol. 68, no. 19, pp. 3738–3743, 2012.

[139] Z. Fu, Z. Li, Y. Song, R. Yang, Y. Liu, and H. Cai, "Decarboxylative halogenation and cyanation of electron-deficient aryl carboxylic acids via cu mediator as well as electron-rich ones through pd catalyst under aerobic conditions," *The Journal of Organic Chemistry*, vol. 81, no. 7, pp. 2794–2803, 2016.

[140] W. B. Smith and O. C. Ho, "Application of the isoamyl nitrite-diiodomethane route to aryl iodites," *Journal of Organic Chemistry*, vol. 55, no. 8, pp. 2543–2545, 1990.

[141] A. A. Cant, R. Bhalla, S. L. Pimlott, and A. Sutherland, "Nickel-catalysed aromatic finkelstein reaction of aryl and heteroaryl bromides," *Chemical Communications*, vol. 48, no. 33, pp. 3993–3995, 2012.

[142] C. Butts, L. Eberson, K. Fulton, M. Hartshorn, W. Robinson, and D. Timmerman-Vaughan, "Photochemical nitration by tetranitromethane. part XXXIII. Adduct formation in the photochemical reactions of 1,2,4,5-and 1,2,3,5-tetramethylbenzene," *Acta Chemica Scandinavica*, vol. 50, no. 11, pp. 991–1008, 1996.

[143] J. M. Masnovi, S. Sankararaman, and J. K. Kochi, "Direct observation of the kinetic acidities of transient aromatic cation radicals. The mechanism of electrophilic sidechain nitration of the methylbenzenes," *Journal of the American Chemical Society*, vol. 111, no. 6, pp. 2263–2276, 1989.

[144] R. R. Yadav, R. A. Vishwakarma, and S. B. Bharate, "Catalyst-free ipso-nitration of aryl boronic acids using bismuth nitrate," *Tetrahedron Letters*, vol. 53, no. 44, pp. 5958–5960, 2012.

[145] A. Preiss, U. Lewin, L. Wennrich, M. Findeisen, and J. Efer, "Analysis of nitrophenols and other polar nitroaromatic compounds in ammunition wastewater by high-field proton nuclear magnetic resonance (1H-NMR) spectroscopy and chromatographic methods," *Fresenius' journal of analytical chemistry*, vol. 357, no. 6, pp. 676–683, 1997.

[146] S. Förster, A. Rieker, K. Maruyama, K. Murata, and A. Nishinaga, "Cobalt schiff base complex-catalyzed oxidation of anilines with tert-butyl hydroperoxide," *The Journal of Organic Chemistry*, vol. 61, no. 10, pp. 3320–3326, 1996.

[147] J. Vinsova, K. Cermakova, A. Tomeckova, M. Ceckova, J. Jampilek, P. Cermak, J. Kunes, M. Dolezal, and F. Staud, "Synthesis and antimicrobial evaluation of new 2-substituted 5,7-di-tert-butylbenzoxazoles," *Bioorganic & Medicinal Chemistry*, vol. 14, no. 17, pp. 5850–5865, 2006.

[148] S. Bhadra, W. I. Dzik, and L. J. Goossen, "Decarboxylative etherification of aromatic carboxylic acids," *Journal of the American Chemical Society*, vol. 134, no. 24, pp. 9938–9941, 2012.

[149] E. Giorgini, R. Petrucci, P. Astolfi, R. P. Mason, and L. Greci, "On the role of nitrogen monoxide (nitric oxide) in the nitration of a tyrosine derivative and model compounds," *European Journal of Organic Chemistry*, vol. 2002, no. 23, pp. 4011–4017, 2002.

[150] J. Dhineshkumar, P. Samaddar, and K. R. Prabhu, "A copper catalyzed azidation and peroxidation of β-naphthols via an oxidative dearomatization strategy," *Chemical Communications.*, vol. 52, no. 74, pp. 11 084–11 087, 2016.

[151] A. Lishchynskyi, M. A. Novikov, E. Martin, E. C. Escudero-Adán, P. Novák, and V. V. Grushin, "Trifluoromethylation of aryl and heteroaryl halides with fluoroform-derived $CuCF_3$: Scope, limitations, and mechanistic features," *The Journal of Organic Chemistry*, vol. 78, no. 22, pp. 11 126–11 146, 2013.

[152] X. Lin, C. Hou, H. Li, and Z. Weng, "Decarboxylative trifluoromethylating reagent $[Cu(O_2CCF_3)(phen)]$ and difluorocarbene precursor $[Cu(phen)_2][O_2CCF_2Cl]$," *Chemistry–A European Journal*, vol. 22, no. 6, pp. 2075–2084, 2016.

[153] J. Iskra and S. S. Murphree, "Rapid aerobic iodination of arenes mediated by hypervalent iodine in fluorinated solvents," *Tetrahedron Letters*, vol. 58, no. 7, pp. 645–648, 2017.

[154] D. Zornik, R. M. Meudtner, T. El Malah, C. M. Thiele, and S. Hecht, "Designing structural motifs for clickamers: Exploiting the 1,2,3-triazole moiety to generate conformationally restricted molecular architectures," *Chemistry – A European Journal*, vol. 17, no. 5, pp. 1473–1484, 2011.

[155] M. E. Sosa Torres, J. P. Saucedo-Vázquez, and P. M. H. Kroneck, "The magic of dioxygen," in *Sustaining Life on Planet Earth: Metalloenzymes Mastering Dioxygen and Other Chewy Gases*, P. M. H. Kroneck and M. E. Sosa Torres, Eds. Cham: Springer International Publishing, 2015, pp. 1–12, ISBN: 978-3-319-12415-5.

[156] D. V. Deubel, "From evolution to green chemistry: Rationalization of biomimetic oxygen-transfer cascades," *Journal of the American Chemical Society*, vol. 126, no. 4, pp. 996–997, 2004.

[157] R. A. Sheldon, "Recent advances in green catalytic oxidations of alcohols in aqueous media," *Catalysis Today*, vol. 247, pp. 4–13, 2015.

[158] C. Parmeggiani and F. Cardona, "Transition metal based catalysts in the aerobic oxidation of alcohols," *Green Chemistry*, vol. 14, no. 3, pp. 547–564, 2012.

[159] S. E. Davis, M. S. Ide, and R. J. Davis, "Selective oxidation of alcohols and aldehydes over supported metal nanoparticles," *Green Chemistry*, vol. 15, no. 1, pp. 17–45, 2013.

[160] M. J. Schultz and M. S. Sigman, "Recent advances in homogeneous transition metal-catalyzed aerobic alcohol oxidations," *Tetrahedron*, vol. 62, no. 35, pp. 8227–8241, 2006.

[161] B. L. Ryland and S. S. Stahl, "Practical aerobic oxidations of alcohols and amines with homogeneous copper/TEMPO and related catalyst systems," *Angewandte Chemie International Edition*, vol. 53, no. 34, pp. 8824–8838, 2014.

[162] S. Wertz and A. Studer, "Nitroxide-catalyzed transition-metal-free aerobic oxidation processes," *Green Chemistry*, vol. 15, no. 11, pp. 3116–3134, 2013.

[163] R. A. Sheldon, I. W. Arends, G.-J. ten Brink, and A. Dijksman, "Green, catalytic oxidations of alcohols," *Accounts of Chemical Research*, vol. 35, no. 9, pp. 774–781, 2002.

[164] R. Liu, X. Liang, C. Dong, and X. Hu, "Transition-metal-free: A highly efficient catalytic aerobic alcohol oxidation process," *Journal of the American Chemical Society*, vol. 126, no. 13, pp. 4112–4113, 2004.

[165] F. Minisci, O. Porta, F. Recupero, C. Punta, C. Gambarotti, M. Pierini, and L. Galimberti, "New selective metal-free oxidations of primary alcohols by HNO_3 or HNO_3 and O_2, catalyzed by Br_2," *Synlett*, vol. 15, no. 12, pp. 2203–2205, 2004.

[166] Y. Kuang, H. Rokubuichi, Y. Nabae, T. Hayakawa, and M.-a. Kakimoto, "A nitric acid-assisted carbon-catalyzed oxidation system with nitroxide radical cocatalysts as an efficient and green protocol for selective aerobic oxidation of alcohols," *Advanced Synthesis & Catalysis*, vol. 352, no. 14-15, pp. 2635–2642, 2010.

[167] C. Aellig, C. Girard, and I. Hermans, "Aerobic alcohol oxidations mediated by nitric acid," *Angewandte Chemie International Edition*, vol. 50, no. 51, pp. 12 355–12 360, 2011.

[168] S. Tanielyan, R. Augustine, N. Marin, G. Alvez, and J. Stapley, "Transition metal free catalytic aerobic oxidation of methyl-α-D-glucopyranoside under mild conditions using stable nitroxyl free radicals," *Topics in Catalysis*, vol. 55, no. 7-10, pp. 556–564, 2012.

[169] A. Rahimi, A. Azarpira, H. Kim, J. Ralph, and S. S. Stahl, "Chemoselective metal-free aerobic alcohol oxidation in lignin," *Journal of the American Chemical Society*, vol. 135, no. 17, pp. 6415–6418, 2013.

[170] A. Levina and S. Trusov, "Nitrous acid-catalysed oxidation of alcohols by oxygen in strongly acidic aqueous solutions," *Journal of Molecular Catalysis*, vol. 88, no. 2, pp. L121–L123, 1994.

[171] C. Aellig, D. Scholz, and I. Hermans, "Metal-free aerobic alcohol oxidation: Intensification under three-phase flow conditions," *ChemSusChem*, vol. 5, no. 9, pp. 1732–1736, 2012.

[172] C. Aellig, D. Scholz, S. Conrad, and I. Hermans, "Intensification of TEMPO-mediated aerobic alcohol oxidations under three-phase flow conditions," *Green Chemistry*, vol. 15, no. 7, pp. 1975–1980, 2013.

[173] T. Del Giacco, A. Faltoni, and F. Elisei, "Anomalous reactivity of radical cations produced by photosensitized oxidation of 4-methoxybenzyl alcohol derivatives: Role of the sensitizer," *Physical Chemistry Chemical Physics*, vol. 10, no. 1, pp. 200–210, 2008.

[174] S. R. Joshi, K. L. Kataria, S. B. Sawant, and J. B. Joshi, "Kinetics of oxidation of benzyl alcohol with dilute nitric acid," *Industrial & Engineering Chemistry Research*, vol. 44, no. 2, pp. 325–333, 2005.

[175] C. Aellig, U. Neuenschwander, and I. Hermans, "Acid-catalyzed decomposition of the benzyl nitrite intermediate in HNO_3-mediated aerobic oxidation of benzyl alcohol," *ChemCatChem*, vol. 4, no. 4, pp. 525–529, 2012.

[176] M. P. Doyle, J. W. Terpstra, R. A. Pickering, and D. M. LePoire, "Hydrolysis, nitrosyl exchange, and synthesis of alkyl nitrites," *The Journal of Organic Chemistry*, vol. 48, no. 20, pp. 3379–3382, 1983.

[177] J. B. Arterburn, "Selective oxidation of secondary alcohols," *Tetrahedron*, vol. 57, no. 49, pp. 9765–9788, 2001.

[178] J. N. Chheda, G. W. Huber, and J. A. Dumesic, "Liquid-phase catalytic processing of biomass-derived oxygenated hydrocarbons to fuels and chemicals," *Angewandte Chemie International Edition*, vol. 46, no. 38, pp. 7164–7183, 2007.

[179] G. Tojo and M. I. Fernández, *Oxidation of alcohols to aldehydes and ketones: A guide to current common practice*. Springer Science & Business Media, 2006, ISBN: 9780387236070.

[180] N. Wang, R. Liu, J. Chen, and X. Liang, "$NaNO_2$-activated, iron–TEMPO catalyst system for aerobic alcohol oxidation under mild conditions," *Chemical Communications*, no. 42, pp. 5322–5324, 2005.

[181] G. Stavber, M. Zupan, and S. Stavber, "Iodine induced transformations of alcohols under solvent-free conditions," *Tetrahedron Letters*, vol. 47, no. 48, pp. 8463–8466, 2006.

[182] S. E. Aldred, D. L. H. Williams, and M. Garley, "Kinetics and mechanism of the nitrosation of alcohols, carbohydrates, and a thiol," *Journal of the Chemical Society, Perkin Transactions 2*, no. 7, pp. 777–782, 1982.

[183] A. Fürstner, "Iron catalysis in organic synthesis: A critical assessment of what it takes to make this base metal a multitasking champion," *ACS Central Science*, vol. 2, no. 11, pp. 778–789, 2016.

[184] A. Gonzalez-de-Castro and J. Xiao, "Green and efficient: Iron-catalyzed selective oxidation of olefins to carbonyls with O_2," *Journal of the American Chemical Society*, vol. 137, no. 25, pp. 8206–8218, 2015.

[185] X. Jiang, J.-M. Wang, Y. Zhang, Z. Chen, Y.-M. Zhu, and S.-J. Ji, "Palladium-catalyzed formylation of aryl halides with tert-butyl isocyanide," *Organic Letters*, vol. 16, no. 13, pp. 3492–3495, 2014.

[186] J. Ma, C. Hong, Y. Wan, M. Li, X. Hu, W. Mo, B. Hu, N. Sun, L. Jin, and Z. Shen, "Aerobic oxidation of secondary alcohols in water with ABNO/tert-butyl nitrite/KPF_6 catalytic system," *Tetrahedron Letters*, vol. 58, no. 7, pp. 652–657, 2017.

[187] P. Wang, J. Cai, J. Yang, C. Sun, L. Li, H. Hu, and M. Ji, "Zinc(II)-catalyzed oxidation of alcohols to carbonyl compounds with chloramine-T," *Tetrahedron Letters*, vol. 54, no. 6, pp. 533–535, 2013.

[188] R. Prebil, G. Stavber, and S. Stavber, "Aerobic oxidation of alcohols by using a completely metal-free catalytic system," *European Journal of Organic Chemistry*, vol. 2014, no. 2, pp. 395–402, 2014.

[189] B. Morandi, Z. K. Wickens, and R. H. Grubbs, "Practical and general palladium-catalyzed synthesis of ketones from internal olefins," *Angewandte Chemie International Edition*, vol. 52, no. 10, pp. 2944–2948, 2013.

[190] A. Nikolaou, G. Kokotos, and V. Magrioti, "Efficient microwave-assisted synthesis of hydroxymethyl ketones using NHC organocatalysts," *Tetrahedron*, vol. 72, no. 47, pp. 7628–7632, 2016.

[191] Y. M. A. Yamada, C. K. Jin, and Y. Uozumi, "H_2O_2-oxidation of alcohols promoted by polymeric phosphotungstate catalysts," *Organic Letters*, vol. 12, no. 20, pp. 4540–4543, 2010.

[192] F. Li, N. Wang, L. Lu, and G. Zhu, "Regioselective hydration of terminal alkynes catalyzed by a neutral gold(I) complex [(IPr)AuCl] and one-pot synthesis of optically active secondary alcohols from terminal alkynes by the combination of [(IPr)AuCl] and Cp*RhCl[(R,R)-TsDPEN]," *The Journal of Organic Chemistry*, vol. 80, no. 7, pp. 3538–3546, 2015.

[193] N. de Kimpe, R. Verhé, S. Patai, and Z. Rappoport, *The chemistry of α-haloketones, α-haloaldehydes, and α-haloimines*, ser. Updates from the Chemistry of the functional groups. Wiley, 1988, ISBN: 9780471917083.

[194] T. Ankner, M. Fridén-Saxin, N. Pemberton, T. Seifert, M. Grøtli, K. Luthman, and G. Hilmersson, "KHMDS enhanced SmI_2-mediated reformatsky type α-cyanation," *Organic Letters*, vol. 12, no. 10, pp. 2210–2213, 2010.

[195] K. Shibatomi and H. Yamamoto, "Stereoselective synthesis of α,α-chlorofluoro carbonyl compounds leading to the construction of fluorinated chiral quaternary carbon centers," *Angewandte Chemie International Edition*, vol. 47, no. 31, pp. 5796–5798, 2008.

[196] S.-G. Li and S. Z. Zard, "A convenient metal-free reagent for the generation and capture of trifluoromethanethiol," *Organic Letters*, vol. 15, no. 22, pp. 5898–5901, 2013.

[197] P. M. Lundin, J. Esquivias, and G. C. Fu, "Catalytic asymmetric cross-couplings of racemic α-bromoketones with arylzinc reagents," *Angewandte Chemie International Edition*, vol. 48, no. 1, pp. 154–156, 2009.

[198] P. M. Lundin and G. C. Fu, "Asymmetric suzuki cross-couplings of activated secondary alkyl electrophiles: Arylations of racemic α-chloroamides," *Journal of the American Chemical Society*, vol. 132, no. 32, pp. 11 027–11 029, 2010.

[199] C. Liu, Y. Deng, J. Wang, Y. Yang, S. Tang, and A. Lei, "Palladium-catalyzed C-C bond formation to construct 1,4-diketones under mild conditions," *Angewandte Chemie International Edition*, vol. 50, no. 32, pp. 7337–7341, 2011.

[200] S. Lou and G. C. Fu, "Nickel/bis (oxazoline)-catalyzed asymmetric kumada reactions of alkyl electrophiles: Cross-couplings of racemic α-bromoketones," *Journal of the American Chemical Society*, vol. 132, no. 4, pp. 1264–1266, 2010.

[201] A. W. Erian, S. M. Sherif, and H. M. Gaber, "The chemistry of α-haloketones and their utility in heterocyclic synthesis," *Molecules*, vol. 8, no. 11, pp. 793–865, 2003.

[202] Z.-W. Chen, D.-N. Ye, M. Ye, Z.-G. Zhou, S.-H. Li, and L.-X. Liu, "AgF/TFA-promoted highly efficient synthesis of α-haloketones from haloalkynes," *Tetrahedron Letters*, vol. 55, no. 7, pp. 1373–1375, 2014.

[203] N. Ahlsten, A. Bermejo Gómez, and B. Martín-Matute, "Iridium-catalyzed 1,3-hydrogen shift/chlorination of allylic alcohols," *Angewandte Chemie International Edition*, vol. 52, no. 24, pp. 6273–6276, 2013.

[204] N. Ahlsten and B. Martin-Matute, "Ir-catalysed formation of C-F bonds. from allylic alcohols to α-fluoroketones," *Chemical Communications.*, vol. 47, no. 29, pp. 8331–8333, 2011.

[205] A. B. Gómez, E. Erbing, M. Batuecas, A. Vázquez-Romero, and B. Martín-Matute, "Iridium-catalyzed isomerization/bromination of allylic alcohols: Synthesis of α-bromocarbonyl compounds," *Chemistry – A European Journal*, vol. 20, no. 34, pp. 10 703–10 709, 2014.

[206] N. Ahlsten, A. Bartoszewicz, and B. Martin-Matute, "Allylic alcohols as synthetic enolate equivalents: Isomerisation and tandem reactions catalysed by transition metal complexes," *Dalton Trans.*, vol. 41, pp. 1660–1670, 6 2012.

[207] S. Stavber, M. Jereb, and M. Zupan, "Electrophilic iodination of organic compounds using elemental iodine or iodides," *Synthesis*, vol. 40, no. 10, pp. 1487–1513, 2008.

[208] C. A. Horiuchi and S. Kiji, "A new α-iodination of ketones using iodine–cerium (IV) ammonium nitrate," *Chemistry Letters*, vol. 17, no. 1, pp. 31–34, 1988.

[209] A. Bekaert, O. Barberan, M. Gervais, and J.-D. Brion, "Direct α-iodination of ketones using iodine/SeO_2," *Tetrahedron Letters*, vol. 41, no. 16, pp. 2903–2905, 2000.

[210] M. L. Rao and D. N. Jadhav, "Metal catalyst-free direct α-iodination of ketones with molecular iodine," *Tetrahedron Letters*, vol. 47, no. 38, pp. 6883–6886, 2006.

[211] M. M. Reddy, P. Swamy, M. Naresh, K. Srujana, C. Durgaiah, T. V. Rao, and N. Narender, "One-pot synthesis of α-iodoketones from alcohols using ammonium iodide and oxone® in water," *RSC Advances*, vol. 5, no. 16, pp. 12 186–12 190, 2015.

[212] J. Barluenga, M. Marco-Arias, F. Gonzalez-Bobes, A. Ballesteros, and J. M. Gonzalez, "New reactions in water: Metal-free conversion of alcohols and ketones into α-iodoketones," *Chemical Communications*, no. 22, pp. 2616–2617, 2004.

[213] J. C. Lee and Y. S. Jin, "Efficient method for α-iodination of ketones," *Synthetic Communications*, vol. 29, no. 16, pp. 2769–2774, 1999.

[214] D. Dolenc, "Iodination of enol acetates and 1,3-diones using N-iodosaccharin," *Synthetic Communications*, vol. 33, no. 16, pp. 2917–2924, 2003.

[215] J. S. Yadav, B. V. S. Reddy, A. P. Singh, and A. K. Basak, "IBX/I_2-mediated oxidation of alkenes and alkynes in water: A facile synthesis of α-iodoketones," *Tetrahedron Letters*, vol. 49, no. 41, pp. 5880–5882, 2008.

[216] L. Bedrač and J. Iskra, "Dihaloiodates (I): Synthesis with hydrogen peroxide and their halogenating activity," *Tetrahedron Letters*, vol. 53, no. 41, pp. 5555–5558, 2012.

[217] T. Gough, W. Lin, and R. Woolford, "Conformational studies of α-substituted ketones by nuclear magnetic resonance," *Canadian Journal of Chemistry*, vol. 45, no. 21, pp. 2529–2535, 1967.

Bibliography

Publications Related to the Thesis

Journal Articles

Original scientific article

Š. Možina, S. Stavber, and J. Iskra, "Dual catalysis for the aerobic oxidation of benzyl alcohols – nitric acid and fluorinated alcohol," *European Journal of Organic Chemistry*, vol. 2017, no. 3, pp. 448–452, 2017.

Conference paper

Published scientific conference contribution

Š. Možina, A. B. Gómez, B. Martín-Matute, S. Stavber, and J. Iskra, "Iridium-catalysed synthesis of alpha-haloketones," in *Zbornik: part 2, 7th Jožef Stefan International Postgraduate School Students' Conference*, Ljubljana: Mednarodna podiplomska šola Jožefa Stefana, 2015, pp. 33–40.

Š. Možina, S. Stavber, and J. Iskra, "Mimicking nature - iron catalysed oxidation of alcohols," in *Zbornik: part 1, 8th Jožef Stefan International Postgraduate School Students' Conference*, Ljubljana: Mednarodna podiplomska šola Jožefa Stefana, 2016, pp. 69–75.

Published scientific conference contribution abstract

Š. Možina, A. B. Gómez, B. Martín-Matute, S. Stavber, and J. Iskra, "Iridium-catalysed isomerization/halogenation of allylic alcohols - synthesis of α-haloketones," in *9th Young researchers' day*, Ljubljana: Institut Jožef Stefan, 2015.

Š. Možina and J. Iskra, "Activation of nitration of aromatic molecules in fluorinated alcohols : Template catalysis?" In *International Symposium and Fluorous Technology*, Budapest, Hungary: ISoFT'13, 2013.

——, "Activation of nitration of aromatic compounds by template catalysis," in *Program and abstract book, 8th Young Researchers' Day*, Ljubljana: Institut Jožef Stefan, 2014.

——, "Activation of nitration of aromatic compounds by template catalysis," in *20th International Conference on Organic Synthesis*, Budapest, Hungary: ICOS-20, 2014.

——, "Aromatic nitration in fluorinated alcohols and its evaluation with green chemistry metrics," in *Zbornik referatov in povzetkov, 22. Slovenski kemijski dnevi*, Portorož: Slovensko kemijsko društvo, 2016.

——, "Evaluation of nitration of aromatics with nitric acid in fluorinated alcohols with literature methods by green chemistry metrics," in *Sustainability through Green chemistry, 6th International IUPAC Conference on Green Chemistry*, Venezia, Italy: IUPAC, 2016.

Š. Možina, S. Stavber, and J. Iskra, “Fluorinated alcohol as template catalyst for aerobic oxidation of alcohols catalyzed by nitric acid,” in *Zbornik referatov in povzetkov, Slovenski kemijski dnevi 2015*, Ljubljana: Slovensko kemijsko društvo, 2015.

——, “Nitric acid catalysed aerobic oxidation of alcohols activated by hexafluoroisopropanol,” in *Programme of lectures, 40th "A. Corbella" International Summer School on Organic Synthesis*, Gargnano, Italy: ISOS 2015, 2015.

——, “Activation of fe-catalyzed aerobicoxidation of alcohols by solvent - template catalysis of fluorinated alcohols,” in *Book of abstracts, 4th CARISMA Meeting*, Ljubljana: Institut Jožef Stefan, 2016.

——, “Activation of oxidation by template catalysis : The power of weak forces,” in *10th Young researchers’ day*, Ljubljana: Institut Jožef Stefan, 2016.

Š. Možina, S. Stavber, J. Iskra, A. B. Gómez, and B. Martín-Matute, “In situ preparation of iodine(i) reagent by oxidation with H_2O_2 and its use in iridium-catalyzed isomerisation/halogenation of allylic alcohols,” in *Book of abstracts, 4th CARISMA Meeting*, Ljubljana: Institut Jožef Stefan, 2016.

To be submitted original scientific articles

Š. Možina, S. Stavber, and J. Iskra, "Triple catalysis in aerobic oxidation of secondary alcohols: nitric acid, iron(III) chloride and fluorinated alcohol".

Š. Možina, S. Stavber, and J. Iskra, "Nitric acid as sole reagent for aromatic nitration: the case of templated catalysis by fluorinated alcohols".

Š. Možina, A. Kokalj, J. Štrancar, S. Stavber, and J. Iskra, "Radical intermediates in nitration of aromatic molecules with nitric acid under template catalysis by fluorinated alcohol".

Š. Možina, S. Stavber, and J. Iskra, "Evaluation of environmental parameters of methods for aromatic nitration".

Biography

I was born on 19. 8. 1989 in Ljubljana. After I finished high school I started studying Chemistry at Faculty for chemistry and chemical technology, University Ljubljana. I graduated on 9. 9. 2013 under supervisor Assoc. Prof. Marjan Jereb and co-supervisor Assoc. Prof. Jernej Iskra. With 1st October same year I became Young researcher at the Centre of Excellence for Integrated Approaches in Chemistry and Biology of Proteins (CIPKeBiP) in Laboratory of Organic and Bioorganic Chemistry at the Department of Physical and Organic Chemistry, "Jožef Stefan" Institute. My Ph.D. study was done under supervisor Prof. Stojan Stavber and co-supervisor Assoc. Prof. Jernej Iskra at Jožef Stefan International Postgraduate School (IPS) in Ecotechnology study program.